CHARACTERIZATION OF THE FUNCTIONAL ROLES OF HISTIDINE-RICH GLYCOPROTEIN IN COAGULATON

By:

Trang T. Vu, B.Sc (Hons)

A Thesis

Submitted to the School of Graduate Studies in Partial

Fulfillment of the Requirements for the Degree

Doctor of Philosophy

McMaster University

DOCTOR OF PHILOSOPHY (2014) McMaster University
(Department of Medical Sciences) Hamilton, Ontario

TITLE: CHARACTERIZATION OF THE FUNCTIONAL ROLES OF HISTIDINE-RICH GLYCOPROTEIN IN COAGULATION

AUTHOR: Trang T. Vu
B. Sc. (Honours) Biochemistry Co-op
(Molecular Biology Specialization)
(McMaster University)

SUPERVISOR: Jeffrey I. Weitz, M.D.

NUMBER OF PAGES: xix, 262

ABSTRACT

Histidine-rich glycoprotein (HRG) is a protein present in plasma at ~ 2 μM, but whose physiologic function is unclear. HRG is a multi-domain protein that contains a unique histidine-rich core that interacts with zinc and hydrogen ions to modulate ligand binding. Due to its modular structure and capacity to sense local changes in zinc and pH, HRG binds several ligands including complement proteins, phospholipids, DNA, fibrin(ogen), heparin, factor (F) XIIa and plasmin. Thus, it is hypothesized that HRG functions as an accessory or adapter protein that bridges different ligands together. Despite the array of ligands and potential involvement in immunity, angiogenesis, coagulation and fibrinolysis, no clear role for HRG has emerged. Congenital HRG deficiency in humans has been associated with a variable phenotype; some investigators report increased susceptibility to thrombosis while others do not. However, studies in HRG-deficient mice reveal that HRG attenuates coagulation.

Coagulation is initiated via the intrinsic (or contact) and extrinsic (or tissue factor) pathways and culminates in the generation of thrombin. Thrombin catalyzes the conversion of fibrinogen into a fibrin meshwork that reinforces the platelet plug at sites of vascular injury. There are two circulating isoforms of fibrinogen that differ with respect to their γ-chains. Bulk fibrinogen is composed of a pair of γ_A-chains, and is designated γ_A/γ_A-fibrinogen, whereas a minor variant contains a γ_A-chain and a γ′-chain, and is designated γ_A/γ'-fibrinogen. The γ′-chain contains an anionic 20-amino acid residue extension at its COOH-terminus, which provides an accessory binding site for thrombin. Thrombin possesses an anion binding pocket termed exosite II that flanks the active site

and mediates its interaction with the γ′-chain of fibrinogen. Exosite II is an evolutionary feature that is unique to thrombin, as this region is not observed on the prototypic serine protease trypsin or on other defibrinogenating enzymes from snake venom such as batroxobin. Although the physiologic function of the thrombin-γ′-chain interaction is unclear, it is proposed that this interaction modulates thrombin's activity when it is bound to fibrin clots. Consistent with this, we show that γ_A/γ'-fibrin attenuates thrombin's capacity to promote clot expansion compared with thrombin bound to γ_A/γ_A-fibrin clots, thereby demonstrating that γ_A/γ'-fibrin attenuates thrombin's activity. In the presence of physiologic concentrations of zinc, HRG binds the γ′-chain of fibrino(gen) and competes with thrombin for binding, thereby suggesting that HRG is a unique modulator of thrombin activity on fibrin clots. Platelets store zinc and HRG in their α-granules and release both components when they undergo activation at sites of injury, which localizes HRG in the vicinity of fibrin-bound thrombin.

Consistent with the role of HRG in modulating coagulation, we also show that HRG attenuates contact activation of coagulation, but has no impact on clotting initiated by the extrinsic pathway. The intrinsic pathway is initiated when FXII is activated by polyanions such as RNA and DNA, which are released into the blood after cellular activation, injury or death. FXIIa activates FXI, thereby propagating coagulation and leading to thrombin generation and fibrin formation. Recently, studies using rodent, rabbit and non-human primate models of thrombosis have shown that knock down of FXII or FXI with antisense oligonucleotides or blocking FXIIa or FXIa activity with inhibitors attenuates thrombosis, while having a minimal impact on hemostasis. With increasing

evidence that the intrinsic pathway plays an important role in thrombosis, FXII and FXI have emerged as prominent targets for new anticoagulants. However, little is known about how the intrinsic pathway is regulated, so as to prevent uncontrolled clotting.

HRG attenuates the intrinsic pathway by binding both FXIIa and the contact activators, RNA and DNA. By binding nucleic acids, HRG is localized to the site of contact activation, where it is poised to inhibit FXIIa. HRG binds to an allosteric region on FXIIa and attenuates its capacity to feedback activate FXII and to activate FXI, thereby inhibiting the initiating steps of contact activation. In addition, HRG attenuates the cofactor role of RNA and DNA in thrombin activation of FXI, which is an important feedback step. With the capacity to modulate multiple steps in the intrinsic pathway, HRG likely serves as a dynamic regulator of contact activation.

We tested our hypothesis that HRG is a novel inhibitor of the intrinsic pathway in a murine model of $FeCl_3$-induced arterial injury. HRG-deficient mice exhibit accelerated thrombosis compared with wild type controls, an effect that was abolished by repletion with human HRG. Therefore, these studies indicate that HRG deficiency induces a prothrombotic phenotype. Consistent with the role of HRG as a modulator of the intrinsic pathway, we show that thrombosis after the $FeCl_3$-induced arterial injury is attenuated by administration of RNase, but not DNase, or by knock down of FXII, but not FVII. Therefore, these studies show that thrombosis in this model is induced by RNA and occurs in a FXII-dependent manner. Furthermore, blood loss after tail tip amputation is similar in HRG-deficient and wild type mice, demonstrating that HRG does not modulate

hemostasis. Therefore, these studies suggest that HRG is a dynamic regulator of the intrinsic pathway, and acts as a molecular brake to limit procoagulant stimuli.

The observations that HRG binds fibrin(ogen), FXIIa and nucleic acids and modulates the thrombin-γ′-interaction and intrinsic pathway of coagulation, suggest that HRG is a key regulator of coagulation. HRG, the contact system and fibrin are also important in the innate immune response, demonstrating that the interaction of HRG with these factors may provide a unique link between coagulation and immunity. Since immune cells and the coagulation system contribute to both deep vein thrombosis and sepsis, further characterization of the role of HRG in these conditions will contribute to a better understanding of the pathophysiological role of HRG, and may identify novel therapeutic directions.

ACKNOWLEDGEMENTS

I would like to express my gratitude to my supervisor and role model Dr. Jeffrey Weitz for his mentorship, generosity and support during graduate school. Although I was enrolled in co-operative education in undergrad and worked in several labs, it was Dr. Weitz who really gave me the first opportunity to prove myself as a scientist. Through his mentorship, Dr. Weitz really gave me the confidence to be creative with my projects and enabled me to do my best research. As a supervisor, Dr. Weitz always makes time for me and I'm always impressed at the lightning speed at which he replies to my enquires and the enthusiasm at which he edits my manuscripts. Most importantly, Dr. Weitz has showed me that medicine and science are a powerful combination and this has inspired me to follow in his footsteps to become a clinician scientist. I look forward to applying what I've learned with Dr. Weitz on my new journey in medicine.

Equally important to my success in graduate school are the "pillars" in the Weitz lab, Dr. Jim Fredenburgh, Alan Stafford, Beverly Leslie and Dr. Ji Zhou. First, I would like to thank my mentor Dr. Jim Fredenburgh for his continual guidance, patience and mentorship. I thank Jim for patiently listening to my ideas, helping me troubleshoot and for the countless hours he spent editing my reports, manuscripts and presentations. I also owe much of my success in graduate school to you, Jim. Second, I'd like to thank Alan Stafford for helping me troubleshoot and inspiring me to do better science everyday. Third, I'd like to thank my two collaborators Beverly Leslie and Dr. Ji Zhou. Both of you have helped me execute really technically challenging experiments and I'm really proud of the work we have done together. Thank you Bev and Ji for your kindness, patience and

continual support. I am very fortunate to work with Dr. Weitz and his team and together, they have taught me to be a better scientist and person.

I am fortunate to have many mentors at TaARI and I would like to express my appreciation to my supervisory committee members, Dr. Patricia Liaw and Dr. Peter Gross. Thank you both for your continued guidance and support. You both inspire me to do my best.

I also want to thank my colleagues and friends in the Weitz (Dr. Paul Kim, Calvin, Sara and Jonathan), Gross (Ran and Nima) and Liaw (Dr. Laura Swystun, Laura Pepler Dhruva, Zakhar and Travis) labs, who make going to the lab every day enjoyable-even when my experiments fail. Thank you to my peers for their camaraderie and memories. I look forward to collaborating with many of you in the future.

Lastly, I'd like to thank my parents, Tuyet and Nam for giving me the opportunity to pursue an education and my dreams. Thank you both for always putting my interests first and always being supportive and loving. It was a long journey for us to get to Canada and I owe a lot of my success to you both. To my sister, Nhung and my brother, Duong, who always have my best interest at heart and are my constant cheerleaders. I dedicate this thesis to my family for always being there for me.

TABLE OF CONTENTS

LIST OF FIGURES

LIST OF TABLES

LIST OF ABBREVIATIONS

ANOVA−	Analysis of variance
aPTT−	Activated partial thromboplastin time
ASOs−	Antisense oligonucleotides
ATIII−	Antithrombin III
B−	Biotin
C1-Inh−	C1 inhibitor
CLP−	Cecal ligation and puncture
CTI−	Corn trypsin inhibitor
DAMPs−	Danger associated molecular patterns
DNase−	Deoxyribonuclease
DVT−	Deep vein thrombosis
EC_{50}−	Effective concentration that attenuates effect by 50%
ETP−	Endogenous thrombin potential
F−	Factor
Fab−	Fragment antibody binding
$FeCl_3$−	Ferric chloride
Fp−	Fibrinopeptide
FPRck−	D-Phe-Pro-Arg chloromethyl ketone
γ'-peptide−	Synthetic analog of the COOH-terminal portion of the γ-peptide of γ_A/γ'-fibrinogen
GAGs−	Glycosaminoglycans
Gla−	γ-carboxyglutamic acid
GP−	Glycoprotein
HBS−	Hepes buffered saline
HBS-Tw−	Hepes buffered saline-Tween 20
HBS-Tw-Ca−	Hepes buffered saline-Tween 20-calcium chloride
HCII−	Heparin cofactor II
H&E−	Hematoxylin & eosin staining
HRG−	Histidine-rich glycoprotein
HRR−	Histidine-rich region
HK−	High molecular weight kininogen
LPS−	Lipopolysaccharide component in cell wall of gram negative bacteria
NDSK−	NH_2-terminal disulfide knot
NETs−	Neutrophil extracellular traps
N1N2−	NH_2-cystatin like domain of HRG
PAMPs−	Pathogen associated molecular patterns
PARs−	Protease activated receptors
PBS−	Phosphate buffered saline
PC−	Protein C
PK−	Prekallikrein
PolyP−	Polyphosphate

PRR−	Proline rich region
PS−	Phosphatidyl serine
PT−	Prothrombin time
RU−	Response units
Req−	Amount of ligand bound to immobilized protein at equilibrium
RNase−	Ribonuclease
Serpin−	Serine protease inhibitor
SI−	Supplemental information
SPR−	Surface plasmon resonance
STI−	Soybean trypsin inhibitor
TBS−	Tris buffered saline
TBS-Tw-Ca−	Tris buffered saline-Tw 20-calcium
TF−	Tissue factor
TFPI−	Tissue factor pathway inhibitor
TM−	Thrombomodulin
TSV-PA−	*T. stejnejeri* venom plasminogen activator
TTO−	Time to vessel occlusion following $FeCl_3$ injury
Tw−	Tween 20
YPRck−	D-Tyr-Pro-Arg chloromethyl ketone

CHAPTER 1: GENERAL INTRODUCTION

1.1 OVERVIEW OF HEMOSTASIS

Circulating blood contains proteins and cellular components, and under physiological conditions is maintained in a fluid state (*reviewed in* (Rasche, 2001)). Hemostasis is attained when the procoagulant, anticoagulant and fibrinolytic processes are balanced. However, after vascular injury, subendothelial components in the vessel wall are exposed to the blood and this triggers activation of platelets and the coagulation cascade. Following vascular injury, subendothelial collagen is exposed to the blood. Platelets bind to collagen, which triggers several signaling events that leads to platelet activation and aggreagation, thereby, resulting in the formation of a platelet plug. During coagulation, a series of proteolytic reactions occur and complexes form, which convert zymogens in the blood into active enzymes. Coagulation culminates in thrombin generation. Thrombin can further activate platelets and also converts insoluble fibrinogen into a fibrin network that reinforces the platelet plug (Rasche, 2001).

Anticoagulant processes are positioned to oppose the procoagulant response by inhibiting or redirecting the activity of proteases. There are a number of inhibitors, of which the most prominent is antithrombin (AT). The capacity of AT to inhibit coagulation factors (i.e., thrombin, FIXa, FXa, FXIa, FXIIa) is enhanced by medicinal heparin and by heparan sulfate proteoglycans on the endothelial cell surface (Rau *et al.*, 2007). The Protein C (PC) pathway is also important in regulating clotting. Thrombin binds to thrombomodulin (TM) and activates PC, which is associated with the endothelial protein C receptor. Activated PC efficiently dampens coagulation by inactivating FVa and

FVIIIa, which are important cofactors in protein complexes that propagate coagulation (Esmon, 2003). Therefore, natural anticoagulants tightly regulate the activity of the coagulation proteases, so as to prevent excessive clotting.

Once a blood clot is formed, fibrinolysis, the process that results in fibrin clot degradation, facilitates wound healing (Cesarman-Maus and Hajjar, 2005). Fibrinolysis is initiated when plasminogen activators released from the vessel wall convert the zymogen plasminogen to the active serine protease, plasmin. Plasmin binds to and degrades the fibrin mesh to dissolve the clot. Therefore, hemostasis depends on the dynamic balance between clot formation and breakdown. Clots that persist can obstruct blood flow, whereas unstable clots that are rapidly degraded can lead to hemorrhage (Cesarman-Maus and Hajjar, 2005).

1.2 OVERVIEW OF THROMBOSIS

Both blood coagulation and platelet activation and aggregation are important for maintaining normal hemostasis, but these processes also play a role in thrombosis. Whereas blood clots formed during hemostasis are cleared from the circulation, clots formed under pathological conditions can persist to occlude vessels or they can embolize to distal sites and obstruct blood flow to the tissues and organs (Mackman, 2008). Consequently, thrombosis is generally viewed as a pathological extension of hemostasis. Arterial thrombosis is most commonly the result of the formation of a platelet-rich thrombus on top of ruptured atherosclerotic plaques in the arteries of the heart or brain, which can lead to myocardial infarction or stroke, respectively (Mackman, 2008). Thrombosis in the venous system is thought to reflect interplay among blood stasis, a

hypercoagulable state and/or injury to the endothelium (Saha *et al.*, 2011). Deep vein thrombosis (DVT) generally starts in the deep veins of the calf and can extend into the more proximal veins. The thrombus can break off and travel to the lungs and lodge in the pulmonary arteries to produce a pulmonary embolism, which can be fatal (Saha *et al.*, 2011).

Arterial clots, which form under high shear conditions, are rich in platelets and contain relatively little fibrin. In contrast, venous thrombi, which form under low shear conditions, are rich in fibrin and trapped red blood cells and contain relatively few platelets. The trapped red cells endow venous clots with a red color, whereas the abundant platelets in arterial clots gives them a white color (Mackman, 2008).

Anticoagulants are widely used for the prevention and treatment of arterial and venous thrombosis. However, despite advances in drug development, thrombosis remains the leading cause of death and disability in Canada and worldwide (Mackman, 2008). Thus, it is important to understand how coagulation is regulated so as to develop novel strategies to prevent and treat thrombosis.

1.3 OVERVIEW OF THE COAGULATION SYSTEM

The process of coagulation can be described in 3 phases: initiation, amplification and termination (Monroe and Hoffman, 2006). Exposure of tissue factor (TF) at sites of vascular injury or release of polyanions into the blood initiates coagulation via the extrinsic or contact pathways, respectively (Fig. 1.1). Both initiating steps trigger a series of enzymatic reactions that culminate in FXa generation at the common pathway (Monroe and Hoffman, 2006). TF binds FVIIa to form the extrinsic tenase, which activates FIX

and FX. Binding of FIXa and FVIIIa forms the intrinsic tenase, which also activates FX (Mann *et al.*, 1988). Initially, FXa only produces small quantities of thrombin. However, once generated, thrombin feeds back and activates FVIII to FVIIIa and FV to FVa, which are important cofactors in the intrinsic tenase and prothrombinase complexes, respectively. Thus, the small burst of thrombin that is initially formed primes the system for amplification (Perzborn *et al.*, 2011).

The intrinsic pathway mainly mediates the amplification step, since tissue factor pathway inhibitor (TFPI) rapidly inhibits extrinsic tenase (TF/FVIIIa). The capacity of thrombin to feedback activate FXI to FXIa further potentiates FXa production, since FXIa activates FIX to FIXa (van't Veer and Mann, 1997). In addition, thrombin also activates platelets by cleaving protease activated receptors (PARs) (Huntington, 2005). The activated platelet surface accelerates the formation of intrinsic tenase and prothrombinase complex and potentiates catalysis by localizing the coagulation factors to a specific region (Monroe and Hoffman, 2006). Thus, during the amplification phase, the intrinsic tenase complex provides a flux of FXa that feeds into the prothrombinase complex and results in a burst of thrombin generation. However, this process cannot be sustained indefinitely, as depletion of prothrombin effectively slows the amplification steps (van't Veer and Mann, 1997). The coagulation cascade is regulated by natural anticoagulants and thrombin generation is effectively terminated when the rate of inhibition exceeds the rate of thrombin formation (see (Rau *et al.*, 2007) *for review*).

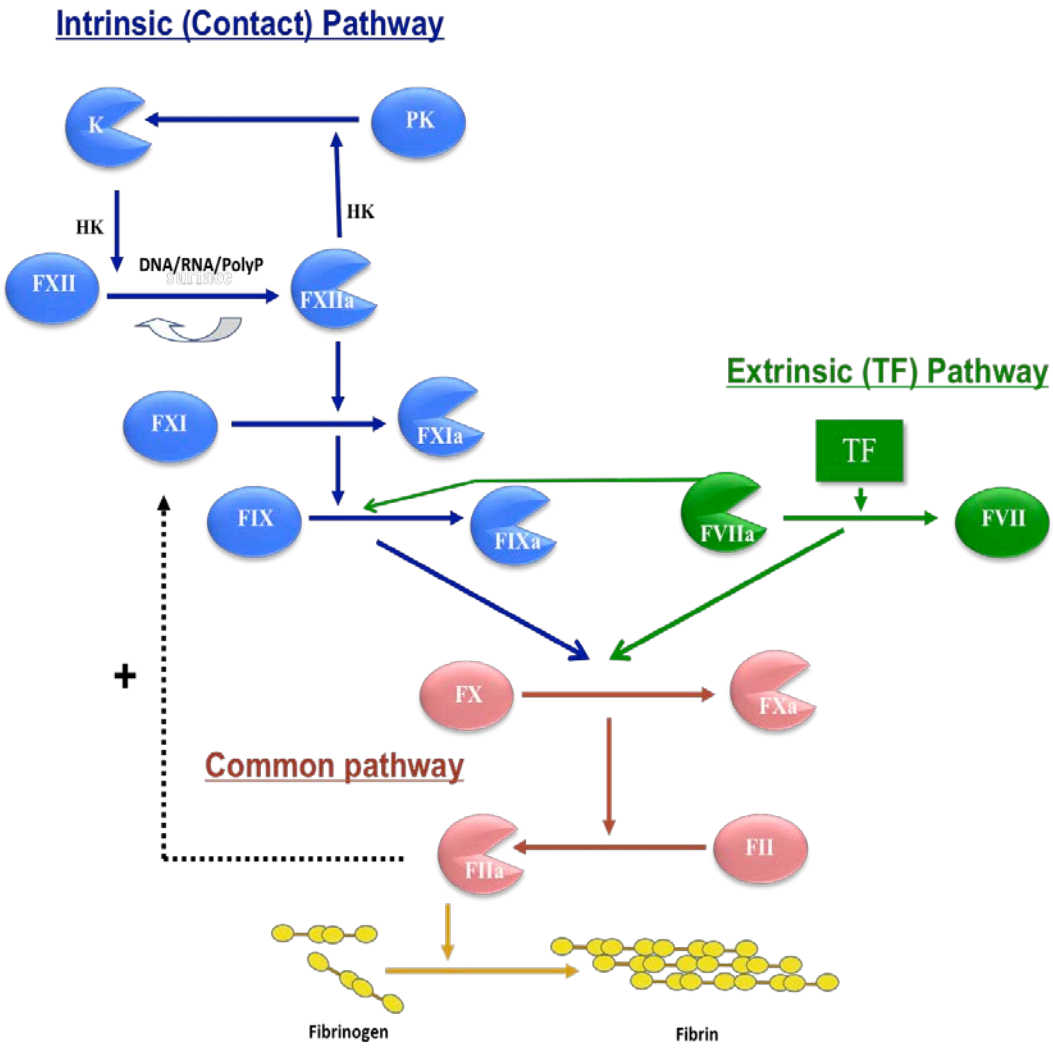
Intrinsic (Contact) Pathway
K
PK
HK
HK
FXII
DNA/RNA/PolyP
FXIIa
Extrinsic (TF) Pathway
FXI
FXIa
TF
FIX
FIXa
FVIIa
FVII
+
FX
FXa
Common pathway
FII
FIIa
Fibrinogen
Fibrin

Figure 1.1 Schematic of the coagulation cascade.

Coagulation is initiated by a series of enzymatic reactions that culminate in thrombin generation. Coagulation is initiated by the extrinsic (or TF) pathway (*green*) and by the intrinsic (or contact) pathway (*blue*). The common pathway (*pink*) represents the convergence of the intrinsic and extrinsic pathways, which both generate FXa. FXa converts prothrombin into thombin. Thrombin activates platelets and converts fibrinogen into insoluble fibrin monomers that self-associate to form a fibrin network. This results in the formation of a blood clot that contains a platelet plug that is reinforced by a fibrin mesh. For simplicity, coagulation factors FV, FVIII and FXIII are omitted from the diagram. The role of these factors in cogualation is described in detail in later sections.

1.4 EXTRINSIC (or TISSUE FACTOR) PATHWAY OF COAGULATION

The extrinsic pathway is initiated by the TF/FVIIa complex (Mackman, 2009). TF is a transmembrane glycoprotein protein that is normally located in the subendothelial layers of vessels or on cells (Eigenbrot and Kirchhofer, 2002). FVII, and to a lesser extent FVIIa, circulate in the blood, but are relatively inert without TF (Mackman, 2009). However, during vascular injury, TF is exposed to the blood where it can bind FVII/FVIIa (Eigenbrot and Kirchhofer, 2002). The TF/FVII(a) complex is localized to cell membranes; TF is membrane bound and FVIIIa contains a γ-carboxyglutamic acid (Gla) domain, which facilitates its binding cell surfaces that contain phosphatidyl serine (PS). The interaction of the Gla-domain-containing proteins to PS is mediated by calcium (Mann *et al.*, 1988). FVII can be activated by an autoactivation mechanism whereby FVIIa activates the zymogen, or by other coagulation proteases such as FXa or thrombin. Binding of FVIIa to TF induces a conformational change in the enzyme that augments its proteolytic activity by 1000-fold (Eigenbrot and Kirchhofer, 2002). The TF/FVIIa complex, which is also known as the extrinsic tenase complex, activates FX and FIX. Extrinsic tenase is thought to be the major initiator of coagulation. In laboratory studies, reconstitution of plasma with relipidated TF forms the basis for the prothrombin time (PT) assay, which is a global test of coagulation that is used to assess the integrity of the extrinsic and common pathways (Eigenbrot and Kirchhofer, 2002, Mackman, 2009).

1.5 INTRINSIC (or CONTACT) PATHWAY OF COAGULATION

The intrinsic pathway of coagulation is triggered by the exposure of FXII in blood to polyanionic activators that provide a platform or surface for assembly of the intrinsic pathway proteins (Gailani and Renne, 2007). For decades, it was known that synthetic substances such as kaolin, silica, ellagic acid and dextran sulfate activate FXII *in vitro*. While these agents form the basis for the activated partial thromboplastin time (aPTT) assay, which is a global coagulation test used to assess the integrity of the intrinsic and common pathways of coagulation, the identity of potent physiologic activators of FXII remained elusive (Renne *et al.*, 2005). However, in the last decade, naturally occurring polyphosphate containing molecules such as inorganic polyphosphates (polyP), DNA and RNA have been shown to activate FXII. Whereas polyP is stored in platelets and is released upon platelet activation, DNA and RNA are released from activated, damaged or dying cells (Kannemeier *et al.*, 2007, Muller *et al.*, 2009, Smith *et al.*, 2006). In addition, the observation that the intrinsic pathway also initiates coagulation on catheters or extracorporeal circuits, suggests that this pathway also contributes to thrombosis on medical devices (Larsson *et al.*, 2014, Yau *et al.*, 2014). The discovery of these physiological agents and the phenomenon that medical devices induce thrombosis has led to a renewed interest in the intrinsic pathway. Novel physiological activators of the intrinsic pathway will be discussed in detail in section 1.12.

FXII and high molecular weight kininogen (HK) possess anionic binding motifs that can directly bind to activators with a polyanionic structure (Colman and Schmaier, 1997). The intrinsic pathway is triggered when FXII binds to polyanions and undergoes a

conformational change, which renders the zymogen more susceptible to proteolysis. As a result of polyanion surface binding, FXII becomes autoactivated, a process whereby FXIIa cleaves its own zymogen to amplify its activation. The majority of FXI and PK circulate in complex with HK, and HK bridges these zymogens to the activating polyanion. Once generated, FXIIa cleaves PK into kallikrein, which feedbacks to activate additional FXII. Therefore, kallikrein generation provides a second positive feedback mechanism to amplify FXIIa generation. Following this, FXIIa activates FXI to FXIa (Colman and Schmaier, 1997). Thrombin activation of FXI is an important feedback step that is dependent on polyanions such as polyP. Thus, this feed back step provides an alternative pathway, whereby FXI can be activated in a manner that is independent of FXII (Choi *et al.*, 2011). FXIa subsequently activates FIX to FIXa, which together with its cofactor FVIIIa, forms the intrinsic tenase complex (FIXa/FVIIIa) (Monroe and Hoffman, 2006).

The term “contact” system/pathway generally refers to FXII, HK and PK, and this designation came about because these zymogens required “contact” with polyanions for activation. The contact system is also known as the plasma kallikrein-kinin system. In contrast, the term intrinsic pathway is more encompassing and in addition to the contact system, includes FXI, FIX and FVIII (Colman and Schmaier, 1997). This distinction is useful for understanding the relative contributions of the different components of the intrinsic pathway to pathophysiology.

1.6 COMMON PATHWAY OF COAGULATION

Because the intrinsic and extrinsic pathways generate FXa, the subsequent enzymatic complex is part of the common pathway (Monroe and Hoffman, 2006). FXa in the prothrombinase complex activates the substrate, prothrombin to thrombin. The prothrombinase complex is composed of the protease FXa and its cofactor FVa, which are assembled on PS-expressing membranes in the presence of calcium (Mann *et al.*, 1988). The Gla-domains of FXa and prothrombin mediate membrane binding, whereas FVa binds via its lectin-like C domains (Gilbert *et al.*, 2012). When associated with the prothrombinase complex, the catalytic efficiency of FXa is increased by $>10^5$-fold. Thus, under these conditions, FXa efficiently cleaves prothrombin to generate α-thrombin (Mann *et al.*, 1988).

1.7 THROMBIN

Thrombin is the only factor in the coagulation cascade that converts fibrinogen into fibrin (Huntington, 2005). Thrombin is a 37 kDa glycoprotein, composed of A (light) and B (heavy) chains linked by a disulfide bridge. Based on its primary structure, thrombin exhibits a 35-49% sequence identity to the chymotrypsin family of serine proteases and its structure and catalytic mechanism resembles that of the prototype, trypsin (Bode *et al.*, 1989). Both thrombin and trypsin possess a catalytic triad of His^{57}, Asp^{102} and Ser^{195} and both proteases cleave at basic residues (Bode *et al.*, 1989). However, thrombin exhibits stricter substrate specificity than trypsin, owing largely to the surface loops, termed the 60- and γ-insertion loops, that surround the active site cleft and

restrict substrate binding. The 60-loop forms hydrophobic interactions with substrates, whereas the γ-loop forms hydrophilic interactions (Di Cera and Cantwell, 2001).

Two basic regions that flank the active site, termed exosites 1 and 2, provide an additional level of regulation. Exosite interactions are important for the formation of thrombin-substrate complexes and this augments proteolysis (Huntington, 2005). It is becoming increasingly evident that all of the thrombin substrates and cofactors interact with at least one exosite. Exosite 1, which is also known as the fibrinogen recognition exosite, also is important for thrombin's interactions with FV, FVIII and PARs on platelets (Huntington, 2005). In addition to interacting with procoagulant molecules, exosite 1 of thrombin also mediates its interaction with anticoagulant factors such as TM and heparin cofactor II (HCII) (Fredenburgh *et al.*, 2001, Huntington, 2005). Of the two exosites, exosite 2 is more basic and was originally identified as the heparin binding site. Furthermore, thrombin is inhibited and cleared from the circulation by the serpins AT and HCII in a manner that is dependent on glycosaminoglycans (GAGs) such as heparin (Fredenburgh *et al.*, 2001, Huntington, 2005). Therefore, the capacity of the exosites to bind both pro- and anti-coagulant substrates provides a dynamic molecular switch that directs thrombin activity and regulates coagulation.

1.8 FIBRIN(OGEN)

Fibrinogen is a 340 kDa dimeric glycoprotein composed of two pairs of Aα-, Bβ- and γ-chains, connected by numerous disulfide bonds. The NH_2-termini of the six chains form the central E domain, which are connected by the coiled-coil regions to the peripheral D-domains formed by the COOH-termini (Mosesson, 2005) (Fig. 1.2). When

thrombin catalyzes the conversion of fibrinogen to fibrin, exosite 1 binds to NH_2-termini of the Aα- and Bβ-chains in the central E-domain of fibrin(ogen), and this orients the substrate and brings the fibrinopeptide (Fp) cleavage sequences in close proximity to the active site of thrombin (Mosesson, 2005). Thrombin cleaves the $A\alpha Arg^{16}$-Gly^{17} and $B\beta Arg^{14}$-Gly^{15} bonds, releasing Fp A and B, respectively (Binnie and Lord, 1993). After cleavage of FpA, fibrin polymerization occurs spontaneously when the newly exposed NH_2-termini on one fibrin monomer bind to pre-existing complementary sites on the D-domains of adjacent fibrin monomers to form protofibrils. This is followed by a second step, whereby FpB is released and promotes lateral assembly of the protofibrils (Mosesson, 2005). Formation of desAA-fibrin facilitates FpB release by either: (a) rendering the $B\beta Arg^{14}$-Gly^{15} bond more susceptible to cleavage, or (b) positioning FpB in close proximity to thrombin's active site (Binnie and Lord, 1993). The assembly of protofibrils results in formation of long, branched fibers, which creates a fibrin network. Thrombin activates FXIIIa in a calcium-dependent manner. The stability of the fibrin clot is enhanced when FXIIIa, a transglutaminase, covalently cross-links the α- and γ-chains of adjacent fibrin monomers, which increases the mechanical strength of the clots and renders them more resistant to lysis (Standeven *et al.*, 2007).

Figure 1.2 Fibrinogen structure. Fibrinogen Aα-, Bβ- and γ-chains are labeled accordingly. The amino acid residues of the γ_A- and γ'-chain sequences are shown below. tThe 20-residue extension of the γ'-chain that serves as the thrombin binding site (exosite 2) is indicated.

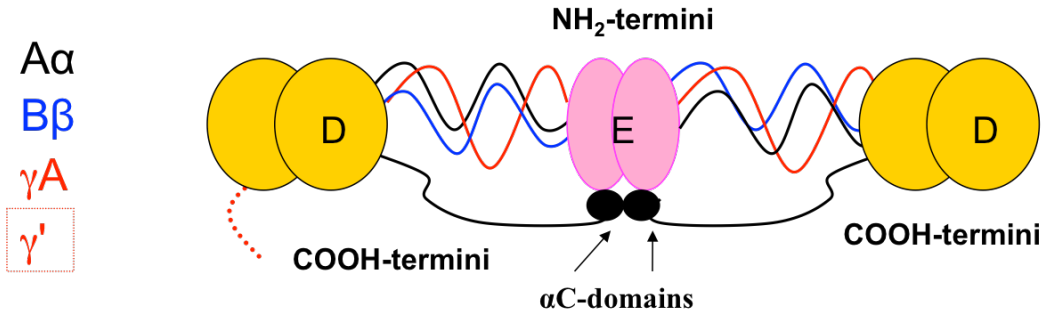

γ_A-chain (residues 404-411):

NH_3-**G-A-K-Q**-A-G-D-V-COOH

γ'-chain (residues 404-427):

IIa exosite 2 binding site

NH_3-**G-A-K-Q**-V-R-P-E-H-P-A-E-T-E-Y(SO_3)-D-S-L-Y(SO_3)-P-E-D-D-L-COOH

1.8.1 γ'–Fibrinogen

About 8-15% of circulating fibrinogen is heterodimeric, containing one γ_A-chain and one variant γ'-chain and is designated γ_A/γ'-fibrinogen (Chung and Davie, 1984, Fornace, Jr. *et al.*, 1984). In contrast, γ'/γ'-fibrinogen makes up less than 0.5% of total fibrinogen (Uitte de Willige *et al.*, 2009). As a result of alternative processing of the γ-chain mRNA transcript, two isoforms of the γ-chain are generated. In the γ'-chain, the COOH-terminal AGDV sequence is replaced by a 20 residue segment (Chung and Davie, 1984, Fornace, Jr. *et al.*, 1984). The γ'-chain extension is anionic due to the presence of 7 Asp/Glu and 2 sulfated-Tyr residues (Fig. 1.2) (Lovely *et al.*, 2003). The presence of the γ'-chain modulates thrombin activity, influences clot structure and alters the capacity of fibrin to interact with platelets (Uitte de Willige *et al.*, 2009).

1.8.2 The γ'–chain modulates the activity of fibrin-bound thrombin

Whereas exosite 1 of thrombin binds to the NH_2-termini of the α- and β-chains of the E-region, exosite 2 of thrombin binds to the γ'-chain (Meh *et al.*, 1996, Pospisil *et al.*, 2003). Consequently, thrombin binds to γ_A/γ_A-fibrin(ogen) via a single site with a K_d value of 2 to 4 μM. In contrast, thrombin binds to γ_A/γ'-fibrin(ogen) in a bivalent manner, whereby one thrombin molecule binds to the central E region of one fibrin molecule and the γ'-chain of a second molecule. Consequently, thrombin binds to γ_A/γ'- fibrin(ogen) with a K_d value of 80 to 200 nM, which is ~20-fold higher affinity than its interaction with γ_A/γ_A-fibrin (Meh *et al.*, 1996, Pospisil *et al.*, 2003).

The capacity of thrombin to bind the γ'-region modulates the activity of the protease when it is bound to fibrin. Several studies were undertaken to elucidate the

physiological importance of thrombin-γ'-region interaction. Fibrin-bound thrombin retains catalytic activity and is protected from inhibition by ATIII and HCII (Fredenburgh *et al.*, 2008, Weitz *et al.*, 1990). However, fibrin sequesters thrombin and thus, its proteolytic activity and capacity to propagate coagulation is significantly reduced compared with unbound thrombin (Mosesson, 2007). Consequently, the fibrin clot is referred to as antithrombin I (Mosesson, 2007). Since thrombin forms a higher affinity interaction with γ_A/γ'-than γ_A/γ_A-fibrin clots, γ_A/γ'-fibrin may sequester thrombin to a greater extent than γ_A/γ_A-fibrin. Thus, γ_A/γ'-fibrin clots may be less thrombogenic than γ_A/γ_A-fibrin clots (Walton *et al.*, 2014).

However, there is an abundance of active thrombin in the thrombi of patients removed after autopsy or surgery (Mutch *et al.*, 2001). Thus, the fibrin clot also serves as a reservoir of active thrombin that promotes clot expansion by locally activating platelets and FXI, FVIII and FV (Mutch *et al.*, 2001, Weitz *et al.*, 1990). Normally, ATIII, in conjunction with heparin, efficiently inhibits thrombin and facilitates its clearance from the blood (Becker *et al.*, 1999, Fredenburgh *et al.*, 2001, Griffith, 1982). However, when thrombin is bound to the fibrin clot, it is protected from inhibition (Weitz *et al.*, 1990). This phenomenon is due to the fact that exosite 1 of thrombin interacts with fibrin, whereas exosite 2 binds heparin, thereby forming a ternary complex of heparin-thrombin-fibrin that sequesters heparin from AT (Becker *et al.*, 1999, Fredenburgh *et al.*, 2008). Moreover, bivalent binding of thrombin to γ_A/γ'-fibrin confers added protection, since the heparin-catalyzed rate of thrombin inhibition by AT is 5-fold slower with γ_A/γ'-fibrin than with γ_A/γ_A-fibrin. These results suggest that γ_A/γ'-fibrin may serve as a reservoir for active

thrombin, rendering these clots more thrombogenic (Becker *et al.*, 1999, Fredenburgh *et al.*, 2008). Thus, there are competing hypotheses as to the role of thrombin bound to γ_A/γ'-fibrin clots and this is addressed in research objective #2.

1.8.3 The γ'–chain modulates fibrin clot formation and structure

There is evidence that the γ'-chain itself, irrespective of its interactions with thrombin, can directly impede protofibril formation and modulate fibrin clot structure (Allan *et al.*, 2012). Support for this concept comes from structural comparisons between γ_A/γ_A- and γ_A/γ'-fibrin(ogen) (Cooper *et al.*, 2003, Siebenlist *et al.*, 2005). Clots containing γ_A/γ'-fibrin have thinner fibril strands that are organized into a denser fibrin network than those in γ_A/γ_A-fibrin clots. Furthermore, γ_A/γ'-fibrin polymerizes at a slower rate than γ_A/γ_A-fibrin because thrombin-mediated FpB release from γ_A/γ'-fibrinogen is delayed (Cooper *et al.*, 2003, Siebenlist *et al.*, 2005).

Although controversial, there is some evidence that the γ'-region is also a FXIII binding site (Falls and Farrell, 1997, Gersh and Lord, 2006, Siebenlist *et al.*, 1996). Thus, γ_A/γ'-rich fibrin clots may contain elevated levels of FXIII, which has been shown to influence fibrin clot structure and lysis (Falls and Farrell, 1997, Siebenlist *et al.*, 2005). Epidemiological studies in a cohort of South Africans confirmed that elevated levels of γ_A/γ'-fibrinogen in plasma results in delayed clot lysis times (Pieters *et al.*, 2013). Collectively, these results suggest that there are at least three mechanisms by which γ_A/γ'-fibrin(ogen) regulates clot formation by: (i) modulating the prothrombotic activity of clot-bound thrombin, (ii) altering the fibrin polymerization and (iii) interacting with FXIII.

1.8.4 Impact of γ'-chain on fibrin(ogen) binding to platelets

Platelet aggregation is crucial for formation of the platelet plug and is mediated by adhesive proteins such as fibrinogen. The COOH terminus of the γ_A-chain of fibrinogen interacts with $\alpha_{IIb}\beta_3$ integrin to facilitate platelet aggregation (Uitte de Willige *et al.*, 2009, Wencel-Drake *et al.*, 1996). Because of the modified structure, the γ'-chain lacks the $\alpha_{IIb}\beta_3$ binding site, which attenuates platelet activation and aggregation. However, the high affinity interaction between thrombin and the γ'-chain inhibits the capacity of fibrinogen to interact with glycoprotein receptor (GP) Ibα and thrombin cleavage of PARs on platelets (Lancellotti *et al.*, 2008). Thrombin binds GPIbα and this facilitates thrombin cleavage of PARs 1 and 4 on platelets. Thrombin's interaction with GPIbα is mediated by exosite 2 (De Cristofaro *et al.*, 2001, Li *et al.*, 2001), which is the same region of thrombin that interacts with the γ'-chain. Thus, γ_A/γ'-fibrinogen competes with GPIbα for thrombin binding and hinders key catalytic events that are vital for platelet signaling and activation (Lancellotti *et al.*, 2008).

1.8.5 Role of γ_A/γ'-fibrinogen in pathophysiology

Although the γ'-chain modulates fibrin clot formation and the capacity of thrombin to promote fibrin clot expansion, little is known about the physiological role of γ_A/γ'-fibrin(ogen) in thrombosis. To address this gap in knowledge, several investigators attempted to assess the role of γ_A/γ'-fibrin(ogen) in murine models of thrombosis (Mosesson *et al.*, 2009, Walton *et al.*, 2014). The murine γ'-chain ends at Tyr^{417}, which is truncated compared with the human counterpart, and possesses half as many anionic residues as the human γ'-chain. Therefore, thrombin does not bind to the murine γ'-region

(Mosesson *et al.*, 2009). Transgenic mice were created in which the murine γ'-chain was replaced with the human counterpart, which resulted in fibrinogen isoforms with chimeric human γ'-chains that could bind thrombin. In a femoral vein thrombosis model, no difference in thrombus weight was observed between wild type and heterozygous mice containing γ_A/γ'-fibrinogen (Mosesson *et al.*, 2009). FV Leiden is a variant of FV that is resistant to proteolytic inactivation by activated PC and is therefore a risk factor for thrombosis as evidenced by the fact that FV Leiden$^{+/-}$ mice exhibit a prothrombotic phenotype. However, when mice are heterozygous for both the chimeric γ_A/γ'-fibrinogen and FV Leiden, this reduced the thrombus size in a venous thrombosis model, thereby suggesting that the γ_A/γ'-fibrinogen exhibits antithrombotic properties. This study suggests that the human γ_A/γ'-fibrinogen is a thrombosis risk modifier (Mosesson *et al.*, 2009).

However, the role of γ_A/γ'-fibrinogen in pathophysiology is still not clear. Recently, murine studies demonstrated that infusion of γ_A/γ_A-fibrinogen, but not γ_A/γ'-fibrinogen shortened the vessel occlusion time in a carotid artery thrombosis model. In support of this, γ_A/γ'-fibrinogen infusion led to lower levels of thrombin-AT complexes (Walton *et al.*, 2014). Thus, in this murine study, elevated levels of γ_A/γ_A-fibrinogen, but not γ_A/γ'-fibrinogen, promote arterial thrombosis. These observations suggest that γ_A/γ'-fibrinogen exhibits antithrombotic properties (Walton *et al.*, 2014).

Conflicting correlations have been drawn between human plasma concentrations of γ_A/γ'-fibrinogen and a predisposition for thrombosis (Uitte de Willige *et al.*, 2005, Walton *et al.*, 2014). In patients with coronary artery disease, the ratio of γ_A/γ'-fibrinogen

to γ_A/γ_A-fibrinogen is higher than normal, but in patients with DVT, the ratio of γ_A/γ'-fibrinogen to γ_A/γ_A-fibrinogen is lower (Lovely *et al.*, 2002, Uitte de Willige *et al.*, 2005). The differences between the γ_A/γ'-fibrinogen ratio may reflect the differences between the pathologies of arterial and venous thrombosis (Mackman, 2008). Because there is emerging evidence that γ_A/γ'-fibrinogen plays a role in thrombosis, it is important to understand how γ'-chain binding proteins modulate fibrin clot formation (Research objective #1).

1.9 BATROXOBIN

Batroxobin is a 33 kDa serine protease isolated from *Bothrops atrox moojeni* snake venom that, like thrombin, converts fibrinogen into fibrin. However, unlike thrombin, batroxobin generates fibrin by solely releasing FpA from the Aα-chain of fibrinogen (You *et al.*, 2004). Whereas thrombin has numerous substrates, fibrinogen is the only known substrate for batroxobin. Furthermore, unlike thrombin, batroxobin is not efficiently inhibited by AT or HCII, but it is inhibited by α2-macroglobulin (Aronson, 1976). Because of these properties, batroxobin is routinely used in biochemical studies to elucidate the mechanisms of Fp release and to characterize thrombin-fibrin(ogen) interactions. Likewise, batroxobin is also used in clinical laboratories to determine whether heparin contamination or abnormal fibrinogen contributes to prolonged thrombin clotting times (Braud *et al.*, 2000). Due to its capacity to lower circulating fibrinogen levels, batroxobin is being investigated for preventing and treating thrombosis (Liu *et al.*, 2004, Liu *et al.*, 2011). Although it is well known that batroxobin induces defibrinogenation, little is known about how it interacts with the isoforms of fibrin(ogen)

and whether, like thrombin, fibrin-bound batroxobin can promote clot expansion. Likewise, it is unclear if batroxobin possesses regulatory regions that are analogous to the exosites of thrombin and whether these interactions contribute to its selectivity in releasing FpA during catalysis. Investigation of these distinctions could elucidate critical structural and functional information about the action of thrombin and the unique specificity of batroxobin (Research objective #2).

1.10 ROLES OF THE EXTRINSIC AND INTRINSIC PATHWAYS IN HEMOSTASIS AND THROMBOSIS

Studies with transgenic mice deficient in TF and FVIIa almost 20 years ago demonstrated that the extrinsic pathway is indispensible for hemostasis (Bugge *et al.*, 1996, Rosen *et al.*, 1997). The prevailing thought in coagulation research was that the mechanisms leading to thrombin generation under pathologic conditions are similar to those involved in normal hemostasis. Therefore, the extrinsic pathway was also considered to be important in thrombosis. In contrast, humans deficient in FXII, the activator of the intrinsic pathway do not exhibit a bleeding diathesis (Renne *et al.*, 2005). Thus, the prevailing paradigm was that the extrinsic pathway, but not the intrinsic pathway, plays a primary role in the pathogenesis of thrombosis. The following section will discuss the relative contribution of the extrinsic and intrinsic (contact) pathways to hemostasis and thrombosis.

1.10.1 Evidence for involvement of the extrinsic pathway in hemostasis and thrombosis

1.10.1.1 ***Hemostasis-*** Studies in murine models have shown that the TF/FVIIa complex is essential for normal hemostasis. Mice deficient in TF or FVII die in utero or during the perinatal period because of severe hemorrhage (Bugge *et al.*, 1996, Rosen *et al.*, 1997). However, mice expressing low levels or <1% of TF or FVII live to adulthood, although they develop cardiac fibrosis and ventricular dysfunction (Pawlinski *et al.*, 2002). Cardiac fibrosis in these mice appears to be the result of bleeding of the cardiac vessels (Pawlinski *et al.*, 2002). The importance of the extrinsic pathway in coagulation is highlighted by observations that in humans: (a) congenital TF deficiency has not been reported, likely because TF is imperative for survival and (b) severe FVII deficiency (< 2% of normal levels) is rare (affecting 1 in 500, 000) and results in a bleeding disorder (Mackman, 2009, Mariani *et al.*, 2006). Therefore, these observations demonstrate that the extrinsic pathway is indispensible for hemostasis.

1.10.1.2 ***Thrombosis-*** There is also ample evidence that the extrinsic pathway plays a role in thrombosis (Mackman *et al.*, 2007, Zhou *et al.*, 2009). Atherosclerotic plaques are hypothesized to be a reservoir of TF, which is expressed on macrophage-derived foam cells and subendothelial smooth muscle cells. Upon plaque rupture, high levels of TF are exposed to the blood and this triggers thrombosis, which can lead to myocardial infarction (Mackman *et al.*, 2007, Zhou *et al.*, 2009). Furthermore, there is evidence that the extrinsic pathway also contributes to coagulopathy associated with sepsis and cancer. First, inhibition of TF/FVIIa activity reduces coagulation observed in an animal model of sepsis (Taylor, Jr. *et al.*, 1991). Second, patients with pancreatic cancer have higher levels of TF-bearing microparticles, which potentiate thrombin generation and are believed to

contribute to thromboembolic events (Tesselaar *et al.*, 2007). Because of these observations, it is widely accepted that the extrinsic pathway contributes to both hemostasis and thrombosis (Mackman *et al.*, 2007).

1.10.2 Evidence for involvement of the intrinsic (contact) pathway in hemostasis and thrombosis

1.10.2.1 ***Hemostasis*****-** When plasma from FXII-, PK- or HK-deficient individuals is subjected to *in vitro* clotting assays, the PT is normal, while the aPTT is prolonged, confirming a clotting defect in the intrinsic pathway. However, hereditary deficiency of FXII, PK or HK does not result in a bleeding phenotype. Therefore, the contact system proteins are dispensable for hemostasis (Colman and Schmaier, 1997, Gailani and Renne, 2007). However, intrinsic tenase (FIXa/FVIIIa), which is activated downstream of the contact system, is pivotal in the amplification phase of coagulation. Thus, FVIII- or FIX-deficiency leads to hemophilia A or B, respectively; and these individuals exhibit spontaneous bleeding (Monroe *et al.*, 2002). In patients with hemophilia A or B, the TF/FVIIa complex is intact and, should therefore be able to promote thrombin generation; yet, life-threatening bleeding still occurs (Zimmerman and Valentino, 2013). This suggests that the extrinsic and intrinsic pathways are not redundant and serve distinct roles in coagulation. Moreover, in FXI-deficient individuals, a bleeding diathesis is only observed with trauma or surgery, thereby suggesting that FXI plays a role, albeit a minor one, in hemostasis (Gailani and Renne, 2007). Consequently, the contact system proteins are dispensible, whereas, downstream components of the intrinsic pathway are vital for

maintaining hemostasis. If the contact system is not important in hemostasis, does it have a role in thrombosis?

1.10.2.2 ***Thrombosis-*** In the last 10 years, several notable animal studies focusing on contact system proteins and novel physiological activators have shed new light on the role of the intrinsic pathway in thrombosis. First, mice deficient in FXII, PK or HK exhibit impaired arterial thrombosis, without associated bleeding (Kleinschnitz *et al.*, 2006, Merkulov *et al.*, 2008, Renne *et al.*, 2005, Revenko *et al.*, 2011). Likewise, FXII deficient mice are protected from ischemic stroke (Kleinschnitz *et al.*, 2006). In addition, administration of small molecule inhibitors, termed antisense oligonucleotides (ASOs), that attenuate the expression of FXII or PK have a thromboprotective effect (Revenko *et al.*, 2011). ASOs are short nucleotide sequences that hybridize to complementary regions on a target mRNA. ASOs attenuate gene expression by interfering with the translation of mRNA into protein (Dias and Stein, 2002). In support of the FXII murine studies, an antibody directed against the FXIIa active site (3F7) protected rabbits from thrombosis in an extracorporeal bypass system, while having no impact on bleeding during injury (Larsson *et al.*, 2014).

In addition to the contact system proteins, studies in rodents, rabbits and primates suggest that FXI also contributes to thrombogenesis. Desmolaris, an inhibitor from vampire bat saliva, attenuates thrombosis after carotid artery injury in mice and only mild bleeding is observed with higher doses of inhibitor; findings that confirm that FXI has a minor role in hemostasis (Ma *et al.*, 2013). Similarly, rabbits treated with FXI ASOs are protected from catheter-induced thrombosis (Yau *et al.*, 2014). In a shunt model of

thrombosis, FXI ASOs produce an antithrombotic effect in baboons, without increasing the risk of bleeding (Crosby *et al.*, 2013).

With a minimal role in hemostasis and increasing evidence that the contact pathway proteins and FXI contribute to thrombogenesis, FXII and FXI have emerged as promising targets for the development of safer anticoagulants (Muller *et al.*, 2009).

1.11 FXII STRUCTURE, ACTIVATION AND REGULATION

Because of its therapeutic potential, it is critical to understand the structure, function, and regulation of FXII, which are discussed below.

1.11.1 FXII Structure

FXII or Hageman factor is a single-chain, 80 kDa glycoprotein that is synthesized in the liver. Structurally, FXII is a modular protein containing 6 domains that are organized into a heavy and a light chain region (Fig. 3). The heavy chain contains: (a) two epidermal growth factor domains that regulate cell growth and proliferation; (b) a kringle domain, and (c) two fibronectin-like domains termed type I and type II (Citarella *et al.*, 2000). The type II domain is the polyanion binding site and is presumed to be important in FXII activation. The light chain contains the catalytic domain with the prototypical serine protease catalytic triad consisting of Asp^{442} and His^{393} and Ser^{554} (Miyata *et al.*, 1989). Kallikrein and FXIIa cleave FXII at the Arg^{353}-Val^{354} bond, thereby generating the protease, α-FXIIa (Fig. 1.3). Subsequent cleavage of α-FXIIa by kallikrein generates β-FXIIa, which is composed of the light chain containing the catalytic region. Consequently, β-FXIIa loses its capacity to bind polyanions and to activate FXI (Brill *et al.*, 2012, Cool *et al.*, 1985) (Fig. 1.3). Thus, the capacity of kallikrein to cleave FXIIa at

multiple sites is important for converting the protease into different forms, which direct its activity. Whereas α-FXIIa triggers coagulation, β-FXIIa is proposed to have important roles in inflammation (van den Herik *et al.*, 2011).

Figure 1.3 FXII structure, activation and regulation. FXII is comprised of a heavy chain and light chain. Kallikrein or FXIIa can cleave FXII at Arg^{353}-Val^{354} thereby generating α-FXIIa. A second cleavage of α-FXIIa outside of the disulfide bond forms β-FXIIa, which lacks the anionic surface bining motifs. FXIIa activity is inhibited by HRG, CTI or the serpin, C1-Inh.

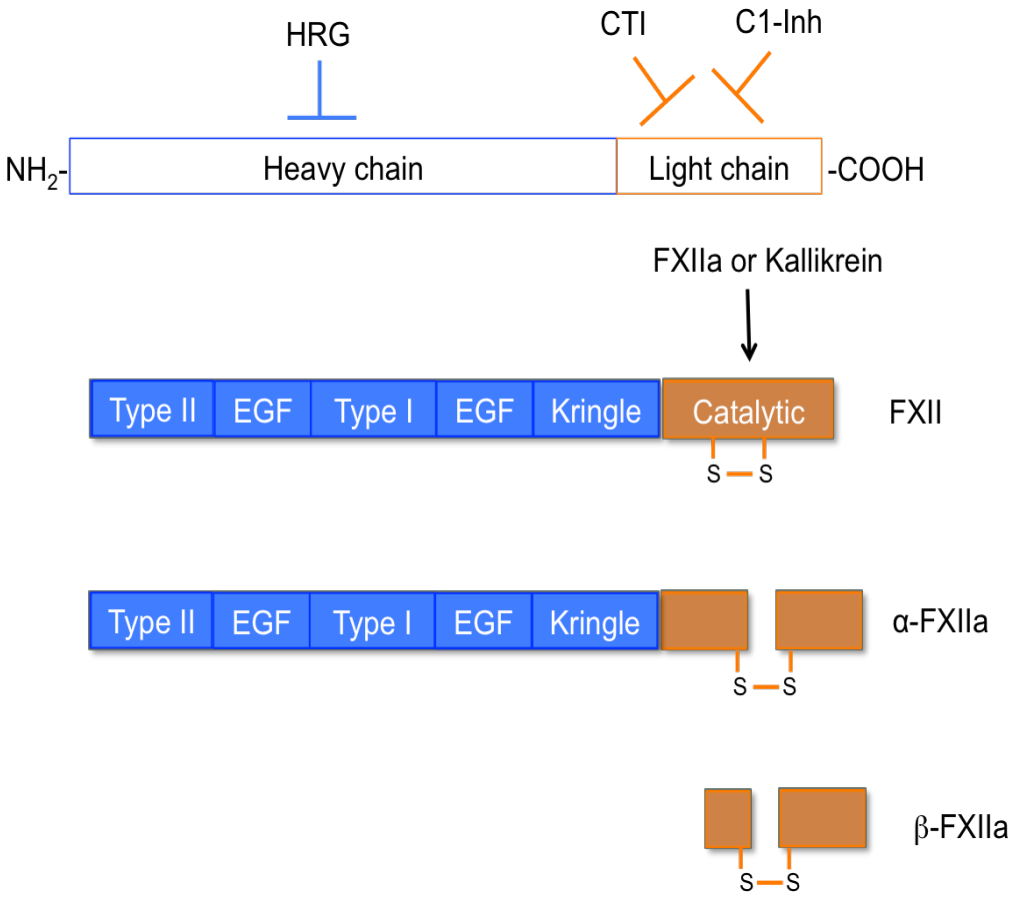

1.11.2 FXII activation

The intrinsic pathway is initiated when FXII is activated to FXIIa. The precise mechanism promoting FXIIa generation is unclear, although there are two prevailing theories. FXIIa can be generated in the absence of a surface and it is hypothesized that this contributes to the small reservoir of FXIIa that is thought to exist in plasma. The origin of this FXIIa is unclear, but it may reflect basal activation of coagulation. In contrast, solid-phase activation refers to the capacity of polyanions to stimulate FXIIa generation (Schmaier *et al.*, 1987). Although the precise mechanism is not known, it is hypothesized that the binding of FXII to polyanions induces a conformational change in the zymogen, which primes it for autocatalysis (Rojkjaer and Schousboe, 1997, Samuel *et al.*, 1992). This is likely a concerted process that is augmented by both polyanion and zinc binding. The heavy chain of FXII interacts with polyanions and the histidine residues bind zinc, with the latter interaction augmenting the rate of FXII activation by 10-fold (Bernardo *et al.*, 1993b, Bernardo *et al.*, 1993a). When FXII is incubated with polyanions, FXIIa is generated and this is thought to occur via an autoactivation process. However, it is not clear whether autoactivation occurs via: (a) activation of FXII on polyanions by basal amounts of FXIIa; or (b) induction of a conformational change in FXII by its interaction with polyanions, which partially activates the catalytic domain of the zymogen to "self" cleave (Schmaier *et al.*, 1987). Because of the ambiguity, this report will refer to the term FXII autoactivation as the process whereby FXIIa activates its own zymogen, regardless of the mechanism involved.

1.11.3 Inhibitors of FXIIa

FXIIa is inhibited by C1 inhibitor (C1-Inh), α2-antiplasmin, α2-macroglobulin and AT, which facilitate FXIIa clearance from the circulation. However, studies in purified and plasma systems demonstrate that C1-Inh accounts for >90% of FXIIa inhibition (de Agostini *et al.*, 1984). C1-Inh is a 105 kDa serine protease inhibitor (serpin) that is present in plasma at 2.3 μM (Caliezi *et al.*, 2000). C1-Inh forms an irreversible 1:1 covalent complex with the active site of FXIIa via the prototypical serpin mechanism, and this renders FXIIa inactive (de Agostini *et al.*, 1984). The rate at which C1-Inh inhibits FXIIa is relatively slow (k_{app} of $<10^5$ $M^{-1}min^{-1}$), which is almost two orders of magnitude slower than other serpin regulated steps in coagulation. The reasons why this inhibition step is so slow are not fully understood, although the high plasma levels of C1-Inh may off-set the slow rate of inhibition (Sulikowski *et al.*, 2002).

Corn trypsin inhibitor (CTI) is a 12 kDa protein that is present in corn kernels and is commonly used in coagulation studies (Korneeva *et al.*, 2014, Swartz *et al.*, 1977). Although CTI inhibits trypsin, in the coagulation cascade, it specifically attenuates the activity of FXIIa. CTI binds to the active site of FXIIa in a 1:1 ratio and reversibly inhibits FXIIa activity via the "standard mechanism of inhibition" (Behnke et al., 1998). In this mechanism, FXIIa interacts with CTI via a substrate-like mechanism. CTI binds to the active site of FXIIa and the protease cleaves the Arg^{34}-Leu^{35} bond, which resembles the scissile bond present on other FXIIa substrates. FXIIa both cleaves and ligates the scissile bond in the reactive loop of CTI and this effectively blocks the active site of FXIIa, thereby, preventing it from cleaving its macromolecular substrates (Behnke et al.,

1998; Korneeva et al., 2014). Consequently, addition of CTI to plasma prolongs the aPTT, but not the PT (Korneeva *et al.*, 2014, Swartz *et al.*, 1977).

1.11.4 Novel inhibitors of FXIIa

Recently, our group identified an additional FXIIa inhibitor. Histidine rich glycoprotein (HRG) binds FXIIa, but not FXII, with high affinity (K_d value of 21 nM) and this binding is enhanced 10^3-fold by zinc (MacQuarrie *et al.*, 2011). HRG binds to the heavy chain region on FXIIa and inhibits its capacity to activate FXII and FXI. HRG-FXIIa complexes are also detected in contact activated plasma. HRG specifically modulates the intrinsic pathway, since the aPTT is shortened in HRG-deficient plasma compared with control plasma, whereas the PT is unaffected. Because of its relative abundance, potency and high affinity for FXIIa, HRG is more likely to be the physiological inhibitor of FXIIa than C1-Inh (MacQuarrie *et al.*, 2011). Thus, HRG is a novel regulator of FXIIa activity. In support of this concept, a genome wide association study in a Scottish cohort demonstrated a correlation between polymorphisms in the FXII and HRG genes and variations in the aPTT (Houlihan *et al.*, 2010).

1.11.5 Mechanisms of HRG inhibition of FXIIa

Unlike C1-Inh and CTI, which bind to and inhibit the active site of FXIIa, the HRG binding site is likely located outside of the catalytic domain (MacQuarrie *et al.*, 2011). Whereas HRG binds α-FXIIa, it does not bind β-FXIIa, which consists of the catalytic domain. Furthermore, HRG does not impair the capacity of C1-Inh or CTI to inhibit FXIIa, thereby substantiating the observation that HRG binds to the heavy chain of

FXIIa (MacQuarrie *et al.*, 2011). However, it is unclear if HRG binds to an allosteric site on FXIIa and whether this modulates proteolysis.

Characterization of the mechanisms of FXIIa inhibition with nanobodies, a single domain antigen binding fragment from llamas that binds to an allosteric site on α-FXIIa, revealed an unidentified protein in plasma that interfered with binding (de Maat *et al.*, 2013). Furthermore, in the presence of CTI, which is an active-site inhibitor, nanobody binding was attenuated, providing additional evidence for allosteric modulation (de Maat *et al.*, 2013). Thus, these observations suggest that the unidentified plasma protein may be HRG.

1.11.6 Epidemiological studies of FXII and the risk for thrombosis

Animal studies suggest that FXII-deficiency confers a thromboprotective phenotype. However, mixed results have emerged from epidemiological studies assessing the correlation between FXII-deficiency and thrombosis. Studies in a Swiss cohort showed that hereditary deficiency of FXII does not contribute to a thrombophilic condition, which supports the animal studies. However, in a Dutch cohort, elevated FXII levels were associated with a decreased risk of myocardial infarction (van Montfoort and Meijers, 2013). Additional studies have also reported no association between hereditary deficiency of FXII and the risk of thrombosis (Cushman *et al.*, 2009, Girolami *et al.*, 2009). The observation that in most cases FXII deficiency is accompanied by other congenital or acquired prothrombotic risk factors complicates conclusions about the link between FXII and thrombosis (Larsson *et al.*, 2014). Therefore, further studies are needed to validate the role of FXII in thrombosis.

1.12 POLYANIONIC ACTIVATORS OF THE INTRINSIC PATHWAY

FXII activation by nonphysiologic polyanions such as glass, silica and kaolin is well established. Of these agents, the minerals kaolin and celite (silica-rich compounds) are amongst the most potent activators of FXII and are thus, commonly used in aPTT coagulation assays to identify contact system defects (Renne *et al.*, 2012). However, physiological counterparts of these polyanions remained elusive. In the 1980s, it was proposed that during vascular injury, polyanionic components such as GAGs (eg. heparin) and collagen are exposed to the blood and stimulate FXII activation (van der Meijden *et al.*, 2009). However, heparin does not promote FXII autoactivation (Pixley *et al.*, 1991). Moreover, studies of FXII activation with collagen, yielded contradictory results (van der Meijden *et al.*, 2009). Therefore, it was unclear whether potent physiological activators of FXII existed.

The discovery that FXII is crucial for thrombosis led to a renewed search for endogenous activators of the contact system. Recently, it was shown that naturally occurring polymers with a polyphosphate backbone such as inorganic polyphosphate (polyP), DNA and RNA are physiological activators of FXII (Fig. 1.4). Of these activators, the role of polyP in coagulation has been studied more extensively. The roles of polyP, DNA and RNA in contact activation of coagulation are discussed below.

1.12.1 Polyphosphate

PolyP is class of linear polymer of phosphate molecules found in prokaryotic and eukaryotic organisms (Fig. 1.4A). In platelets, polyP is stored in the dense granules and is released upon activation. Microorganisms also produce polyP, which facilitates motility

and host invasion. Whereas platelet-derived polyP polymers consist of 60-100 phosphate units, bacterial-derived polyP is typically >500 phosphate units in length (Morrissey *et al.*, 2012). PolyP has a half-life of 1.5-2 hours in human blood due to endogenous phosphatases (Morrissey *et al.*, 2012). The importance of polyP in clotting is highlighted by several observations: (a) human platelets contain 0.7 nM polyP/10^{11} platelets, therefore blood may contain 1-3 μM of polyP following platelet activation and these levels may increase in the vicinity of a platelet-rich thrombi (Morrissey *et al.*, 2012); (b) patients with Hermansky-Pudlak syndrome have reduced or absent platelet dense granules and exhibit a bleeding diathesis, and supplementation of purified polyP restores the clot times to baseline (Muller *et al.*, 2009); (c) inhibition of polyP synthesis in the dense granules protects mice from thrombosis (Ghosh *et al.*, 2013); (d) infusion of platelet polyP into mice promotes the formation of microthrombi in lungs and this processes is attenuated by phosphatase (Muller *et al.*, 2009); and (e) polyP-binding polymers neutralize polyP activity, and attenuate arterial and venous thrombosis in mice (Smith *et al.*, 2012).

PolyP triggers the contact system by potentiating FXII autoactivation (Muller *et al.*, 2009, Smith *et al.*, 2010). PolyP also binds HK, which localizes PK and FXI to the surface where FXIIa is generated (Muller *et al.*, 2009). PolyP augments PK activation to K and augments thrombin feedback activation of FXI (Choi *et al.*, 2011, Muller *et al.*, 2009). However, polyP appears to exert differential effects on clotting depending on the polymer length. Long polymers, such as those found in microorganisms, are better activators of FXII than the shorter polymers from platelets (Smith *et al.*, 2010).

Moreover, in addition to thrombosis, polyP may modulate hemostasis since mice deficient in inositol hexakisphosphate kinase 1, a key enzyme regulating polyP production in platelets, have prolonged bleeding times (Ghosh *et al.*, 2013).

How important is platelet-derived polyP in contact activation of coagulation? The role of platelet-derived polyP has recently been called into question (Faxalv *et al.*, 2013). First, platelet polyP was shown to only weakly promote autoactivation of FXII. Second, activated platelets do not promote activation of FXII. Third, the initial observation that polyP infusion into mice promotes microthrombosis could not be reproduced in a follow-up study. Most importantly, when platelets were stimulated with PAR activating peptides, they did not release sufficient amounts of polyP to promote thrombosis in mice (Faxalv *et al.*, 2013). Thus, the role of polyP in contact activation remains controversial.

Figure 1.4 Physiological activators of the intrinsic pathway. Hydrogen bonds.

A) polyP

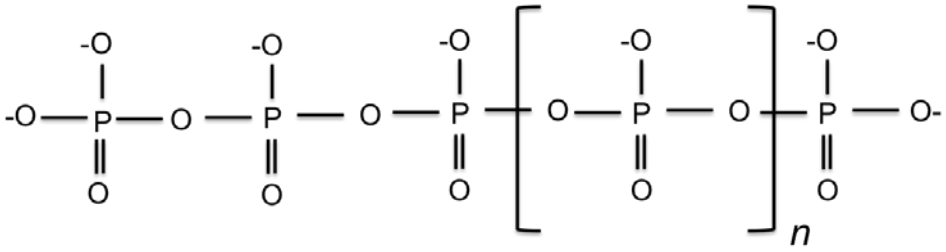

B) RNA

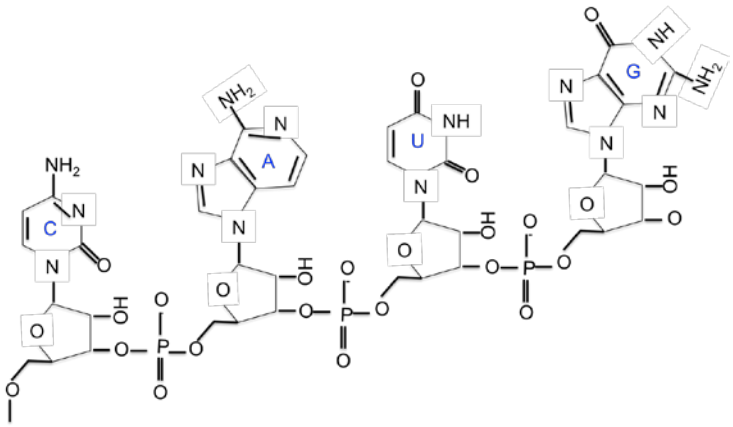

C) DNA

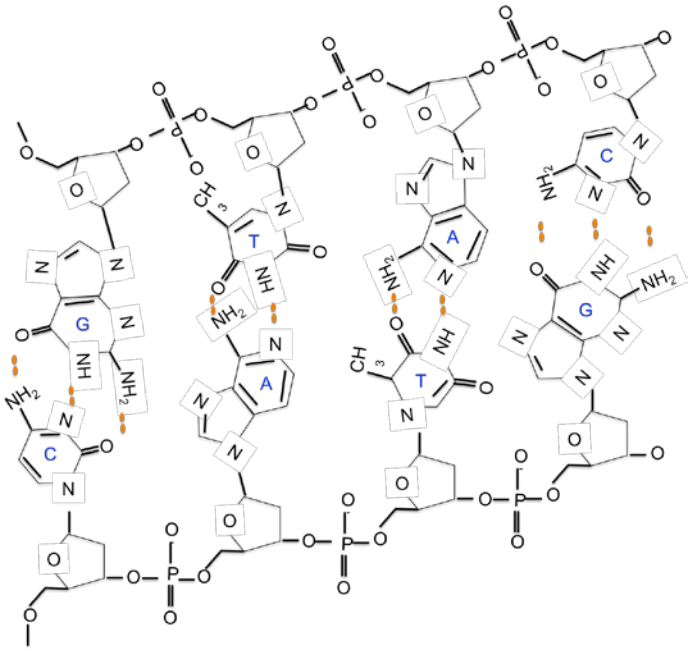

1.12.2 DNA and RNA

DNA and RNA are normally contained within cells, but are expelled from cells that are stimulated, necrotic or dying (Fig. 1.4B-C) (van der Vaart and Pretorius, 2008). The size of the DNA and RNA circulating in the blood depends on various factors such as: (i) the mode of cellular stimulation or injury, (ii) the signaling pathway that is activated in the cells and (iii) the cell type. Because of these varying factors, the size of nucleic acids released into the blood is likely polydispersed (varying from 10^2 to $>10^4$ base pairs) (Fuchs *et al.*, 2010, Rumore and Steinman, 1990, Semeraro *et al.*, 2011, Swystun *et al.*, 2011). Furthermore, circulating DNA and RNA can be associated with proteins, lipids, or vesicles (El Hefnawy *et al.*, 2004, Gormally *et al.*, 2007). Deoxyribonuclease (DNase) and ribonuclease (RNase) are also present in blood and serve to degrade DNA and RNA, respectively. Therefore, circulating DNA and RNA are proposed to have short half-lives, ~5-16 min (Kannemeier *et al.*, 2007, Lo *et al.*, 1999). Several pioneering studies in animals have shed new light on the role of DNA and RNA in thrombosis and they are discussed in the following sections.

1.12.3 Role of DNA in thrombosis

Circulating DNA levels are elevated in rodent and baboon models of DVT (Brill *et al.*, 2012, Fuchs *et al.*, 2010). Stimulated neutrophils release neutrophil extracellular traps (NETs), which are thought to be the main source of plasma DNA in these models (*reviewed in* (Yipp and Kubes, 2013)). When neutrophils are activated with stimulants such as interleukin-8 or gram-negative bacterial cell wall components such as lipopolysaccharides (LPS), a signaling pathway is triggered that leads to disintegration of

the cell membranes and extrusion of web-like structures composed of DNA, histones and various cytoplasmic proteins. NETs are important components of the innate immune system, but recently, they have also been implicated in thrombosis (Yipp and Kubes, 2013).

NETs are prothrombotic because they contain DNA and histones. DNA triggers contact activation of coagulation and histones trigger platelet activation and thrombin generation in a manner that is dependent on toll-like receptors and polyP (Fuchs *et al.*, 2010, Semeraro *et al.*, 2011, Swystun *et al.*, 2011). Therefore, the prevailing thought is that NETs serve as a scaffold for fibrin formation and platelet activation (Fuchs *et al.*, 2010). Animal models of DVT and stroke have provided new insight into the role of NETs in thrombosis. The contention that NETs contribute to DVT is supported by observations that: (a) DNA associated with NETs is detected in rodent and baboon models of DVT, (b) administration of DNase inhibits DVT in mice (Brill *et al.*, 2012), and (c) mice deficient in peptidylarginine deaminase-4, a chromatin remodeling enzyme necessary for NET formation, exhibit attenuated thrombosis (Martinod *et al.*, 2013). Moreover, there is an increase in circulating levels of DNA in murine models of stroke, and addition of DNase improved the outcomes in these animals (De Meyer *et al.*, 2012). Therefore, pathological neutrophil activation likely plays a role in thrombosis and targeting DNA may prove beneficial in preventing DVT.

1.12.4 Role of RNA in thrombosis

While not investigated in the DVT models, the role of RNA in models of arterial thrombosis has been more thoroughly examined. $FeCl_3$ is arguably the most widely used

agent to initiate thrombosis in rodent models, and it is amenable to studying coagulation in both arterial and venous systems (Diaz *et al.*, 2012, Westrick *et al.*, 2007). Typically, a filter paper soaked in $FeCl_3$ is applied to the exterior surface of a vessel, which initiates thrombosis (Owens, III *et al.*, 2011). Although this method is commonly used, little is known about the mechanisms that promote thrombosis in this model. Observations that both $FXII^{-/-}$ and $FXI^{-/-}$ mice are protected from $FeCl_3$-induced vascular injury, suggest that the intrinsic pathway contributes to thrombogenesis (Renne *et al.*, 2005, Wang *et al.*, 2005, Wang *et al.*, 2006). $FeCl_3$ triggers clotting in a RNA-dependent manner in murine models because administration of RNase attenuates thrombosis (Kannemeier *et al.*, 2007). In addition, RNase protects rats from $FeCl_3$-induced thrombosis of the superior sagittalis sinus in the brain (Fischer *et al.*, 2007). RNA, therefore, triggers thrombosis in the $FeCl_3$-model. However, the mechanisms contributing to $FeCl_3$-induced thrombosis are still unclear and thus, this is an important question that will be addressed in Research Objective #4.

1.12.5 Circulating DNA and RNA as prognostic markers of thrombosis

The importance of nucleic acids in coagulation is highlighted by the following observations: (a) nucleic acid levels are relatively low in normal individuals (Tamkovich *et al.*, 2006); (b) plasma DNA and nucleosome (DNA bound to histones) levels are elevated in patients with severe coronary artery disease (Borissoff *et al.*, 2013) and thrombotic microangiopathies (Fuchs *et al.*, 2012); and (c) DNA and RNA levels are elevated in patients with sepsis and cancer, where thrombotic complications are common (Dwivedi *et al.*, 2012, Preissner, 2007).

1.12.6 Mechanisms of nucleic acid-mediated activation of the intrinsic pathway

DNA and RNA promote contact activation in plasma, but compared with polyP, less is known about how they promote FXII and FXI activation. This gap in knowledge is partly due to the assumption that their mechanism of action is similar to polyP. DNA and RNA promote clotting in plasma and whole blood (Kannemeier *et al.*, 2007, Swystun *et al.*, 2011). Characterization of the mechanism by which DNA and RNA trigger clotting reveals that nucleic acids promote clotting in a manner that is dependent on FXII, PK and FXI (Kannemeier *et al.*, 2007, Swystun *et al.*, 2011). Nucleic acids bind FXII and HK (Gansler *et al.*, 2012, Kannemeier *et al.*, 2007). However, in the absence of added factors, DNA and RNA alone are poor activators of FXII. Optimal FXIIa generation is only observed in the presence of PK and HK, suggesting that reciprocal activation by the kallikrein-kinin system potentiates this reaction (Kannemeier *et al.*, 2007). In support of this concept, it is observed that RNA acts as a template to promote PK activation in an HK-dependent manner. In contrast, polyP can promote FXII activation in a PK- and HK-independent manner (Muller *et al.*, 2009). As observed with polyP, nucleic acids are also cofactors that augment feedback activation of FXI by thrombin. Investigations into the requirements for clotting demonstrate that only RNA molecules with a minimum length of 50 nucleotides potentiate clotting reactions (Kannemeier *et al.*, 2007). Furthermore, nucleic acids with secondary structures such as a hairpin loop are more potent triggers of contact activation than their single-stranded or linear counterparts (Gansler *et al.*, 2012). Therefore, DNA and RNA are important activators of the intrinsic pathway. However,

little is known about how their activity is regulated, so as to prevent uncontrolled clotting. This gap in knowledge is addressed in Research Objective #3.

1.12.7 Role of nucleases in regulating nucleic acid-mediated activation of coagulation

In rodent studies, administration of RNase A or DNase I dampens the procoagulant activity of RNA and DNA, respectively (Brill *et al.*, 2012, Fischer *et al.*, 2007, Kannemeier *et al.*, 2007). Thus, endogenous nucleases are hypothesized to be the counterpart that neutralizes the procoagulant activity of nucleic acids. Nucleases are generally thought of as digestive enzymes, but they are also expressed in non-digestive tissues such as the kidneys and liver (Nadano *et al.*, 1993). However, the biological roles of nucleases have not been fully elucidated (Nadano *et al.*, 1993). When stimulated, some cells release nucleases, but the biological relevance of this phenomenon is unclear (Fischer *et al.*, 2011).

There is some evidence that RNase 1, which is a member of the RNase A family, is stored in the Weibel-Palade bodies of endothelial cells where it localizes with von Willebrand factor. When endothelial cells are stimulated with RNA, RNase 1 is released (Fischer *et al.*, 2011). This observation suggests that when RNA is released into the blood, it stimulates endothelial cells to secrete RNase, which degrades the activator and likely prevents it from triggering contact activation (Fischer *et al.*, 2011, Kannemeier *et al.*, 2007). DNase is also released from cells when necrotic or apoptotic pathways are activated, which suggests that DNase plays an important role in DNA clearance and

removal of dead cells (Gaipl *et al.*, 2004, Nagata *et al.*, 2003). Thus, DNAse may be regulated in a manner that is distinct from RNase.

Despite these processes, the plasma levels of DNA and RNA are elevated in thrombosis and they may contribute to its pathogenesis (Fuchs *et al.*, 2012, Preissner, 2007). Under pathological conditions, nucleases are ineffective at attenuating the procoagulant activity of nucleic acids. Although C1-Inh is the major regulator of FXIIa, its rate of inhibition is slow (de Agostini *et al.*, 1984). Therefore, it is unclear what mechanisms are in place to prevent uncontrolled activation of the intrinsic pathway.

The observation that HRG binds to DNA (Gorgani *et al.*, 2002) suggests that HRG may act as a molecular brake that dampens nucleic acid activation of FXII. This hypothesis is explored in Research Objectives #3 and #4.

1.13 HISTIDINE-RICH GLYCOPROTEIN

Because HRG is a potent inhibitor of the contact system, it is important to understand the protein and how it is regulated. Although the precise physiological role of HRG is unknown, it is proposed to have numerous roles in vascular biology and immunity (Poon *et al.*, 2011). The synthesis of HRG, its structure, regulation and proposed physiological role in hemostasis are discussed below.

1.13.1 Protein synthesis and plasma levels

HRG circulates in plasma at 1.6-2 μM and has a half-life of ~3 days in humans (Lijnen *et al.*, 1981). HRG is synthesized in the liver, and is found in monocytes, macrophages, megakaryocytes and platelets, although it is unclear whether these cells synthesize HRG or whether they actively take it up from the blood (Jones *et al.*, 2005,

Sabbatini *et al.*, 2011). Evidence for extracellular uptake of HRG comes from studies with muscle and T-cells. These studies show that HRG can bind to cellular receptors such as GAGs (ie. heparan sulfate) and this facilitates its uptake into these cells (Sabbatini *et al.*, 2011).

Levels of HRG increase with age and there is some evidence to suggest that protein levels also vary with blood type (Drasin and Sahud, 1996). HRG is a negative acute phase protein whose levels decrease during the acute response to injury or with chronic inflammation (Jones *et al.*, 2005). In addition, local concentrations of HRG can increase in the vicinity of a platelet-rich thrombus because activated platelets secrete HRG from their α-granules (Leung *et al.*, 1983).

1.13.2 Domain structure and proteolytic cleavage by plasmin and kallikrein

HRG is a multidomain protein, which consists of two NH_2-terminal cystatin-like domains (N1N2), a central histidine-rich region (HRR) flanked by two proline-rich regions (PRR) and a COOH-terminal domain (Fig. 1.5A) (Borza *et al.*, 1996, Jones *et al.*, 2005). HRG has a high content of histidine and proline residues, each comprising ~13% of the total residues. The HRR domain is composed of tandem repeats of an X-His-His-Pro-His motif, which results in a tertiary structure predicted to be elongated and helical (Borza *et al.*, 1996, Jones *et al.*, 2005). Imidazole groups in the histidine side chains are exposed to solvent and consequently, can bind zinc and hydrogen ions in solution. Thus, the HRR domain endows HRG with the unique ability to sense local changes in pH and fluctuations in zinc concentration (Fig. 1.5B) (Jones *et al.*, 2005). Activated platelets also secrete zinc (Marx *et al.*, 1993). Zinc binds to HRG (K_d of ~200 nM) and promotes the

binding of HRG to its ligands (Table 1.1) (Bird *et al.*, 2012). HRG is also considered a pH sensor because binding of HRG to its ligands such as heparin is regulated by changes in hydrogen ion concentration (Borza and Morgan, 1998). When zinc or hydrogen ions bind to the PRR-HRR region of HRG, they induce local conformation changes that are transmitted throughout the molecule. Such changes are believed to indirectly modulate the binding of the N1N2 and COOH domains to their ligands (Borza *et al.*, 1996, Jones *et al.*, 2005).

HRG activity is regulated by proteolytic cleavage (Poon *et al.*, 2011). Cleaved derivatives of HRG are found in plasma. In patients undergoing thrombolytic therapy, HRG-derived bands of 9-67 kDa are observed, suggesting that plasmin modulates HRG activity (Smith *et al.*, 1985). Plasmin cleaves HRG into disulfide-linked HRR-PRR, N1N2 and COOH-terminal fragments. The susceptibility of HRG to degradation is dependent on the zinc concentration and pH because both elevated levels of zinc and hydrogen ions protect HRG from plasmin degradation (Poon *et al.*, 2009). Upon plasmin cleavage, HRG binding to GAGs is attenuated, whereas binding to necrotic cells and plasminogen is augmented (Poon *et al.*, 2011). Although kallikrein cleaves HRG in a manner distinct from plasmin, the functional consequence of this has not been determined (Poon *et al.*, 2009). Therefore, protease cleavage of HRG provides an additional level of regulation that directs HRG activity.

1.13.3 HRG ligands in coagulation and fibrinolysis

HRG is a dynamic modulator and regulates coagulation and fibrinolysis at multiple steps (Table 1.1). Since HRG prolongs the aPTT, but has no impact on the PT, these data suggest that HRG is a specific regulator of the intrinsic pathway (MacQuarrie *et al.*, 2011). HRG attenuates contact activation of coagulation by interacting with FXIIa, kallikrein and DNA, which are components of the contact system that are important in the initiation phase of coagulation (Gorgani *et al.*, 2002, MacQuarrie *et al.*, 2011). HRG exhibits anticoagulant activity, as it attenuates both FXII activation and FXIIa activity. The capacity of HRG to bind and inhibit FXIIa activity dampens contact activation of coagulation (MacQuarrie *et al.*, 2011). HRG also binds kallikrein and impairs its capacity to activate FXII. Since the affinity of HRG for kallikrein is 16-fold lower than for FXIIa, this suggests that kallikrein modulation is secondary to FXIIa inhibition (MacQuarrie *et al.*, 2011). Nucleic acids promote FXII activation and thrombin activation of FXI (Kannemeier *et al.*, 2007). HRG binds DNA and facilitates apoptotic cell clearance (Gorgani *et al.*, 2002), suggesting that HRG may modulate nucleic-acid mediated protease activation during contact activation. Thus, HRG likely regulates the contact system at multiple levels.

Downstream of the intrinsic pathway, HRG regulates fibrin clot formation and lysis. HRG binds fibrinogen (K_d of 6 nM) and this prolongs the thrombin clot time. Like thrombin, HRG remains associated with the fibrin clot, and its binding was shown to modulate fibrin clot structure (Leung, 1986). In addition, fibrin clots formed from plasma of $HRG^{-/-}$ mice are more prone to lysis than those formed in plasma from wild type mice,

thereby suggesting that HRG has anti-fibrinolytic effects (Tsuchida-Straeten *et al.*, 2005). In support of this, HRG binds plasminogen and sequesters the protein, so as to prevent it from binding to fibrin clots and promoting fibrinolysis (Lijnen *et al.*, 1980). Taken together, these observations posit a novel role for HRG in modulating processes that are important in hemostasis.

1.13.4 HRG modulation of hemostasis and thrombosis

Although HRG binds to several proteins that are important in coagulation and fibrinolysis, its physiological function is unclear. In families with a congenital HRG deficiency, where the HRG levels are 20-35% of normal, hemostatic and immune function abnormalities were not detected (Poon *et al.*, 2011). Studies in HRG-deficient mice have shed some light on the physiological role of the protein. $HRG^{+/-}$ and $HRG^{-/-}$ mice are viable and fertile (Tsuchida-Straeten *et al.*, 2005). $HRG^{-/-}$ mice exhibit a shorter PT and accelerated fibrinolysis compared with wild type controls. Furthermore, in a tail bleeding model of hemostasis, HRG-deficiency results in a shortened bleeding time, suggesting that HRG modulates hemostasis (Tsuchida-Straeten *et al.*, 2005). The intrinsic pathway contributes to thrombosis, and since HRG attenuates contact activation of coagulation *in vitro*, it may be a unique molecular brake that prevents uncontrolled thrombosis (Morrissey, 2011). Nucleic acids are novel activators of the contact system and HRG has been shown to bind DNA (Gorgani *et al.*, 2002). The possibility that HRG modulates FXII-driven coagulation is addressed using a murine model of thrombosis (Research Objective #4).

A) Domain structure of HRG

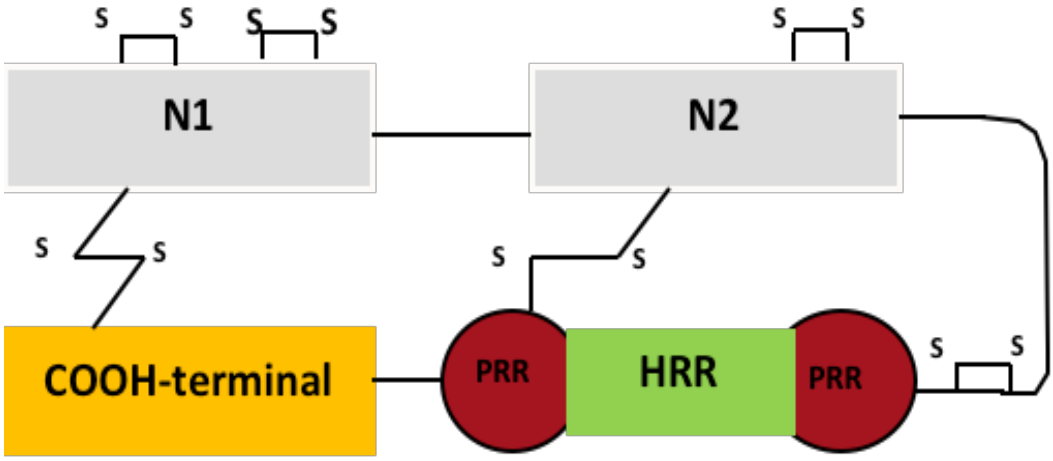

B) HRR

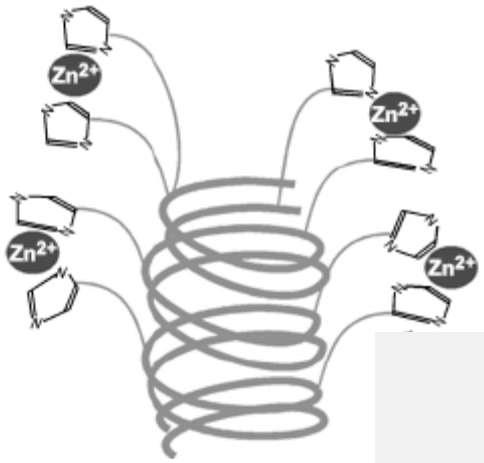

Figure 1.5 Domain structure of HRG and coiled-coiled structure of HRR with imidazole rings exposed to zinc. HRG is composed of 2 NH_2-terminal cystatin-like domains (N1 and N2), a histidine-rich region (HRR) that is flanked by 2 proline-rich regions (PRR) and a COOH-terminal domain. These domains facilitate HRG binding to its various ligands (Table 1.1). The HRR is predicted to have a coiled-coil structure, with the imidazole rings of the histidine residues being exposed to solvent. The nitrogen on the histidine rings can act as hydrogen bond donors or acceptors and the imidazole ring can also interact with divalent metal ions such as zinc. Binding of hydrogen ions and zinc is proposed to induce conformational change in the HRR that is transmitted throughout the molecule, which modulates ligand binding. Images are adapted from Jones et al., 2005.

Table 1. 1 HRG ligands in coagulation and fibrinolysis. This table is adapted from Jones et al., 2005, but also contains work that was observed by the Weitz lab.

Ligands	K_d	Stoichiometry (HRG:Ligand)	HRG domain
Zinc	200 nM	1:1 to 1:10	HRR
H^+	?	?	?
FXIIa	21 nM 7.5 pM (+) Zn^{2+}	?	?
Kallikrein	340 nM (+) Zn^{2+}	?	?
Fibrinogen and Fibrin monomers	10 nM	≥ 2:1	HRR (?)
Fibrin clots	30-100 nM	≥ 2:1	HRR (?)
DNA and RNA	1 nM	?	?
PolyP	6 nM	?	?
Heparin and Heparan sulfate	10 nM	1:1	NIN2-
Plasminogen and Plasmin	500-1000 nM	1:1	NIN2-, COOH-

CHAPTER 2: OVERVIEW, HYPOTHESIS & OBJECTIVES

2.1 Thesis Overview: The overall objective of this Ph.D thesis is to explore the role of HRG in coagulation as a means of further understanding hemostasis, and identifying new strategies for prevention and treatment of thrombosis.

2.2 Rationale: HRG is a relatively abundant plasma protein whose physiological function is unclear (Jones *et al.*, 2005, Poon *et al.*, 2011). Because of its modular structure, HRG binds numerous ligands such as zinc, FXIIa, kallikrein, DNA, fibrin(ogen) and plasmin(ogen). HRG is proposed to be an adaptor or accessory protein that bridges together different ligands. Consequently, HRG is implicated in diverse processes such as coagulation, fibrinolysis, immunity and angiogenesis (Jones *et al.*, 2005, Poon *et al.*, 2011).

The intrinsic pathway is initiated by FXIIa and this process is augmented in the presence of polyanions such as DNA and RNA (Kannemeier *et al.*, 2007). HRG forms a high affinity interaction with FXIIa (K_d 21 nM), but not FXII, the zymogen (MacQuarrie *et al.*, 2011). In doing so, HRG inhibits FXIIa activation of FXI and feedback activation of FXII (MacQuarrie *et al.*, 2011). Inhibition of FXIIa impairs clot formation and stability, without affecting hemostasis (Larsson *et al.*, 2014, Renne *et al.*, 2005). Thus, characterization of the mechanisms by which HRG modulates contact activation of coagulation may provide novel strategies to prevent or treat thrombosis, while limiting bleeding complications.

Downstream to the common pathway, HRG also modulates fibrin clot formation. HRG binds fibrinogen and fibrin and is incorporated into the fibrin clots. The presence of

HRG lowers the clot turibidy measured by absorbance, which suggests that HRG modulates the fibrin clot structure (Leung *et al.*, 1983). However, the physiological relevance of the HRG-fibrin(ogen) interaction during coagulation was unclear.

2.3 Hypothesis: Based on these observations, we hypothesized that HRG is a novel regulator of the contact pathway and fibrin formation and as such, serves as a dynamic modulator of coagulation.

2.4 Overall Objectives: To address this hypothesis, 4 main objectives were proposed.

2.4.1 <u>Objective 1:</u> *Characterization of the HRG interaction with γ_A/γ_A- and γ_A/γ'-fibrin(ogen).*

γ_A/γ'-Fibrin(ogen) contains a unique anionic binding site that interacts with thrombin (Meh *et al.*, 1996, Pospisil *et al.*, 2003). Since HRG binds to polyanionic molecules (Borza and Morgan, 1998), we hypothesized that HRG also binds the γ'-chain. To test this hypothesis, we set out to quantify the binding of HRG to both isoforms of fibrin(ogen) and to determine whether there is overlap between the HRG and thrombin binding sites on fibrin(ogen). Characterization of proteins that interact with the γ'-region is important, since epidemiological studies suggest that elevated levels of γ_A/γ'-fibrin(ogen) are associated with an increased risk of cardiovascular disease (Lovely *et al.*, 2002, Uitte de Willige *et al.*, 2005).

2.4.2 <u>Objective 2:</u> *Characterization of the mechanisms of batroxobin binding to γ_A/γ_A- and γ_A/γ'-fibrin(ogen).*

In characterizing HRG binding to the isoforms of fibrinogen, we observed that in contrast to thrombin, batroxobin, a thrombin-like serine protease that converts fibrinogen

into fibrin, does not bind to the γ'-chain on γ_A/γ'-fibrin(ogen). Unlike thrombin, which releases FpA and FpB, batroxobin generates fibrin solely by releasing FpA from fibrinogen (You *et al.*, 2004). Clinically, batroxobin is used in clinical laboratories to identify abnormal fibrinogen molecules and to exclude the possibility that a prolonged thrombin time is the result of heparin contamination (Braud *et al.*, 2000). Batroxobin also is being explored as a defibrinogenating agent for the treatment of ischemic stroke (Liu *et al.*, 2004, Wang *et al.*, 2010, Xu *et al.*, 2007). Since thrombin and batroxibin have different patterns of Fp release, we hypothesized that batroxobin binds fibrin(ogen) in a manner that is distinct from that of thrombin. Therefore, we set out to characterize the binding of batroxobin to both isoforms of fibrin(ogen) and to determine if like thrombin, batroxobin binds to fibrin and promotes clot expansion.

2.4.3 <u>Objective 3:</u> *Characterization of the mechanisms of HRG attenuation of DNA- and RNA-mediated activation of the contact pathway.*

DNA and RNA are physiological activators of the contact pathway (Kannemeier *et al.*, 2007). Since HRG binds DNA (Gorgani *et al.*, 2002), we hypothesized that HRG also binds RNA and by doing so, modulates the capacity of nucleic acids to promote FXII and FXI activation. To explore this hypothesis, we set out to characterize the molecular mechanisms by which HRG modulates DNA/RNA-mediated activation of the intrinsic pathway.

2.4.4 **Objective 4:** *Characterization of the role of HRG in hemostasis and thrombosis using a mouse model.*

We previously showed that HRG binds FXIIa with high affinity and attenuates contact activation of coagulation (MacQuarrie *et al.*, 2011). The contact system is imperative for thrombosis, but not hemostasis (Gailani and Renne, 2007). Therefore, we hypothesized that HRG modulates thrombosis driven via the intrinsic pathway, but has no effect on hemostasis. To test these hypotheses, we used murine models of thrombosis and hemostasis to: (a) compare, the time to occlusion after $FeCl_3$-induced carotid artery injury in HRG-deficient mice with that in wild type mice, with the expectation that HRG deficiency would endow the mice with a prothrombotic phenotype; (b) determine whether HRG supplementation would render the time to occlusion in HRG-deficient mice similar to that in wild type mice; and (c) compare blood loss after tail tip amputation in HRG-deficient and wild type mice with the expectation that blood loss would be comparable if HRG has no impact on hemostasis. In addition, to explore the relative contribution of the intrinsic and extrinsic pathways to $FeCl_3$-induced thrombosis, mice were pre-treated with FXII or FVII directed ASOs to selectively knock down the levels of these key components of the intrinsic and extrinsic pathway, respectively, prior to subjecting them to $FeCl_3$-induced injury. Finally, to examine the role of RNA and/or DNA in $FeCl_3$-induced thrombosis, mice were infused with RNase or DNase prior to injury.

CHAPTER 3: Histidine rich glycoprotein binds fibrin(ogen) with high affinity and competes with thrombin for binding to the γ'-chain

3.1 Forward: The interactions between HRG and fibrin(ogen) are described in this manuscript. We demonstrated that HRG has multiple binding sites on fibrin(ogen). Of interest, HRG interacts with the γ'-region of γ_A/γ'-fibrin(ogen) and in doing so, displaces thrombin from the γ'-chain.

This manuscript has been published in the *Journal of Biological Chemistry* (Vol. 286, pp. 30314-30323, September 2, 2011). The authors are: Trang T. Vu, Alan R. Stafford, Beverly A. Leslie, Paul Y. Kim, James C. Fredenburgh and Jeffrey I. Weitz. Dr. Weitz is the corresponding author. According to the policies of the American Society for Biochemistry and Molecular Biology (ASBMB), no formal permission is required to reproduce this mauscript for non-commercial purposes.

Trang Vu performed the experiments in this manuscript. Alan Stafford and Beverly Leslie provided technical assistance and reagents. Dr. Paul Kim provided reagents. The project was designed and the manuscript written by Trang Vu, Dr. James Fredenburgh and Dr. Jeffrey Weitz.

Chapter 3 is a direct representation of the above referenced manuscript (Copyright © 2011 by ASBMB).

3.2 Summary

Histidine-rich glycoprotein (HRG) is an abundant protein that binds fibrinogen and other plasma proteins in a Zn^{2+}-dependent fashion but whose function is unclear. HRG has antimicrobial activity, and its incorporation into fibrin clots facilitates bacterial entrapment and killing and promotes inflammation. Although these findings suggest that HRG contributes to innate immunity and inflammation, little is known about the HRG-fibrin(ogen) interaction. By immunoassay, HRG-fibrinogen complexes were detected in Zn^{2+}-supplemented human plasma, a finding consistent with a high affinity interaction. Surface plasmon resonance determinations support this concept and show that in the presence of Zn^{2+}, HRG binds the predominant γ_A/γ_A-fibrinogen and the γ-chain elongated isoform, γ_A/γ'-fibrinogen, with K_d values of 9 nM. Likewise, ^{125}I-labeled HRG binds γ_A/γ_A- or γ_A/γ'-fibrin clots with similar K_d values when Zn^{2+} is present. There are multiple HRG binding sites on fibrin(ogen) because HRG binds immobilized fibrinogen fragment D or E and γ′-peptide, an analog of the COOH terminus of the γ′-chain that mediates the high affinity interaction of thrombin with γ_A/γ'-fibrin. Thrombin competes with HRG for γ′-peptide binding and displaces ^{125}I-HRG from γ_A/γ'-fibrin clots and vice versa. Taken together, these data suggest that (*a*) HRG circulates in complex with fibrinogen and that the complex persists upon fibrin formation, and (b) by competing with thrombin for γ_A/γ'-fibrin binding, HRG may modulate coagulation. Therefore, the HRG-fibrin interaction may provide a novel link between coagulation, innate immunity, and inflammation.

3.3 Introduction

Fibrinogen is the soluble precursor of fibrin, a critical component of blood clots that endows them with strength and elasticity. Fibrinogen is a glycoprotein composed of three pairs of polypeptide chains, termed Aα, Bβ, and γ, that are connected by disulfide bonds (Henschen-Edman *et al.*, 1999). Approximately 10–15% of circulating fibrinogen has a variant γ-chain termed the γ′-chain, which results from differential processing of the γ_A-chain mRNA transcript (Chung and Davie, 1984, Fornace, Jr. *et al.*, 1984, Wolfenstein-Todel and Mosesson, 1980). The γ′-chain is distinguished from the γ_A-chain by the presence of an acidic 20-residue extension at its COOH terminus (Meh *et al.*, 1996, Wolfenstein-Todel and Mosesson, 1980).

Thrombin catalyzes the conversion of fibrinogen to insoluble fibrin, and during this process some thrombin remains bound to the fibrin network (Weitz *et al.*, 1990). Exosites 1 and 2 are two regulatory domains that flank the active site of thrombin and mediate its binding to fibrin (Jackman *et al.*, 1992, Liu *et al.*, 1991). Exosite 1 of thrombin interacts with the central E-domain of fibrin, whereas exosite 2 binds only to the COOH terminus of the γ′-chain. Consequently, thrombin binds γ_A/γ_A-fibrin in a univalent fashion with a K_d value of 2–4 μM. In contrast, both exosites are engaged when thrombin binds to γ_A/γ'-fibrin, resulting in a higher affinity interaction (K_d value of 0.08–0.18 μM) (Meh *et al.*, 1996, Pospisil *et al.*, 2003). Fibrin-bound thrombin remains active, and the protease is protected from inhibition by fluid-phase inhibitors, such as AT and HCII (Weitz *et al.*, 1990). Because of its bivalent interaction with γ_A/γ'-fibrin, thrombin bound

to γ_A/γ'-fibrin is more protected from inhibition by fluid-phase inhibitors than thrombin bound to γ_A/γ_A-fibrin (Becker *et al.*, 1999, Fredenburgh *et al.*, 2008).

Like thrombin, histidine-rich glycoprotein (HRG) binds to fibrinogen and is incorporated into fibrin clots (Leung, 1986). Although the plasma concentration of HRG ranges from 1.6 to 2 μM, the concentration in platelet-rich thrombi may be higher because HRG is stored in the alpha granules of platelets and is released when platelets are activated (Leung *et al.*, 1983, Lijnen *et al.*, 1980). A 75-kDa glycoprotein, HRG, is composed of two NH_2-terminal cystatin-like domains, a central histidine-rich region (HRR) flanked by two proline-rich regions, and a COOH-terminal domain (Jones *et al.*, 2005). In addition to fibrinogen, HRG also binds plasminogen, heparan sulfate, and divalent cations, such as Zn^{2+} (Jancso *et al.*, 2009, Jones *et al.*, 2004a, Lijnen *et al.*, 1980). Therefore, HRG is hypothesized to be an important accessory or adapter protein that brings different ligands together under specific conditions (Jones *et al.*, 2005).

HRG-deficient mice exhibit a shorter prothrombin time and accelerated fibrinolysis compared with wild-type mice, raising the possibility that HRG modulates coagulation and fibrinolysis (Tsuchida-Straeten *et al.*, 2005). In addition to its potential role in hemostasis, HRG also has been implicated in innate immunity and inflammation (Poon *et al.*, 2011). HRG exhibits antifungal and antimicrobial activity *in vitro*, and these activities are enhanced at low pH or in the presence of Zn^{2+}, conditions that promote ligand binding (Rydengard *et al.*, 2006, Rydengard *et al.*, 2007, Rydengard *et al.*, 2008). The antimicrobial activity of HRG has also been demonstrated *in vivo* and appears to be fibrin-dependent (Shannon *et al.*, 2010). Thus, compared with wild-type mice, HRG-

deficient mice are more susceptible to the lethal effect of *Streptococcus pyogenes* infection and are rescued with HRG supplementation (Shannon *et al.*, 2010). This phenomenon is fibrin-dependent because fibrin is essential for HRG-mediated bacterial entrapment and killing, processes that prevent bacterial dissemination. In addition, the HRG-fibrin interaction modulates inflammation because HRG-deficient mice exhibit attenuated abscess formation in response to subcutaneous injection of bacteria. Based on these findings, it has been postulated that HRG plays a fibrin-dependent role in both inflammation and innate immunity (Shannon *et al.*, 2010).

Despite emerging evidence that the HRG-fibrin(ogen) interaction is physiologically important, little is known about the biochemical foundation of this interaction or its functional consequences. To address these gaps in knowledge, we set out to (*a*) quantify the binding of HRG to fibrin(ogen), (*b*) identify the HRG binding domains on fibrin(ogen), and (*c*) determine whether there is overlap between the HRG and thrombin binding domains on fibrin(ogen).

3.4 EXPERIMENTAL PROCEDURES

3.4.1 Materials

3.4.1.1 Reagents

Human thrombin, prothrombin, and plasminogen-free fibrinogen were from Enzyme Research Laboratories (South Bend, IN). Plasmin and factor XIII were from Haematologic Technologies Inc. (Essex Junction, VT). Prionex was from Pentapharm (Basel, Switzerland). A 20-amino acid analog of the COOH terminus of the γ′-chain of

fibrinogen, γ′-peptide (VRPEHPAETEYDSLYPEDDL), was prepared by Bachem Bioscience, Inc. (King of Prussia, PA), and a sheep antibody against this peptide was from Affinity Biologicals (Ancaster, ON). The two Tyr residues within the γ′-peptide were modified with phosphate groups in place of sulfate to enhance stability (Lovely *et al.*, 2003). The γ′-peptide-directed IgG was subjected to affinity chromatography using immobilized γ′-peptide (SulfoLink Immobilization Kit for Peptides, Thermo Scientific, Rockford, IL). D-Phe-Pro-Arg chloromethyl ketone and D-Tyr-Pro-Arg chloromethyl ketone (FPRck and YPRck, respectively) were from EMD Chemicals (Gibbstown, NJ). Fibrinogen was rendered factor XIII-free, and γ_A/γ_A- and γ_A/γ'-fibrinogen were separated by fractionation on DEAE-Sepharose (GE Healthcare) and characterized as previously described (Fredenburgh *et al.*, 2008, Schaefer *et al.*, 2006). HRG was purified by metal-chelate chromatography, and HRG-deficient plasma was prepared as described previously (MacQuarrie *et al.*, 2011). Non-immune sheep IgG and a human HRG-directed IgG from sheep were prepared by Affinity Biologicals, and the HRG-specific IgG fraction was isolated by affinity chromatography using immobilized HRG (MacQuarrie *et al.*, 2011). Unless otherwise specified, other reagents were from Sigma.

3.4.1.2 Preparation of Fibrinogen Fragments

Fragment X was prepared by limited plasmin digestion of fibrinogen (Schaefer *et al.*, 2006). Fragments D and E were generated by plasmin digestion of γ_A/γ_A-fibrinogen (Kaczmarek and McDonagh, 1988). Digested material was applied to a 12-ml UNO Q-12 ion exchange column (Bio-Rad) using a Bio-Rad Biologic Duoflow system at a flow rate of 5 ml/min. To elute non-specifically bound proteins, the column was washed with 30 ml

of 0.02 M sodium phosphate, 0.01 M citric acid, pH 7.6. Fragment D was eluted with 100 ml of 0.1 M sodium phosphate, 0.05 M citric acid, pH 5.0, whereas fragment E was subsequently eluted with 40 ml of the same buffer at pH 4.4 (Olman *et al.*, 1998). Protein-containing fractions were identified by absorbance at 280 nm and pooled. Purified fragments were dialyzed into 10 mM Hepes-NaOH, 150 mM NaCl, pH 7.4 (HBS) and concentrated. Final concentrations were determined at 280 nm (Marder *et al.*, 1969). The integrity of the fragments was assessed by SDS-PAGE analysis on 4–15% polyacrylamide gels (Ready-Gel, Bio-Rad) under reducing and non-reducing conditions. Samples were stored in aliquots at −80°C.

3.4.1.3 Preparation of γ′-directed IgG Fab Fragments

For some experiments, fragment antibody binding (Fab) regions from the affinity-purified γ′-peptide-directed IgG were generated by papain digestion (Nikula *et al.*, 1995), isolated with a Fab preparation kit (Pierce), assessed for purity by SDS-PAGE analysis, and then concentrated and dialyzed against HBS.

3.4.1.4 Labeling of Proteins

γ′-Peptide was labeled with fluorescein isothiocyanate as previously described (Pospisil *et al.*, 2003). α–Thrombin was radiolabeled by reaction with ^{125}I-labeled YPRck, and HRG was radiolabeled with Na^{125}I (McMaster University Nuclear Reactor, Hamilton, ON) using Iodo-beads (Pierce) as described (Fredenburgh *et al.*, 2001). ^{125}I-YPRck-thrombin and ^{125}I-HRG concentrations were 5–6 μM, as determined by absorbance at 280 nm, with radioactivity of 500,000–800,000 cpm/μg of protein. FPRck-thrombin was prepared as described (Petrera *et al.*, 2009).

3.4.2 Methods

3.4.2.1 Surface Plasmon Resonance (SPR)

The interaction of HRG with immobilized γ_A/γ_A- or γ_A/γ'-fibrin(ogen), biotinylated-γ′-peptide, or fragments X, D, or E was assessed by SPR using a BIAcore 1000 (GE Healthcare) as previously described (MacQuarrie *et al.*, 2011, Petrera *et al.*, 2009) but with some modifications. Briefly, proteins were covalently linked to separate flow cells of a carboxymethylated dextran (CM4) biosensor chip at a flow rate of 5 μl/min using an amine coupling kit (GE Healthcare). Proteins were immobilized using 10 mM acetate buffer at varying pH values to maximize adsorption. γ_A/γ_A- or γ_A/γ'-fibrinogen or fragments X and D were immobilized at pH 5.5 to ~3000–7000 response units (RU). Fragment E was immobilized at pH 4.5 to ~2000–3000 RU. For fibrin binding studies, immobilized γ_A/γ_A- or γ_A/γ'-fibrinogen was converted to fibrin by three successive 60-min injections of 100 nM thrombin at 5 μl/min (Petrera *et al.*, 2009). To prepare streptavidin-conjugated CM4 flow cells, 0.4 mg/ml streptavidin (Sigma) at pH 4.5 was injected. Biotinylated γ′-peptide (Petrera *et al.*, 2009) was adsorbed to the immobilized streptavidin to 200–300 RU. Remaining reactive groups were neutralized with 1 M ethylenediamine, and non-specifically adsorbed proteins were removed by treatment with 0.5 M NaCl. An unmodified flow cell served as the control. All SPR procedures were done in HBS containing 0.005% Tween 20 and 2 mM $CaCl_2$, and flow cells were regenerated with 250 mM imidazole and 2 mM EDTA between runs.

To measure the affinity of HRG for immobilized fibrinogen, fibrin, or fibrinogen fragments, aliquots of HRG (0–1 μM) in buffer containing 20 μM $ZnCl_2$ were injected at

a flow rate of 30 μl/min. To quantify Zn^{2+} dependence, binding of 200 nM HRG to immobilized γ_A/γ_A- or γ_A/γ'-fibrinogen was monitored in the presence of varying concentrations of $ZnCl_2$ (0–60 μM) using dual injection mode. The binding of thrombin to immobilized fragment D or E was monitored by injection of FPRck-thrombin (0–15 μM) into flow cells.

The γ′-peptide-directed IgG was used to assess the contribution of the γ′-chain to the interaction of HRG with immobilized γ′-peptide or fibrinogen. A saturating amount of γ′-peptide-directed IgG or a non-immune IgG (2 μM) was first injected into flow cells containing immobilized γ′-peptide or γ_A/γ'- or γ_A/γ_A-fibrinogen. The binding of HRG to fibrinogen or fibrinogen fragments was then measured as described above, except that flow cells were re-saturated with 0.5 μM γ′-peptide-directed IgG or control IgG before each HRG injection.

Binding of HRG to immobilized γ′-peptide in the absence or presence of FPRck-thrombin was monitored using a BIAcore T200. Biotinylated γ′-peptide was adsorbed to streptavidin-conjugated CM4 flow cells to 100 RU in the presence of 20 μM $ZnCl_2$ at a flow rate of 5 μl/min. An unmodified flow cell served as a control. Using dual injection mode, 1 μM HRG was injected at 10 μl/min followed by a second injection of FPRck-thrombin or prothrombin at concentrations ranging from 0 to 8 μM. Flow cells were regenerated with 250 mM imidazole, 2 mM EDTA, and 1 M NaCl. All experiments were performed at least twice.

3.4.2.2 SPR Data Analysis

K_d values were determined by kinetic analysis of on- and off-rates of HRG binding to immobilized ligands using Scrubber2 version 2.0a (Bio-Logic Software Co., Campbell, Australia) as described previously (MacQuarrie *et al.*, 2011, Petrera *et al.*, 2009). For further assessment of binding, the amount of HRG bound at the equilibrium position (Req) was determined using the Langmuir 1:1 binding model (BIAEvaluation software Version 3.2) and was plotted against the titrant concentration. Molar stoichiometries were determined as described in the BIAtechnology handbook (BIAcore 1000). The correction factor to account for the orientation of the immobilized fibrinogen and fibrin was 0.25, which corresponds to 25% of the amount of immobilized fibrin accessible to the γ′-peptide-directed IgG as determined in a separate study (Fredenburgh *et al.*, 2008). The correction factor for immobilized γ′-peptide was 0.7, which corresponds to 70% correct orientation of peptide accessible to an analyte (BIAcore).

3.4.2.3 Interaction of ^{125}I-HRG with Fibrin Clots

In a series of microcentrifuge tubes, γ_A/γ_A- or γ_A/γ'-fibrinogen, in concentrations ranging from 0 to 1.25 μM, was clotted with 10 nM thrombin in the presence of 40 nM ^{125}I-HRG as previously described (Petrera *et al.*, 2009). Clots were formed in 20 mM Tris-HCl and 150 mM NaCl, pH 7.4 (TBS), containing 0.005% Tween (TBS-Tween) and 2 mM $CaCl_2$ and 20 μM $ZnCl_2$ or 10 μM sodium diethyldithiocarbamate trihydrate. The concentration of ^{125}I-HRG bound to fibrin was calculated by subtracting the concentration in the clot supernatant from the value obtained in controls prepared in the absence of fibrinogen. Plots of bound ^{125}I-HRG *versus* fibrin concentration were analyzed by

nonlinear regression of a rectangular hyperbola to determine K_d. Experiments were performed twice in duplicate.

3.4.2.4 Effect of Competitors on the Binding of ^{125}I-HRG to Fibrin Clots

Clots were formed in TBS-Tween containing 2 mM $CaCl_2$ and 20 μM $ZnCl_2$. Fab fragments derived from γ′-peptide-directed IgG were used to assess the contribution of the γ′-chain to ^{125}I-HRG binding to clots. After preincubation of 0.25 μM γ_A/γ_A- or γ_A/γ'-fibrinogen with γ′-peptide-directed Fab fragments or control sheep IgG (0–4 μM) for 1 h at 23°C, 60 nM ^{125}I-HRG was added, and clots were generated with 20 nM thrombin. To determine whether HRG and thrombin share fibrin binding sites, the effect of FPRck-thrombin on the binding of ^{125}I-HRG was assessed. Samples containing 2 μM γ_A/γ_A- or γ_A/γ'- fibrinogen, 20 nM^{125}I-HRG, and FPRck-thrombin (0–8 μM) in 0.25% Prionex were clotted with 20 nM thrombin. The effect of varying concentrations of HRG on the binding of ^{125}I-YPRck-thrombin was assessed in a reciprocal experiment. Samples containing 2 μM γ_A/γ_A- or 0.25 μM γ_A/γ'-fibrinogen, 20 nM ^{125}I-YPRck-thrombin, and HRG (0–2 μM) were clotted with 10 nM thrombin. The fraction of ^{125}I-HRG or ^{125}I-YPRck-thrombin bound was determined as described above. All experiments were performed twice in duplicate.

3.4.2.5 HRG Diffusion from Preformed Fibrin Clots

The rate of ^{125}I-HRG dissociation from γ_A/γ_A- or γ_A/γ'-fibrin clots was determined as previously described (Fredenburgh *et al.*, 2008, Petrera *et al.*, 2009). Briefly, fibrin clots were formed around plastic inoculation loops (Bac-Loop, Thermo-Fisher Scientific, Waltham, MA) by adding 10 nM thrombin to solutions containing 5 μM γ_A/γ_A- or γ_A/γ'-

fibrinogen, 20 nM FXIII, and 50 nM ^{125}I-HRG in TBS-Tween containing 2 mM $CaCl_2$ and 20 μM $ZnCl_2$. After incubation for 45 min at 23°C, clots were removed and immersed in buffer containing 2 mM $CaCl_2$ plus 20 μM $ZnCl_2$, 2 mM $CaCl_2$ plus 10 μM diethyldithiocarbamate trihydrate, or 2 M NaCl plus 2 mM EDTA. The fraction of clot-associated ^{125}I-HRG remaining at various times was determined, and time courses were fit to a two-phase exponential decay curve (Table Curve, Jandel Scientific, San Rafael, CA) (Fredenburgh *et al.*, 2008). Experiments were repeated three times.

3.4.2.6 Detection of HRG-Fibrinogen Complexes in Plasma

HRG-fibrinogen complexes in plasma were detected using a previously described sandwich ELISA (MacQuarrie *et al.*, 2011) with some modifications. Briefly, 100 μl of fibrinogen-directed capture antibody (Affinity Biologicals) diluted to 20 μg/ml in 50 mM $NaHCO_3$, pH 9.6, was added to wells of a 96-well Immunlon 4 HBX plate (Thermo Scientific) and incubated overnight at 4°C. To block nonspecific binding, 200 μl of 10 mg/ml bovine serum albumin (Sigma) was added to each well and incubated for 1 h at 23°C. Wells were washed 3 times with 150 μl of phosphate-buffered saline (PBS) containing 10 μM $ZnCl_2$ and 0.1% Tween 20. Normal and HRG-deficient plasma samples were dialyzed against TBS to remove citrate, reconstituted with 18 μM $ZnCl_2$, and then serially diluted up to 1600-fold with HBS containing 1% ovalbumin, 0.1% Tween 20, 2 mM $CaCl_2$, 100 nM hirudin (Behring), and 18 μM $ZnCl_2$. To prepare a reference curve, HRG-fibrinogen complexes were generated by incubating varying concentrations of HRG (0–1.6 μg/ml) with fibrinogen (0–0.8 μg/ml) in a 2:1 molar ratio. 100 μl of each of these mixtures or plasma was added to wells and incubated for 2 h at 23°C. After three

sequential washes with PBS containing $ZnCl_2$, HRG-fibrinogen complexes were detected in purified and plasma systems using a HRG-directed IgG-horseradish peroxidase (HRP) conjugate, prepared as specified by the manufacturer using a Lightning-link HRP conjugation kit (Cedarlane, Burlington, ON). After incubation for 1 h at 23°C, bound HRP conjugates were detected as specified by the supplier. Experiments were repeated three times.

3.4.2.7 Interaction of HRG with Fluorescein-labeled γ′-Peptide in the Absence or Presence of $ZnCl_2$

The binding of 1.1 μM HRG to 0.05 μM fluorescein-γ′-peptide was monitored by fluorescence in the absence or presence of Zn^{2+} using a PerkinElmer Life Sciences LS 50B luminescence spectrometer (Pospisil *et al.*, 2003). Briefly, the base-line fluorescence (I_o) was determined at excitation and emission wavelengths (slit widths) of 492 (5 nm) and 532 nm (2.5 nm), respectively, and an emission filter at 515 nm. The mixture was then titrated with aliquots of $ZnCl_2$ up to 20 μM, and fluorescence intensity (I) was monitored after each addition. I/I_ovalues were plotted against the concentration of $ZnCl_2$, and the data were subjected to nonlinear regression analysis as previously described (Pospisil *et al.*, 2003).

3.4.2.8 Statistical Analyses

Results are presented as the mean ± S.D., and the significance of differences in the means was determined using *t* tests. For these analyses, $p<0.05$ was considered statistically significant.

3.5 RESULTS

3.5.1 Interactions of HRG with $\gamma_A/_A$- or γ_A/γ'-Fibrinogen

Although HRG has previously been shown to bind fibrinogen (Leung 1986), the distinction between γ_A/γ_A- and γ_A/γ'-fibrinogen binding has not been investigated. SPR was used to characterize the interaction between HRG and the two isoforms of fibrinogen. γ_A/γ_A- or γ_A/γ'-fibrinogen was immobilized on separate flow cells of a CM4 sensor chip, and an unmodified flow cell served as the control. HRG did not bind either form of fibrinogen in the presence of Ca^{2+} alone (data not shown). Because Zn^{2+} facilitates the binding of ligands to HRG (Jones *et al.*, 2005), we examined the effect of Zn^{2+} on the HRG-fibrinogen interaction. The Req increased as a function of the Zn^{2+} concentration and saturated at ~30 μM $ZnCl_2$ (Fig. 3.1). At each Zn^{2+} concentration, more HRG bound to γ_A/γ'-fibrinogen than to γ_A/γ_A-fibrinogen. The apparent K_d values of $ZnCl_2$ necessary to promote HRG binding to γ_A/γ_A- or γ_A/γ'-fibrinogen were 4.9 ± 0.2 and 1.2 ± 0.8 μM, respectively. The Zn^{2+} dependence of the interaction of HRG with fibrin(ogen) is in apparent contradiction to previous work demonstrating HRG binding to fibrin without Zn^{2+}addition (Leung, 1986). Because no binding was detected in the absence of Zn^{2+} in our study, it is likely that the HRG preparation used in the previous report contained sufficient amounts of Zn^{2+} to enable the interaction. For the remainder of the study, $ZnCl_2$ was used at a concentration of 20 μM. This concentration was chosen because the physiological concentration of Zn^{2+} in plasma ranges from 10 to 20 μM (Gorgani *et al.*, 1999, Jones *et al.*, 2004b). As evidenced from the similarity in saturation profiles

illustrated in Fig. 3.1, more than 80% of HRG is bound to both forms of fibrinogen at 20 μM $ZnCl_2$.

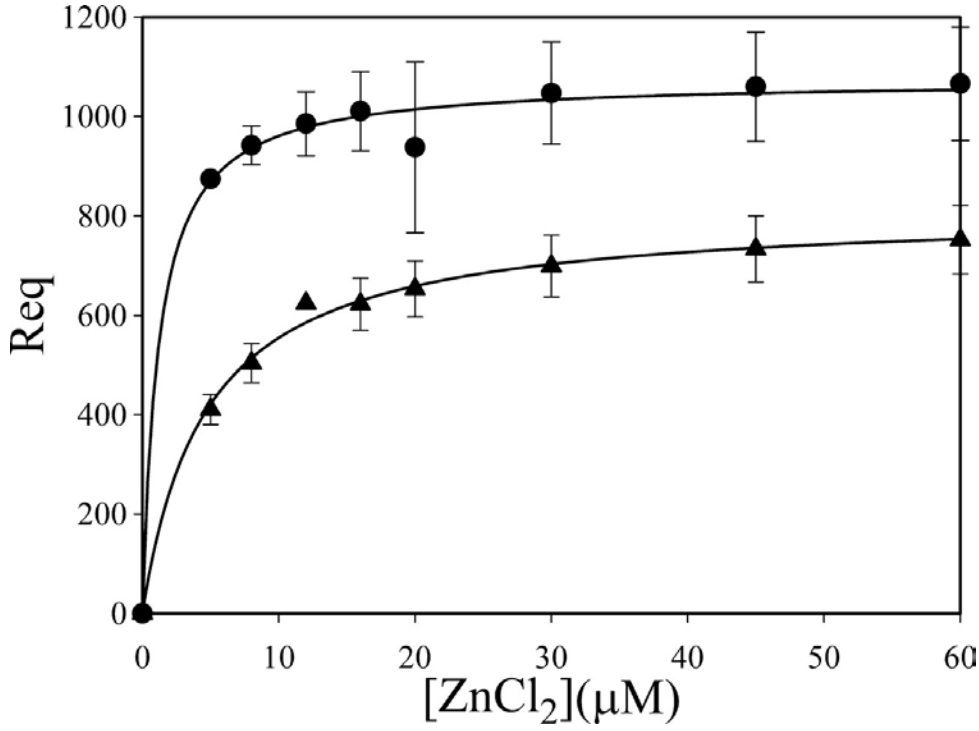
1200
1000
800
600
400
200
0
Req
0
10
20
30
40
50
60
[ZnCl2](μM)

Figure 3.1 Effect of $ZnCl_2$ on the binding of HRG to γ_A/γ_A- or γ_A/γ'-fibrinogen.

γ_A/γ_A-Fibrinogen (*triangles*) or γ_A/γ'-fibrinogen (*circles*) was immobilized to 6000–7000 RU on separate flow cells of a CM4 BIAcore chip. An unmodified flow cell served as control. HRG (0.2 μM) was injected into flow cells in the absence or presence of $ZnCl_2$ at the concentrations indicated. The RU at equilibrium (Req) was calculated and, after background correction, is plotted against the input $ZnCl_2$ concentrations. Data represent the mean ± S.D. of two experiments, and *lines* represent nonlinear regression analyses of the data.

To determine the affinity of HRG for fibrinogen, increasing concentrations of HRG were sequentially injected into flow cells containing immobilized fibrinogen in the presence of 20 μM $ZnCl_2$. The sensograms reveal slow association and dissociation phases for HRG binding to both isoforms of fibrinogen (Fig. 3.2 *A* and *B*). K_d values were obtained by kinetic analysis of the on- and off-rates by globally fitting the binding data. In the presence of Zn^{2+}, HRG binds γ_A/γ_A- and γ_A/γ'-fibrinogen with similar affinity, K_d values of 8.8 ± 0.9 and 8.9 ± 3.9 nM, respectively (Table 3.1). These values agree with the previously reported K_d of 6.7 nM determined by immunoassay (Leung, 1986). Plots of calculated Req values for each HRG concentration revealed saturable binding and demonstrated that binding of HRG to γ_A/γ'-fibrinogen was significantly ($p<0.005$) higher than that for γ_A/γ_A-fibrinogen (Fig. 3.3), suggesting that 2-fold more HRG is bound to the γ_A/γ'-fibrinogen isoform. The molar stoichiometries for the interaction of HRG with γ_A/γ_A-fibrinogen and γ_A/γ'-fibrinogen are 1.7 ± 0.3 and 3.2 ± 0.5, respectively (Table 3.1). Because the extended COOH terminus of the γ′-chain is the feature that distinguishes γ_A/γ'-fibrinogen from γ_A/γ_A-fibrinogen, the increased binding of HRG to γ_A/γ'-fibrinogen suggests that the γ′-chain provides the additional HRG binding site.

3.5.2 Effect of the γ′-Peptide-directed IgG on the Binding of HRG to γ_A/γ_A- or γ_A/γ'-Fibrinogen

To confirm that HRG binds specifically to the γ′-chain of γ_A/γ'-fibrin(ogen), we examined the effect of an affinity-purified IgG directed against this region. As an initial control, we demonstrated specific binding of the antibody to immobilized γ_A/γ'-fibrinogen but not to γ_A/γ_A-fibrinogen (data not shown). We next examined the effect of the antibody

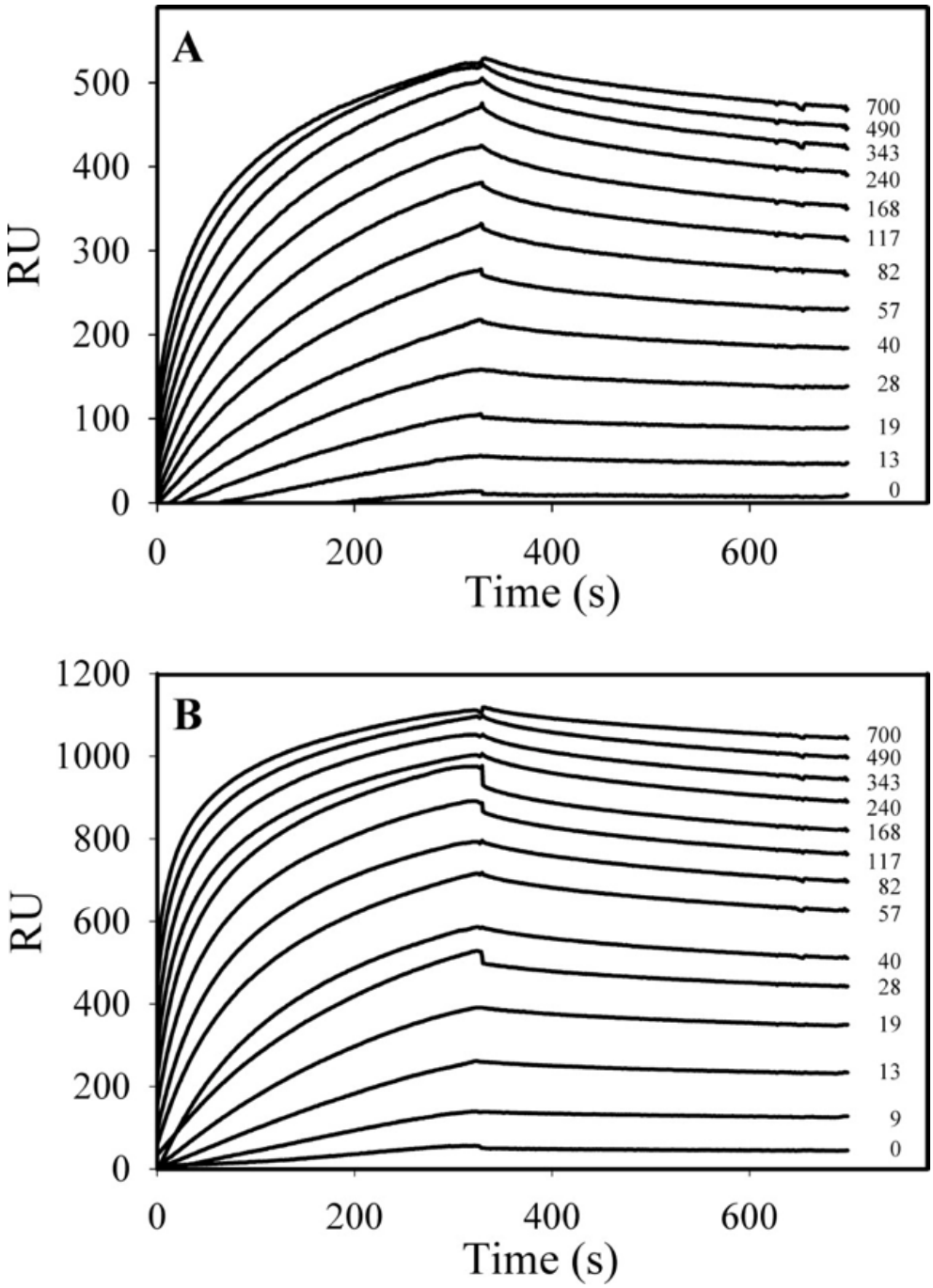
A
RU
500
400
300
200
100
0
0
200
400
600
Time (s)
700
490
343
240
168
117
82
57
40
28
19
13
0
B
RU
1200
1000
800
600
400
200
0
0
200
400
600
Time (s)
700
490
343
240
168
117
82
57
40
28
19
13
9
0

Figure 3.2 Determination of the affinity of HRG for γ_A/γ_A- or γ_A/γ'-fibrinogen in the presence of $ZnCl_2$.

γ_A/γ_A-Fibrinogen (*A*) or γ_A/γ'-fibrinogen (*B*) was adsorbed to separate flow cells on a CM4 chip. HRG (0–700 nM) was injected into flow cells for 300 s in the presence of 20 μM $ZnCl_2$, and the cells were then washed with HBS buffer containing 2 mM $CaCl_2$ and 20 μM $ZnCl_2$ for 500 s to monitor dissociation. HRG concentrations in nM are indicated adjacent to each sensogram tracing. These are data from a single experiment, which was performed three times.

	K_d	Stoichiometry
	nM	HRG/molecule
γ_A/γ_A-Fibrinogen	8.8 ± 0.9	1.7 ± 0.3
γ_A/γ'-Fibrinogen	8.9 ± 3.9	3.2 ± 0.5
γ_A/γ_A-Fibrin	19.3 ± 2.6	1.8 ± 0.3
γ_A/γ'-Fibrin	10.9 ± 0.9	2.9 ± 0.6
γ'-Peptide	0.8 ± 0.01	0.7 ± 0.02

Table 3.1 Dissociation constants and stoichiometries for the binding of HRG to γ_A/γ_A-fibrin(ogen), γ_A/γ'-fibrin(ogen), or γ'-peptide.

The binding of HRG to immobilized fibrin(ogen) isoforms or γ′-peptide in the presence of 20 μM Zn^{2+} was quantified using SPR. K_d values were determined by kinetic analysis of the data, and stoichiometries were calculated according to the BIAtechnology handbook.

on HRG binding to γ_A/γ'- or γ_A/γ_A-fibrinogen. The γ′-chain-directed antibody reduced HRG binding to γ_A/γ'-fibrinogen to that observed with γ_A/γ_A-fibrinogen (Fig. 3.3). As a control, a sheep non-immune IgG was used; the control IgG had no effect on the binding of HRG to fibrinogen (data not shown). Because the interaction of HRG with γ_A/γ_A-fibrinogen is already of high affinity, the addition of the γ′-peptide-directed IgG did not alter the affinity of HRG for γ_A/γ'-fibrinogen. However, in the presence of the antibody, the molar stoichiometry of HRG for γ_A/γ'-fibrinogen was similar to that for γ_A/γ_A-fibrinogen (1.8 ± 0.5 and 1.8 ± 0.6, respectively), providing further support for the concept that the γ′-chain on γ_A/γ'-fibrinogen represents a unique HRG binding site. These data suggest that HRG has multiple high-affinity binding sites on fibrinogen and that blocking one binding site has minimal effects on the others.

3.5.3 HRG Binding to the γ′-Peptide

To confirm that the γ′-chain affords HRG an additional binding site, binding of HRG to synthetic γ′-peptide was examined. First, the interaction of HRG with fluorescein-γ′-peptide was examined by fluorescence. Neither HRG nor Zn^{2+} alone altered the fluorescence intensity of the f-γ′-peptide, suggesting that in the absence of Zn^{2+}, there is no interaction. However, when Zn^{2+} was titrated in the presence of HRG, the fluorescence intensity of fluorescein-γ′-peptide decreased in a dose-dependent and saturable manner (Fig. 3.4 *A*), suggesting that Zn^{2+} facilitates the binding of HRG to the peptide. Nonlinear regression analysis of the data revealed that the apparent K_d for $ZnCl_2$ required to promote the HRG-fluorescein-γ′-peptide interaction was 9.1 ± 4.5 μM. This

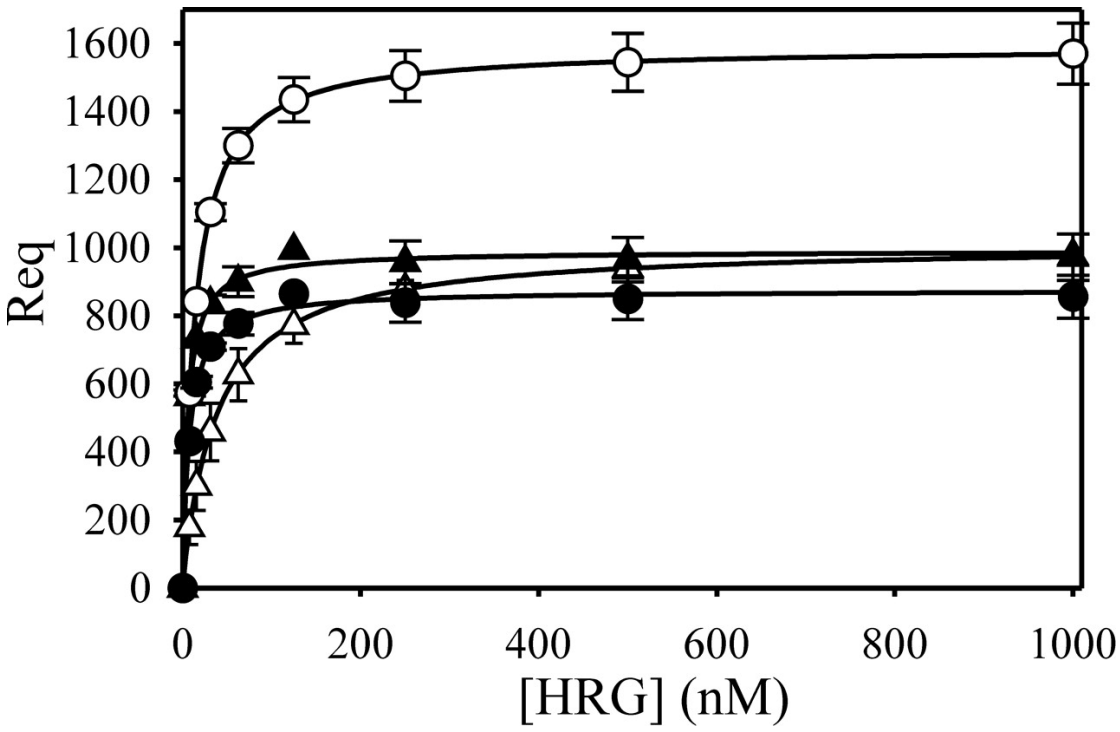
Req
1600
1400
1200
1000
800
600
400
200
0
0
200
400
600
800
1000
[HRG] (nM)

Figure 3.3 Effect of the γ′-peptide-directed IgG on HRG binding to γ_A/γ_A- or γ_A/γ'-fibrinogen.

Flow cells containing immobilized γ_A/γ_A-fibrinogen (*triangles*) or γ_A/γ'-fibrinogen (*circles*) were pretreated with (*closed*) or without (*open*) 0.5 μM γ′-peptide-directed IgG before injection of HRG (0–1.0 μM). *Symbols* represent the mean ± S.D. of two experiments, and *lines* represent nonlinear regression analyses of the data.

value is similar to the apparent K_d of 1.2 μM for Zn^{2+}-mediated promotion of HRG binding to γ_A/γ'-fibrinogen (Fig. 3.1).

To confirm these results, the interaction of HRG with γ′-peptide was examined by SPR. Biotinylated γ′-peptide was adsorbed to a streptavidin-modified flow cell, and HRG binding was monitored in the presence of 20 μM $ZnCl_2$. HRG bound immobilized γ′-peptide in a concentration-dependent and saturable manner, and binding was blocked by the γ′-peptide-directed IgG (Fig. 3.4 *B*). Based on kinetic analysis, HRG binds the γ′-peptide with a K_d value of 0.79 ± 0.01 nM in the presence of Zn^{2+}; there is no detectable binding in the absence of Zn^{2+} (data not shown). These data offer independent confirmation that HRG binds to the COOH terminus of the γ′-chain of γ_A/γ'-fibrinogen in a Zn^{2+}-dependent fashion.

3.5.4 Effect of the γ′-Peptide-directed IgG on the Binding of HRG to γ_A/γ_A- or γ_A/γ'-Fibrin

Having shown that HRG binds fibrinogen with high affinity in a Zn^{2+}-dependent fashion, we next used SPR to determine the affinity of HRG for fibrin. To convert immobilized fibrinogen to fibrin, flow cells were treated with thrombin (Petrera *et al.*, 2009). HRG bound to both isoforms of fibrin with affinities (Table 3.1) and Req values similar to those for fibrinogen, suggesting that HRG binding is unaltered when fibrinogen is converted to fibrin. To complement the SPR studies, we also assessed the binding of ^{125}I-HRG to fibrin clots. Clots containing varying concentrations of fibrinogen were prepared, and the amount of ^{125}I-HRG in the supernatants of compacted clots was determined. In keeping with our SPR data, ^{125}I-HRG did not bind to fibrin clots in the

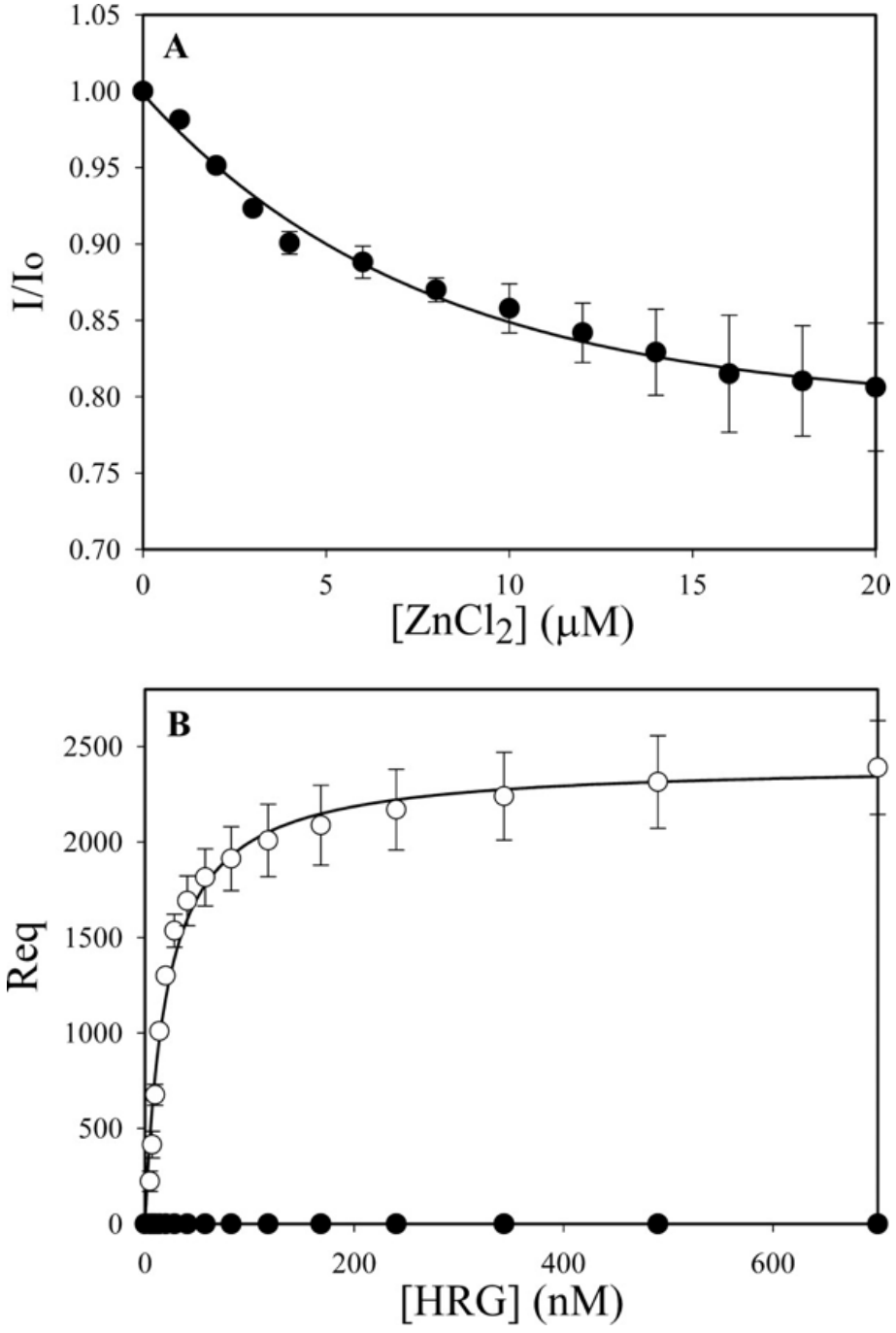
A
I/Io
1.05
1.00
0.95
0.90
0.85
0.80
0.75
0.70
0
5
10
15
20
[ZnCl2] (μM)
B
Req
2500
2000
1500
1000
500
0
0
200
400
600
[HRG] (nM)

Figure 3.4 Binding of HRG to γ′-peptide.

A, the binding of 1.1 μM HRG to fluorescein-labeled γ′-peptide (50 nM) was monitored in the presence of $ZnCl_2$ (0–20 μM) at λ_{ex}= 492 nm and λ_{em}= 532 nm. Initial fluorescence was determined in the presence of HRG but in the absence of $ZnCl_2$ (I_o). Aliquots of $ZnCl_2$ were then added, and the fluorescence intensity (I) was measured after each addition. I/I_o values are plotted *versus* $ZnCl_2$ concentrations. *B*, binding of HRG to immobilized γ′-peptide was measured by SPR. Biotinylated γ′-peptide was adsorbed to a streptavidin-immobilized CM4 chip. Binding of HRG (0–700 nM) to γ′-peptide in the presence of 20 μM $ZnCl_2$ was then determined in the absence (*open symbols*) or presence (*closed symbols*) of the γ′-peptide-directed IgG. Corrected Req values are plotted against the input HRG concentrations. *Symbols* represent the mean ± S.D. of two experiments, and *lines* represent nonlinear regression analyses of the data.

absence of Zn^{2+} (data not shown). With 20 μM Zn^{2+}, ^{125}I-HRG bound to γ_A/γ_A- and γ_A/γ'-fibrin clots with K_d values of 105.9 ± 21.0 and 33.3 ± 6.2 nM, respectively (Fig. 3.5 *A*). Similar results were obtained in the reciprocal experiment using varying concentrations of ^{125}I-HRG and a fixed concentration of fibrinogen (data not shown). The binding constants obtained here are comparable with the previously reported K_d value of 250 nM for the interaction of ^{125}I-HRG with fibrin formed from unfractionated fibrinogen, which consists of both isoforms of fibrinogen (Leung, 1986). Taken together, these results suggest that HRG binds fibrinogen and remains bound when fibrinogen is converted to fibrin.

Next, we examined the effect of varying concentrations of Fab fragments derived from the γ′-peptide-directed IgG on ^{125}I-HRG binding to γ_A/γ_A- or γ_A/γ'-fibrin clots. Fab fragments had minimal effects on HRG binding to γ_A/γ_A-fibrin clots (Fig. 3.5 *B*). In contrast, at 4 μM, the Fab fragments reduced HRG binding to γ_A/γ'-fibrin clots by 50%, providing further evidence that HRG binds to the γ′-chain of γ_A/γ'-fibrin. A non-immune sheep IgG was used as a control and demonstrated no effect.

3.5.5 HRG Binding to Fibrinogen Fragments

To localize the HRG binding domains on fibrinogen, binding of HRG to immobilized fibrinogen fragments was examined by SPR (data not shown). To avoid potential contribution of the γ′-chain to HRG binding, fragments X, D, and E were prepared from γ_A/γ_A-fibrinogen. In the presence of Zn^{2+}, HRG bound fragment X with a K_d value of 63.5 ± 11.8 nM, suggesting that the αC-domain of fibrinogen does not represent the primary HRG binding site. HRG also bound fragments D and E with high affinity in a Zn^{2+}-dependent manner, with K_d values of 8.0 ± 1.3 and 23.3 ± 2.2 nM,

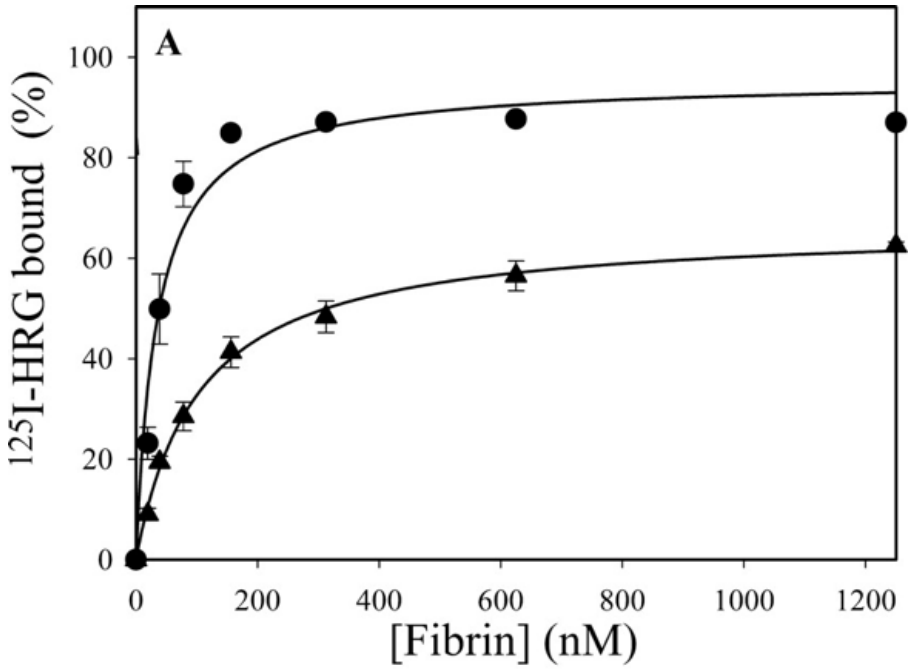
A
100
80
60
40
20
0
^{125}I-HRG bound (%)
0
200
400
600
800
1000
1200
[Fibrin] (nM)

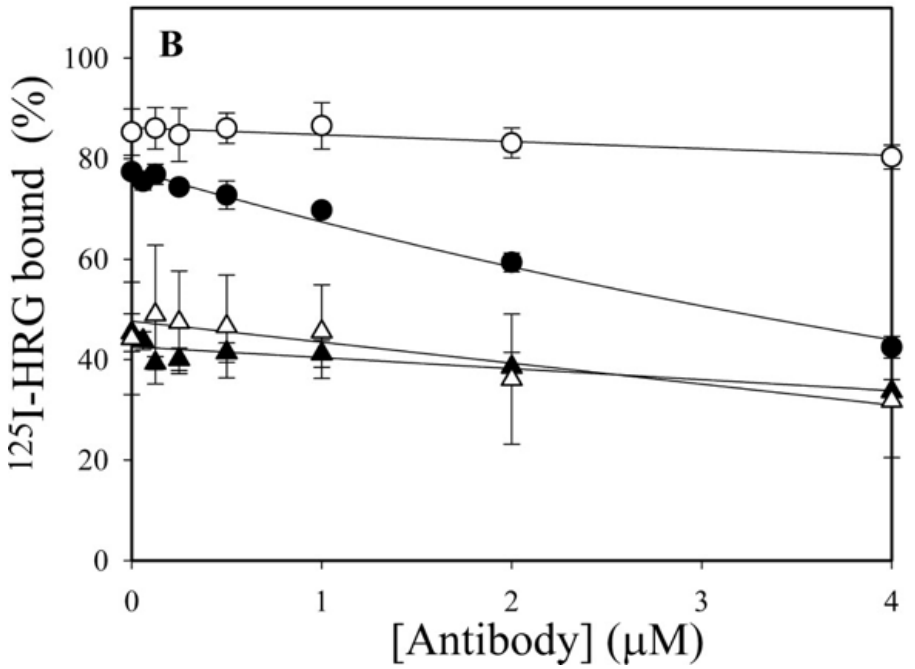
B
100
80
60
40
20
0
^{125}I-HRG bound (%)
0
1
2
3
4
[Antibody] (μM)

Figure 3.5 Binding of ^{125}I-HRG to γ_A/γ_A- or γ_A/γ'-fibrin clots.

A, 0–1.25 μM γ_A/γ_A- (*triangles*) or γ_A/γ'-fibrinogen (*circles*) was added to microcentrifuge tubes, and the binding of ^{125}I-HRG (40 nM) to clots was assessed after thrombin addition. *B*, the binding of ^{125}I-HRG (20 nM) to 0.25 μM γ_A/γ_A- (*triangles*) or γ_A/γ'-fibrin clots (*circles*) was assessed in the presence of 0–4 μM γ′-peptide-directed Fab fragments (*closed symbols*) or a control sheep IgG (*open symbols*). Experiments were performed in TBS-Tween containing 20 μM $ZnCl_2$ and 2 mM $CaCl_2$ and clots were generated with 10 nM thrombin. After incubation at 23°C for 45 min, fibrin clots were pelleted by centrifugation, and the amount of free ^{125}I-HRG in the supernatant was used to calculate the fraction bound. The percent of HRG bound to the clots is plotted *versus* fibrin or antibody concentrations. *Symbols* represent the mean ± S.D. of two experiments, each performed in duplicate, whereas the *lines* represent nonlinear regression analyses of the data.

respectively. As a negative control, we demonstrated that HRG did not bind immobilized FPRck-thrombin in the absence or presence of Zn^{2+}. As a positive control, we showed that FPRck-thrombin bound fragment E, with a K_d value of 5.0 ± 0.4 μM, but did not bind fragment D, findings in agreement with previously published results (Kaczmarek and McDonagh, 1988). Therefore, these data suggest that, in addition to its interaction with the γ′-chain, HRG binds to other unique sites on fibrinogen.

3.5.6 Diffusion of HRG from Fibrin Clots

To identify differences in the binding of HRG to γ_A/γ_A- and γ_A/γ'-fibrin clots, we monitored the dissociation of ^{125}I-HRG from preformed fibrin clots (Fig. 3.6). Diffusion in the presence of 2 M NaCl and 2 mM EDTA served as the base-line control because ionic and divalent cation-dependent interactions are abrogated (Fredenburgh *et al.*, 2008, Petrera *et al.*, 2009). In the presence of Zn^{2+}, the rates of diffusion of ^{125}I-HRG from γ_A/γ_A- and γ_A/γ'-fibrin clots were significantly (p<0.05) slowed by 3- and 11-fold, respectively, compared with those determined in the presence of diethyldithiocarbamate trihydrate, a specific Zn^{2+} chelator (Lakomaa *et al.*, 1982). Consistent with the concept that γ_A/γ'-fibrin affords HRG an additional binding site, the rate of ^{125}I-HRG diffusion from γ_A/γ'-fibrin was 3-fold slower than that from γ_A/γ_A-fibrin (p<0.05). Collectively, our results offer independent confirmation that the HRG-fibrinogen interaction is Zn^{2+}-dependent and that there is an additional HRG binding site on γ_A/γ'-fibrin.

3.5.7 Effect of FPRck-thrombin on HRG Binding to the γ′-Chain

In addition to binding HRG, the γ′-chain COOH extension binds thrombin (Meh *et al.*, 1996, Pospisil *et al.*, 2003). SPR was used to determine whether the two proteins

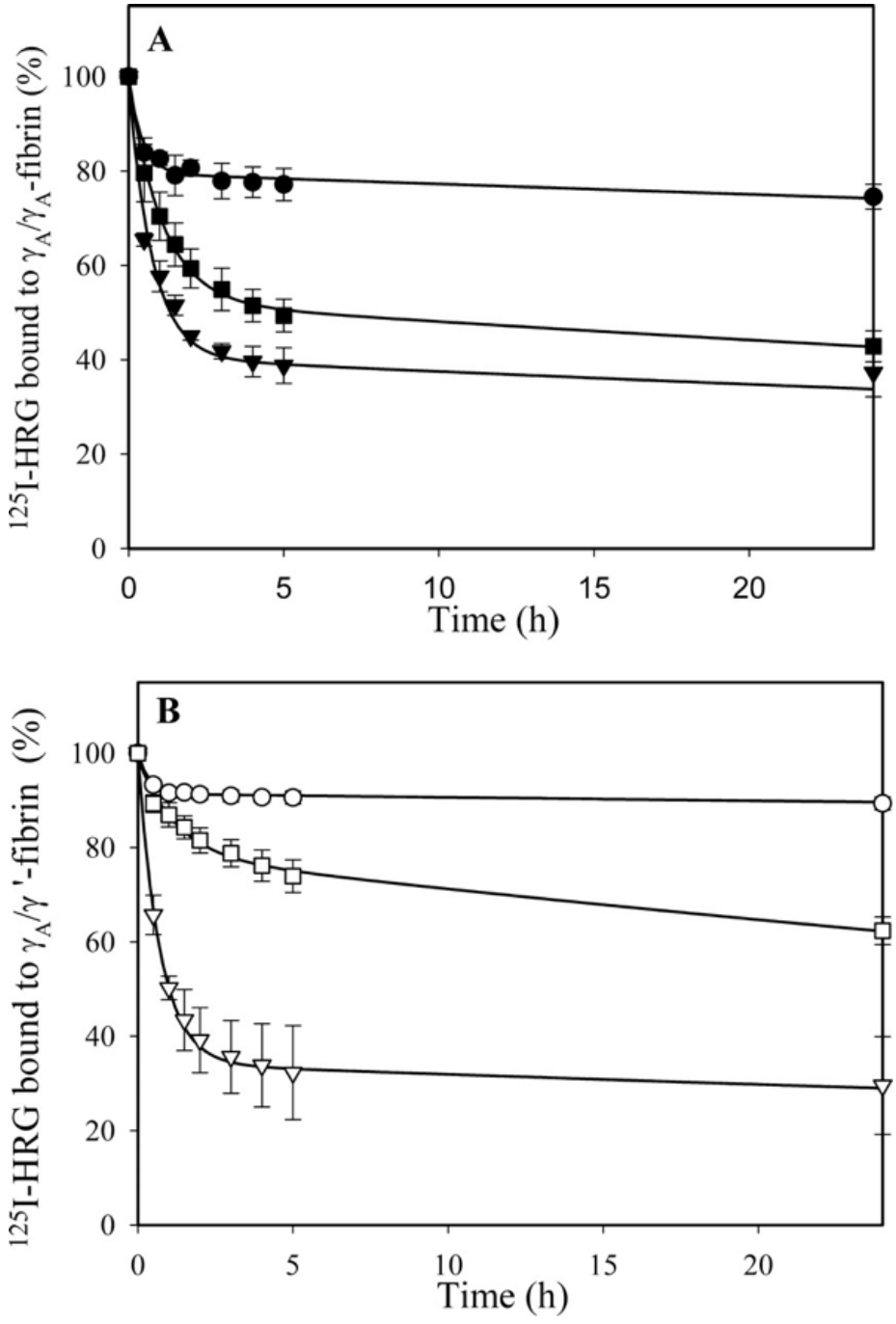
A
^{125}I-HRG bound to γ_A/γ_A-fibrin (%)
100
80
60
40
20
0
0
5
10
15
20
Time (h)
B
^{125}I-HRG bound to γ_A/γ'-fibrin (%)
100
80
60
40
20
0
0
5
10
15
20
Time (h)

Figure 3.6 Dissociation of ^{125}I-HRG from preformed γ_A/γ_A- or γ_A/γ'-fibrin clots.

Aliquots of 5 μM γ_A/γ_A- (*A*) or γ_A/γ'-fibrinogen (*B*) containing 2 mM $CaCl_2$, 20 μM $ZnCl_2$, 20 nM FXIII, and 50 nM ^{125}I-HRG were clotted with 10 nM thrombin around plastic inoculation loops. After incubation at 23°C for 45 min, clots were counted for radioactivity and incubated in tubes containing 5 ml of 2 M NaCl and 2 mM of EDTA (*triangles*), 2 mM $CaCl_2$ and 10 μM diethyldithiocarbamate trihydrate (*squares*), or 2 mM $CaCl_2$ and 20 μM $ZnCl_2$ (*circles*). At intervals, clots were removed, and residual radioactivity was used to determine the percent of ^{125}I-HRG that remained clot-associated. The *symbols* represent the mean ± S.D. of three experiments, whereas the *lines* represent nonlinear regression analyses of the data using two-component exponential decay model.

compete for binding to this region. This approach exploits the fact that the dissociation rate of HRG from immobilized γ′-peptide is much slower than that of thrombin. HRG (1 μM) was injected into flow cells containing immobilized biotinylated γ′-peptide, and the subsequent dissociation phase was monitored in the absence or presence of FPRck-thrombin or prothrombin in concentrations up to 8.0 μM. Prothrombin was used as a negative control because it does not bind to the γ′-peptide (Kretz *et al.*, 2006). Whereas FPRck-thrombin displaced HRG from the γ′-peptide in a concentration-dependent manner, prothrombin did not (Fig. 3.7). These data confirm that thrombin and HRG compete for binding to the γ′-peptide.

To determine whether the same was true with fibrin clots, we next examined the effect of increasing concentrations of FPRck-thrombin on ^{125}I-HRG binding to γ_A/γ_A- or γ_A/γ'-fibrin clots. At 10 μM, FPRck-thrombin reduced the amount of HRG bound to γ_A/γ'-fibrin clots by 90% but only reduced HRG bound to γ_A/γ_A-fibrin clots by 15% (Fig. 3.8 *A*). Similar results were obtained in the reciprocal competition experiments using varying concentrations of HRG and a fixed concentration of ^{125}I-YPRck-thrombin (Fig. 3.8 *B*). Collectively, these data confirm that HRG and thrombin compete for binding to the γ′-chain on γ_A/γ'-fibrin(ogen) in a mutually exclusive fashion.

3.5.8 Detection of HRG-Fibrinogen Complexes in Plasma

Because HRG binds fibrinogen with high affinity, it was of interest to determine whether HRG-fibrinogen complexes can be detected in plasma by immunoassay. Plasma was first dialyzed to remove citrate and then reconstituted with 18 μM $ZnCl_2$. The concentration of HRG-fibrinogen complexes detected in normal plasma was 1 μM, whereas no complexes

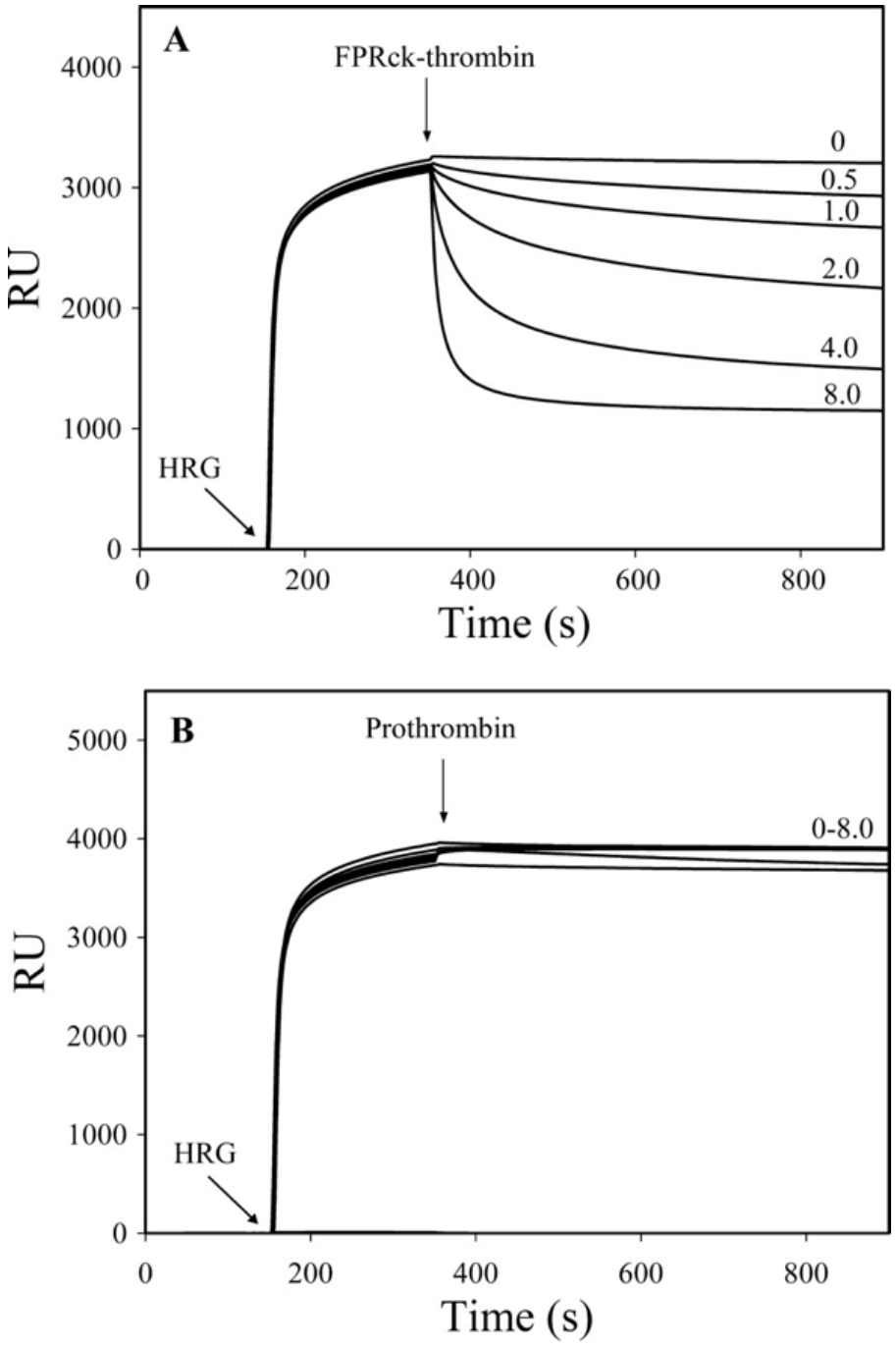
A
FPRck-thrombin
0
0.5
1.0
2.0
4.0
8.0
HRG
RU
Time (s)
B
Prothrombin
0-8.0
HRG
RU
Time (s)

Figure 3.7 Effect of FPRck-thrombin or prothrombin on the interaction of HRG with γ′-peptide.

Biotinylated γ′-peptide was immobilized on a streptavidin-modified flow cell to 200 RU, and an unmodified flow cell served as a control. *Arrows* indicate injection of 1 μM HRG for 200 s followed by injections of FPRck-thrombin (*panel A*) or prothrombin (*panel B*) at the concentrations (μM) indicated. Injections were carried out in the presence of 20 μM Zn^{2+}. These are data from a single experiment, which was performed three times.

were detected in HRG-deficient plasma. Because the plasma concentration of HRG ranges from 1.6 to 2 μM (Leung *et al.*, 1983, Lijnen *et al.*, 1980, MacQuarrie *et al.*, 2011), our findings suggest that in the presence of Zn^{2+} ~50–60% of HRG in plasma circulates in complex with fibrinogen.

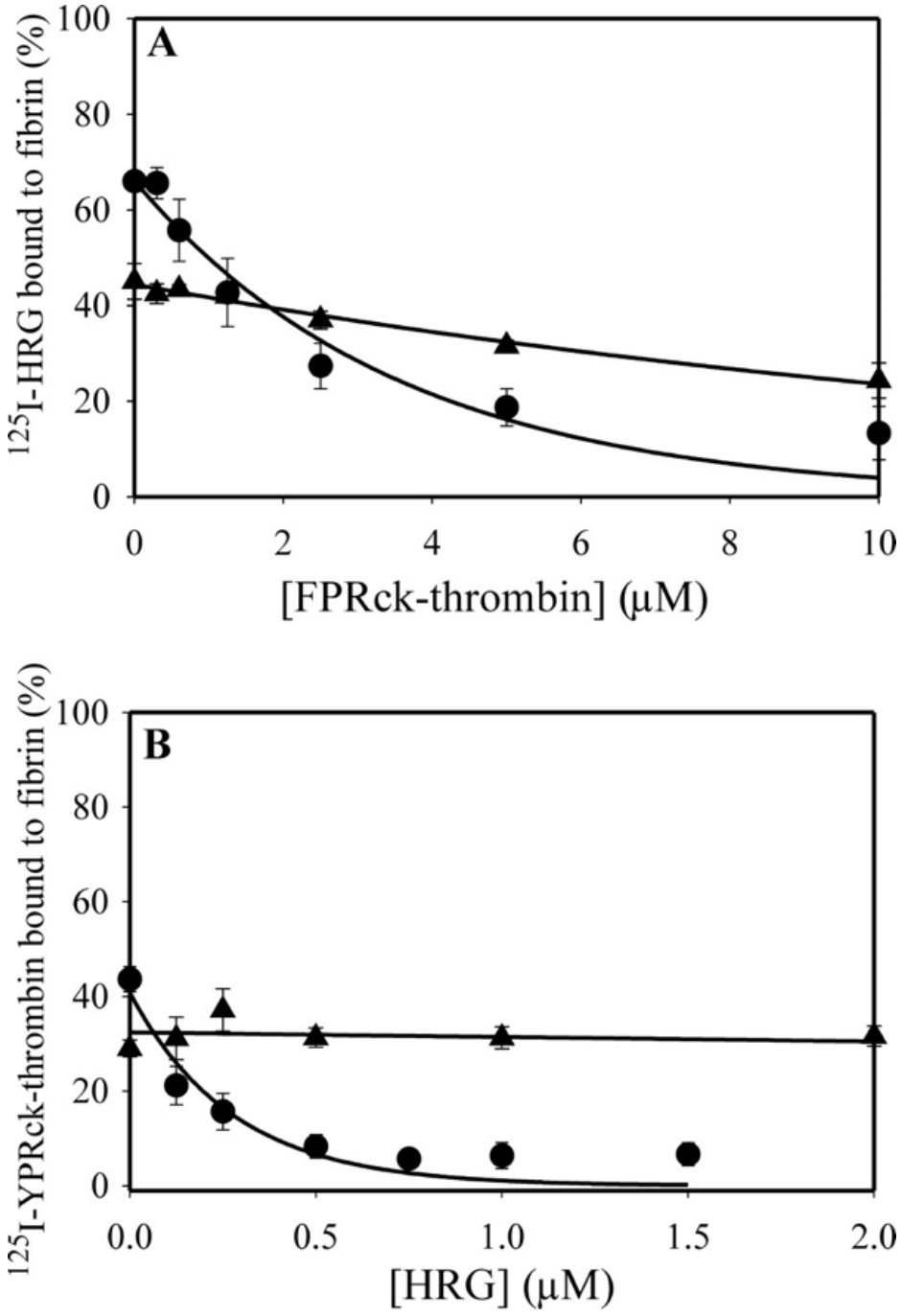
A
^{125}I-HRG bound to fibrin (%)
100
80
60
40
20
0
0
2
4
6
8
10
[FPRck-thrombin] (μM)
B
^{125}I-YPRck-thrombin bound to fibrin (%)
100
80
60
40
20
0
0.0
0.5
1.0
1.5
2.0
[HRG] (μM)

Figure 3.8 Effect of competitors on the binding of ^{125}I-HRG or ^{125}I-YPRck-thrombin to γ_A/γ_A- or γ_A/γ'-fibrin clots.

A, ^{125}I-HRG (20 nM) was added to microcentrifuge tubes containing 2 μM γ_A/γ_A-fibrinogen (*triangles*) or γ_A/γ'-fibrinogen (*circles*) in the presence of FPRck-thrombin (0–10 μM). *B*, ^{125}I-YPRck-thrombin (20 nM) was added to microcentrifuge tubes containing 2 μM γ_A/γ_A-fibrinogen (*triangles*) or 0.25 μM γ_A/γ'-fibrinogen (*circles*) in the presence of HRG (0–2 μM). In both experiments 2 mM $CaCl_2$ plus 20 μM $ZnCl_2$ were present and clotting was initiated with 10 nM thrombin. After incubation at 23°C for 45 min, fibrin was pelleted by centrifugation, and free ^{125}I-HRG or ^{125}I-YPRck-thrombin in the supernatant was used to calculate the bound fraction. The percent of fibrin-bound ^{125}I-HRG or ^{125}I-YPRck-thrombin is plotted *versus* the FPRck-thrombin or HRG concentration, respectively. The *symbols* represent the mean ± S.D. of two experiments, each performed in duplicate, whereas the *lines* represent nonlinear regression analyses of the data.

3.6 DISCUSSION

Despite increasing evidence that the interaction of HRG with fibrin(ogen) plays an important role in innate immunity, inflammation, and coagulation, little is known about this interaction. To address this gap, we characterized the binding of HRG to γ_A/γ_A- and γ_A/γ'-forms of fibrinogen and fibrin. In the presence of physiological concentrations of Zn^{2+}, HRG binds γ_A/γ_A- and γ_A/γ'-fibrinogen with similar affinities (K_d values of ~9 nM). The affinities of HRG for both isoforms of fibrin are comparable to those for fibrinogen, suggesting that the conversion of fibrinogen to fibrin does not alter the binding of HRG. In addition to its interaction with the unique COOH terminus of the γ′-chain of γ_A/γ'-fibrin(ogen), HRG binds to fragments D and E, suggesting that there are several HRG binding sites on fibrinogen. In support of these observations, HRG-fibrinogen complexes were detected in plasma. Taken together, our findings suggest that HRG circulates in plasma bound to fibrinogen and that the complex remains intact when fibrinogen is converted to fibrin.

The absolute requirement for Zn^{2+} to promote the HRG-fibrinogen interaction underscores the regulatory role this cation may have in hemostasis. Zn^{2+} is important for the binding of HRG to bacteria, cells, and hemostatic factors, such as glycosaminoglycans, plasminogen, and factor XIIa (Borza and Morgan, 1998, Lijnen *et al.*, 1980, MacQuarrie *et al.*, 2011, Rydengard *et al.*, 2006). It is likely that there are still other HRG interactions that have been overlooked because of the widespread use of citrate as an anticoagulant. The total Zn^{2+} concentration in plasma is ~20 μM, and the majority of Zn^{2+} is bound to albumin (Stewart *et al.*, 2009). Although the concentration of

Zn^{2+} that is not bound to proteins is only 0.5–1 μM (Foote and Delves, 1984, Gorgani *et al.*, 1999), the free Zn^{2+} concentration can increase under a variety of conditions. For example, platelets can secrete Zn^{2+} when they are activated at sites of vascular injury (Marx *et al.*, 1993). Furthermore, when fatty acids bind to albumin, they displace Zn^{2+} from the protein, thereby providing another mechanism whereby the concentration of free Zn^{2+} in plasma can be augmented (Stewart *et al.*, 2009). In addition to alterations in the Zn^{2+} concentration, the activity of HRG can also be modulated by changes in pH, with optimal binding to ligands observed under more acidic conditions. Consequently, the decrease in pH that occurs with reduced tissue perfusion may also enhance the affinity of HRG for both Zn^{2+} and its ligands (Jones *et al.*, 2005). Therefore, the current data extend the concept that Zn^{2+} serves as a dynamic switch that regulates HRG activity and directs it to various pathways involved in hemostasis (Borza and Morgan, 1998, Jones *et al.*, 2005).

Although we show that Zn^{2+} is essential for the interaction of HRG with fibrin(ogen), the mechanism by which Zn^{2+} mediates this binding is unknown. Both HRG and fibrin(ogen) bind Zn^{2+} (Marx *et al.*, 1993, Vu *et al.*, 2011). Therefore, Zn^{2+} may act as a cofactor that simultaneously binds HRG and fibrin(ogen) in a coordinated fashion (Maret, 2004). Alternatively, Zn^{2+} binding to HRG may induce conformational changes that facilitate its interaction with fibrin(ogen), a concept supported by the observation that Zn^{2+} alters the conformation of a synthetic His-Pro-rich peptide (Jancso *et al.*, 2009). Furthermore, the intrinsic fluorescence of HRG decreases upon Zn^{2+} titration (data not shown), providing additional support for the notion that Zn^{2+} alters HRG conformation.

Binding of Zn^{2+} to the HRR domain of HRG indirectly promotes the interaction of heparan sulfate or plasminogen with the NH_2-terminal cystatin domains of HRG, suggesting that Zn^{2+} binding to the HRR domain modulates other domains (Jones *et al.*, 2004b, Jones *et al.*, 2004a). These data point to a mechanism whereby Zn^{2+} modulates the structure and function of HRG.

Because HRG binds to the γ′-chain on γ_A/γ'-fibrin(ogen), novel roles of HRG can be envisioned. In addition to binding HRG, the COOH terminus of the γ′-chain also binds thrombin and factor XIIIa and, by so doing, may modulate coagulation and fibrinolysis (Fredenburgh *et al.*, 2008, Lorand, 2001). The importance of fibrin as a reservoir of thrombin is highlighted by the observation that thrombi harvested at autopsy contain abundant amounts of active thrombin (Mutch *et al.*, 2001). Fibrin-bound thrombin has been postulated to be an important mediator of thrombus expansion because of its capacity to locally activate platelets and to promote its own generation through activation of factor V and factor VIII (Kumar *et al.*, 1995, Weitz and Bates, 2003). The procoagulant activity of thrombin bound to γ_A/γ'-fibrin appears to be greater than that of thrombin bound to γ_A/γ_A-fibrin because the γ′-chain mediates the high affinity interaction of thrombin with fibrin, and γ_A/γ'-fibrin affords bound thrombin more protection from inhibition by the antithrombin-heparin complex than γ_A/γ_A-fibrin (Fredenburgh *et al.*, 2008). Further support for this concept comes from epidemiological studies that suggest that higher circulating levels of γ_A/γ'-fibrinogen are associated with an increased risk of cardiovascular disease (Lovely *et al.*, 2002, van den Herik *et al.*, 2011). HRG competes with thrombin for binding to the γ′-chain as evidenced by its capacity to displace FPRck-

thrombin from γ′-peptide or from γ_A/γ′-fibrin clots. Consequently, by displacing fibrin-bound thrombin, HRG may have antithrombotic properties. HRG may also compete with factor XIII, which is proposed to bind the γ′-chain (Siebenlist *et al.*, 1996), thereby attenuating fibrin cross-linking and endowing HRG with pro-fibrinolytic activity. Studies in HRG-deficient mice support the concept that HRG affects hemostasis. HRG-deficient mice have a shorter prothrombin time and a longer bleeding time than their wild-type counterparts. In addition, thrombi formed in HRG-deficient mice are more susceptible to fibrinolysis than those generated in control mice (Tsuchida-Straeten *et al.*, 2005). The contribution of the HRG interaction with the γ′-chain to the anticoagulant and anti-fibrinolytic activities of HRG remains to be determined.

In addition to its role in hemostasis, fibrinogen appears to be an important mediator of inflammation and innate immunity because fibrinogen and fibrin stimulate peripheral blood mononuclear cells and vascular smooth muscle cells to synthesize proinflammatory cytokines (Guo *et al.*, 2009, Jensen *et al.*, 2007, Liu *et al.*, 2011). Furthermore, bacteria trapped within fibrin clots are protected from host defenses and the action of antibiotics (Turcotte and Bergeron, 1992). However, because HRG has antimicrobial properties, the HRG-fibrin interaction promotes bacterial entrapment and killing (Shannon *et al.*, 2010). The capacity of HRG to enhance bacterial killing has been localized to its NH_2-terminal and HRR domains. Thus, in the presence of Zn^{2+} or when the pH is low, HRG induces lysis of the bacterial cell wall (Rydengard *et al.*, 2006, Rydengard *et al.*, 2007, Rydengard *et al.*, 2008). These conditions can occur at sites of injury or wound-healing where activated platelets release Zn^{2+} and local ischemia lowers

pH (LaManna, 1996, Leung *et al.*, 1983). Activated platelets also release HRG (Leung *et al.*, 1983) and, by so doing, may amplify the antimicrobial effect. Our observation that HRG binds fibrinogen and fibrin provides a regulatory mechanism by which HRG may mediate bacterial killing within a clot. The importance of HRG in modulating the inflammatory response has been confirmed in mouse models. Thus, compared with wild-type mice, HRG-deficient mice given subcutaneous injections of *S. pyogenes* exhibit attenuated abscess formation and reduced recruitment of neutrophils and macrophages to the site of infection (Shannon *et al.*, 2010), suggesting that HRG modulates the inflammatory response. In support of this concept, a synthetic peptide analog of the HRR of HRG attenuated the secretion of interleukin-8 from lipopolysaccharide-stimulated, CD14-transfected monocytes (Bosshart and Heinzelmann, 2003). These observations raise the possibility that HRG plays a part in the inflammatory response to infection.

Although HRG is an abundant plasma protein with multiple ligands, its physiological role remains unknown (*for review, see* (Poon *et al.*, 2011)). HRG is hypothesized to be an important effector of hemostasis and immunity. The ability of HRG to bind fibrinogen and displace thrombin from fibrin may provide an important link between these two systems and reveals a potential mechanism by which this could occur. Additional regulation may result from variations in the local pH and/or Zn^{2+} concentration.

CHAPTER 4: Batroxobin binds fibrin with higher affinity and promotes clot expansion to a greater extent than thrombin

4.1 Forward: The interactions between batroxobin and fibrin(ogen) and the mechanisms by which batroxobin cleaves fibrinogen are described in this manuscript. We demonstrated that unlike thrombin, batroxobin forms a high affinity interaction with both isoforms of fibrin(ogen) that resembles thrombin binding to γ_A/γ'-fibrin(ogen). The batroxobin binding sites on fibrin(ogen) only partially overlap with those of thrombin. Like thrombin, batroxobin also remains bound to the fibrin clot and promotes clot expansion.

This manuscript has been published in the *Journal of Biological Chemistry* (Vol. 288, pp. 16862-16871, June 7, 2013). The authors are: Trang T. Vu, Alan R. Stafford, Beverly A. Leslie, Paul Y. Kim, James C. Fredenburgh and Jeffrey I. Weitz. Dr. Weitz is the corresponding author. According to the policies of the American Society for Biochemistry and Molecular Biology (ASBMB), no formal permission is required to reproduce this mauscript for non-commercial purposes.

The experiments in this manuscript were performed by Trang Vu. Dr. James Fredenburgh prepared the structural models and provided reagents. Alan Stafford and Beverly Leslie provided technical assistance and reagents. Dr. Paul Kim provided reagents. The project was designed and the manuscript written by Trang Vu, Dr. James Fredenburgh and Dr. Jeffrey Weitz.

Chapter 4 is a direct representation of the above referenced manuscript (Copyright © 2013 by ASBMB).

4.2 Capsule

4.2.1 Background: Snake venom protease batroxobin clots fibrinogen in a manner distinct from thrombin.

4.2.2 Results: Batroxobin binds fibrin(ogen) with higher affinity than thrombin and promotes greater clot expansion.

Conclusion: Batroxobin's distinctive interaction with fibrin(ogen) may contribute to its unique pattern of fibrinopeptide release.

4.2.3 Significance: Clinically, batroxobin is used as a defibrinogenating agent, but its capacity to promote clot expansion may promote microvascular thrombosis.

4.3 Summary

Batroxobin is a thrombin-like serine protease from the venom of *Bothrops atrox moojeni* that clots fibrinogen. In contrast to thrombin, which releases fibrinopeptide A and B from the NH_2-terminal domains of the Aα- and Bβ-chains of fibrinogen, respectively, batroxobin only releases fibrinopeptide A. Because the mechanism responsible for these differences is unknown, we compared the interactions of batroxobin and thrombin with the predominant γ_A/γ_A isoform of fibrin(ogen) and the γ_A/γ' variant with an extended γ-chain. Thrombin binds to the γ′-chain and forms a higher affinity interaction with γ_A/γ'-fibrin(ogen) than γ_A/γ_A-fibrin(ogen). In contrast, batroxobin binds both fibrin(ogen) isoforms with similar high affinity (K_d values of about 0.5 μM) even though it does not interact with the γ′-chain. The batroxobin-binding sites on fibrin(ogen) only partially overlap with those of

thrombin because thrombin attenuates, but does not abrogate, the interaction of γ_A/γ_A-fibrinogen with batroxobin. Furthermore, although both thrombin and batroxobin bind to the central E-region of fibrinogen with a K_d value of 2–5 μM, the α(17–51) and Bβ(1–42) regions bind thrombin but not batroxobin. Once bound to fibrin, the capacity of batroxobin to promote fibrin accretion is 18-fold greater than that of thrombin, a finding that may explain the microvascular thrombosis that complicates envenomation by *B. atrox moojeni*. Therefore, batroxobin binds fibrin(ogen) in a manner distinct from thrombin, which may contribute to its higher affinity interaction, selective fibrinopeptide A release, and prothrombotic properties.

4.4 Introduction

Fibrinogen is important for optimal primary and secondary hemostasis because of its critical role in platelet aggregation and fibrin clot formation (Wolberg, 2012). Fibrinogen is a dimeric glycoprotein composed of two pairs of Aα-, Bβ-, and γ-chains connected by numerous disulfide bonds (Mosesson, 2005). The NH_2 termini of the six chains form the central E-domain, which is connected by the coiled-coil regions to the peripheral D-domains formed by the COOH termini (Mosesson, 2005). There are two circulating isoforms of fibrinogen that differ with respect to their γ-chains. The predominant fibrinogen isoform is a homodimer that contains two γ_A-chains consisting of 411 residues and is designated γ_A/γ_A-fibrinogen. About 10–15% of circulating fibrinogen is heterodimeric, containing one γ_A-chain and one variant γ′-chain that possesses a 16-residue anionic extension at its COOH terminus. This minor fibrinogen population is designated γ_A/γ'-fibrinogen (Chung and Davie, 1984, Fornace, Jr. *et al.*, 1984, Wolfenstein-Todel and Mosesson, 1980). Epidemiological studies suggest that elevated levels of circulating γ_A/γ'-fibrinogen are associated with an increased risk of cardiovascular disease (Lovely *et al.*, 2002, van den Herik *et al.*, 2011).

Thrombin is the protease that converts fibrinogen to insoluble fibrin by releasing fibrinopeptides (Fp) A and B from the NH_2 termini of the Aα- and Bβ-chains, respectively (Blomback *et al.*, 1978). Fibrin polymerization occurs when the newly exposed NH_2termini on one fibrin monomer bind to pre-existing complementary sites on the D-domains of adjacent fibrin monomers (Blomback *et al.*, 1978, Mosesson, 2005, Mullin *et al.*, 2000). During this process, some thrombin remains bound to the fibrin clot

(Weitz *et al.*, 1990). Thrombin possesses two anion-binding exosites that flank the active site and mediate substrate binding and catalysis (Adams and Huntington, 2006, Huntington, 2005). Exosite 1 mediates thrombin binding to the Aα- and Bβ-chains in the central E-region of fibrin(ogen), whereas exosite 2 is responsible for thrombin's interaction with the unique COOH terminus of the γ′-chain of a second fibrin(ogen) molecule (Fredenburgh *et al.*, 2004, Mosesson, 2007). Consequently, thrombin binds γ_A/γ_A-fibrin solely via exosite 1 with a K_d value of 2–4 μM. In contrast, both exosites are engaged when thrombin binds to γ_A/γ'-fibrin(ogen), which results in an ~ 20-fold higher affinity interaction than that with γ_A/γ_A-fibrin (K_d value of 80–200 nM) (Meh *et al.*, 1996, Pospisil *et al.*, 2003). Because fibrin-bound thrombin retains activity and is protected from inhibition by AT and HCII, the fibrin clot serves as a reservoir of thrombin that promotes thrombus expansion by locally activating platelets and FXI, FVIII, and FV (Becker *et al.*, 1999, Weitz *et al.*, 1990, Weitz and Bates, 2003). The higher affinity, bivalent interaction of thrombin with γ_A/γ'-fibrin affords thrombin more protection from fluid-phase inhibitors than the univalent interaction of thrombin with γ_A/γ_A-fibrin (Fredenburgh *et al.*, 2008).

Batroxobin is a serine protease isolated from *Bothrops atrox moojeni* venom that clots fibrinogen (Da Graca Salomao *et al.*, 1997). In contrast to thrombin, fibrinogen is the sole substrate for batroxobin, and batroxobin only releases FpA and is not inhibited by antithrombin or heparin cofactor II (Aronson, 1976). Because of these properties, batroxobin is often used in clinical laboratories to determine whether prolonged thrombin clotting times are the result of heparin contamination or abnormal fibrinogen molecules

(Braud *et al.*, 2000). In addition, batroxobin has been used clinically for prevention and treatment of thrombosis because of its capacity to lower circulating fibrinogen levels (Latallo, 1983, Stocker, 1998, Wang *et al.*, 2010, Xu *et al.*, 2007).

Although it is well established that batroxobin induces defibrinogenation, the interaction of batroxobin with fibrinogen has not been studied nor is it known whether, like thrombin, batroxobin binds to fibrin and triggers thrombus expansion. The potential procoagulant activity of batroxobin is important because patients envenomated by *B. atrox moojeni* often experience thrombotic complications (White, 2005). To address these questions, (*a*) we characterized the binding of batroxobin to γ_A/γ_A- and γ_A/γ'-fibrinogen to determine whether its fibrinogen-binding sites overlap with those of thrombin because both enzymes release FpA; (*b*) we assessed the binding of batroxobin to γ_A/γ_A- and γ_A/γ'-fibrin clots to determine whether the protease remains bound to the product following catalysis; and (*c*) we measured the procoagulant activity of fibrin-bound batroxobin to determine whether, like fibrin-bound thrombin, batroxobin promotes clot expansion.

4.5 EXPERIMENTAL PROCEDURES

4.5.1 Materials

4.5.1.1 Reagents

Human α-thrombin and plasminogen-free fibrinogen were from Enzyme Research Laboratories (South Bend, IN), and FXIII was from Haematologic Technologies Inc. (Essex Junction, VT). Fibrinogen was endered FXIII-free, and γ_A/γ_A- and γ_A/γ'-fibrinogens were separated by fractionation on DEAE-Sepharose (GE Healthcare) as

described previously (Fredenburgh *et al.*, 2008, Schaefer *et al.*, 2006). Batroxobin from the venom of *B. atrox moojeni* was from Pentapharm (Basel, Switzerland). A 20-amino acid analog of the COOH terminus of the γ′-chain of fibrinogen with a Cys at the NH_2 terminus, termed γ′-peptide (VRPEHPAETEYDSLYPEDDL), and a γ′-peptide-directed IgG from sheep were prepared by Bachem Bioscience, Inc. (King of Prussia, PA). The two Tyr residues of the γ′-peptide were modified with phosphate groups to mimic the sulfated Tyr residues found in the native γ′-chain and to increase the affinity for thrombin (Lovely *et al.*, 2003). The γ′-peptide-directed IgG was subjected to affinity chromatography using immobilized γ′-peptide as described previously (Vu *et al.*, 2011). The α(17–51)-peptide (GPRVVERHQSAAKDSDWPFASDEDWNYKAPSGCRM) with Cys-28, Cys-36, and Cys-45 changed to Ala and an NH_2-terminal Cys residue was synthesized by LifeTein (Plainfield, NJ). Chromogenic substrates H-D-Phe-Pip-Arg-*p*-nitroaniline (S-2238) and Glu-Pro-Arg-nitroaniline (CS-21(66)) were from Chromogenix (Milano, Italy) and Aniaria (Neuville-sur-Oise, France), respectively. D-Phe-Pro-Arg-chloromethyl ketone (FPR) and D-Tyr-Pro-Arg-chloromethyl ketone (YPR) were from Calbiochem. Full-length hirudin was from Dade-Behring (Marburg, Germany). Citrated human plasma was prepared as described (Kretz *et al.*, 2010). Unless otherwise specified, other reagents were from Sigma.

4.5.1.2 Preparation of Fibrinogen Derivatives and Fragments

Fibrinogen derivatives and fragments were isolated from γ_A/γ_A-fibrinogen to eliminate the contribution of the γ′-chain. Des-Bβ(1–42) fibrinogen was prepared by incubating γ_A/γ_A-fibrinogen with protease III fraction from *Crotalus atrox* venom and

purified using ethanol precipitation as described (Pospisil *et al.*, 2003). Fragments D and E were generated by plasmin digestion and purified as reported previously (Vu *et al.*, 2011). The NH_2-terminal disulfide knot (NDSK) was obtained with cyanogen bromide treatment and purified as described (Olexa and Budzynski, 1979).

4.5.1.3 Modification of Proteins and Peptides

Batroxobin and thrombin were radiolabeled by reaction with ^{125}I-YPR, prepared using Na^{125}I (McMaster University Nuclear Reactor, Hamilton, Ontario, Canada) and IODO-BEADs (Pierce) as described (Fredenburgh *et al.*, 2008, Vu *et al.*, 2011). ^{125}I-YPR-batroxobin and ^{125}I-YPR-thrombin concentrations were 1–2 and 6–7 μM, respectively, as determined by absorbance at 280 nm, and had specific radioactivities of ~500,000–700,000 cpm/μg. Unfractionated fibrinogen (0.5 mg in phosphate-buffered saline) was radiolabeled with 1 mCi of Na^{125}I using 1 IODO-BEAD for 5 min at 23°C. The sample was then subjected to gel filtration on a PD-10 column (GE Healthcare). The labeled fibrinogen was over 90% clottable and had a specific radioactivity of 925,000 cpm/μg. FPR-batroxobin, FPR-thrombin, and biotin conjugated γ′- and α(17–51)-peptides were prepared as described (Petrera *et al.*, 2009).

4.5.2 Methods

4.5.2.1 Characterization of Thrombin and Batroxobin

The integrity of thrombin and batroxobin was assessed by SDS-PAGE analysis on 4–15% polyacrylamide gradient gels (Bio-Rad) under nonreducing conditions. Thrombin and batroxobin migrated as single bands with expected apparent molecular weights of 37,000 and 32,000, respectively (Fig. 4.1). The identity of batroxobin was confirmed by

amino acid sequence analysis. Briefly, batroxobin was resolved by SDS-PAGE, and protein bands were transferred to a PVDF membrane (Bio-Rad), and identified by Ponceau Red staining. The bands of interest were submitted for amino acid sequence analysis (Hospital for Sick Children Advanced Protein Technology Centre, Toronto, Ontario, Canada). In addition, SDS-PAGE analysis of batroxobin-treated fibrinogen revealed bands corresponding solely to α-, Bβ-, and γ-chains, indicating the absence of contaminating proteases in the batroxobin preparation (data not shown). The specificity of batroxobin was confirmed by comparing its capacity to cleave FpA and/or FpB from fibrinogen with that of thrombin. FpA and FpB release were quantified by HPLC using synthetic FpA (Bachem) and FpB (LifeTein) as internal standards (Cooper *et al.*, 2003), and the identities of released FpA and FpB were confirmed by mass spectrometry (Bioanalytical and Mass Spectrometry Laboratory, McMaster University). As expected, batroxobin only released FpA from fibrinogen, whereas thrombin released both FpA and FpB (data not shown); these findings are in agreement with previously published results (Moen *et al.*, 2003).

4.5.2.2 Surface Plasmon Resonance (SPR)

The interaction of FPR-batroxobin and FPR-thrombin with immobilized γ_A/γ_A- or γ_A/γ'-fibrin(ogen), biotinylated-γ′- and α(17–51)-peptides, NDSK, and fragments D or E was assessed by SPR on a BIAcore 1000 (GE Healthcare) as described (Fredenburgh *et al.*, 2008, Petrera *et al.*, 2009, Vu *et al.*, 2011), but with some modifications. Briefly, fibrinogen and fibrinogen fragments were covalently linked to separate flow cells of a

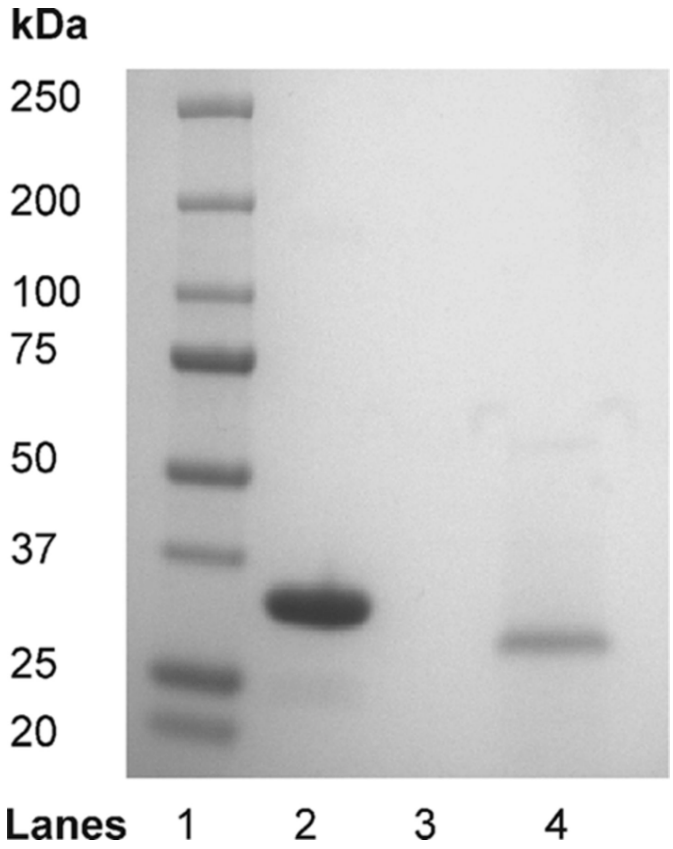
kDa
250
200
100
75
50
37
25
20
Lanes 1 2 3 4

Figure 4.1 Integrity of thrombin and batroxobin as assessed by SDS-PAGE analysis.

Thrombin (*lane 2*) and batroxobin (*lane 4*) were subjected to SDS-PAGE analysis on a 4–15% polyacrylamide gradient gel under nonreducing conditions. The molecular weights of the mobility markers are shown on the *left* (*lane 1*).

carboxymethylated dextran CM5 biosensor chip at a flow rate of 5 μl/min using an amine coupling kit (GE Healthcare). Proteins were immobilized in 10 mM acetate buffer at varying pH values to maximize adsorption. γ_A/γ_A- and γ_A/γ'-fibrinogen and fragment D were immobilized at pH 5.5 to ~6000–8000 response units (RU). Fragment E and NDSK were immobilized at pH 4.5 and 5.0 to ~6000–8000 RU, respectively. For fibrin studies, immobilized γ_A/γ_A- and γ_A/γ'-fibrinogen were converted to fibrin by three successive 60-min injections of 100 nM α-thrombin, each followed by a wash with 0.5 M NaCl (Petrera *et al.*, 2009, Vu *et al.*, 2011). To prepare streptavidin-conjugated CM5 cells, 0.4 mg/ml streptavidin was immobilized at pH 4.5. Biotinylated γ′-peptide and α(17–51) were adsorbed onto separate streptavidin-containing cells to 200–600 RU, whereas 0.4 mg/ml ovalbumin was immobilized at pH 4.5 to ~6000–8000 RU in control flow cells. The remaining reactive amine groups were neutralized with 1 M ethanolamine. All SPR procedures were done in 10 mM Hepes-NaOH, 150 mM NaCl at pH 7.4 (HBS) containing 0.005% Tween 20 and 2 mM $CaCl_2$ (HBS-Tw-Ca). Flow cells were regenerated with 0.5 M NaCl between runs. To measure the affinity of proteases for immobilized fibrinogen, fibrin, and fibrinogen fragments, aliquots of FPR-batroxobin or FPR-thrombin (0–40 μM) were injected at a flow rate of 30 μl/min. In reciprocal experiments, FPR-batroxobin and FPR-thrombin were immobilized at pH 4.5 to ~4000–6000 RU, and the binding of fibrinogen to the adsorbed proteins was assessed. The sensorgram tracings were obtained from the instrument software, and all experiments were performed at least twice.

To determine the extent to which the batroxobin and thrombin-binding sites on fibrinogen overlap, the binding of γ_A/γ_A-fibrinogen to immobilized FPR-batroxobin was measured as described previously in the absence or presence of FPR-thrombin up to 40 μM. As a positive control, the experiment was repeated in the presence of 80 μM hirudin; as a negative control, ovalbumin (0–40 μM) was used in place of FPR-thrombin. The amount of γ_A/γ_A-fibrinogen bound to adsorbed batroxobin in the presence of FPR-thrombin was normalized to that determined in the absence of competitor. All competition experiments were performed three times.

4.5.2.3 SPR Data Analysis

K_d values for one-site binding were determined by kinetic analysis of on- and off-rates of batroxobin or thrombin binding to immobilized ligands using Scrubber2 version 2.0a (Bio-Logic Software Co., Campbell, Australia) as described (Petrera *et al.*, 2009). To calculate two-site binding of thrombin to γ_A/γ'-fibrin(ogen), the amount of analyte bound at equilibrium (Req) was plotted against input protease concentrations and analyzed by nonlinear regression analysis of a two-site binding equation (Table Curve, Jandel Scientific, San Rafael, CA) as described (Pospisil *et al.*, 2003).

4.5.2.4 Binding of Batroxobin and Thrombin to Fibrin Clots

In a series of microcentrifuge tubes, up to 30 μM γ_A/γ_A-, γ_A/γ'-, or des-Bβ(1–42) γ_A/γ_A-fibrinogen was clotted with 10 nM thrombin in the presence of 20–40 nM ^{125}I-YPR-batroxobin or ^{125}I-YPR-thrombin in 20 mM Tris-HCl, pH 7.4, 150 mM NaCl (TBS) containing 0.005% Tween 20 and 2 mM $CaCl_2$ (TBS-Tw-Ca) (Petrera *et al.*, 2009). After 60 min of incubation at 23°C, clots were compacted by centrifugation at 14,000 × *g* for 4

min. Fibrin-bound ^{125}I-protease was quantified by subtracting the radioactivity in the clot supernatant from that obtained in controls prepared without fibrinogen. Plots of bound ^{125}I-protease *versus* fibrin concentration were analyzed by nonlinear regression of a rectangular hyperbola to determine the composite K_d value. Experiments were performed twice in duplicate.

4.5.2.5 Effect of Competitors on the Binding of ^{125}I-YPR-Batroxobin or ^{125}I-YPR-Thrombin to Fibrin

Affinity-purified γ′-peptide-directed IgG (Vu *et al.*, 2011) was used to assess the importance of the γ′-region in protease binding to fibrin clots. After preincubating 1 μM γ_A/γ_A- or γ_A/γ'-fibrinogen with γ′-peptide-directed IgG (0–8 μM) for 60 min at 23°C, 40 nM ^{125}I-YPR-thrombin or ^{125}I-YPR-batroxobin was added, and clotting was initiated with 10 nM thrombin. The fraction of ^{125}I-YPR-protease bound to the clot was then calculated as described above.

To determine whether batroxobin and thrombin have overlapping binding sites, clots were formed with 1 μM γ_A/γ_A- or γ_A/γ'-fibrinogen, 10 nM thrombin, 20–40 nM ^{125}I-YPR-batroxobin or ^{125}I-YPR-thrombin, and 0–25 μM FPR-thrombin in TBS-Tw-Ca. Fibrin-bound ^{125}I-protease was quantified as described above. Experiments were performed twice in duplicate.

4.5.2.6 Batroxobin and Thrombin Diffusion from Preformed Fibrin Clots

The rate of ^{125}I-protease diffusion from clots formed from γ_A/γ_A- or γ_A/γ'-fibrinogen was determined as described (Petrera *et al.*, 2009, Vu *et al.*, 2011). Briefly, 120-μl fibrin clots were formed around plastic loops (Bac-Loop, Thermo-Fisher

Scientific, Waltham, MA) in microcentrifuge tubes by adding 100 nM thrombin to 9 μM γ_A/γ_A- or γ_A/γ'-fibrinogen, 30 nM FXIII, and 25 nM ^{125}I-YPR-batroxobin or -thrombin. After incubation at 37 °C for 45 min, clots were removed and immersed in 5 ml of TBS-Tw-Ca or 2 M NaCl containing 5 mM EDTA. At intervals, the fraction of clot-bound ^{125}I-YPR-protease was quantified, and time courses were fit to a two-phase exponential decay curve (Table Curve, Jandel scientific, San Rafael, CA). Experiments were repeated three times.

4.5.2.7 Fibrin Clot Accretion

The capacity of fibrin-bound batroxobin or thrombin to promote clot accretion was assessed by counting clots for radioactivity after incubation in plasma containing ^{125}I-fibrinogen. Briefly, clots were formed around plastic loops with concentrations of batroxobin or thrombin that yielded comparable clot times. Thus, 8.3 μM γ_A/γ_A- or γ_A/γ'-fibrinogen in HBS-Tw-Ca containing 500 cpm ^{125}I-fibrinogen (for clot standardization) and 30 nM FXIII was incubated with 76.5 units/ml batroxobin or 45 nM thrombin for 30 min at 37°C. Clots were then incubated in citrated human plasma supplemented with ~800,000 cpm/ml of ^{125}I-fibrinogen for up to 3.3 h at 23°C. At intervals, clots were removed from the plasma, washed with HBS-Tw, and counted for radioactivity. Experiments were performed three times, each in triplicate.

4.5.2.8 Statistical Analysis

Results are presented as the mean ± S.D. The extent of clot accretion over time induced by batroxobin and thrombin was compared by two-way repeated measures

analysis of variance using the Greenhouse Geisser correction, whereas *t*-tests were used for other analyses. In all cases, $p<0.05$ was considered statistically significant.

4.6 RESULTS

4.6.1 Binding of Batroxobin and Thrombin to γ_A/γ_A- and γ_A/γ'-Fibrinogen

Although the interaction of thrombin with γ_A/γ_A- and γ_A/γ'-fibrinogen is well characterized, binding of batroxobin to fibrinogen has not been investigated. SPR was used to quantify binding, and Req values from the sensorgrams are plotted against input protease concentrations. As reported previously, the amount of FPR-thrombin bound to γ_A/γ'-fibrinogen is about 2-fold greater than that bound to γ_A/γ_A-fibrinogen ($p<0.05$) (Fig. 4.2 *A*). In contrast, similar amounts of FPR-batroxobin bind to both isoforms of fibrinogen (Fig. 4.2 *B*). Sensorgrams showing real time binding to γ_A/γ_A-fibrinogen reveal rapid association and dissociation phases for both proteases. However, the off-rate of FPR-batroxobin is about 16-fold slower than that of FPR-thrombin ($p<0.005$), which suggests that batroxobin binds γ_A/γ_A-fibrinogen with higher affinity than thrombin (Fig. 4.2, *A* and *B, insets*). Kinetic analyses of the on- and off-rates reveal that FPR-thrombin binds γ_A/γ_A-fibrinogen via a single site (K_d of 2.3 ± 0.3 μM), whereas thrombin binds γ_A/γ'-fibrinogen via high and low affinity sites (K_d values of 0.05 ± 0.02 and 1.5 ± 0.1 μM, respectively); these findings are in agreement with previous studies (Fredenburgh *et al.*, 2008, Pospisil *et al.*, 2003). In contrast, FPR-batroxobin binds both γ_A/γ_A- and γ_A/γ'-fibrinogen via a single high affinity site (K_d values of 0.6 ± 0.1 and 0.5 ± 0.04 μM, respectively, $p = 0.9$). As illustrated in Table 4.1, the affinities of batroxobin for both isoforms of fibrinogen are 3–4-fold higher than that of thrombin for γ_A/γ_A-fibrinogen and

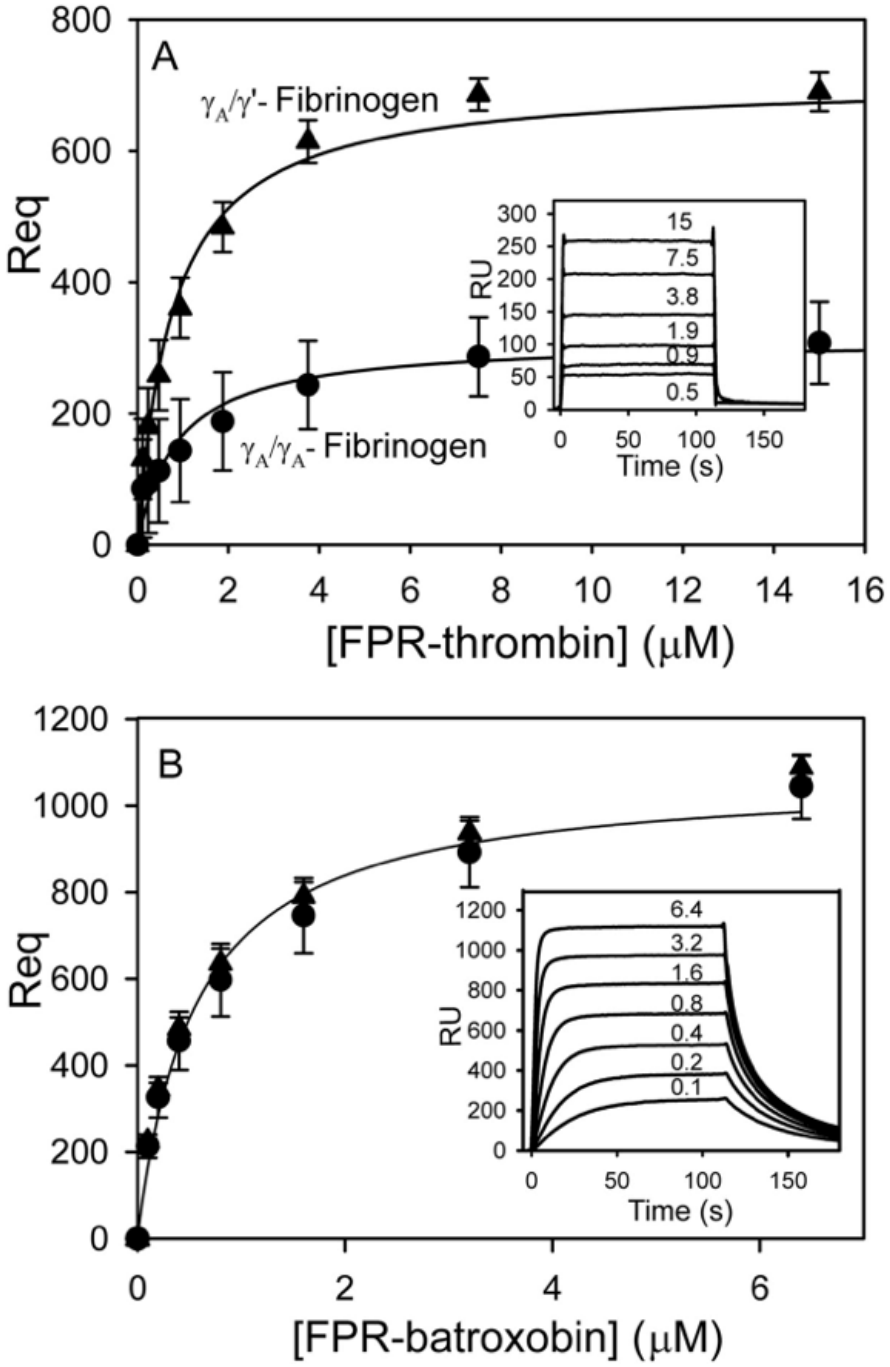
A
γA/γ'- Fibrinogen
γA/γA- Fibrinogen
Req
[FPR-thrombin] (μM)
RU
Time (s)
15
7.5
3.8
1.9
0.9
0.5
B
Req
[FPR-batroxobin] (μM)
RU
Time (s)
6.4
3.2
1.6
0.8
0.4
0.2
0.1

Figure 4.2 SPR analysis of the interaction of FPR-batroxobin and FPR-thrombin with immobilized γ_A/γ_A- or γ_A/γ'-fibrinogen.

γ_A/γ_A- (●) and γ_A/γ'-fibrinogen (▲) were adsorbed on individual flow cells to ~6000–8000 RU. Increasing concentrations (0–15 μM) of FPR-thrombin (*A*) or FPR-batroxobin (*B*) were successively injected into flow cells for 2 min, followed by a 4-min wash to monitor dissociation. The amount of protease bound at equilibrium (Req) after background correction is plotted against the input FPR-protease concentration. The *insets* show representative sensorgrams for the interaction of FPR-thrombin (*A*) and FPR-batroxobin (*B*) with γ_A/γ_A-fibrinogen in concentrations up to 15 and 6.4 μM, respectively. Data points represent the mean ± S.D. of 2-3 experiments, and the *lines* represent nonlinear regression analyses.

resemble the high affinity interaction of thrombin with γ_A/γ'-fibrinogen. Similar results were obtained in reciprocal experiments, where the binding of fibrinogen to immobilized FPR-batroxobin or FPR-thrombin was assessed (data not shown). The γ′-chain, which distinguishes γ_A/γ'-fibrinogen from γ_A/γ_A-fibrinogen, affords thrombin a high affinity binding site. Because batroxobin binds γ_A/γ_A- and γ_A/γ'-fibrinogen with similar affinities, it is unlikely to bind to the γ′-chain. To verify this, SPR was used to compare the affinity of batroxobin for immobilized γ′-peptide with that of thrombin. Whereas thrombin binds γ′-peptide with a K_d value of 1.1 ± 0.1 μM, batroxobin does not bind (Table 4.1). These findings suggest that the γ′-region on γ_A/γ'-fibrinogen is important for thrombin but not batroxobin binding.

4.6.2 Interaction of Batroxobin and Thrombin with γ_A/γ_A- and γ_A/γ'-Fibrin

Thrombin binds fibrinogen and fibrin with similar affinities. To determine whether the same is true for batroxobin, SPR was used to compare the affinity of batroxobin for immobilized γ_A/γ_A- and γ_A/γ'-fibrin with that of thrombin (Petrera *et al.*, 2009, Vu *et al.*, 2011). Like thrombin, batroxobin binds both isoforms of fibrin with affinities similar to those for fibrinogen (Table 4.1); these findings suggest that batroxobin binds fibrin as well as fibrinogen.

To confirm the SPR results, the binding of ^{125}I-YPR-proteases to fibrin clots was assessed. ^{125}I-YPR-thrombin binds γ_A/γ_A-fibrin clots with a K_d of 2.5 ± 0.3 μM, whereas it binds γ_A/γ'-fibrin clots with a composite K_d of 230 ± 70.0 nM (Fig. 4.3 *A*), and 1.5-fold more thrombin binds γ_A/γ'-fibrin clots than γ_A/γ_A-fibrin clots; these findings are in agreement with previous work (Petrera *et al.*, 2009). In contrast, ^{125}I-YPR-batroxobin

	FPR-thrombin		
	K_{d1}	K_{d2}	FPR-batroxobin K_d
	μM	μM	μM
γ_A/γ_A-Fibrinogen	2.3 ± 0.3		0.6 ± 0.1
γ_A/γ'-Fibrinogen	1.5 ± 0.1	0.05 ± 0.02	0.5 ± 0.04
γ_A/γ_A-Fibrin	2.0 ± 0.9		0.5 ± 0.9
γ_A/γ'-Fibrin	2.1 ± 0.4	0.1 ± 0.06	0.5 ± 0.9
Fragment D	NB		NB
Fragment E	3.2 ± 1.5		2.1 ± 0.5
NDSK	3.0 ± 1.0		4.5 + 1.7
γ′-Peptide	1.1 ± 0.1		NB
α(17–51)-Peptide	2.2 ± 1.0		>25

Table 4.1 Dissociation constants for the binding of FPR-thrombin and FPR-batroxobin to fibrinogen, fibrin, and related fragments.

The affinities of FPR-thrombin or FPR-batroxobin for immobilized fibrin(ogen), fibrinogen fragments, or peptides was determined using SPR. K_d values were determined by kinetic analysis of the binding sensorgrams. The interaction of thrombin with γ_A/γ'-fibrin(ogen) was analyzed using a two-site binding model. Each value represents the mean ± S.D. of two to three experiments. NB represents no binding.

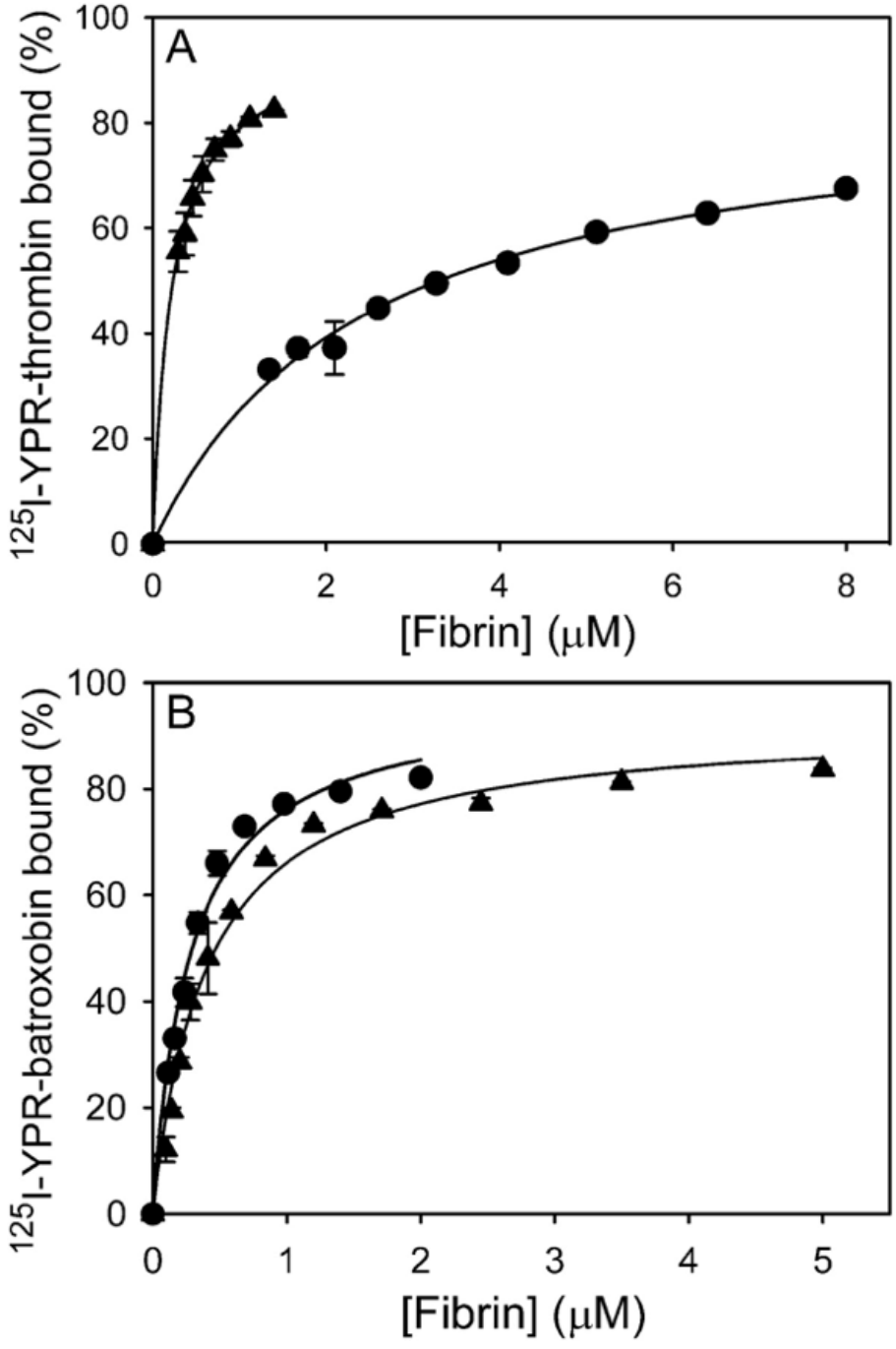
A
^{125}I-YPR-thrombin bound (%)
[Fibrin] (μM)
B
^{125}I-YPR-batroxobin bound (%)
[Fibrin] (μM)

Figure 4.3 Binding of ^{125}I-YPR-batroxobin and ^{125}I-YPR-thrombin to γ_A/γ_A- or γ_A/γ'-fibrin clots.

20 nM ^{125}I-YPR-thrombin (*A*) or 40 nM ^{125}I-YPR-batroxobin (*B*) was added to microcentrifuge tubes containing 0–8 μM γ_A/γ_A- (●) or γ_A/γ'-fibrinogen (▲), and 10 nM α-thrombin was used to initiate clotting. After incubation for 60 min, clots were pelleted by centrifugation, and free ^{125}I-YPR-protease in the supernatant was used to calculate the bound fraction. Data are plotted as the percentage of ^{125}I-YPR-protease bound to fibrin clots *versus* the fibrinogen concentration. Data points represent the mean ± S.D. of two experiments, each performed in duplicate, and the *lines* represent nonlinear regression analyses.

binds γ_A/γ_A- and γ_A/γ'-fibrin clots with K_d values of 268 ± 18.5 and 409 ± 48.4 nM (p = 0.18), respectively (Fig. 4.3 *B*), and similar amounts of batroxobin bind to clots formed from either isoform of fibrinogen. Consistent with their distinct modes of binding to γ_A/γ'-fibrin, the γ′-peptide-directed IgG has no effect on ^{125}I-YPR-batroxobin binding to γ_A/γ'-fibrin clots, but it decreases the binding of ^{125}I-YPR-thrombin to γ_A/γ'-fibrin clots by ~70% at 8 μM (Fig. 4.4). In contrast, the γ′-peptide-directed IgG has only nonspecific effects on ^{125}I-YPR-batroxobin and ^{125}I-YPR-thrombin binding to γ_A/γ_A-fibrin clots (Fig. 4.4, *inset*). Thus, the findings with fibrin clots are similar to those with immobilized fibrin and demonstrate that batroxobin does not bind to the COOH terminus of the γ′-chain.

4.6.3 Comparison of the Rates of Batroxobin and Thrombin Diffusion from γ_A/γ_A- and γ_A/γ'-Fibrin Clots

To further characterize batroxobin binding to fibrin, we compared the rates of dissociation of batroxobin and thrombin from preformed γ_A/γ_A- or γ_A/γ'-fibrin clots. Consistent with previously reported results, the rate of ^{125}I-YPR-thrombin dissociation from γ_A/γ'-fibrin clots is 9-fold slower than that from γ_A/γ_A-fibrin clots (p<0.005) (Fig. 4.5 *A*); this is a difference that reflects the bivalent interaction of thrombin with γ_A/γ'-fibrin and its univalent interaction with γ_A/γ_A-fibrin (Fredenburgh *et al.*, 2008). In contrast, the rates of ^{125}I-YPR-batroxobin diffusion from γ_A/γ_A- and γ_A/γ'-fibrin clots are similar and comparable with the rate of ^{125}I-YPR-thrombin diffusion from γ_A/γ'-fibrin clots (Fig. 4.5 *B*). Thus, even though batroxobin does not interact with the γ′-chain, it binds both isoforms of fibrin with affinities similar to the high affinity bivalent interaction of thrombin with γ_A/γ'-fibrin. As a control, rates of diffusion were determined in the

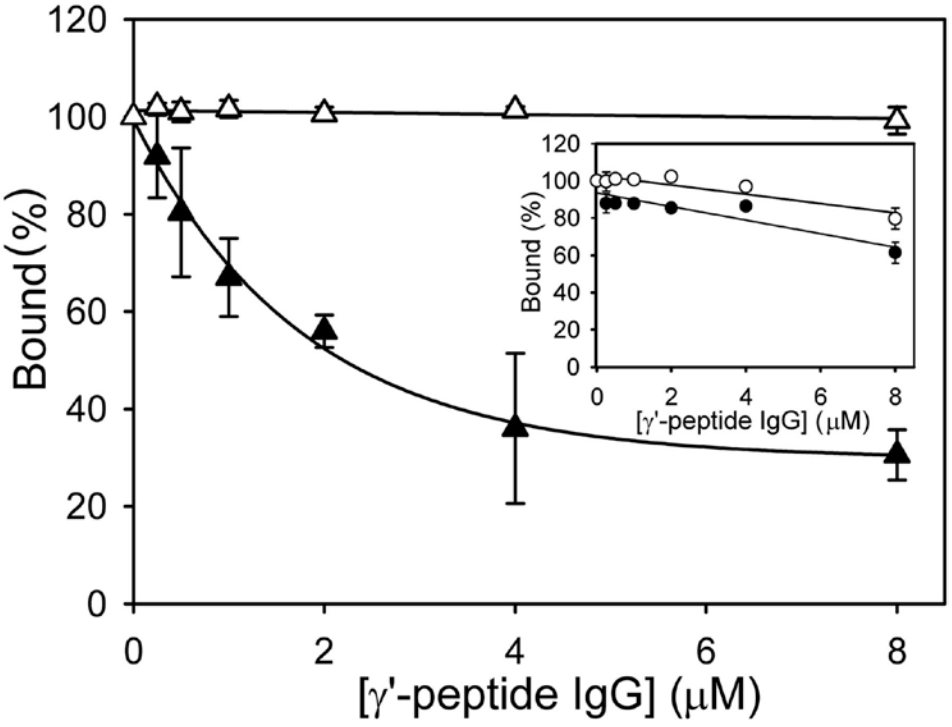
Bound(%)
[γ'-peptide IgG] (μM)
Bound (%)
[γ'-peptide IgG] (μM)

Figure 4.4 Effect of γ′-peptide-directed IgG on ^{125}I-YPR-batroxobin and ^{125}I-YPR-thrombin binding to γ_A/γ_A- or γ_A/γ'-fibrin clots.

The binding of 40 nM ^{125}I-YPR-thrombin (●/▲) or ^{125}I-YPR-batroxobin (○/Δ) to clots formed from 1 μM γ_A/γ_A- (*circles*) or γ_A/γ'-fibrinogen (*triangles*) was assessed in the absence or presence of γ′-peptide-directed IgG up to 8 μM. Clots were generated with thrombin and pelleted, and clot-bound ^{125}I-YPR-protease was determined. The percentage of ^{125}I-YPR-protease bound in the absence of antibody is plotted *versus* antibody concentration. The *main figure* illustrates the percentage of ^{125}I-YPR-protease bound to γ_A/γ'-fibrin clots, and the *inset* shows the percentage of ^{125}I-YPR-protease bound to γ_A/γ_A-fibrin clots. *Symbols* represent the mean ± S.D. of two experiments, each performed in duplicate, and the *lines* represent nonlinear regression analyses of the data.

presence of 2 M NaCl and 5 mM EDTA. Under these conditions, the rates of diffusion of batroxobin from both γ_A/γ_A- and γ_A/γ'-fibrin clots are 3–4-fold slower than those of thrombin ($p < 0.05$) (Fig. 4.5). This finding raises the possibility that ionic interactions are less important for batroxobin binding to fibrin than they are for thrombin.

4.6.4 Thrombin Competition of Batroxobin Binding to Fibrin(ogen)

SPR was used to determine whether thrombin and batroxobin have overlapping binding sites. The extent to which increasing concentrations of FPR-thrombin attenuate γ_A/γ_A-fibrinogen (2.5 μM) binding to immobilized FPR-batroxobin was assessed. FPR-thrombin attenuates γ_A/γ_A-fibrinogen binding to adsorbed FPR-batroxobin in a concentration-dependent fashion with an IC_{50} of 2.5 ± 0.5 μM. At 40 μM, FPR-thrombin reduces fibrinogen binding by 39% (Fig. 4.6 *A*). Because hirudin binds exosite 1 on thrombin (Stone and Hofsteenge, 1986), we hypothesized that hirudin would attenuate the capacity of FPR-thrombin to compete with adsorbed FPR-batroxobin for fibrinogen binding. As expected, hirudin reduces competition by FPR-thrombin by 1.3–1.7-fold. This is not a nonspecific protein effect because, even at 40 μM, ovalbumin has no effect on γ_A/γ_A-fibrinogen binding to immobilized FPR-batroxobin (data not shown). The finding that saturating concentrations of FPR-thrombin reduce γ_A/γ_A-fibrinogen binding to FPR-batroxobin by a maximum of 39% suggests that the batroxobin-binding sites on fibrinogen partially overlap with those of thrombin.

We next examined the effect of increasing concentrations of FPR-thrombin on ^{125}I-YPR-batroxobin or ^{125}I-YPR-thrombin binding to γ_A/γ_A-fibrin clots. At 25 μM, FPR-thrombin reduces ^{125}I-YPR-thrombin binding by ~60%. In contrast, 25 μM FPR-thrombin

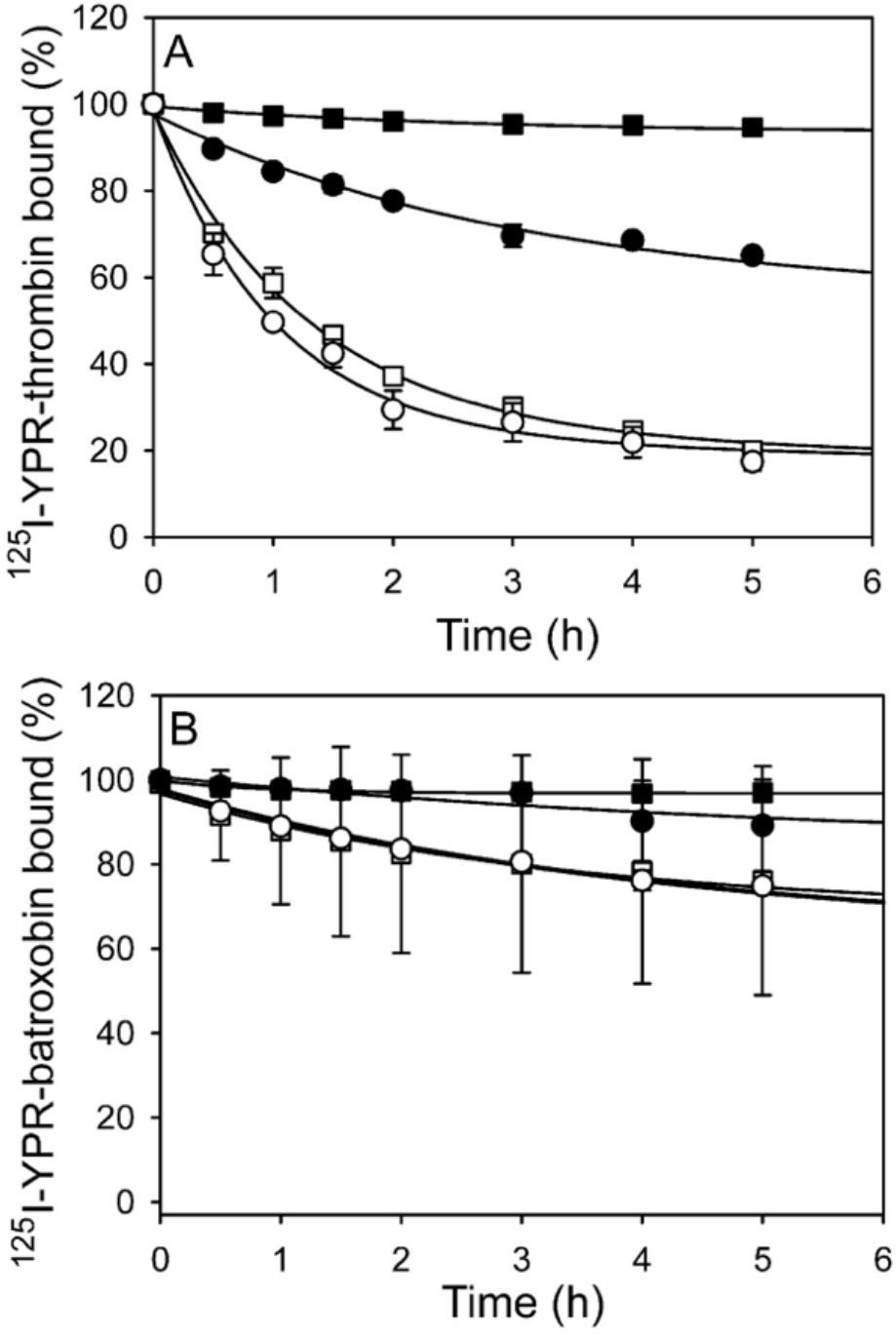
A
^{125}I-YPR-thrombin bound (%)
Time (h)
B
^{125}I-YPR-batroxobin bound (%)
Time (h)

Figure 4.5 Diffusion of ^{125}I-YPR-batroxobin and ^{125}I-YPR-thrombin from γ_A/γ_A- or γ_A/γ'-fibrin clots.

Clots were formed around plastic loops by incubating 9 μM γ_A/γ_A- (●/○) or γ_A/γ'-fibrinogen (■/□) with 100 nM thrombin and 30 nM FXIII in the presence of 20 nM ^{125}I-YPR-thrombin (*A*) or 40 nM ^{125}I-YPR-batroxobin (*B*) and then immersed in solutions containing TBS-Ca (●/■) or 2 M NaCl and 5 mM EDTA (○/□). At the indicated time points, 0.5-ml aliquots of the bathing solutions were removed and counted for radioactivity to quantify bound ^{125}I-YPR-protease. Data are plotted as the percentage of clot-bound ^{125}I-YPR-protease *versus* time, and *lines* represent nonlinear regression analyses. Data points represent the mean ± S.D. of three separate determinations.

reduces ^{125}I-YPR-batroxobin binding by 40%; this value is consistent with the SPR results with fibrinogen (Fig. 4.6 *B*). Collectively, these data suggest that the batroxobin-binding sites on fibrin(ogen) partially overlap with those of thrombin.

4.6.5 Localization of the Batroxobin-binding Sites on Fibrinogen

To begin to localize the batroxobin-binding sites on fibrinogen, the interaction of batroxobin with immobilized fibrinogen fragments was examined using SPR and compared with that of thrombin. The fibrinogen derivatives include fragment X, which lacks the αC-domains, fragment E, and NDSK, which consist of the NH_2 termini of all six chains, and fragment D, which contains the COOH-terminal portions of the three chains. Fragments were generated from γ_A/γ_A-fibrinogen to avoid possible contribution of the γ′-chain to thrombin binding. FPR-batroxobin and FPR-thrombin bind to fragment E and NDSK (K_d values of 3–5 μM) but not to fragment D (Table 4.1). Thrombin binds fragment E and NDSK with affinities comparable with that of intact γ_A/γ_A-fibrinogen, suggesting that most of the sequences necessary for thrombin binding to fibrinogen are localized to the E-domain. Like thrombin, batroxobin binds fragment E and NDSK, suggesting that the protease primarily binds to the central region of fibrinogen. However, because batroxobin binds the central E-region with affinities 4–8-fold lower than that for intact γ_A/γ_A-fibrinogen, the batroxobin-binding sites may extend beyond the E-domain.

To further distinguish the batroxobin and thrombin-binding sites on fibrin(ogen), their interaction with α(17–51) was compared because this sequence contains a thrombin-binding site (Lord *et al.*, 1995). Biotinylated α(17–51)-peptide was adsorbed onto a streptavidin-containing cell, and the binding of FPR-batroxobin and FPR-thrombin was

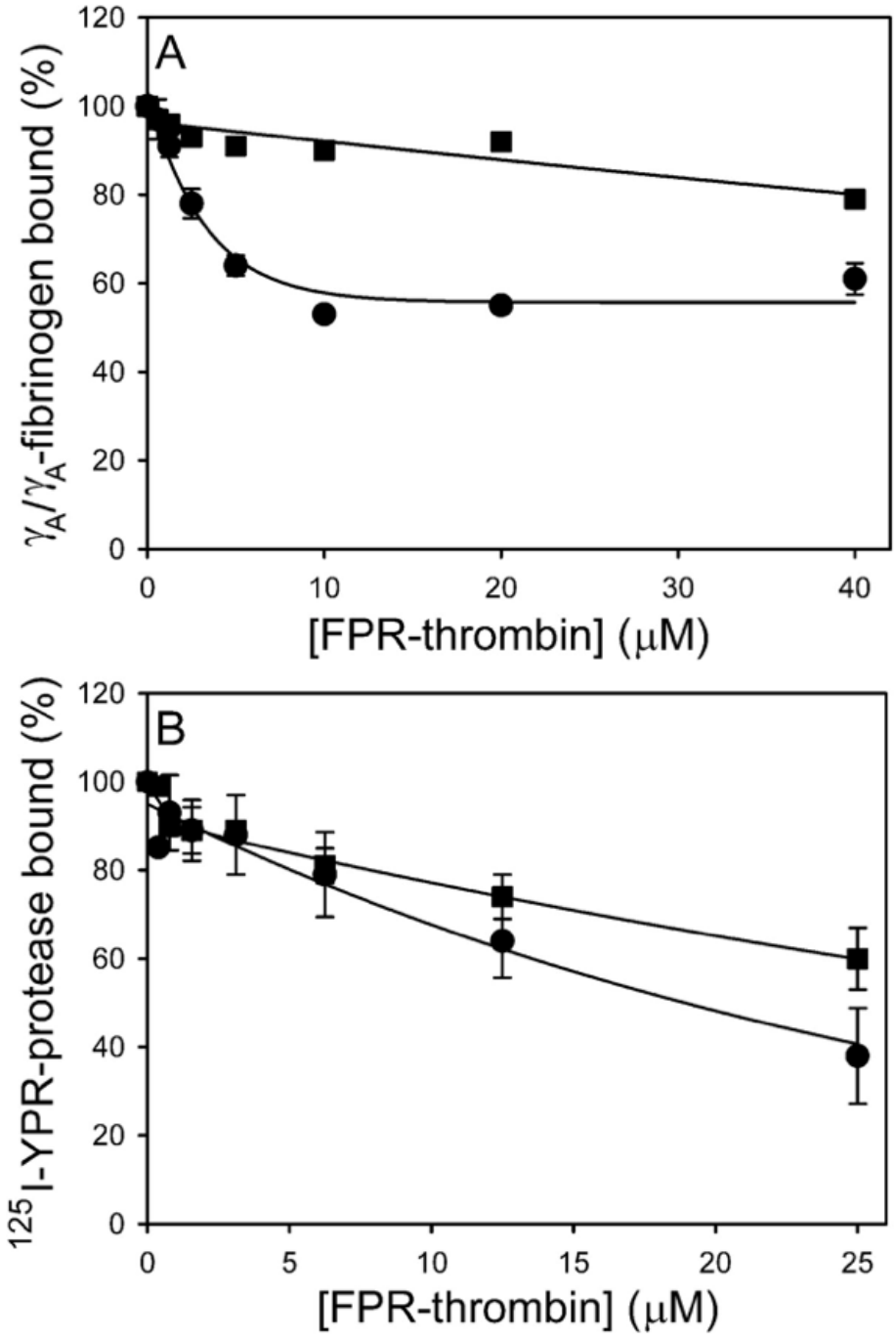
A
γ_A/γ_A-fibrinogen bound (%)
[FPR-thrombin] (μM)
B
^{125}I-YPR-protease bound (%)
[FPR-thrombin] (μM)

Figure 4.6. Effect of FPR-thrombin on batroxobin binding to γ_A/γ_A-fibrinogen or γ_A/γ_A-fibrin clots.

A, effect of FPR-thrombin on γ_A/γ_A-fibrinogen binding to immobilized FPR-batroxobin was determined using SPR. γ_A/γ_A-fibrinogen (2.5 μM) was incubated with FPR-thrombin concentrations up to 40 μM in the absence (●) or presence (■) of 80 μM hirudin, and the mixture was then injected into flow cells containing immobilized FPR-batroxobin. Binding in the presence of competitors was normalized relative to that determined in their absence. Data are plotted as the percentage of γ_A/γ_A-fibrinogen bound *versus* the FPR-thrombin concentration. *B,* binding of ^{125}I-YPR-batroxobin (■) and ^{125}I-YPR-thrombin (●) to γ_A/γ_A-fibrin clots was measured in the absence or presence of FPR-thrombin concentrations up to 25 μM. Clots were formed by incubating 2 or 0.06 μM γ_A/γ_A-fibrinogen with 20 nM ^{125}I-YPR-thrombin or 40 nM ^{125}I-YPR-batroxobin, respectively, and 10 nM thrombin. After 60 min, clots were counted for radioactivity to quantify bound ^{125}I-YPR-protease. Data are plotted as the percentage of ^{125}I-YPR-protease bound *versus* the FPR-thrombin concentration. Data points represent the mean ± S.D. of 3–4 experiments, and the *lines* represent nonlinear regression analyses.

assessed by SPR. Whereas FPR-thrombin binds α(17–51)-peptide (K_d value of 2.2 ± 1.0 μM), FPR-batroxobin displays minimal binding (K_d >25 μM), suggesting that the NH_2 terminus of the α-chain is only important for thrombin binding (Table 4.1). To determine the role of the NH_2 terminus of the β-chain, the binding of ^{125}I-YPR-batroxobin and ^{125}I-YPR-thrombin to clots generated from intact or des-Bβ(1–42) γ_A/γ_A-fibrinogen was examined. ^{125}I-YPR-batroxobin binds intact and des-Bβ(1–42) γ_A/γ_A-fibrin with similar affinities (K_d values of 0.27 ± 0.02 and 0.24 ± 0.1 μM, respectively). In contrast, the affinity of thrombin for des-Bβ(1–42) γ_A/γ_A-fibrin is 2.6-fold lower than that for intact γ_A/γ_A-fibrin (K_d values of 6.5 ± 1.5 and 2.5 ± 0.3 μM, respectively; p = 0.07); this finding is in agreement with previous work (Pospisil *et al.*, 2003). These results further support the contention that the batroxobin-binding sites on fibrin(ogen) are distinct from those of thrombin.

4.6.6 Comparison of the Capacities of Fibrin-bound Batroxobin and Thrombin to Promote Clot Accretion

To determine whether, like fibrin-bound thrombin, fibrin-bound batroxobin also promotes clot accretion, γ_A/γ_A- and γ_A/γ'-fibrinogen were clotted with batroxobin or thrombin, and the clots were counted for radioactivity after incubation in citrated plasma containing ^{125}I-labeled fibrinogen. Both fibrin-bound batroxobin and thrombin trigger progressive fibrin accretion over time (Fig. 4.7). The extent of fibrin accretion onto γ_A/γ_A-fibrin clots prepared with thrombin is 1.5–2.0-fold greater than that onto γ_A/γ'-fibrin clots (Fig. 4.7, *inset*, p<0.001). Therefore, thrombin bound to γ_A/γ_A-fibrin clots promotes more fibrin accretion than thrombin bound to γ_A/γ'-fibrin clots. In contrast, clot accretion

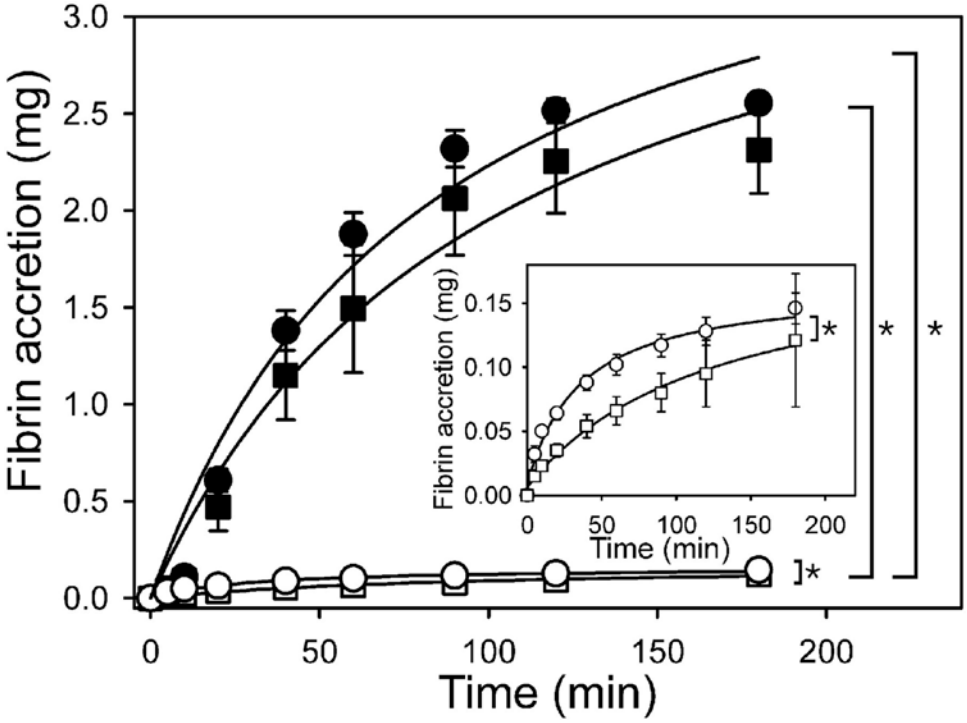
Fibrin accretion (mg)
Time (min)
0.0
0.5
1.0
1.5
2.0
2.5
3.0
0
50
100
150
200
*
*
*
Fibrin accretion (mg)
Time (min)
0.00
0.05
0.10
0.15
0
50
100
150
200
*
*

Figure 4.7. Clot accretion induced by batroxobin or thrombin bound to γ_A/γ_A- or γ_A/γ'-fibrin clots.

Clots were formed around plastic loops by incubating 8.3 μM γ_A/γ_A-fibrinogen (●/○) or γ_A/γ'-fibrinogen (■/□) with 76.5 units/ml of batroxobin (●/■) or 45 nM thrombin (○/□) in the presence of 2 mM $CaCl_2$, 30 nM FXIII, and 500 cpm of ^{125}I-fibrinogen for 30 min at 37°C. After determining radioactivity, clots were incubated in 1 ml of citrated human plasma containing ~800,000 cpm/ml of ^{125}I-fibrinogen. At intervals, clots were washed twice with 1 ml of HBS and again counted for radioactivity so that fibrin accretion could be determined. The *inset* provides an expanded view of clot accretion induced by thrombin. Data points represent the mean ± S.D. of three experiments, each performed in triplicate, and the *lines* represent nonlinear regression analyses. (*, $p<0.001$).

induced by batroxobin is similar regardless of whether batroxobin is bound to γ_A/γ_A- or γ_A/γ'-fibrin clots (p = 0.18). It is notable that clot accretion induced by fibrin-bound batroxobin is ~18-fold greater than that induced by fibrin-bound thrombin (p<0.001); this indicates that the procoagulant activity of fibrin-bound batroxobin is greater than that of fibrin-bound thrombin, likely reflecting the fact that batroxobin is not inhibited by antithrombin or heparin cofactor II (Aronson, 1976).

4.7 DISCUSSION

Although the thrombin-like activity of batroxobin is well known, the interaction of batroxobin with fibrinogen has not been studied. To address this, we compared the interaction of batroxobin with γ_A/γ_A- and γ_A/γ'-fibrin(ogen) with that of thrombin. Batroxobin forms a high affinity interaction with both isoforms of fibrin(ogen), which resembles the high affinity thrombin interaction with γ_A/γ'-fibrin(ogen). The batroxobin-binding sites on fibrin(ogen) only partially overlap with those of thrombin because thrombin incompletely displaces batroxobin from fibrinogen and fibrin clots. In keeping with the concept that the batroxobin-binding sites on fibrin(ogen) are distinct from those of thrombin, batroxobin binds NDSK and fragment E with lower affinity than intact γ_A/γ_A-fibrinogen, whereas the affinity of thrombin for these fragments is similar to that for fibrinogen, suggesting that the batroxobin-binding sites on fibrinogen extend beyond the E-domain. Furthermore, the α(17–51) and Bβ(1–42) regions in the E-domain are important for thrombin binding but not for batroxobin binding. In addition, fibrin-bound batroxobin retains catalytic activity and is a more potent stimulus for fibrin accretion than fibrin-bound thrombin.

Structural and functional studies have elucidated the structural determinants of thrombin's interaction with fibrinogen (Adams and Huntington, 2006, Bode *et al.*, 1989, Di Cera and Cantwell, 2001, Pechik *et al.*, 2004, Rose *et al.*, 2003). In the absence of a crystal structure for batroxobin, structural appraisal relies on sequence comparison and modeling. Based on primary sequence alignments, batroxobin exhibits 25 and 37% sequence identity to thrombin and trypsin, respectively. Notably, batroxobin lacks the 60- and γ-loops and the Na^+-binding site, domains that endow thrombin with its specificity for a wide repertoire of macromolecular substrates (Di Cera and Cantwell, 2001, Lord *et al.*, 1995). The absence of these domains may explain why fibrinogen is the sole substrate of batroxobin (Aronson, 1976). Without the 60- and γ-loops and the Na^+-binding site, the interaction of batroxobin with fibrinogen is likely to depend on other residues in the vicinity of the active site of batroxobin (Castro *et al.*, 2004, Parry *et al.*, 1998).

The exosites flanking the active site of thrombin also are critical determinants of its interaction with fibrin(ogen) and other substrates (Di Cera and Cantwell, 2001, Huntington, 2005, Petrera *et al.*, 2009). Exosite 1 on thrombin contains hydrophobic and basic regions that mediate substrate and cofactor binding (Pechik *et al.*, 2004, Rose *et al.*, 2003). In particular, Tyr-76 of thrombin provides the anchor for a hydrophobic patch surrounded by basic residues that interact with a complementary region on fibrinogen (Pechik *et al.*, 2004, Rose *et al.*, 2003). Although only 50% of the corresponding residues are retained, a homologous fibrinogen recognition exosite in batroxobin has been proposed (Castro *et al.*, 2004, Henschen-Edman *et al.*, 1999). The observation that the interaction of batroxobin with γ_A/γ_A-fibrin clots is less readily disrupted by high salt than

that of thrombin raises the possibility that hydrophobic interactions may be more important for batroxobin binding to the fibrinogen recognition exosite than they are for thrombin binding. Although both proteases have similar affinities for fibrinogen, batroxobin does not bind other thrombin exosite 1-mediated ligands, such as hirudin or HD1 aptamer (data not shown). These findings support the concept that exosite specificity contributes to the distinct functional properties of batroxobin and thrombin.

Although sequence alignments reveal conserved exosite regions consisting of hydrophobic and basic residues, snake venom proteases possess fewer basic residues in the region corresponding to exosite 1 (Henschen-Edman *et al.*, 1999, Maroun and Serrano, 2004, Serrano and Maroun, 2005). This is demonstrated by modeling the putative exosite residues in batroxobin onto the crystal structure of *Trimeresurus stejnejeri* venom plasminogen activator (TSV-PA), which has 64% sequence identity to batroxobin (Parry *et al.*, 1998). The spatial organization of these residues reveals a putative exosite that resembles exosite 1 on thrombin and may contribute to the interaction of batroxobin with fibrin(ogen) (Fig. 4.8 *A*) (Maroun and Serrano, 2004, Zhang *et al.*, 1997). Although the existence of a second exosite on batroxobin cannot be excluded, there is little surface homology with thrombin in the exosite 2 region, and a thrombin variant with mutations in exosite 2 displays normal fibrin binding (Pospisil *et al.*, 2003).

In addition to the structural differences between the proteases, binding site differences on fibrinogen may also affect specificity. The importance of the β-chain to binding is demonstrated by the observation that FpA release from fibrinogen Naples I, a variant with

a point mutation at residue 68 in the Bβ-chain, is normal with batroxobin but impaired with thrombin (Koopman *et al.*, 1992). The crystal structure of thrombin bound to fragment E provides further insight into the differences between the batroxobin and thrombin-binding sites on fibrinogen (Pechik *et al.*, 2004). Thrombin exosite 1 interacts with a patch populated by residues from both the α- and β-chains, including αPhe-35, αAsp-38, βAla-68, βAsp-69, and βAsp-71. Likewise, the α-chain segment DSDWPF (α(30–35)), which lies proximal to where FpA resides, contains a similar combination of acidic and hydrophobic residues that may support batroxobin binding (Fig. 4.8 *B*). However, our observation that the affinity of thrombin, but not batroxobin, for α(17–51) is comparable with its affinity for intact fibrinogen suggests that a tertiary structure consisting of multiple fibrinogen chains also may be necessary to optimally position batroxobin for FpA cleavage. These results suggest that the proteases have related, but unique, modes of interaction with fibrinogen.

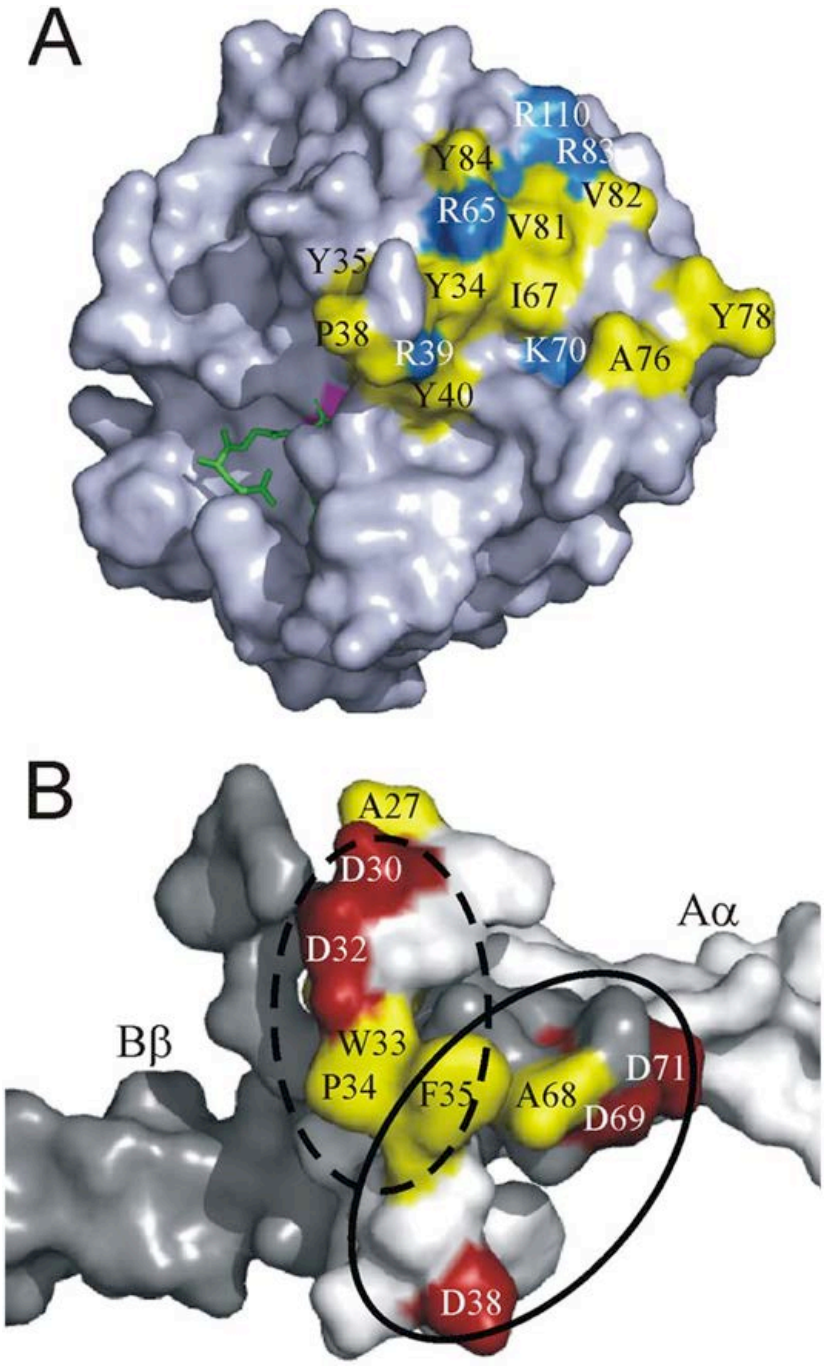
A
R110
Y84
R83
V82
R65
V81
Y35
Y34
I67
Y78
P38
R39
K70
A76
Y40
B
A27
D30
Aα
D32
Bβ
W33
D71
P34
F35
A68
D69
D38

Figure 4.8 Models of binding sites on batroxobin and fibrinogen.

A, crystal structure of TSV-PA (Protein Data Bank accession number 1BQY) in complex with Glu-Gly-Arg chloromethyl ketone (*green*) is shown in space-filling format using PyMOL. The image is rotated clockwise ~90° from standard view with the active site Ser-195 (*magenta*) facing *left*. Hydrophobic (*yellow*) and basic (*blue*) residues in batroxobin that constitute a putative exosite are mapped onto the TSV-PA structure. Residues are identified using chymotrypsin numbering system. *B*, crystal structure of the NH_2 termini of fibrinogen α- and β-chains forming the thrombin-binding site (Protein Data Bank accession number 2A45) is shown in space-filling format. Both the γ-chains and the reciprocal α- and β-chains are omitted for clarity. The α- and β-chain surfaces are *white* and *gray*, respectively. Thrombin binding residues α-chain Phe-35 and Asp-38 and β-chain Ala-68, Asp-69, and Asp-71 are shown within a *solid black oval* with hydrophobic residues in *yellow* and acidic residues in *red*. Residues comprising the putative batroxobin-binding site include α-chain Asp-30, Asp-32, Trp-33, Pro-34, and Phe-35 (*hatched black oval*). The site where the unmapped α1–26 segment exits the α-chain at Ala-27 indicates the vicinity of FpA.

The distinct batroxobin-binding sites in the E-domain of fibrinogen may explain why batroxobin only induces FpA release. Current thinking is that fibrin generation and fibrin monomer assembly in solution occur in two distinct steps. In the first step, thrombin releases FpA, thereby generating des-AA-fibrin monomers that associate to form protofibrils (Mosesson, 2005). This is followed by a second step whereby FpB is released, resulting in lateral growth of the fibrin protofibrils; this is a process dependent on des-AA-fibrin polymerization (Mosesson, 2005, Weisel *et al.*, 1993). Thus, the generation of des-AA-fibrin facilitates FpB release either by rendering the BβArg-14–Gly-15 bond more susceptible to thrombin hydrolysis or by positioning FpB in close proximity to the active site of thrombin (Blomback *et al.*, 1978, Mullin *et al.*, 2000, Riedel *et al.*, 2011). A conformational change in the vicinity of the BβArg-14–Gly-15 bond cannot be the sole explanation for FpB release because, like thrombin, batroxobin also generates des-AA-fibrin polymers, yet it does not induce FpB release (Aronson, 1976, Moen *et al.*, 2003). Whereas thrombin cleaves the BβArg-14–Gly-15 bond on Bβ(1–42)-peptide, thereby releasing FpB, batroxobin does not, which suggests that unlike thrombin, batroxobin does not bind to the Bβ(1–42) region (data not shown). In support of this concept, the affinity of batroxobin for intact and des-Bβ(1–42) γ_A/γ_A-fibrinogen is the same, whereas the affinity of thrombin for γ_A/γ_A-fibrinogen is reduced by 2.6-fold when the Bβ(1–42) sequence is removed. Therefore, these data suggest that thrombin interaction with the Bβ(1–42) region is an important determinant of its capacity to release FpB. Because batroxobin fails to bind to this region, it does not induce FpB release.

Batroxobin is a potent defibrinogenating enzyme, which is a property that has been exploited in studies of batroxobin for prevention or treatment of thrombosis. Batroxobin binds fibrin(ogen) with high affinity, and fibrin-bound batroxobin is more potent than fibrin-bound thrombin at triggering fibrin accretion, likely because batroxobin is not inhibited by AT and HCII (Aronson, 1976). Therefore, the procoagulant activity of fibrin-bound batroxobin may contribute to the microvascular thrombosis observed in patients envenomated with *B. atrox moojeni* (Isbister, 2010, White, 2005). The defibrinogenating effects of batroxobin and other venom-derived thrombin-like serine proteases underlie their therapeutic potential. Our results suggest that treatment with these agents may be complicated by microvascular thrombosis, which may explain the disappointing results of studies that explored the use of fibrinogen-depleting snake venom enzymes for treatment of acute ischemic stroke (Liu *et al.*, 2011).

In summary, we have characterized the interaction of batroxobin with fibrin(ogen) and have shown how it differs from that of thrombin. These differences likely reflect the fact that batroxobin is missing the surface loops and allosteric sites that modulate thrombin's interaction with fibrin(ogen) (Di Cera and Cantwell, 2001, Lord *et al.*, 1995). The structural features on batroxobin that mediate the high affinity interaction with fibrin(ogen) remain to be elucidated.

CHAPTER 5: Histidine rich glycoprotein binds DNA and RNA with high affinity and attenuates contact-activation of coagulation

5.1 Forward: The interactions between HRG and nucleic acids are described in this manuscript. We demonstrated that DNA and RNA promote FXII and FXI activation and by binding nucleic acids, HRG attenuates this process.

This manuscript is in preparation for submission to *Journal of Biological Chemistry* The authors are: Trang T. Vu, Beverly A. Leslie, Alan R. Stafford, Ji Zhou, James C. Fredenburgh and Jeffrey I. Weitz. Dr. Weitz is the corresponding author.

The experiments in this manuscript were performed by Trang Vu and Beverly Leslie. Alan Stafford and Dr. Ji Zhou provided technical assistance and reagents. The project was designed and the manuscript written by Trang Vu, Dr. James Fredenburgh and Dr. Jeffrey Weitz.

5.2 Capsule

5.2.1 Background: Histidine-rich glycoprotein (HRG) binds factor (F) XIIa and inhibits contact activation of coagulation.

5.2.2 Results: HRG binds DNA and RNA with high affinity and attenuates their procoagulant activity.

5.2.3 Conclusion: HRG attenuates the contact pathway of coagulation by inhibiting the initiation, amplification and propagation steps.

5.2.4 Significance: HRG attenuates contact-mediated coagulation by modulating the pro-thrombotic properties of FXIIa and extracellular nucleic acids.

5.3 Summary

Histidine-rich glycoprotein (HRG) is an abundant plasma protein, but whose function is unclear. The activated partial thromboplastin time (aPTT), which is a global test to measure the contact pathway is shortened in HRG deficient plasma; and we have previously shown that HRG modulates the contact pathway by binding factor (F) XIIa and inhibiting its activity. Because DNA and RNA serve as physiological activators of the contact pathway, the capacity of HRG to bind polyanions may endow it with a regulatory role in thrombosis. Therefore, we set out to (*a*) characterize the mechanisms by which nucleic acids promote contact activation and (*b*) assess the role of HRG in this system. In characterizing DNA and RNA in the intrinsic pathway, we found that both surfaces promote clotting in plasma in a dose-dependent fashion. However, the effective concentration of DNA and RNA required to initiate clotting in plasma is reduced by 7- to 14-fold,

respectively in HRG-deficient human plasma, suggesting that HRG inhibits nucleic acid mediated activation of coagulation. Investigations into the mechanisms of contact activation revealed that DNA and RNA promote FXIIa generation in a manner that is dependent on prekallikrein and high molecular weight kininogen. However, when physiological levels of HRG are added, HRG inhibits DNA-mediated FXII activation (IC_{50}= 183.3 ± 35.1 nM) and activation of FXI by FXIIa (IC_{50}= 466.7 ± 55.1 nM). HRG has a similar affect on RNA-mediated processes. Analysis of nucleic acid binding by surface plasmon resonance (SPR) revealed that FXII, FXIIa, FXI, FXIa and thrombin bind DNA and RNA. Similarly, HRG also binds to nucleic acids (K_d value of 1.3 ± 0.7 nM). The capacity of HRG to directly modulate the procoagulant activity of DNA and RNA was also assessed in an assay where HRG only binds to nucleic acids. Nucleic acids are cofactors for feedback activation of FXI by thrombin; however, HRG attenuates this process (IC_{50} of ~ 200-300 nM). The capacity of HRG to interfere with the procoagulant activity of nucleic acids was confirmed in competition assays, which showed that HRG competes with thrombin, but not FXI or FXIa for nucleic acid binding. Collectively, these data show that HRG inhibits FXIIa activity and the procoagulant activity of nucleic acids and in doing so, modulates contact activation at multiple levels.

5.4 Introduction

Coagulation is initiated by the extrinsic or intrinsic pathway, which converge at the common pathway where thrombin is formed. The extrinsic pathway is thought to predominate in hemostasis because the tissue factor (TF)/factor (F) VIIa complex forms following injury when TF is exposed on cells or in the subendothelium (Mackman *et al.*, 2007). In contrast, the intrinsic pathway is initiated by activation of the contact system, in which FXII is activated in the presence of a polyanionic cofactor and circulating prekallikrein (PK) and high molecular weight kininogen (HK) (Colman and Schmaier, 1997). The physiological significance of the contact system was downplayed in the past because FXII, PK and HK deficiencies do not result in a bleeding phenotype, and deficiency of FXI, the protein downstream of FXII, results in only a mild bleeding diathesis (Gailani and Renne, 2007, Muller *et al.*, 2011). These results prompted a revision of the coagulation model that minimized the role of the intrinsic pathway in coagulation (Gailani and Renne, 2007, Muller *et al.*, 2011).

However, re-examination of the role of the contact system in animal models has challenged this assumption. First, while mice deficient in FXII, FXI, PK or HK do not have a bleeding diathesis, they are protected from thrombosis (Merkulov *et al.*, 2008, Renne *et al.*, 2005, Revenko *et al.*, 2011, Wang *et al.*, 2005, Wang *et al.*, 2006). Second, identification of naturally occurring polyphosphates such as DNA and RNA and inorganic polyphosphate (polyP) as endogenous contact activators has shed new light on the role of the intrinsic pathway in coagulation (Kannemeier *et al.*, 2007, Muller *et al.*, 2009). PolyP is released from activated platelets or bacteria, and nucleic acids are

released from host cells that are stimulated, injured, or dying. Nucleic acids and polyP are potent activators of the intrinsic pathway *in vitro* (Kannemeier *et al.*, 2007, Muller *et al.*, 2009). The capacity of polyP to activate FXII is dependent on the chain length, with longer chains being more potent activators (Smith *et al.*, 2010). In addition, polyP is a cofactor for FXI activation by thrombin, which is an important feedback activation step of the intrinsic pathway (Choi *et al.*, 2011). The physiological relevance of polyP as a FXII activator and its role in thrombosis has recently been challenged (Faxalv *et al.*, 2013). Compared with polyP, relatively little is known about the mechanisms by which nucleic acids trigger contact activation. DNA levels are elevated in murine models of deep vein thrombosis and stroke, and administration of deoxyribonuclease (DNase) attenuates thrombosis in both models (Brill *et al.*, 2012, De Meyer *et al.*, 2012). Likewise, arterial and venous thrombosis in rodents is attenuated by ribonuclease A (RNase), providing evidence that RNA also is a procoagulant stimulus (Fischer *et al.*, 2007, Kannemeier *et al.*, 2007). Because nucleic acid levels are elevated in pathological conditions where thrombosis is a complication (Fuchs *et al.*, 2010, Preissner, 2007), it is important to characterize the role of DNA and RNA in contact activation of coagulation.

We have recently identified histidine-rich glycoprotein (HRG) as a potent inhibitor of the intrinsic pathway that does not affect the extrinsic pathway (MacQuarrie *et al.*, 2011). HRG is a 75 kDa glycoprotein that is present in plasma at 1.5-2 μM, but whose physiological function is unclear (Jones *et al.*, 2005, Poon *et al.*, 2011). Its modular composition includes two NH_2-terminal cystatin domains, a proline-histidine rich region and a COOH-terminal domain. The domains enable HRG to bind to numerous

ligands important in hemostasis, such as fibrin(ogen), heparin, heparan sulfate, DNA and kallikrein (Jones *et al.*, 2005, MacQuarrie *et al.*, 2011). We observed that HRG binds FXIIa and complexes are detected in contact activated plasma (MacQuarrie *et al.*, 2011). HRG binds to FXIIa, but not the zymogen, with a high affinity (K_d 21 nM), and the affinity is increased 1000-fold in the presence of zinc. As a result of HRG binding, the capacity of FXIIa to activate FXII and FXI is attenuated. Consequently, HRG prolongs the FXIIa clot time in plasma, but has little effect on the FIXa and FXIa clotting times, providing additional support that HRG is a potent inhibitor of FXIIa (MacQuarrie *et al.*, 2011). Because HRG is released from activated platelets and also binds fibrin, it is uniquely positioned to be a novel regulator of the intrinsic pathway (Leung *et al.*, 1983).

Since HRG binds DNA (Gorgani *et al.*, 2002), we set out to determine whether HRG attenuates DNA- and RNA-mediated activation of the intrinsic pathway. To address this, we characterized: (a) the procoagulant activity of DNA and RNA in normal and HRG-depleted human plasma, (b) the interaction of HRG with DNA and RNA, (c) the effect of HRG on DNA- and RNA-mediated activation of FXII and FXI and (d) the mechanisms by which HRG modulates thrombin activation of FXI on nucleic acid.

5.5 Experimental Procedures

5.5.1 Materials

5.5.1.1 Reagents

Human α-thrombin, FXII, FXIIa, FXI, FXIa, PK, kallikrein, HK and corn trypsin inhibitor (CTI) were from Enzyme Research Laboratories (South Bend, IN). Pooled, human plasma from 10-15 normal volunteers was prepared by collecting blood into 0.105

M citrate. Platelet poor plasma was prepared by centrifuging blood twice at 4,000 x g for 8 min each to remove cells and stored at -80^{o}C. HRG was isolated from human plasma using a nickel-NTA agarose column as described previously (MacQuarrie *et al.,* 2011) (Kleinschnitz *et al.*, 2006)(MacQuarrie *et al.*, 2011a) and was labeled with fluorescein isothiocyanate (FITC) (Sigma Aldrich) according to the manufacturer's specifications. Dextran sulfate (500 kDa) was from GE Healthcare. Chromogenic substrates H-D-Pro-Phe-Arg-*p*-nitroaniline (S-2302) and pyroGlu-Pro-Arg-*p*-nitroaniline (CS-21(66)) were from Chromogenix (Milano, Italy) and Aniaria (Neuville-sur-Oise, France), respectively. D-Phe-Pro-Arg-chloromethyl ketone (FPR) was from EMD Millipore and FPR-adducts of FXIIa, FXIa and thrombin were prepared as described (Petrera *et al.*, 2009) Full-length hirudin was from Dade-Behring (Marburg, Germany). Phosphatidylcholine and phosphatidylserine (PCPS) (3:1) vesicles were prepared as described (Kretz *et al.*, 2010). 100 bp and 1 kbp DNA ladders were from Invitrogen. Soybean trypsin inhibitor (STI) was from Sigma Aldrich.

5.5.1.2 HRG deficient plasma

Sheep polyclonal antibody against human HRG (Affinity Biologicals, Inc., Ancaster, ON, Canada) was affinity purified using an HRG-Sepharose column, prepared by cyanogen bromide activation. Crude HRG-IgG antiserum was applied to a 4 ml HRG-Sepharose column using a Bio-Rad Biologic Duoflow system at a flow rate of 1 ml/min. The column was equilibrated and washed with 20 mM Tris-HCl, pH 7.4, 150 mM NaCl (TBS)-0.05% Tween 20 (Tw) and the HRG-IgG was eluted with Gentle Elution buffer (GE Healthcare) at 2 ml/min. 2 ml fractions were collected into tubes containing 0.2 ml of

1 M Tris-HCl, pH 8.0. Protein-containing fractions were pooled and the concentration was determined by absorbance at 280 nm. The affinity purified HRG-IgG was then dialyzed into 10 mM Hepes-NaOH, pH 7.4, 150 mM NaCl (HBS) containing 0.05% Tw, precipitated with 50% ammonium sulfate and stored at 4^{o}C. The antibody was immobilized onto cyanogen bromide activated Sepharose. HRG-deficient human plasma was prepared by chromatography over the affinity purified anti-HRG column as described (MacQuarrie *et al.*, 2011). As a control, a second sample of human plasma was subjected to chromatography on unmodified Sepharose. Removal of HRG from human plasma was verified by Western blot analysis using the same affinity purified antibody (MacQuarrie *et al.*, 2011).

5.5.2 Methods

5.5.2.1 Nucleic acid preparation

A549 non-small lung cancer cells (kind gift from Dr. Patricia Liaw) were cultured in petri dishes containing RPMI-1640 media (Invitrogen) with 10% heat inactivated fetal bovine serum (Sigma Aldrich) and 5% penicillin and streptomycin (Sigma Aldrich). For RNA preparations, cell suspensions were stored in RNA Protect reagent (Qiagen, Mississauga, ON, Canada). 200 µl samples of cell suspension were thawed and centrifuged at 10 000 x g for 10-15 min to sediment cells. DNA and RNA were isolated from cells using a DNeasy and RNeasy Plus Blood and Tissue mini isolation kits (Qiagen, Mississauga, ON, Canada), respectively, according to the manufacturer's protocol. Isolated nucleic acids were quantified by absorbance at 260 nm. The integrity of DNA and RNA was assessed by non-denaturing electrophoresis on 1.5 and 2% agarose

gels, respectively. DNA migrated as a narrow band with an apparent size of > 10 kbp whereas two RNA bands migrating at 0.8 and 2 kbp were observed (data not shown). Biotin (B)-labelled DNA and RNA were generated using the Photoprobe (Long Arm) Biotin labeling kit (Vector laboratories, Burlingame, CA) according to the manufacturer's instructions.

5.5.2.2 Plasma Clotting assays

Clotting assays were performed as described (MacQuarrie *et al.*, 2011), with some modifications. To assess the effect of HRG on clot time, 50 µl of citrated mock-depleted or HRG-depleted human plasma containing 15 µM of PCPS was added to a multi-well plate containing 50 µl DNA or RNA (0-25 µg/ml). For HRG repletion experiments, 50 µl of HRG-depleted plasma was added to wells containing 25 µl DNA or RNA (30 µg/ml) and 25 µl HRG (0-3 µM). In all assays, clotting was initiated with addition of 50 µl of $CaCl_2$ (8.3 mM, final). All reagents were diluted into a 41.7 mM imidazole buffer, pH 7.0. Clotting was monitored by turbidity at 405 nm at 37^{o}C using a SpectroMax plate reader (Molecular Devices, Sunnyvale, CA) and the clot time was taken as the time to reach half-maximal absorbance, as determined with instrument software. Experiments were repeated 3 times, each in duplicate.

5.5.2.3 Factor activation assays

The effect of PK and HK on FXII activation in the presence of DNA or RNA (25 µg/ml) or dextran sulfate (0.7 µg/ml) was assessed by monitoring FXIIa chromogenic activity. FXII (150 nM) was added to different reaction mixtures containing no polyanion, DNA, or RNA in the absence or presence of PK (15 nM), HK (37.5 nM), or both.

Reaction mixtures were incubated for 30 min at 37^{o}C, following which STI was added to 100 ug/ml to inhibit kallikrein activity, and 417 uM S-2302 was added to monitor FXIIa activity. FXIIa generation was monitored by absorbance at 405 nm in a Spectromax platereader (Molecular Devices, Sunnyvale CA) and the activity of FXIIa generated was normalized to the activity of FXIIa generated in the absence of nucleic acids and added factors. Experiments were repeated 3 times.

The effects of HRG (0-4.0 μM) on contact activation of FXII and FXI were assessed in the presence of DNA, RNA (20 μg/ml) or dextran sulfate (0.7 μg/ml). FXII activation was monitored in wells containing HRG, nucleic acid or dextran sulfate, FXII (150 nM), PK (15 nM) and HK (37.5 nM). Reactions were incubated for 30 min at 37^{o}C, followed by addition of 100 μg/ml STI. The activity of FXIIa generated was determined by monitoring hydrolysis of 417 μM S-2302. The activity of FXIIa generated was normalized to the activity of FXIIa generated in the absence of HRG. Experiments were repeated 3 times.

Effects of HRG on FXIIa activation of FXI were assessed by adding HRG into wells containing nucleic acids (20 μg/ml) or dextran sulfate (0.2 μg/ml), FXIIa (10 nM), FXI (100 nM) and HK (100 nM). Reactions were incubated at 37^{o}C for 35 min, following, which CTI (30 nM) was added to inhibit FXIIa, and CS-21(66) (529 μM) hydrolysis was monitored at 405 nm to assess the activity of FXIa generated.

The effect of HRG (0-4 μM) on activation of FXI (40 nM) by thrombin (10 nM) was assessed in the absence and presence of nucleic acids. Reactions were incubated at

37^{o}C for 35 min, followed by addition of hirudin (100 nM) to inhibit thrombin activity and the activity of FXIa generated was quantified by monitoring CS-21(66) hydrolysis.

For all assays, the concentration of HRG required to attenuate factor activation by 50% (EC_{50}) was determined by nonlinear regression using a rectangular hyperbola curve (Table Curve, Jandel Scientific, San Rafael, CA). All experiments were performed 3 times.

5.5.2.4 Fluorescence measurements

The binding of single-stranded (ss)-DNA (Sigma Aldrich) and double-stranded (ds)-DNA both from salmon sperm (Invitrogen) to FITC-HRG was assessed by monitoring changes in fluorescence using a Perkin Elmer LS 50B luminescence spectrophotometer (Vu *et al.*, 2011). Briefly, fluorescence was monitored at excitation and emission wavelengths of 492 and 532 nm and slit widths of 10 and 15 nm, respectively, with a 515 nm emission filter. Binding was assessed by titrating aliquots of ss- or ds-DNA (0-0.16 µM) into a cuvette containing FITC-HRG (50 nM) in HBS-Tw. Intensity values (I) were obtained and calculated as a fraction of the baseline fluorescence (I_o). I/I_o values were plotted against concentration of DNA, and the data were analyzed using non-linear regression analysis as previously described (Petrera *et al.*, 2009). Experiments were performed 3 times.

5.5.2.5 Surface plasmon resonance (SPR)

The binding of proteins to B-DNA and B-RNA was determined by SPR using a Biacore T200 (GE Healthcare) in HBS-0.05% Tw. B-DNA and B-RNA were adsorbed to 200-300 response units (RU) onto separate flow cells of a streptavadin-coated chip

(XanTec bioanalytics GmbH, Duesseldorf, Germany) at a flow rate of 5 µl/min. Flow cells were regenerated with 1 M NaCl, 250 mM imidazole and 5 mM EDTA between runs. Aliquots of HRG (0-0.125 µM), FXI (0-0.1 µM), FPR-FXIa (0-0.2 µM) or FPR-thrombin (0-8 µM) were injected at a flow rate of 40 µl/min for 300 s, followed by injections of HBS-0.05% Tw buffer for 800 s to monitor dissociation. An unmodified streptavadin-containing flow cell served as the reference control. Binding of FPR-thrombin was analyzed by steady-state analysis, whereas HRG and FXI/FXIa binding were analyzed by global analysis of on- and off-rates using the Langmuir 1:1 binding model, using instrument software. All experiments were performed 3-4 times.

5.5.2.6 Statistical Analysis

Results are presented as the mean ± standard deviation. Significance of differences was determined using student t-tests. For all analyses, $p<0.05$ was considered statistically significant.

5.6 Results

5.6.1 Effect of HRG on DNA and RNA-mediated activation of coagulation in plasma

We previously showed that HRG is a potent inhibitor of dextran sulfate mediated initiation of the contact pathway (MacQuarrie *et al.*, 2011). To assess the effect of HRG on nucleic acid-mediated activation of the contact pathway, DNA and RNA were titrated into control or HRG-depleted human plasma. DNA and RNA accelerated clotting in both control and HRG-depleted plasma in a dose-dependent and saturable manner (Fig. 5.1 *A-B*) However, the effective concentration of DNA required to reduce clot times by 50% (EC_{50}) was 7-fold lower in HRG-depleted plasma than in control plasma (3.8 ± 1.4 µg/ml

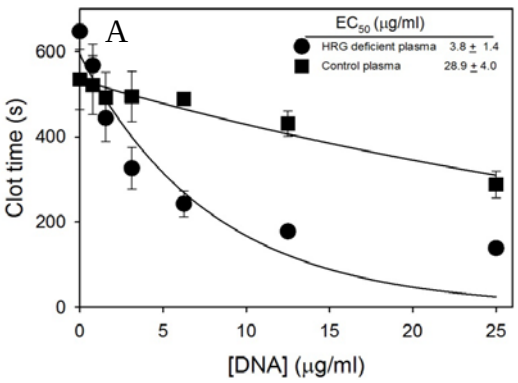
A
EC50 (μg/ml)
HRG deficient plasma 3.8 ± 1.4
Control plasma 28.9 ± 4.0
Clot time (s)
[DNA] (μg/ml)

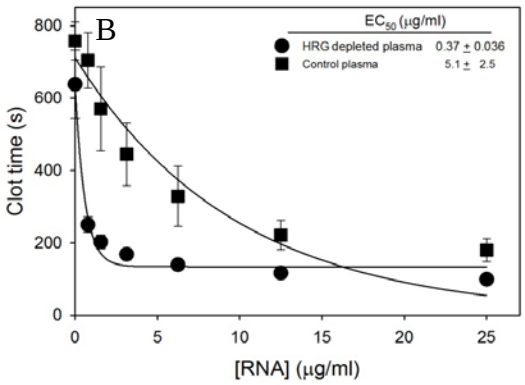
B
EC50 (μg/ml)
HRG depleted plasma 0.37 ± 0.036
Control plasma 5.1 ± 2.5
Clot time (s)
[RNA] (μg/ml)

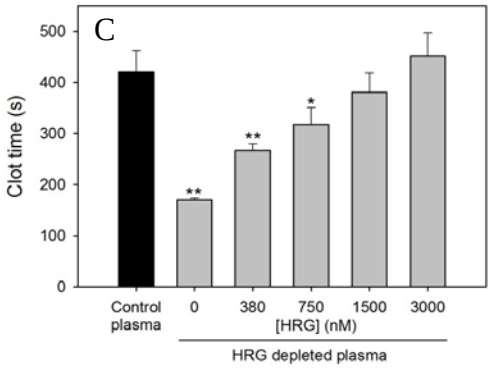
C
Clot time (s)
Control plasma
0
380
750
1500
3000
[HRG] (nM)
HRG depleted plasma

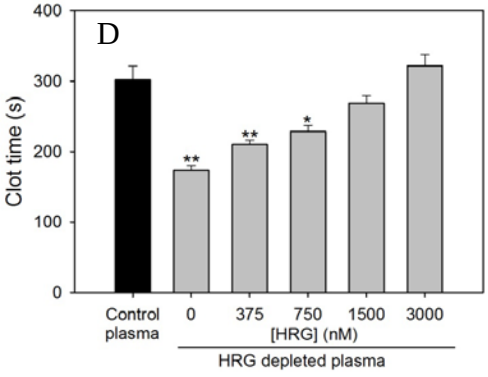
D
Clot time (s)
Control plasma
0
375
750
1500
3000
[HRG] (nM)
HRG depleted plasma

Figure 5.1 Effect of HRG on DNA- and RNA-mediated activation of the contact pathway in plasma.

0-25 μg/ml of (A) DNA or (B) RNA was added to control (■) or HRG-depleted human plasma (●) and clotting was initiated with $CaCl_2$ addition to a final concentration of 8.3 mM. Clot times were determined as the time to reach half-maximal turbidity at 405 nm and plotted versus nucleic acid concentration. EC_{50} values were determined by nonlinear regression (*lines*). Clotting was initiated with (C) DNA (30 μg/ml) or (D) RNA (30 μg/ml) and $CaCl_2$ (8.3 mM) in control (*black bars*) or HRG-depleted human plasma (*gray bars*) supplemented with HRG (0-3000 nM). Data are mean ± SD, of three determinations performed in duplicate. **$p<0.001$, * $p< 0.01$ relative to control plasma.

and 28.9 ± 4.0 μg/ml, respectively ($p<0.01$)). Likewise, the EC_{50} for RNA was 13-fold lower in HRG-depleted plasma compared with control plasma (0.4 ± 0.04 μg/ml and 5.1 ± 2.5 μg/ml, respectively ($p<0.01$)). The role of HRG in nucleic acid-mediated activation was further examined by repletion of HRG in HRG-depleted plasma. When clotting was initiated with 30 μg/ml DNA or RNA, clots times were 1.5-2.0-fold shorter in HRG-depleted plasma than control plasma (~170 s and ~300-400 s, respectively ($p<0.01$)) (Fig. 5.1 *C-D*). Addition of HRG up to 3 μM restored the clot time of HRG-depleted plasma to that of the control plasma in a dose-dependent and saturable manner (Fig. 5.1 *C-D*). These observations extend our previous work by demonstrating that HRG also attenuates DNA- and RNA-mediated activation of coagulation in human plasma.

5.6.2 Effect of HRG on activation of FXII in the presence of nucleic acids, PK and HK

Prior to examining the effect of HRG on the contact system, the capacity of DNA and RNA to promote FXII activation was assessed in the absence and presence of PK and HK. Without HK and PK present, nucleic acids enhanced FXII-activation by ~4-fold (Fig. 5.2 and Table 5.1). Whereas the addition of HK did not augment FXII activation, PK enhanced the capacity of nucleic acids to promote FXII activation by up to 20-fold. However addition of both PK and HK augmented nucleic acid stimulation of the reaction by up to 180-fold (Fig. 5.2 and Table 5.2). Therefore, these observations suggest that nucleic acids alone are poor promoters of FXII activation, and optimal stimulation is observed when both PK and HK are present, in agreement with a recent report (Kannemeier *et al.*, 2007). In contrast, dextran sulfate is more potent because a

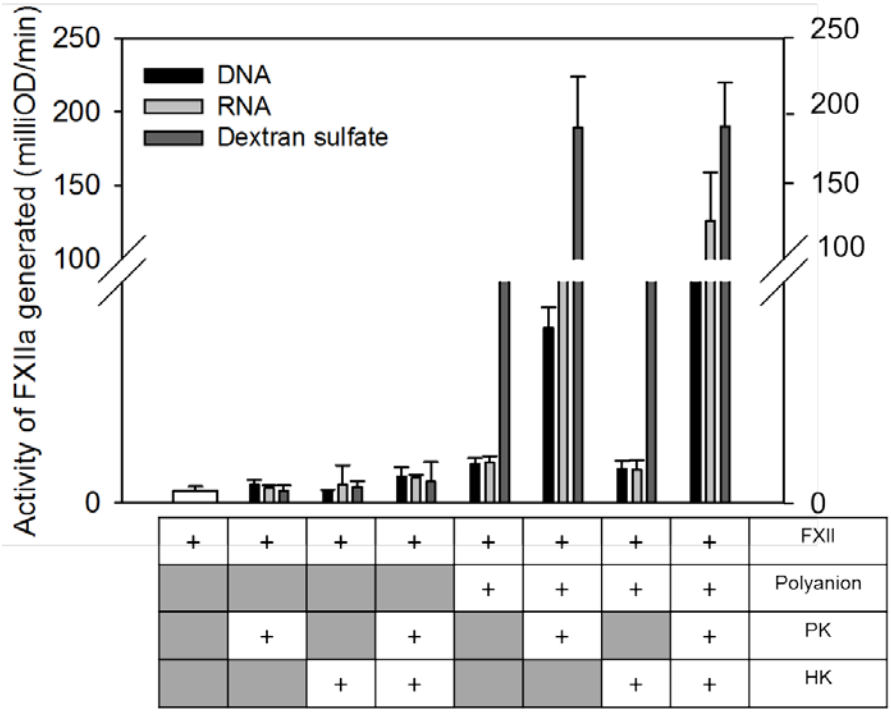
Activity of FXIIa generated (milliOD/min)
250
200
150
100
0
DNA
RNA
Dextran sulfate
FXII
Polyanion
PK
HK

Figure 5.2 Effect of contact proteins on FXIIa generation in the presence of DNA and RNA.

Solutions containing FXII (150 nM), without or with PK (15 nM) or HK (37.5 nM) were prepared in the absence or presence of DNA, RNA (25 μg/ml) or dextran sulfate (0.7 μg /ml). The activity of FXIIa generated was quantified by chromogenic assay using S-3202. In assays where PK was added, kallikrein activity was inhibited with soy trypsin inhibitor (100 μg/ml). Data are mean ± SD, of three determinations.

	FXIIa activity (relative)			
	No polyanion	DNA	RNA	Dextran sulfate
FXII	1.0	3.9	4.0	52.3
FXII + HK	1.3	3.4	3.5	25.3
FXII + PK	2.8	17.5	20.8	209.3
FXII+ PK + HK	2.2	63.0	183.0	212.0

Table 5.1. Effect of DNA and RNA on FXII activation.

Activity of FXIIa generated in the absence or presence of 15 nM PK and 37.5 nM HK and 25 μg/ml DNA, RNA, or 0.7 μg/ml dextran sulfate was normalized to control conditions in the absence of polyanion and added factors. Data are the mean ± SD of three determinations.

concentration of 0.7 μg/ml promotes FXII autoactivation by 52-fold in the absence of PK and HK (Figure 5.2); findings that demonstrate that the mechanism of FXII activation depends on the type of activator.

To assess the effect of HRG on nucleic acid-mediated activation of FXII, experiments were performed in the presence of both PK and HK. HRG attenuated FXIIa generation in a dose-dependent fashion. Activation in the presence of either DNA or RNA was reduced by more than 95% by HRG with an EC_{50} of ~200 nM (Fig. 5.3 *A*). Therefore, by binding to and impairing FXIIa activity, HRG attenuates nucleic acid-mediated activation of FXII, consistent with previous results obtained with dextran sulfate (MacQuarrie *et al.*, 2011).

5.6.3 Effect of HRG on FXIIa activation of FXI in the presence of nucleic acids

Next, we assessed the effect of HRG on activation of FXI by FXIIa. FXI activation was augmented up to 2-fold in the presence of 20 μg/ml nucleic acids ($p<0.05$) (data not shown). However, when HRG was added, there was a dose-dependent inhibition of activation of FXI by FXIIa (Fig. 5.3 *B*). At 2 μM HRG, activation was reduced by 63% and 83% for DNA and RNA with EC_{50} values of ~500 and 100 nM, respectively (Fig. 5.3 *B*). These data show that nucleic acids potentiate FXIIa activation of FXI and HRG abrogates this effect.

5.6.4 Effect of HRG on thrombin activation of FXI in the presence of nucleic acids

Thrombin activation of FXI is a key feedback reaction that is augmented in the presence of surfaces such as dextran sulfate and polyP (Choi *et al.*, 2011, Scott and Colman, 1992). However, it is unknown whether nucleic acids also promote this reaction. To address this,

FXI activation by thrombin was monitored by chromogenic assay in the absence and presence of DNA or RNA. In the absence of surface, thrombin is a poor activator of FXI. The rate of FXI activation by thrombin was increased by 7- to 8-fold in the presence of DNA and RNA, compared with control conditions without surface ($p<0.001$) (Fig. 5.4). For comparison, 0.2 μg/ml of dextran sulfate enhanced FXI activation by thrombin by 71-fold ($p<0.001$; data not shown). Therefore, these data demonstrate that nucleic acids promote FXI activation by thrombin.

The effect of HRG was then tested in this assay. HRG attenuated the capacity of DNA and RNA to promote FXI activation by thrombin in a dose-dependent and saturable manner (Fig. 5.4). Addition of HRG up to 4 μM reduced FXI activation by 60% and 85%, with EC_{50} values of 215 ± 85 nM and 300 ± 160 nM for RNA and DNA, respectively. Likewise, HRG inhibited the capacity of dextran sulfate to promote thrombin activation of FXI (EC_{50} 255 ± 40.4 nM; data not shown). Since HRG does not bind to FXI, FXIa or thrombin (MacQuarrie *et al.*, 2011, Vu *et al.*, 2011), these data suggest that HRG attenuates the stimulatory activity of the nucleic acids.

5.6.5 Binding of HRG to DNA and RNA

To investigate whether HRG attenuates nucleic acid-mediated activation of coagulation by binding nucleic acids, surface plasmon resonance (SPR) was used to characterize the interaction between HRG and DNA and RNA. Nucleic acids were biotinylated and adsorbed onto individual streptavidin-modified flow cells. HRG was injected and binding was quantified. The sensorgrams reveal rapid association and slow dissociation of HRG (Fig. 5.5, *insets*), indicative of high affinity binding. Plotting the RU

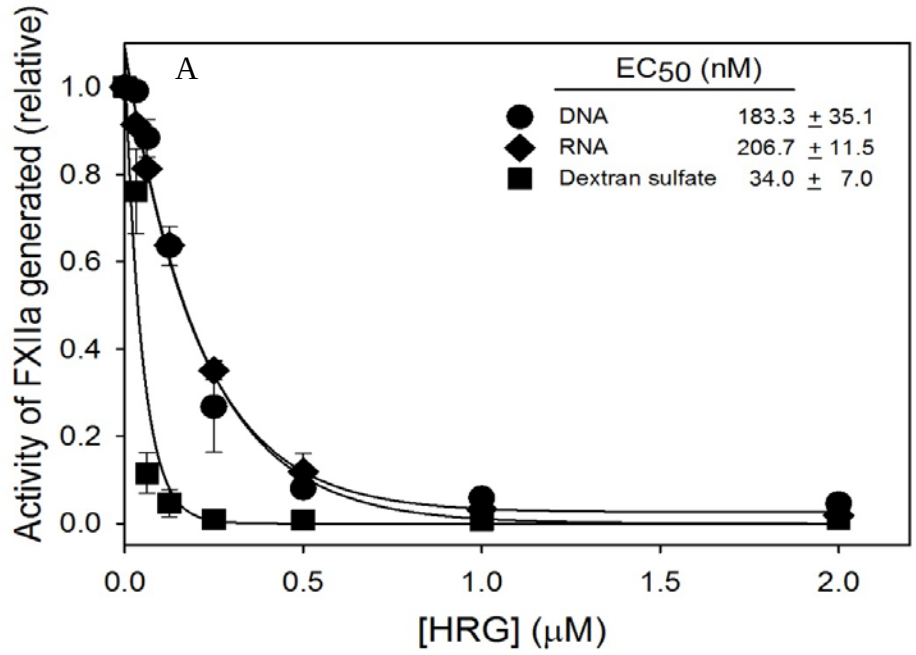
A
EC50 (nM)
DNA 183.3 ± 35.1
RNA 206.7 ± 11.5
Dextran sulfate 34.0 ± 7.0
Activity of FXIIa generated (relative)
[HRG] (μM)

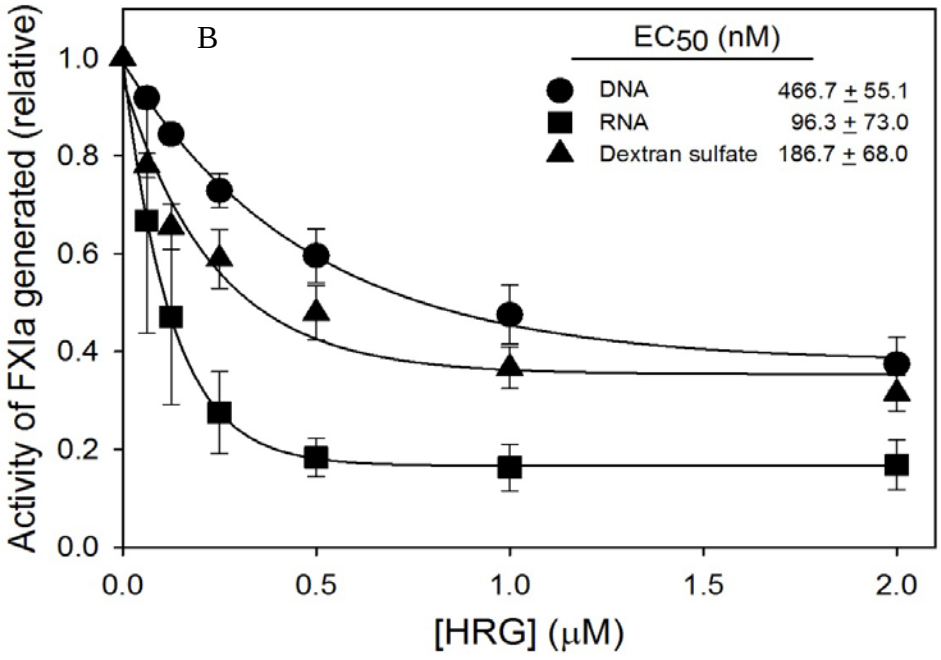
B
EC50 (nM)
DNA 466.7 ± 55.1
RNA 96.3 ± 73.0
Dextran sulfate 186.7 ± 68.0
Activity of FXIIa generated (relative)
[HRG] (μM)

Figure 5.3 Effect of HRG on DNA- and RNA-mediated activation of FXII and FXIIa activation of FXI.

(A) FXII (150 nM), PK (15 nM), HK (37.5 nM) and DNA (●, 20 μg/ml), RNA (◆, 20 μg/ml) or dextran sulfate (■, 0.7 μg/ml) were incubated in the presence of 0-2 μM HRG. In the FXIIa assay, kallikrein was inhibited and FXIIa activity was determined as described in Fig. 3. (B) For FXI activation, FXIIa (10 nM), FXI (100 nM), HK (100 nM) and DNA (●, 20 μg/ml), RNA (◆, 20 μg/ml) or dextran sulfate (■, 0.2 μg/ml) were incubated in the presence of 0-2 μM HRG. After 35 min, FXIIa was inhibited with corn trypsin inhibitor (30 nM) and activity of FXIa generated was determined by monitoring hydrolysis of CS-21(66). The activity of FXIIa or FXIa generated was normalized to that in the absence of HRG and values were plotted versus the concentration of HRG. EC_{50} values were determined by nonlinear regression (*lines*). Data are mean ± SD, of three determinations.

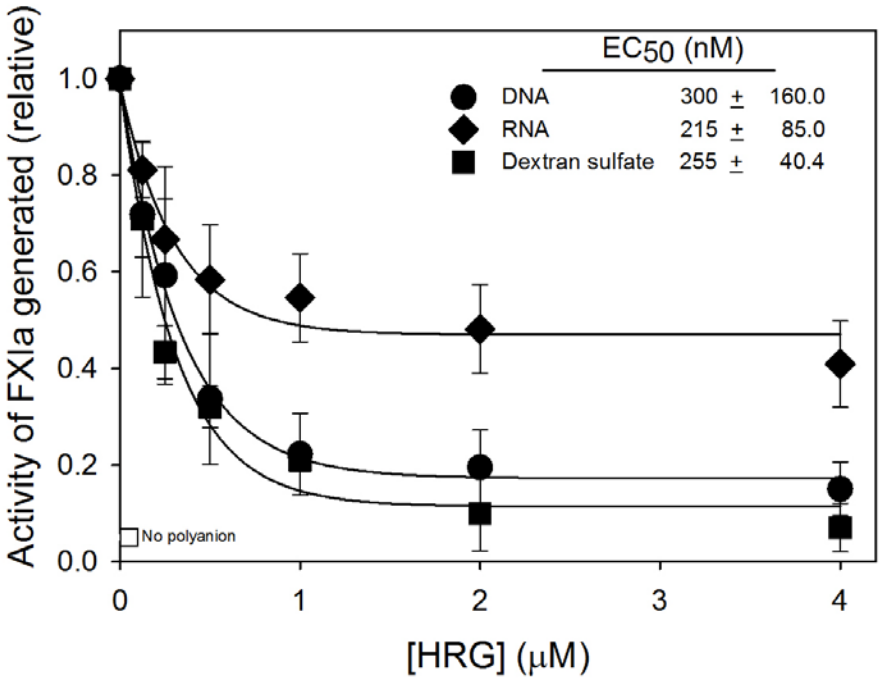
EC50 (nM)
DNA 300 ± 160.0
RNA 215 ± 85.0
Dextran sulfate 255 ± 40.4
No polyanion
Activity of FXIa generated (relative)
[HRG] (μM)
0.0
0.2
0.4
0.6
0.8
1.0
0
1
2
3
4

Figure 5.4 Effect of HRG on thrombin activation of FXI.

HRG (0-4 μM) was incubated with thrombin (10 nM), FXI (40 nM) and DNA (●, 20 μg/ml), RNA (◆, 20 μg/ml) or dextran sulfate (■, 0.2 μg/ml). After 35 min, thrombin was inhibited with hirudin (100 nM) and FXIa activity was determined by monitoring hydrolysis of CS-21(66). The activity of FXIa generated was normalized to that where no HRG was added and values were plotted versus the concentration of HRG. EC_{50} values were determined by nonlinear regression (*lines*). Data are mean ± SD, of three determinations.

values at equilibrium (Req) against input HRG concentrations shows that HRG binds to DNA in a dose-dependent and saturable manner (Fig. 5.5). The affinities of HRG for DNA and RNA are identical, with K_d values of 1.3 ± 0.8 nM (Table 5.2). This is in agreement with previous work, which showed HRG binds DNA with high affinity (Gorgani *et al.*, 2002).

Since processed DNA can contain regions that are single stranded and ss-DNA is structurally different from RNA, we assessed the capacity of FITC-HRG to bind ds- and ss-DNA by fluorescence. FITC-HRG bound to both ds- and ss-DNA with comparable affinities, K_d value of 19.1 ± 1.4 nM and 28.5 ± 10.6 nM, respectively (data not shown). Thus, the data suggest that HRG binds to both ss- and ds-DNA and confirms our observations by SPR. These observations provide additional mechanistic insight and suggest that HRG binds nucleic acids and modulates their procoagulant activity.

5.6.6 Binding of FXI, FXIa and thrombin to DNA and RNA

To assess how HRG attenuates FXI activation by thrombin, we characterized the binding of FXI, FXIa and thrombin to immobilized nucleic acids by SPR. Both FXI and FPR-FXIa bound to B-DNA in a dose-dependent and saturable manner, as shown by the Req plots (Fig. 5.6 *A*-*B*). Both FXI (K_d value of 3-4 nM) and FPR-FXIa (K_d value of 14-16 nM) bind to DNA with high affinity. Similar results were observed with B-RNA (Table 5.2). Therefore, both FXI and FXIa demonstrate high affinity interaction with nucleic acids that is comparable with that of HRG (Table 5.2).

Because thrombin binds polyP (Choi *et al.*, 2011), we asked whether thrombin would also bind to nucleic acids. FPR-thrombin bound to DNA and RNA in a dose-

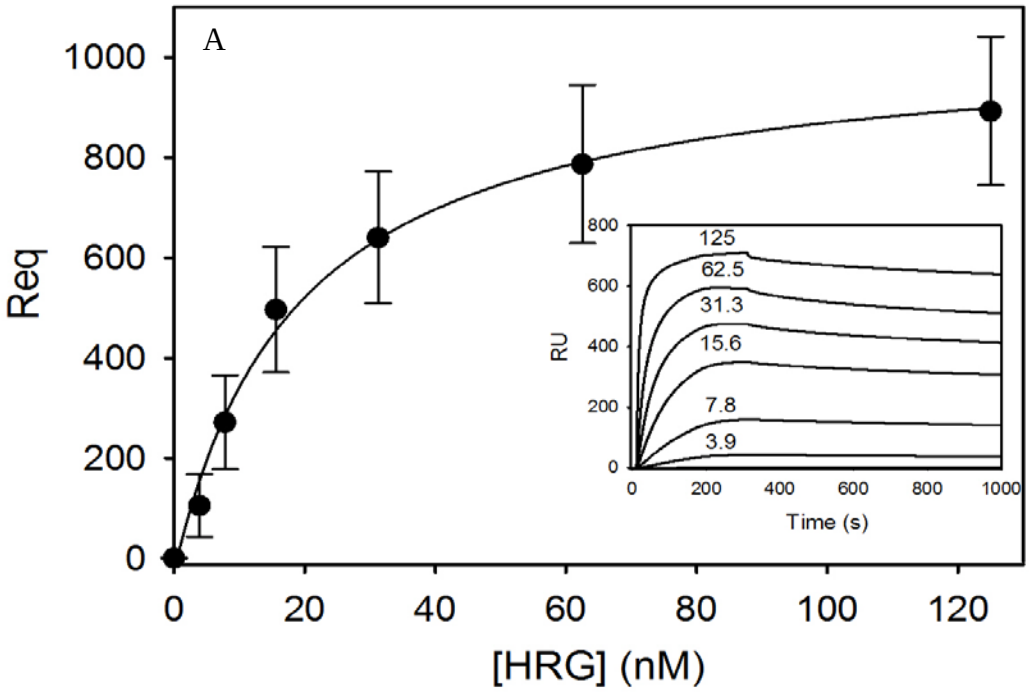
A
Req
[HRG] (nM)
RU
Time (s)
125
62.5
31.3
15.6
7.8
3.9

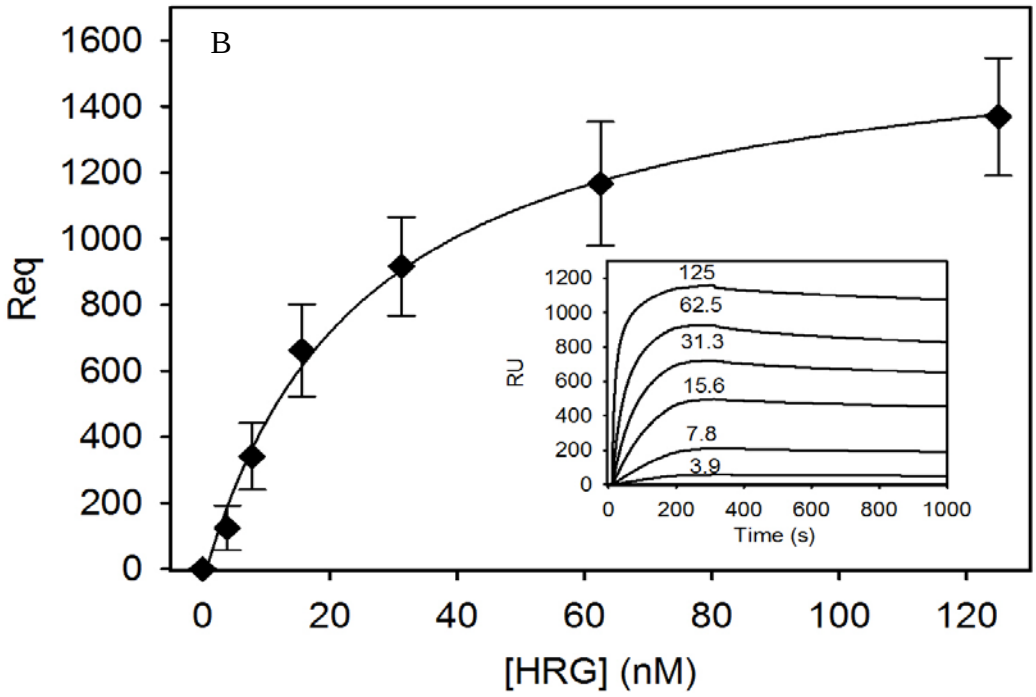
B
Req
[HRG] (nM)
RU
Time (s)
125
62.5
31.3
15.6
7.8
3.9

Figure 5.5 Binding of HRG to DNA and RNA quantified by SPR.

(A) B-DNA and (B) B-RNA were adsorbed to 200-300 RU on separate flow cells containing immobilized streptavadin. An unmodified streptavadin containing cell served as the reference control. HRG (0-0.125 μM) was injected into flow cells for 300 s to assess binding, followed by injections of buffer for 800 s to assess dissociation. The amount of HRG bound at equilibrium (Req) was corrected for background and is plotted against input HRG concentrations. Data are mean ± SD, of three determinations and were fit by non-linear regression analysis using a rectangular hyperbola (*line*). *Insets* show representative binding sensorgrams for DNA and RNA, where input HRG concentrations are indicated adjacent to each tracing.

	DNA	RNA
	K_d (nM)	
HRG	1.3 ± 0.7	1.3 ± 0.7
FXI	3.1 ± 0.4	4.4 ± 0.7
FPR-FXIa	13.6 ± 0.8	15.6 ± 0.2
FPR-thrombin	971.3 ± 211.9	867.7 ± 429.8

Table 5.2 Dissociation constants for the binding of HRG, FXI, FPR-FXIa and FPR-thrombin to DNA and RNA.

The affinities of HRG, FXI, FPR-FXIa and FPR-thrombin for immobilized B-DNA and B-RNA were determined using SPR. K_d values for thrombin binding to nucleic acids are determined by steady state analysis of the Req vs input thrombin concentration plot (Fig. 5.6 *C*). The binding of HRG, FXI and FPR-FXIa to immobilized nucleic acids is quantified by kinetic analysis of the binding sensorgrams (Fig. 5.5 and 5.6, *insets*). Values represent the mean ± SD of three to four determinations.

dependent and saturable fashion (Fig. 5.6 *C, inset),* yielding K_d values of ~0.8-0.9 μM (Table 5.2). Compared with HRG and FXI/FXIa, FPR-thrombin has weaker affinity for nucleic acids. Thus, the capacity of FXI and thrombin to bind nucleic acids supports the contention that DNA and RNA are templates that promote thrombin activation of FXI (Fig. 5.4).

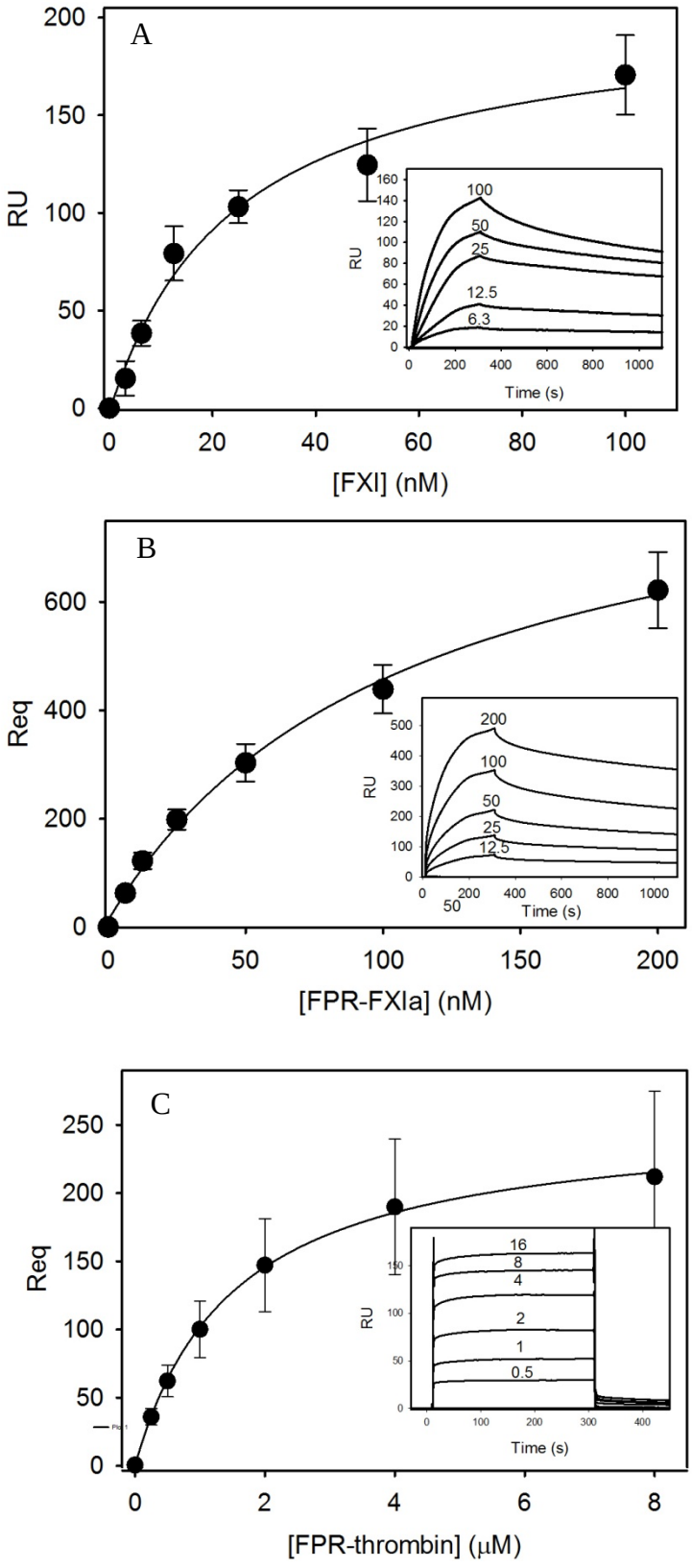
A
RU
[FXI] (nM)
Time (s)
100
50
25
12.5
6.3
B
Req
[FPR-FXIa] (nM)
Time (s)
200
100
50
25
12.5
C
Req
[FPR-thrombin] (μM)
Time (s)
16
8
4
2
1
0.5

Figure 5.6 Binding of FXI, FXIa and thrombin to DNA quantified by SPR.

(A) FXI (0-0.1 μM), (B) FPR-FXIa (0-0.2 μM) and (C) FPR-thrombin (0-8 μM) were separately injected into streptavidin flow cells containing immobilized B-DNA as described for Fig. 5. Req values are plotted against input protein concentration. Data are mean ± SD, of three determinations and were fit by nonlinear regression analysis using a rectangular hyperbola (*line*). *Insets* show representative binding sensorgrams from each experiment, where input protein concentrations are indicated adjacent to each tracing.

5.7 Discussion

Because of the importance of FXII and nucleic acids in thrombosis, it is important to understand how these components are regulated (Fuchs *et al.*, 2010, Kannemeier *et al.*, 2007, Renne *et al.*, 2005). We previously showed that HRG binds FXIIa and attenuates its capacity to promote contact activation of coagulation (MacQuarrie *et al.*, 2011). Therefore, we set out to characterize (a) the mechanism(s) by which RNA and DNA promote FXII and FXI activation and (b) the capacity of HRG to attenuate nucleic acid activation of coagulation. We demonstrated that nucleic acids promote FXII activation and thrombin feedback activation of FXI. Subsequently, we showed that HRG attenuates FXIIa activation of FXII and FXI in the presence of nucleic acids. HRG binds nucleic acids (K_d of ~ 1 nM) and attenuates thrombin feedback activation of FXI by competing with these factors for surface binding. In support of these concepts, HRG was shown to attenuate the procoagulant activity of RNA and DNA in plasma. Collectively, our results confirm that nucleic acids are potent contact activators of coagulation and that HRG is a dynamic regulator of this system.

This study confirms that, in addition to polyP and mast-cell derived heparin, DNA and RNA are potent stimulators of the contact system. The cofactor dependence of FXII activation is sensitive to the type of polyanion (de Maat *et al.*, 2013). For instance, polyP promotes FXII autoactivation (Muller *et al.*, 2009), whereas heparin does so only if PK is present (Pixley *et al.*, 1991). Similar to heparin, we observed that nucleic acids alone are poor activators of FXII, and optimal FXIIa generation was observed in the presence of PK and HK. This reflects the importance of reciprocal activation of FXII and PK on

nucleic acids. Once generated, FXIIa activates FXI, but this process is only weakly promoted by nucleic acids. However, FXI can also be activated by thrombin in a process that is accelerated by polyanions such as dextran sulfate and polyP (Choi *et al.*, 2011). FXI and thrombin bind polyP and the activator augments thrombin activation of FXI, which is an important feedback activation step (Choi *et al.*, 2011). Likewise, we observed that FXI and thrombin also bind RNA and DNA, which are cofactors for thrombin activation of FXI. However, the capacity of nucleic acids to promote this reaction is significantly weaker than dextran sulfate (data not shown); thereby suggesting that thrombin activation of FXI is also sensitive to the nature of the polyanion. Therefore, nucleic acids are physiological activators of FXII and FXI and promote both initiation and amplification of coagulation via the intrinsic pathway.

Although physiological activators of the intrinsic pathway have been identified, it is still unclear how this pathway is regulated to prevent uncontrolled clotting. C1 inhibitor is proposed to be the major regulator of FXIIa, albeit its rate of inhibition is relatively slow compared with other serpin/protease interactions (de Agostini *et al.*, 1984). In addition, when FXIIa is bound to polyanions, it is protected from inhibition (Pixley *et al.*, 1985, Pixley *et al.*, 1987, Wagenaar-Bos and Hack, 2006). However, the ability of HRG to inhibit the activities of FXIIa, RNA, and DNA establishes it as a potentially important regulator of the contact system. Thus, HRG attenuates: (a) FXII activation, (b) FXIIa activity and (c) thrombin feedback activation of FXI. The capacity of HRG to bind RNA and DNA localizes it to the site of contact activation, where it is able to bind and inhibit FXIIa. Further support for a role for HRG comes from the observation that platelets

release zinc and HRG upon activation, and zinc augments HRG-FXIIa affinity by 10^3-fold (MacQuarrie *et al.*, 2011). Thus, the surge of zinc provides a dynamic switch that directs HRG binding to FXIIa, and the HRG-FXIIa interaction may be particularly relevant at sites of vascular injury. Therefore, HRG is equipped to play a prominent role in regulation of FXIIa. In support of this, HRG-FXIIa complexes are detected in contact-activated plasma (MacQuarrie *et al.*, 2011), suggesting that the unidentified protein that interferes with the binding of FXIIa nanobody to FXIIa is HRG (de Maat *et al.*, 2013). These studies identify HRG as a potentially important regulator of the contact system. In support of this, mice deficient in HRG demonstrate accelerated thrombosis in a $FeCl_3$-induced arterial injury model, and administration of HRG reverses this effect (Vu *et al.*, 2013).

The capacity of HRG to bind numerous ligands and modulate different biological pathways is largely ascribed to its multi-domain structure. The NH_2-terminal domain of HRG binds heparin and neutralizes its anticoagulant activity (Borza and Morgan, 1998). Furthermore, the same domain interacts with heparan sulfate on cell surfaces (Jones *et al.*, 2004b). In both instances, HRG binding is augmented in the presence of zinc. Because heparin and nucleic acids are both polyanions, it is likely that they bind to the same domain on HRG. The affinity of HRG for DNA and RNA is comparable in the absence and presence of zinc (data not shown), suggesting that unlike heparin, zinc does not modulate the HRG-nucleic acid interaction. Initial evidence for the ability of HRG to bind nucleic acids comes from the observation that HRG binds to cell surface DNA on apoptotic cells and facilitates their clearance (Gorgani *et al.*, 2002). However, HRG only

weakly binds to chromatin, which is a complex of DNA and histones (Gorgani *et al.*, 2002). Further characterization of the regions of HRG necessary for nucleic acid binding will provide insights into HRG modulation of the contact system.

In addition to binding FXIIa, the capacity of HRG to interact with nucleic acids enhances its ability to regulate the intrinsic pathway. Thus, we demonstrate that HRG is a dynamic modulator of the intrinsic pathway and further characterization of this protein in animal models may lead to the development of novel FXIIa inhibitors that attenuate thrombosis, without impacting bleeding.

CHAPTER 6: Arterial thrombosis is accelerated in histidine-rich glycoprotein deficient mice

6.1 Forward: The effects of HRG deficiency on arterial thrombosis and hemostasis are described in this manuscript. In a RNA-driven, FXII-dependent thrombosis model, HRG-deficiency endows mice with a prothrombotic phenotype and repletion with HRG abrogates this phenotype. Consistent with the role of HRG as a modulator of the contact system, HRG-deficiency has no effect on tail bleeding, thereby demonstrating that it has minimal effects on hemostasis.

A modified version of this manuscript will be submitted to the journal *Blood*. The authors are: Trang T. Vu, Ji Zhou, Beverly A. Leslie, Alan R. Stafford, James C. Fredenburgh, Ran Ni, Shengjun Qiao, Nima Vaezzadaeh, Willi Jahnen-Dechent, Brett Monia and Peter L. Gross and Jeffrey I. Weitz.

Dr. Weitz is the corresponding author.

The experiments in this manuscript were designed and performed by Trang Vu and Dr. Ji Zhou, who are co-first authors. Beverley Leslie also performed experiments. Alan Stafford, Ran Ni, Dr. Shengjuin Qia, Nima Vaezzadaeh, Dr. Willi Jahnen-Dechent, Dr. Brett Monia and Dr. Peter Gross provided technical assistance and/or reagents. The project was designed and the manuscript written by Trang Vu, Dr. James Fredenburgh and Dr. Jeffrey Weitz.

Note: ALL supplemental information (figures and tables) pertaining to this manuscript will proceed the Methods section.

6.2 Summary

Factor (F) XII is a key component of the contact system and triggers clotting via the intrinsic pathway. Although the contact system has little impact on hemostasis, FXII and FXI are important for propagating thrombosis, and naturally occurring polyphosphates have been identified as potent activators of the contact system. Consequently, it is important to understand how the contact system is regulated. Previously, we showed that the plasma protein histidine-rich glycoprotein (HRG) binds FXIIa with high affinity and attenuates its capacity to propagate coagulation. To test the hypothesis that HRG modulates thrombosis without affecting hemostasis, we compared the time to occlusion after $FeCl_3$-induced carotid injury and blood loss after tail tip amputation in HRG-deficient and wild type mice. Although blood loss in HRG-deficient and wild type mice was similar, HRG-deficient mice exhibited accelerated thrombosis, and administration of human HRG abrogated this effect. Neither administration of deoxyribonuclease nor selective depletion of FVII had an impact on thrombosis. However, ribonuclease A or selective depletion of FXII abrogated $FeCl_3$-induced occlusion, indicating that thrombosis is triggered by RNA in a FXII-dependent fashion. Therefore, RNA is a potent stimulator of the contact pathway and by binding RNA and FXIIa with high affinity, HRG attenuates this effect.

6.3 Introduction

Hemostasis depends on rapid blood clot formation at sites of vascular injury to prevent excessive blood loss. Uncontrolled coagulation can lead to life-threatening vascular occlusion, the underlying cause of acute myocardial infarction, ischemic stroke and venous thromboembolism. Despite advances in antithrombotic therapy, thrombotic disorders remain the leading cause of mortality and morbidity worldwide (Mackman, 2008).

According to the classic waterfall model, blood coagulation is initiated via two distinct pathways; the extrinsic pathway, which is initiated by the tissue factor (TF)/factor (F) VIIa complex, and the contact or intrinsic pathway, which is initiated when FXII is activated (MACFARLANE, 1964). Studies in knockout mice highlight the importance of the TF/FVIIa complex not only as a driver of thrombosis, but also as a modulator of hemostasis (Bugge *et al.*, 1996, Mackman *et al.*, 2007, Rosen *et al.*, 1997). In contrast, the contact pathway plays little or no role in hemostasis. Thus, patients with congenital deficiency of FXII or its cofactors, prekallikrein (PK) and high molecular weight kininogen (HK), have no bleeding diathesis, and most of those with FXI deficiency only experience bleeding with surgery or trauma (Gailani and Renne, 2007). Although ignored until recently as a contributor to thrombosis, there is mounting evidence that the contact system is important for thrombus stabilization and propagation (Gailani and Renne, 2007). Thus, mice deficient in FXII or FXI experience attenuated thrombosis at sites of arterial or venous injury (Kleinschnitz *et al.*, 2006, Renne *et al.*, 2005, Wang *et al.*, 2005, Wang *et al.*, 2006). Additionally, selective depletion of FXII or FXI with antisense

oligonucleotides (ASOs), or inhibition of FXIIa or FXIa with targeted antibodies or inhibitors, reduces thrombosis in mouse, rabbit and non-human primate models (Crosby *et al.*, 2013, Larsson *et al.*, 2014, Revenko *et al.*, 2011, Younis *et al.*, 2012, Zhang *et al.*, 2010). With increasing evidence that they contribute to thrombosis, but have only a limited role in hemostasis, FXII and FXI have emerged as attractive targets for new anticoagulant drugs (Gailani and Renne, 2007, Muller *et al.*, 2011).

The intrinsic pathway is initiated when FXII is activated on polyanionic surfaces, a process that is enhanced by PK and HK. FXIIa activates FXI, which propagates the procoagulant response and culminates in thrombin generation and fibrin formation (Colman and Schmaier, 1997). Recent studies suggest that naturally occurring polyphosphates, such as DNA, RNA and inorganic polyphosphate (polyP), may serve as physiological activators of the contact system, findings that provide additional support for the contribution of this system to thrombosis. DNA and RNA are released from stimulated, apoptotic or necrotic cells, whereas polyP is released from activated platelets (Morrissey *et al.*, 2012, van der Vaart and Pretorius, 2008, Yipp and Kubes, 2013). In purified systems, DNA and RNA promote FXII activation; in contrast, platelet polyP, which consists of about 70 phosphate units, is a less potent activator of FXII (Kannemeier *et al.*, 2007, Smith *et al.*, 2010). Plasma levels of cell-free DNA are elevated in murine models of ischemic stroke and venous thrombosis induced by partial ligation of the inferior vena cava, and treatment with deoxyribonuclease (DNase) protects mice from thrombosis in these models (Brill *et al.*, 2012, De Meyer *et al.*, 2012). Likewise, RNA appears to be released after $FeCl_3$-induced arterial injury in mice because administration

of ribonuclease A (RNase), but not DNase, attenuates thrombosis in this model (Fischer *et al.*, 2007, Kannemeier *et al.*, 2007). With potential physiological activators of the contact system now identified and with mounting evidence that this system contributes to thrombosis, it is important to better understand how the contact system is regulated.

Histidine-rich glycoprotein (HRG) is a ~75 kDa glycoprotein that circulates in plasma at a concentration of 1.5-2.0 μM. HRG is a modular protein with distinct structural domains that has been implicated in diverse processes, including coagulation, innate immunity, and angiogenesis (Jones *et al.*, 2005, Lijnen *et al.*, 1980, Poon *et al.*, 2011). HRG binds multiple ligands, including zinc, fibrin(ogen), heparin, plasmin(ogen), DNA, kallikrein and FXIIa (Jones *et al.*, 2005, MacQuarrie *et al.*, 2011, Vu *et al.*, 2011). Because of its numerous interactions, HRG is hypothesized to serve as an adaptor or accessory protein (Jones *et al.*, 2005).

In a previous study, we showed that the activated partial thromboplastin time (aPTT), a test that reflects the integrity of the contact system and intrinsic pathway, is shortened when human plasma is immunodepleted of HRG, whereas the prothrombin time (PT), a test that monitors the extrinsic pathway, is unchanged (MacQuarrie *et al.*, 2011). Therefore, these findings localized the HRG effect to the intrinsic pathway. We went on to show that although HRG does not bind FXII, it binds FXIIa with high affinity and attenuates its capacity to activate FXI and propagate the intrinsic pathway of coagulation (MacQuarrie *et al.*, 2011). In the current study, we have used HRG deficient mice to follow up on these observations and to test the hypothesis that HRG modulates the contact system *in vivo* without affecting hemostasis. To accomplish this, we first

triggered clotting and thrombin generation in plasma from HRG-deficient or wild type mice with an aPTT reagent or with relipidated TF to confirm that HRG deficiency only modulates the intrinsic pathway. Next, using HRG-deficient and wild type mice, we set out to (a) evaluate the effect of HRG deficiency on occlusion time after $FeCl_3$-induced carotid artery injury; (b) use FXII or FVII directed ASOs to examine the relative contribution of the contact system and extrinsic pathway to thrombosis in this model, and (c) determine whether HRG deficiency influences bleeding after tail tip amputation. Finally, additional *in vitro* experiments were performed to better delineate how HRG might modulate the contact system *in vivo*.

6.4 Results

6.4.1 Contact activation and thrombin generation are enhanced in plasma from HRG-deficient mice.

To characterize the role of HRG in the contact system, plasma was obtained from $HRG^{-/-}$, $HRG^{+/-}$ and wild type mice. Complete and partial deficiency of HRG in $HRG^{-/-}$ and $HRG^{+/-}$ mice, respectively, were confirmed by PCR analysis of liver mRNA and immunoblot analysis of plasma samples (data not shown), as previously described (Tsuchida-Straeten *et al.*, 2005). Whereas mean PT values were comparable in $HRG^{-/-}$, $HRG^{+/-}$ and wild type mice (Fig. 6.1A), the mean aPTT values in plasma from $HRG^{-/-}$ and $HRG^{+/-}$ mice were 1.4- and 1.3-fold shorter than that in wild type mice, respectively ($p<0.01$). These findings are consistent with our previous observation that HRG modulates clotting via the contact system (MacQuarrie *et al.*, 2011). To confirm this

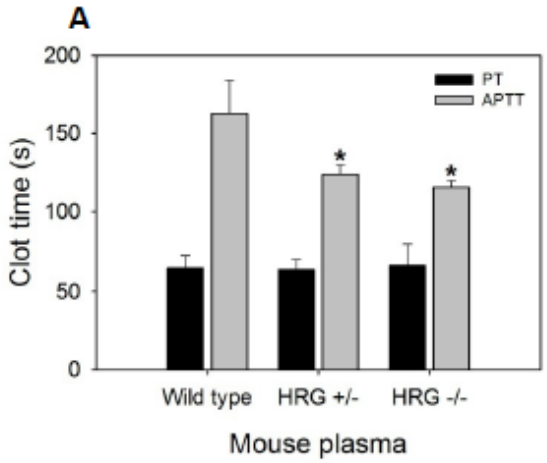

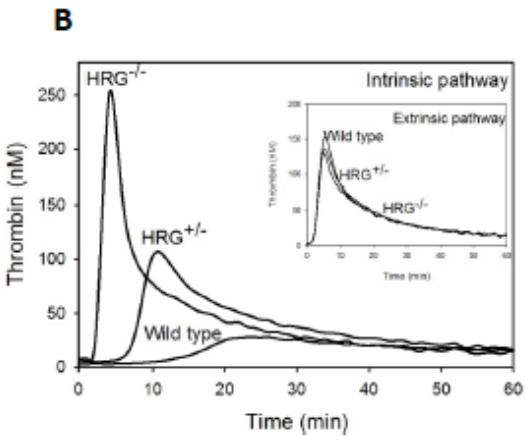

C

	Mouse plasma		
	Wild type	HRG$^{+/-}$	HRG$^{-/-}$
Lag time (min)	9.2 ± 0.8	5.8 ± 0.4*	3.2 ± 0.4*
Peak thrombin (nM)	22.6 ± 3.7	102.6 ± 28.2*	238.3 ± 20.5*
Time to peak (min)	24.2 ± 1.9	10.7 ± 1.5*	4.2 ± 0.4*
Velocity index (nM/min)	1.5 ± 0.3	24.0 ± 13.9*	238.2 ± 20.5*
ETP (nM·min)	1207.5 ± 130.6	2483.0 ± 150.4*	2836.8 ± 32.7*

Figure 6.1 HRG influences the intrinsic pathway of coagulation.

(A) PT and aPTT. The PT (black bars) and aPTT (grey bars) were determined by incubating plasma from wild type, $HRG^{+/-}$ or $HRG^{-/-}$ mice with Recombiplastin or aPTT reagent, respectively. Clotting was initiated by recalcification and was monitored by absorbance. Bars represent the mean of 3 experiments, each performed in duplicate, while the lines above the bars reflect SD. *p<0.001, compared with wild type plasma. (**B**) Representative thrombin generation profiles. Thrombin generation in plasma from wild type, $HRG^{+/-}$ and HRG-$^{/-}$ mice was triggered with aPTT reagent or Recombiplastin to evaluate the intrinsic and extrinsic pathways, respectively (*inset*). Thrombin generation was quantified by monitoring hydrolysis of Z-Gly-Gly-Arg-AMC. (**C**) Summary of thrombin generation data obtained with aPTT reagent. Values represent the mean ± SD of 3 experiments, each performed in duplicate. *p<0.001, compared with results in wild type plasma.

concept, thrombin generation studies were also performed. When initiated with TF, there were no significant differences in thrombin generation variables in plasma from $HRG^{-/-}$, $HRG^{+/-}$ and wild type mice (Fig. 6.2 *inset* and Supplemental Information [SI] Table 6.1). In contrast, when triggered with aPTT reagent (Fig. 6.1B-C), endogenous thrombin potential (ETP) in plasma from $HRG^{+/-}$ and $HRG^{-/-}$ mice was increased 2-fold and 2.4-fold, respectively, compared with that in plasma from wild type mice ($p<0.001$). Likewise, compared with values in plasma from wild type mice, the lag time and time to peak thrombin were shortened by 3- and 6-fold, respectively, and peak thrombin was 10-fold higher, in plasma from $HRG^{-/-}$ mice ($p<0.001$). The thrombin generation variables in plasma from $HRG^{+/-}$ mice were intermediate between those of $HRG^{-/-}$ and wild type mice (Fig. 6.1B-C). Therefore, HRG modulates clotting and thrombin generation initiated via the contact system and has no effect on that initiated via the extrinsic pathway.

6.4.2 HRG attenuates $FeCl_3$-induced arterial thrombosis.

Because HRG attenuates contact activation in murine plasma, we hypothesized that its deficiency would induce a prothrombotic phenotype. To test this hypothesis, we compared blood flow and time to occlusion after $FeCl_3$-induced carotid artery injury in HRG-deficient and wild type mice (Kannemeier *et al.*, 2007, Owens, III *et al.*, 2011). Initially, the model conditions were adjusted such that no arterial occlusion was observed in wild type mice for 30 min after injury. Under these conditions, the mean time to occlusion (TTO) in $HRG^{-/-}$ mice was significantly accelerated to 7.5 ± 2.6 min ($p<0.001$). Although mean TTO in $HRG^{+/-}$ mice was 26.7 ± 14.9 min, blood flow fell by about 60% within the first 10 min after injury and remained decreased thereafter (Fig. 6.2A-B).

Furthermore, the mean area under the blood flow *versus* time curve was significantly ($p<0.001$) reduced by 1.5-fold in $HRG^{+/-}$ and 7.5-fold in $HRG^{-/-}$ mice, compared with that in wild type mice (1507.4 ± 452.3, 304.4 ± 189.4 and 2252.7 ± 392.9 %blood flow·min, respectively). Therefore, thrombosis in the $FeCl_3$-model is significantly accelerated in $HRG^{-/-}$ deficient mice compared with their wild type counterparts, an effect also seen in $HRG^{+/-}$ mice. These findings suggest that deficiency of HRG endows mice with a prothrombotic phenotype and that even a 50% reduction in HRG levels fails to protect the mice from this prothrombotic state.

6.4.3 HRG supplementation abrogates the prothrombotic phenotype in $HRG^{-/-}$ mice.

To further validate the role of HRG in this model of thrombosis, studies were repeated in $HRG^{-/-}$ mice administered human HRG or saline prior to $FeCl_3$-induced injury. To determine the concentration of human HRG required for restoration of HRG levels to normal, we used an enzyme immunoassay to measure plasma HRG concentrations in wild type and $HRG^{-/-}$ mice. Whereas no HRG was detected in plasma from $HRG^{-/-}$ mice, the mean plasma level in wild type mice was 1.5 ± 0.5 μM; a value in agreement with a previous report (Tsuchida-Straeten *et al.*, 2005). When $HRG^{-/-}$ mice were given physiological levels of human HRG, the TTO was > 30 min (Fig. 6.2A-B). In contrast, $HRG^{-/-}$ mice given saline had a mean TTO of 8.9 ± 2.1 min (Fig. 6.2B). Therefore, restoration of HRG to levels similar to those in wild type mice abrogates the prothrombotic phenotype in $HRG^{-/-}$ mice.

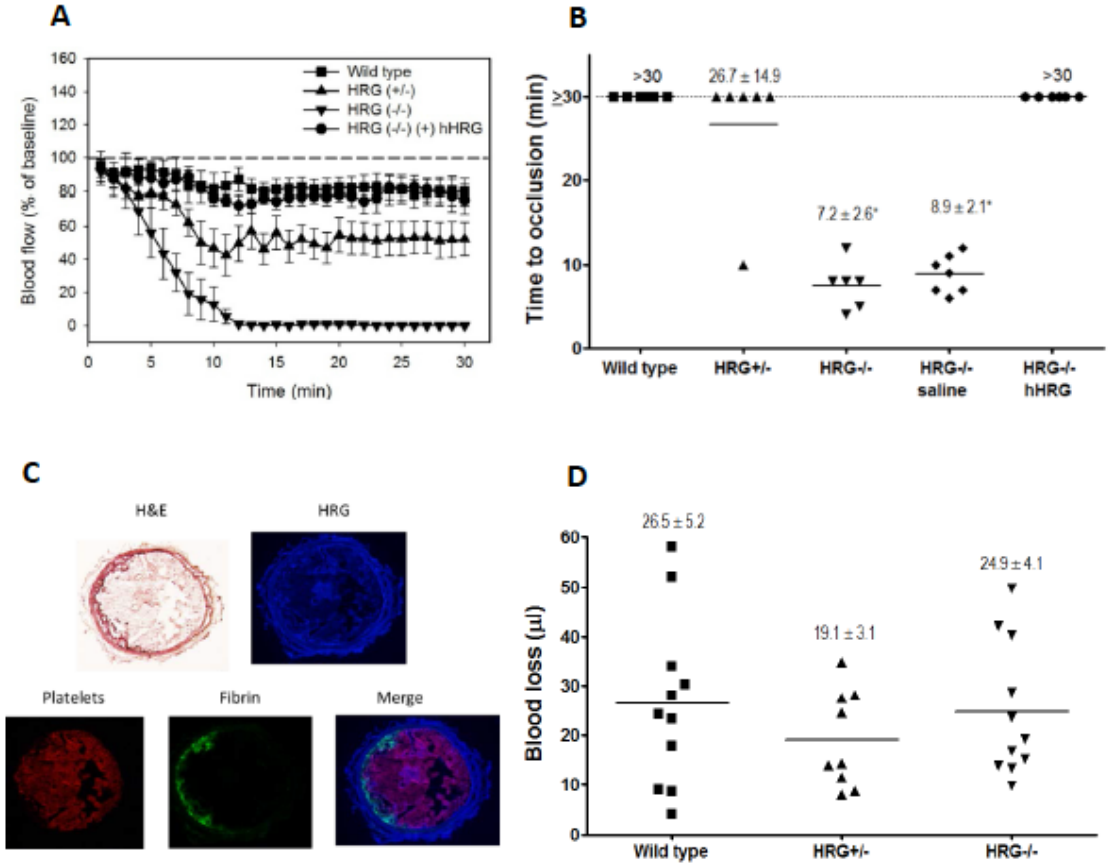
A
Wild type
HRG (+/-)
HRG (-/-)
HRG (-/-) (+) hHRG
Blood flow (% of baseline)
Time (min)
B
Time to occlusion (min)
>30
26.7 ± 14.9
7.2 ± 2.6*
8.9 ± 2.1*
>30
Wild type
HRG+/-
HRG-/-
HRG-/- saline
HRG-/- hHRG
C
H&E
HRG
Platelets
Fibrin
Merge
D
Blood loss (µl)
26.5 ± 5.2
19.1 ± 3.1
24.9 ± 4.1
Wild type
HRG+/-
HRG-/-

Figure 6.2 HRG deficiency in mice is associated with accelerated thrombosis after $FeCl_3$-induced arterial injury, but has minimal effect on hemostasis.

(**A**) 1x1 mm filter paper presoaked in 7.5% $FeCl_3$ was applied for 1 min to the right carotid artery of wild type, $HRG^{+/-}$ and $HRG^{-/-}$, and $HRG^{-/-}$ mice given human HRG to 2 μM or saline (n=6 to 7) to initiate vascular injury. Using an ultrasonic flow probe, blood flow was continuously measured for 30 min after injury. Flow measurements at the times indicated are expressed as a percentage of baseline flow prior to injury. Symbols represent the means, while the bars reflect SE. (**B**) Time to occlusion (TTO) in wild type, $HRG^{+/-}$ and $HRG^{-/-}$, and $HRG^{-/-}$ mice given human HRG or saline. TTO values, defined as the time required for blood flow to fall below 20% of the baseline value for at least 3 consecutive min, are presented as a scatter diagram, where symbols represent individual values, and horizontal lines represent the mean values in each of the 5 groups. *$p<0.001$, compared with data in wild type mice. (**C**) Representative thrombi harvested from the carotid artery of a wild type mouse 30 min after $FeCl_3$-induced injury and subjected to immunohistochemical analysis using antibodies against HRG, platelets and fibrin or stained with hematoxylin and eosin (H&E). (**D**) Influence of HRG on hemostasis. Cumulative blood loss for 30 min after tail tip amputation was quantified in wild type, $HRG^{+/-}$, and $HRG^{-/-}$ mice (n=9-11 per group). Symbols represent individual values, while horizontal lines represent the mean values in each of the 3 groups.

6.4.4 Immunostaining localizes HRG with platelets and fibrin in thrombi formed after $FeCl_3$-induced injury.

To localize HRG, thrombi from wild type mice were removed and subjected to immunohistochemical analysis to determine whether HRG localizes with fibrin and platelets. Whereas platelets were dispersed throughout the thrombi, fibrin deposition was localized to the vessel wall, likely at the site of $FeCl_3$ application (Fig. 6.2C). Because HRG is stored in platelet α-granules and released upon platelet activation and because HRG binds to fibrin (Leung *et al.*, 1983, Vu *et al.*, 2011) we hypothesized that HRG would localize with these components in the thrombi. Consistent with this hypothesis, HRG was detected in thrombi where it localized with platelets and, to a lesser extent, with fibrin (Fig. 6.2C). These data confirm that HRG is found in the thrombi formed after $FeCl_3$-induced arterial injury in mice.

6.4.5 Hemostasis is normal in $HRG^{-/-}$ or $HRG^{+/-}$ mice.

To examine the role of HRG in hemostasis, a tail bleeding assay was used. Cumulative blood loss over the 30 min period after standardized tail transection (Fig. 6.2D) was not significantly different in $HRG^{-/-}$ and $HRG^{+/-}$ mice from that in the wild type controls (24.9 ± 3.9, 19.1 ± 3.1, and 26.5 ± 4.9 μl, respectively; $p>0.2$). These findings are at odds with previous work, which reported a significantly shorter bleeding time in $HRG^{-/-}$ mice than in wild type controls (Tsuchida-Straeten *et al.*, 2005). The discrepancy may reflect differences in the bleeding models; we monitored cumulative blood loss over a 30 min period, whereas the time to bleeding cessation was determined in the previous study

(Tsuchida-Straeten *et al.*, 2005). Taken together, our results suggest that HRG modulates thrombosis with minimal effects on hemostasis.

6.4.6 $FeCl_3$-induced arterial thrombosis occurs via the contact system.

To examine the relative contribution of the contact system and extrinsic pathway to $FeCl_3$-induced arterial thrombosis, we used ASOs to selectively knock down the levels of FXII or FVII in wild type mice and examined their effect on thrombosis after $FeCl_3$-induced carotid injury. To our knowledge, this is the first reported use of a murine-specific FVII-directed ASO to assess the role of the extrinsic pathway in thrombosis. ASOs were administered twice-weekly by subcutaneous injection for up to 6 weeks and a benign ASO sequence was used as a control. Compared with untreated mice and those given the control ASO, the FXII and FVII targeted ASOs reduced plasma levels of their cognate proteins by 99% and 90-95%, respectively, in wild type mice, as determined by immunoblot analysis (Fig. 6.3A). Likewise, the ASOs dampened the expression of their respective proteins in a similar manner in the $HRG^{-/-}$ mice (data not shown). Whereas the aPTT was significantly ($p<0.001$) prolonged by 2-3-fold in plasma from mice given the FXII ASO compared with that in controls, the PT values were similar (SI Fig. 6.1B-C). In contrast, compared with controls, the PT was prolonged 1.4- to 1.7-fold ($p<0.001$) in plasma from mice given the FVII ASO, but the aPTT values were similar (SI Fig. 6.1B-C). Similar results were obtained in ASO-treated $HRG^{-/-}$ mice (SI Fig. 6.1A-C). Together, these results demonstrate that selective depletion of FXII or FVII using ASOs attenuates clotting initiated via the contact system and extrinsic pathways, respectively.

We then examined the effect of ASO treatment on $FeCl_3$-induced arterial thrombosis. To ensure that thrombosis occurred in wild type mice treated with the control ASO, a larger filter paper was used for $FeCl_3$ application and the exposure time was lengthened. Despite selective depletion of FVII, blood flow rapidly decreased and the mean TTO in these mice was similar to that in controls. In contrast, with selective knockdown of FXII, the vessels remained patent for over 30 min (Fig. 6.3B-C), a finding consistent with previous work showing attenuated thrombosis after $FeCl_3$-induced arterial injury in $FXII^{-/-}$ mice (Renne *et al.*, 2005). Together, our data suggest that the contact system is a more important driver of thrombosis after $FeCl_3$-induced injury than the extrinsic pathway, at least under the conditions of our model.

Next, we compared the effect of selective FXII or FVII knockdown on occlusion after $FeCl_3$-induced arterial injury in $HRG^{-/-}$ mice (SI Fig. 6.1A-D). Because $HRG^{-/-}$ mice exhibit accelerated thrombosis compared with wild type mice, less stringent $FeCl_3$ conditions were used in $HRG^{-/-}$ mice than in wild type mice. Like the results in wild type mice, knockdown of FXII, but not FVII, attenuated thrombosis in $HRG^{-/-}$ mice (SI Fig. 6.1D). Thrombosis after $FeCl_3$-induced injury was accelerated in $HRG^{-/-}$ mice compared with wild type mice (Fig. 6.2A-B), findings that not only suggest that HRG attenuates coagulation driven by the contact system, but also are in keeping with our previous report that HRG modulates FXIIa activity (MacQuarrie *et al.*, 2011).

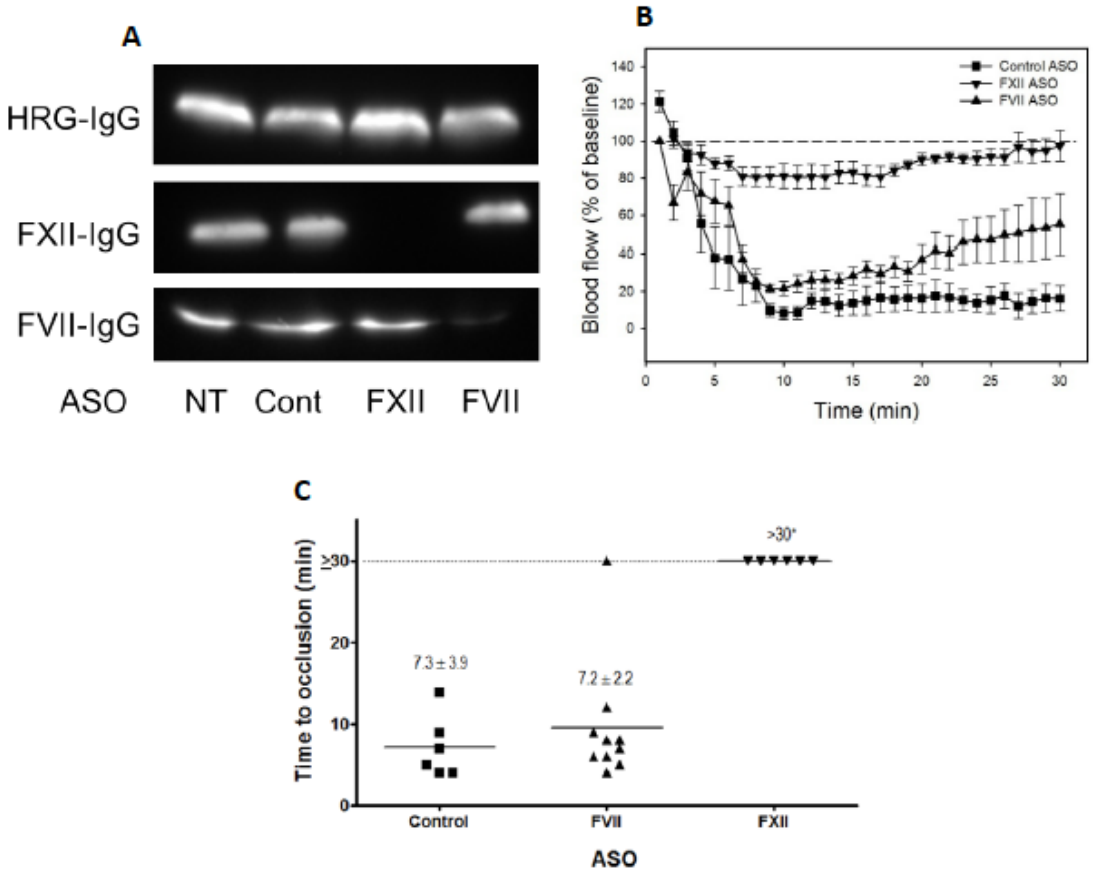
A
HRG-IgG
FXII-IgG
FVII-IgG
ASO NT Cont FXII FVII
B
Control ASO
FXII ASO
FVII ASO
Blood flow (% of baseline)
Time (min)
C
Time to occlusion (min)
≥30
>30'
7.3±3.9
7.2±2.2
Control
FVII
FXII
ASO

Figure 6.3 Thrombosis after $FeCl_3$-induced carotid artery injury occurs via the contact system.

Wild type mice were given FXII, FVII or control (Cont) ASOs by twice weekly subcutaneous injection for up to 6 weeks. (**A**) Plasma from these mice was then subjected to immunoblot analysis to quantify the levels of HRG, FXII and FVII. (**B-C**) Effect of FXII or FVII ASO pretreatment on thrombosis. A 1x2 mm filter paper presoaked in 10% $FeCl_3$ was applied for 1.5 min to the right carotid artery of wild type mice pretreated with FXII, FVII or control ASOs to initiate vascular injury (n=6-10 per group). (**B**) Blood flow was continuously monitored before and for 30 min after injury and data were analyzed and plotted as described in the legend for Fig. 6.2. Symbols represent the means, while the bars reflect SE. (**C**) The TTO values in wild type mice pretreated with FXII, FVII or control ASOs were determined as described in the legend for Fig. 6.2. TTO data are presented as a scatter diagram, where symbols represent individual values, and horizontal lines represent the mean values in each of the 3 groups. *$p<0.001$, compared with the control ASO group.

6.4.7 RNA mediates $FeCl_3$ injury-induced arterial thrombosis.

Having demonstrated that the contact system is a more important driver of thrombosis after $FeCl_3$-induced injury than the extrinsic pathway, we set out to identify the initiator of thrombosis in this model. As controls, we first performed clotting studies in plasma to confirm that DNase and RNase attenuated the procoagulant effects of DNA and RNA, respectively (SI Fig. 6.2A-D). Using saline as a control, we next examined the effects of DNase and RNase administration on $FeCl_3$-induced arterial thrombosis in wild type mice. With conditions that ensured rapid thrombosis after $FeCl_3$ application, the mean TTO in mice given saline or DNase were 10.8 ± 2.9 and 9.4 ± 8.5 min, respectively ($p=0.7$) (Fig. 6.4A-B). In contrast, there was no occlusion after 30 min in mice given RNase ($p<0.001$, compared with saline controls) (Fig. 6.4A-B), a finding in keeping with a previous report (Kannemeier *et al.*, 2007). RNA was detected in thrombi harvested from the mice (Fig. 6.4C) and administration of RNase reduced the amount of RNA in the thrombi compared with that in thrombi from the saline control group (Fig. 6.4D), findings that support RNA as the initiator of thrombosis in this model. In contrast, DNA was not detected in the thrombi (SI Fig. 6.3A-B). Similar results were obtained when the studies were repeated in $HRG^{-/-}$ mice, indicating that HRG-deficiency does not alter the capacity of RNase to modulate thrombosis in the $FeCl_3$-model (SI Fig. 6.4). The observations that HRG-deficiency induces a prothrombotic phenotype and that HRG localizes with RNA in the thrombi harvested from mice after $FeCl_3$-induced injury (Fig. 6.4C), suggest that HRG modulates RNA-driven thrombosis.

6.4.8 HRG attenuates RNA-induced thrombin generation and clot formation in murine plasma.

When initiated with RNA, thrombin generation in plasma from $HRG^{-/-}$ mice was enhanced compared with that in plasma from wild type control mice and intermediate in plasma from $HRG^{+/-}$ mice (Fig. 6.5A-B). Thus, compared with control, the lag time and time to peak thrombin in plasma from $HRG^{-/-}$ mice were shortened by 1.5- and 2-fold, respectively ($p<0.001$), whereas the peak thrombin and ETP values were increased by 3.7- and 1.8-fold, respectively ($p<0.001$). The difference in RNA-induced clotting in

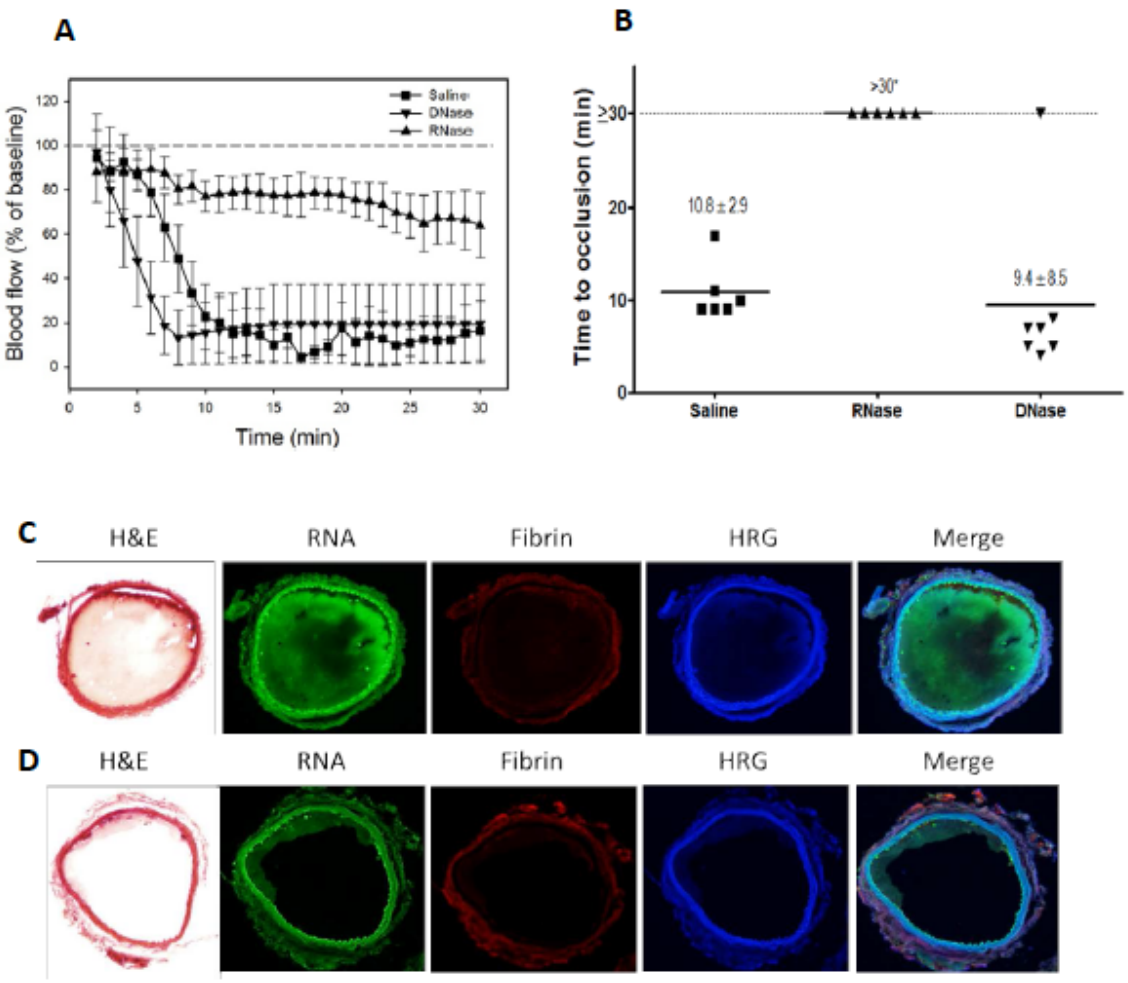
A
Blood flow (% of baseline)
Time (min)
Saline
DNase
RNase
B
Time to occlusion (min)
>30'
10.8±2.9
9.4±8.5
Saline
RNase
DNase
C
H&E
RNA
Fibrin
HRG
Merge
D
H&E
RNA
Fibrin
HRG
Merge

Figure 6.4. RNA initiates thrombosis after $FeCl_3$-induced carotid artery injury.

(**A-B**) Effect of RNase or DNase administration on thrombosis. After injection of 2 mg/ml RNase, 1 mg/ml DNase or saline into the left jugular vein, a 1x2 mm filter paper presoaked in 7.5% $FeCl_3$ was applied to the right carotid artery for 1.5 min to initiate vascular injury (n=6-7 per group). (**A**) Blood flow was continuously monitored and the data are plotted as described in the legend for Fig. 6.2. Symbols represent the means, while the bars reflect SE. (**B**) The TTO values were determined and plotted as described in the legend for Fig. 6.2. *$p<0.001$, compared with saline control. (**C-D**) Representative thrombi harvested from the carotid artery of wild type mice pretreated with (**C**) saline or (**D**) RNase. Prior to injury, mice were given an intravenous injection of a RNA-specific fluorescent stain to identify RNA within the thrombus. Thrombi were sectioned and subjected to immunohistochemical analysis using antibodies against HRG or fibrin, or were stained with H&E.

A

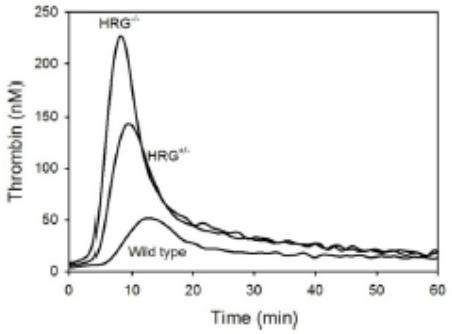

B

	Mouse plasma		
	Wild type	HRG$^{+/-}$	HRG$^{-/-}$
Lag time (min)	6.0 ± 0.0	4.5 ± 0.6*	4.0 ± 0.0*
Peak thrombin (nM)	63.3 ± 14.5	160.1 ± 25.8*	242.0 ± 45.0*
Time to peak (min)	11.8 ± 1.0	8.3 ± 0.5*	6.8 ± 1.0*
Velocity index (nM/min)	11.4 ± 4.1	42.6 ± 10.5*	96.7 ± 44.1*
ETP (nM·min)	1719.3 ± 174.5	2872.8 ± 98.3*	3246.8 ± 98.2*

C

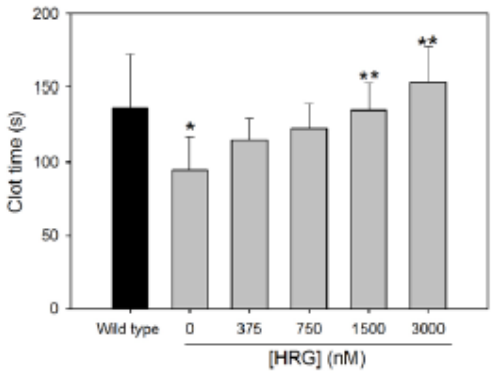

Figure 6.5 HRG attenuates RNA-induced activation of coagulation.

(**A-B**) Thrombin generation was quantified after adding 16 μg/ml RNA to plasma from wild type, $HRG^{+/-}$ or $HRG^{-/-}$ mice. (**A**) Representative thrombin generation profiles. (**B**) Summary of thrombin generation data. Values represent the means ± SD of 3 experiments, each performed in duplicate. *p<0.001, compared with results from wild type controls. (**C**) Effect of HRG on RNA-induced clotting. Clotting was initiated in plasma from wild type (*black*) or $HRG^{-/-}$ (*grey*) mice containing human HRG at the indicated concentrations by addition of 30 μg/ml of RNA and recalcifying. Bars reflect the mean of 3 experiments, each performed in duplicate, while the lines above the bars reflect SD. *p<0.05, compared with wild type plasma; **p<0.01, compared with plasma from $HRG^{-/-}$ mice without HRG supplementation.

plasma from control and $HRG^{-/-}$ mice was abrogated when human HRG was added to the HRG-deficient plasma (Fig. 6.5C). Collectively, these data suggest that HRG modulates the procoagulant effect of RNA.

6.4.9 HRG, FXII and FXIIa bind RNA.

HRG has been reported to bind DNA (Gorgani *et al.*, 2002), and we previously showed that HRG binds FXIIa with high affinity, but not FXII (MacQuarrie *et al.*, 2011). To determine whether RNA could serve as a template onto which HRG, FXII and/or FXIIa assemble, surface plasmon resonance (SPR) was used to quantify the interaction of these proteins with immobilized RNA. The amount of protein bound to RNA at equilibrium (Req) was plotted against titrant concentrations to quantify affinity (Fig. 6.6). All three proteins bound RNA in a concentration-dependent and saturable fashion. HRG formed the highest affinity interaction with RNA (K_d value of 16.2 ± 1.8 nM). Thus, HRG bound RNA with 43-fold higher affinity than FXII and over 100-fold higher affinity than FXIIa, which bound RNA with K_d values of 0.7 ± 0.06 μM and 2.7 ± 0.8 μM, respectively. Further analysis of the sensorgrams revealed that although FXII and FXIIa bound RNA with similar on-rates, FXIIa dissociated from RNA with an initial off-rate that was 31-fold faster than that of FXII (Fig. 6.6B-C, *inset*). These data suggest that once FXII is activated, its affinity for RNA decreases. In support of this concept, the Req plots show that whereas binding of FXII to immobilized RNA saturates at 1 μM, 4-times more FXIIa is needed to achieve saturation. These findings suggest that the capacity of RNA to bind FXIIa is less than that for FXII (Fig. 6.6B-C). Collectively, these observations provide a potential mechanism by which RNA induces contact activation

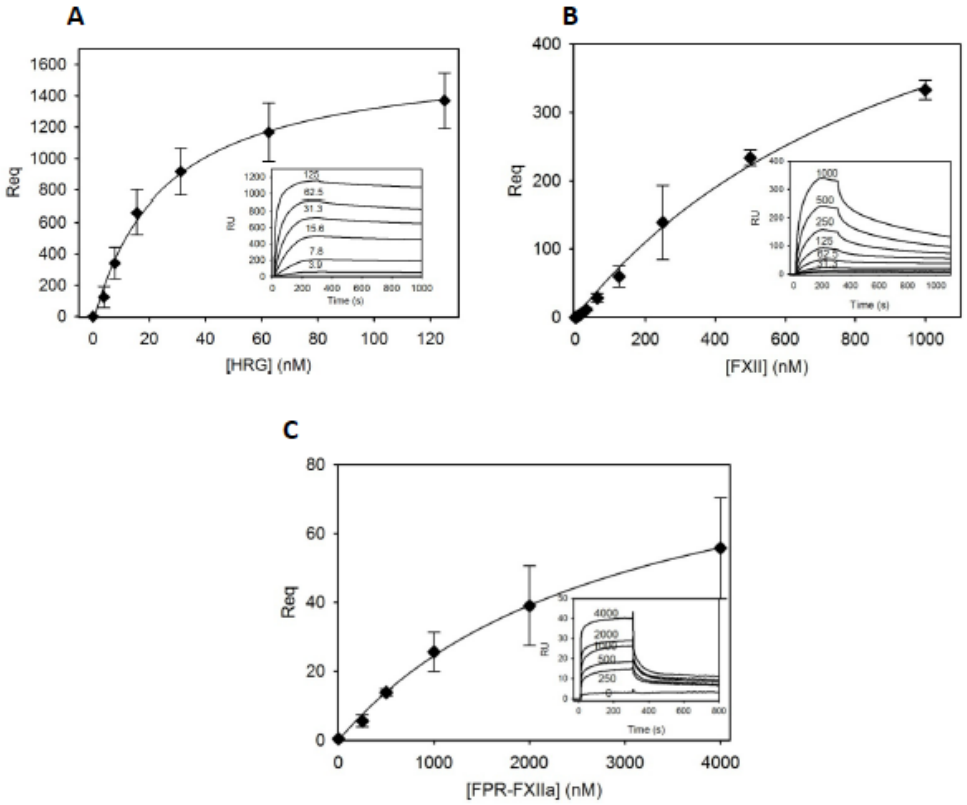
A
Req
[HRG] (nM)
RU
Time (s)
B
Req
[FXII] (nM)
RU
Time (s)
C
Req
[FPR-FXIIa] (nM)
RU
Time (s)

Figure 6.6 HRG, FXII and FXIIa bind to immobilized RNA.

Biotinylated-RNA was adsorbed to 200-300 RU on separate SPR flow cells containing streptavidin. An unmodified streptavadin-containing cell served as the reference control. (**A**) HRG in concentrations ranging from 0-0.125 μM, (**B**) FXII in concentrations ranging from 0-1 μM, (**C**) or FPR-FXIIa in concentrations ranging from 0-4 μM was injected into flow cells to assess protein binding. The binding constants were determined by non-linear regression analysis of the amount of protein bound at the equilibrium point (Req) plotted against the input protein concentrations (*lines*). *Insets* show a representative binding sensorgram for each experiment, with analyte concentrations indicated. Symbols represent the mean of 3 experiments, while the lines above and below the symbols reflect SD.

of coagulation and HRG attenuates this process.

6.5 Discussion

Emerging data highlight the importance of the contact system in the pathogenesis of thrombosis and identify naturally occurring polyphosphates, such as nucleic acids, as potential initiators of this pathway. However, it is unclear how the contact system is regulated so as to prevent uncontrolled clotting. Previously, we demonstrated that HRG binds FXIIa with high affinity and attenuates contact activation of coagulation *in vitro* (MacQuarrie *et al.*, 2011). In this study, we used HRG-deficient mice to test the hypothesis that HRG modulates the contact system without affecting hemostasis.

To confirm that HRG deficiency only modulates the intrinsic pathway, we triggered clotting and thrombin generation in plasma from HRG-deficient or wild type mice with an aPTT reagent or with relipidated TF. Compared with the results in plasma from wild type mice, aPTT reagent accelerated the clotting time and enhanced thrombin generation in plasma from $HRG^{-/-}$ mice, a difference that was attenuated with HRG supplementation of the deficient plasma (Fig. 6.1). In contrast, there was no difference when relipidated TF was used in place of aPTT reagent. Therefore, these results demonstrate that not only does HRG selectively attenuate contact activation of coagulation in human plasma (MacQuarrie *et al.*, 2011), but it also does so in murine plasma.

With the contact system as its target, we speculated that HRG would have no influence on hemostasis. In support of this concept, we demonstrated that tail bleeding in $HRG^{-/-}$ and $HRG^{+/-}$ mice is similar to that in wild type mice (Fig. 6.2D). To test the

hypothesis that HRG modulates thrombosis, we compared the time to occlusion after $FeCl_3$-induced carotid injury in HRG-deficient and wild type mice. $HRG^{-/-}$ mice exhibited accelerated occlusion compared with wild type controls, an effect abrogated with HRG repletion. $HRG^{+/-}$ mice also exhibited more rapid reduction in blood flow after $FeCl_3$-induced injury than their wild type counterparts, indicating that even with a partial reduction in HRG levels, thrombosis is accelerated (Fig. 6.2A-B). These findings suggest that HRG deficiency induces a prothrombotic phenotype, which is in agreement with previous work (Tsuchida-Straeten *et al.*, 2005).

To validate the modulating effect of HRG on the contact system, we characterized the $FeCl_3$-model of thrombosis using ASOs that selectively knockdown FXII or FVII levels. In wild type and $HRG^{-/-}$ mice, knockdown of FXII, but not FVII, attenuated thrombosis; indicating that thrombosis in this model occurs via the intrinsic pathway. Administration of RNase, but not DNase, attenuated thrombosis suggesting that $FeCl_3$-induced thrombosis is mainly driven by RNA (Kannemeier *et al.*, 2007); a finding consistent with another report (Kannemeier *et al.*, 2007). The origin of RNA in the $FeCl_3$-model is currently unknown. There have been conflicting data as to whether $FeCl_3$ induces endothelial denudation (Barr *et al.*, 2013, Eckly *et al.*, 2011), or triggers thrombosis through other mechanisms. A recent report implicates red blood cells in the pathogenesis of $FeCl_3$-induced thrombosis (Barr *et al.*, 2013) and *in vitro* work suggests that when activated, red blood cells can promote thrombin generation (Whelihan *et al.*, 2012). Consequently, RNA may be derived from endothelial cells, red blood cells, or other cells that are injured or activated after $FeCl_3$-induced injury. Regardless of whether

thrombosis is initiated by arterial or venous injury, RNA is consistently detected in thrombi, and administration of RNase, but not DNase, protects rodents from occlusion after $FeCl_3$-induced injury; findings that support the contention that RNA is the driver of thrombosis after $FeCl_3$-induced vascular injury (Fischer *et al.*, 2007, Kannemeier *et al.*, 2007). However, other investigators have shown that DNA in neutrophil extracellular traps and/or histones promote clotting *in vitro* and may contribute to thrombosis in murine models of deep vein thrombosis and stroke (Brill *et al.*, 2012, De Meyer *et al.*, 2012, Fuchs *et al.*, 2010, Semeraro *et al.*, 2011). Taken together, these findings raise the possibility that the type of nucleic acid released into the blood may vary depending on the method used to induce vascular injury.

Having identified RNA as the initiator of thrombosis in the $FeCl_3$-induced arterial injury model, we next set out to determine whether HRG modulates RNA-driven clotting. Compared with plasma from wild type mice, RNA-induced activation of coagulation and thrombin generation are enhanced in plasma from HRG-deficient mice and attenuated with HRG supplementation (Fig. 6.5); findings consistent with our *in vivo* observations (Fig. 6.2A-B). To determine whether the effect of HRG on RNA-driven clotting extends beyond its capacity to attenuate FXIIa activity (MacQuarrie *et al.*, 2011), we measured the affinity of RNA for HRG, FXII and FXIIa using SPR. HRG, FXII and FXIIa bind RNA, which is hypothesized to serve as a template that promotes contact assembly and activation (Gansler *et al.*, 2012, Kannemeier *et al.*, 2007). The affinity of FXII for RNA decreases by ~4-fold when it is activated to FXIIa. With its high affinity for RNA (K_d value of 16 nM), HRG is likely to localize at the site of RNA-induced contact activation,

where it is poised to bind the newly generated FXIIa with high affinity (K_d value of 21 nM). In support of this concept, HRG localizes with RNA in the thrombi formed after $FeCl_3$-induced injury. Once HRG binds to FXIIa, the capacity of FXIIa to propagate coagulation through autoactivation of FXII and activation of FXI is attenuated (MacQuarrie *et al.*, 2011). Platelets store zinc and HRG in their alpha-granules and both components are released upon platelet activation. In the presence of zinc, the affinity of HRG for FXIIa is heightened by 1000-fold (Kd value of 7.5 pM). This creates a potential molecular switch that directs HRG to FXIIa because the affinity of HRG for FXIIa is significantly higher than that for RNA in the presence of zinc. Given its abundance and high affinity for FXIIa, HRG is more likely to bind FXIIa in the vicinity of platelet-rich thrombi than is C1-inhibitor; the putative physiological regulator of FXIIa (MacQuarrie *et al.*, 2011). In support of this concept, an unidentified plasma protein, which may have been HRG, was shown to interfere with the interaction of a FXIIa-directed nanobody with FXIIa (de Maat *et al.*, 2013). RNA binds HRG with 43-fold higher affinity than it binds FXII; findings that posit a secondary role for HRG as a modulator of RNA-mediated activation of FXII. Therefore, by acting as a molecular brake to limit the procoagulant response, HRG is poised to serve as a dynamic regulator of the contact system. This is an important concept because the identification of several novel physiological activators of the contact system demands a compensatory regulatory mechanism.

There is mounting evidence that multifunctional agents, such as HRG and RNA, mediate crosstalk between different biological pathways (Delvaeye and Conway, 2009). HRG is an adapter protein that, in addition to modulating coagulation, also influences

inflammation and immunity (Poon *et al.*, 2011). $HRG^{-/-}$ mice are more susceptible to disseminated sepsis than wild type mice because $HRG^{-/-}$ mice fail to localize bacteria at sites of subcutaneous injection (Shannon *et al.*, 2010). There is emerging evidence that host-derived RNA is involved in immunity and inflammation after injury (Fischer *et al.*, 2007). Bacterial and mitochondrial RNA can activate the innate immune system to enhance clearance of microbial invaders and dead cells from the circulation (Kariko *et al.*, 2005). HRG was previously shown to bind nucleic acids and to promote the removal of necrotic cell debris by macrophages (Gorgani *et al.*, 2002). Cancer and sepsis are pathological conditions that highlight the nexus among coagulation, inflammation and immunity and the HRG-RNA interaction may modulate these disorders. Increased levels of RNA are found in the plasma of patients with cancer and sepsis (Preissner, 2007), and such patients often suffer from compromised immune systems and from thrombosis. HRG is a negative acute phase protein whose levels are decreased in immunocompromised patients (Morgan, 1986); an observation that raises the possibility that when HRG levels fall, the procoagulant and/or proinflammatory properties of RNA may predominate. Taken together, we demonstrate that HRG is a dynamic regulator of the contact system, which in addition to clotting, has also been implicated in processes such as immunity and inflammation.

6.6 Methods

6.6.1 Nucleic acid preparations.

RNA was isolated from cultured A549 non-small lung cancer cells, a generous gift from Dr. P. Liaw, using RNeasy Plus mini isolation kits (Qiagen, Mississauga, ON,

Canada), according to the manufacturer's protocol. RNA was quantified by measuring absorbance at 260 nm with a BioPhotometer Plus spectrophotometer (Eppendorf, Mississauga, ON, Canada). For SPR studies, RNA was biotinylated using the Photoprobe (long arm) biotin labeling kit (Vector laboratories, Burlingame, CA) according to the manufacturer's instructions.

6.6.2 Affinity purification of HRG-directed IgG.

A sheep polyclonal antibody against human HRG (Affinity Biologicals Inc., Ancaster, ON, Canada) was affinity purified using an HRG-Sepharose column prepared by cyanogen bromide activation. The HRG antiserum was affinity purified by application on a 4 ml HRG-Sepharose column using a Bio-Rad Biologic Duoflow system at a flow rate of 1 ml/min. The column was equilibrated and washed with 20 mM Tris-HCl, pH 7.4, 150 mM NaCl (TBS) containing 0.05% Tween (Tw) 20, and the HRG-directed IgG was eluted with Gentle Elution buffer (GE Healthcare) at 2 ml/min. After collecting 2 ml fractions into tubes containing 0.2 ml 1 M Tris-HCl, pH 8.0, protein-containing fractions were pooled and the concentration was determined by measuring absorbance at 280 nm. The HRG-directed IgG was then dialyzed into 10 mM HEPES-NaOH, 150 mM NaCl, pH 7.4 (HBS) containing 0.005% Tw 20, precipitated with 50% ammonium sulfate, and stored in aliquots at 4^{o}C.

6.6.3 Mice.

$HRG^{-/-}$ mice were maintained on a pure C57BL/6 background after more than 10 generations of backcrossing (Shannon *et al.*, 2010). $HRG^{+/-}$ mice were generated by crossing wild type C57BL/6 mice (Charles River Laboratories) with $HRG^{-/-}$ mice. Mice

were housed in micro-isolator cages exposed to constant light-dark cycles and had free access to food and water. Mice were genotyped by PCR analysis as previously described (Tsuchida-Straeten *et al.*, 2005), and HRG levels were determined by immunoblot analysis as described below. For all experiments, female, weight and age-matched mice were used. Unless otherwise stated, blood was collected via a carotid artery cannulus into 0.105 M citrate. Platelet poor plasma was prepared by twice exposing the blood to centrifugation at 4,000 x g for 8 min to remove the cellular elements. The resultant plasma was then harvested and stored in aliquots at -80^{o}C. All animal utilization protocols were approved by the Animal Research Ethics Board at McMaster University, and all studies were performed in accordance with the Canadian Council on Animal Care guidelines.

6.6.4 Antisense oligonucleotides (ASOs).

Mouse-specific FXII- and FVII-directed ASOs were designed and synthesized by Isis Pharmaceuticals (Carlsbad, CA), and prepared as described previously (Revenko *et al.*, 2011). The oligonucleotides for the control, FXII and FVII mRNA knockdown in mice were synthesized and chemically modified as previously reported (Revenko *et al.*, 2011). Wild type and HRG$^{-/-}$ mice were given 20 mg/kg FXII, FVII or control ASO via twice weekly subcutaneous injections for up to 6 weeks. The effect of the ASOs on protein expression was assessed by immunoblot analysis as follows. Briefly, blood was collected via cardiac puncture and after preparing platelet poor plasma as described above, 8 μl was subjected to SDS-PAGE on 4-15% gradient gels (Bio-Rad, Mississauga, ON) under non-reducing conditions. Separated proteins were transferred to a

nitrocellulose membrane and subjected to immunoblot analysis using a goat polyclonal antibody directed against human FXII (GAFXII-AP, Affinity Biologicals), a goat monoclonal IgG directed against mouse FVII (AF3305, R&D Systems, Abingdon, UK), or the affinity purified sheep IgG directed against human HRG. All antibodies were conjugated to horseradish peroxidase using the Lightning-Link conjugation kit (Innova Biosciences, Cambridge, England). After quantification using Bio-Rad ChemiDoc instrument software, FVII and FXII protein levels in ASO treated mice were normalized relative to those in mice given the control ASO.

6.6.5 Plasma clotting assays.

Clotting assays were performed as described (MacQuarrie *et al.*, 2011), with some modifications. The intrinsic pathway was assessed using an aPTT reagent (Instrumentation Laboratory, Bedford, MA) diluted 1/5 in 125 mM imidazole buffer, pH 7.0 (imidazole buffer), whereas TF-induced clotting was examined using Recombiplastin (Instrumentation Laboratory) diluted 1/200 in TBS. To wells of a 96-well plate containing 50 µl of citrated plasma from $HRG^{-/-}$, $HRG^{+/-}$ or wild type mice supplemented with 30 µM PCPS vesicles, which were prepared as previously described (Kretz *et al.*, 2010), was added 50 µl of dilute aPTT reagent or Recombiplastin. The effect of HRG on RNA-mediated activation of the intrinsic pathway was examined by incubating 25 µl of a 30 µg/ml RNA solution diluted in imidazole buffer with 50 µl of murine plasma supplemented with 60 µM PCPS in the absence or presence of 25 µl of human HRG at concentrations up to 3 µM. Clotting was initiated by addition of 50 µl of $CaCl_2$ to a final concentration of 8.3 mM for the aPTT and RNA-induced clotting assays and 5 mM for

the PT assays. To assess the clotting time in plasma from wild type or $HRG^{-/-}$ mice treated with ASOs, the aPTT and PT were performed as described above, except the volume of plasma and aPTT or PT reagent were reduced from 50 µl to 30 µl and clotting was initiated by addition of 30 µl of $CaCl_2$ to a final concentration of 8.3 mM. With all assays, absorbance was monitored at 405 nm at 37^{o}C using a SpectroMax plate reader (Molecular Devices, Sunnyvale, CA) and clot time was taken as the time to reach half-maximal absorbance, as determined by the instrument software.

6.6.6 Thrombin generation assays.

Thrombin generation was assessed in real time using the calibrated automated thrombogram assay as described previously (Swystun *et al.*, 2011), but with some modifications. To wells of a black 96-well plate (Costar, Lowell, MA) containing 40 µl of plasma from wild type, $HRG^{+/-}$ or $HRG^{-/-}$ mice supplemented with 30 µM PCPS vesicles was added 10 µl of aPTT reagent at a 1/2 dilution or 16 µg/ml RNA prepared in imidazole buffer to assess the contact system. The extrinsic pathway was assessed using 10 µl of Recombiplastin diluted to 1/1000 dilution in TBS and 50 µg/ml CTI (Enzyme Research Laboratories) to inhibit contact activation. RNase A is DNase- and protease-free (Thermoscientific, Waltham, MA) and any contaminating proteases were inactivated by heating to 95ºC for 15 min. The capacity of RNase and DNase (Pulmozyme, Roche, Mississauga, ON), to digest RNA or DNA, respectively, was evaluated in human plasma. Briefly, 20 µg/ml RNase or DNase was incubated in HBS buffer at 37^{o}C for 30 min in the absence or presence of 20 µg/ml RNA or DNA in reaction mixtures containing 0.1 mM $CaCl_2$ and 2.5 mM $MgCl_2$. The extent of RNA and DNA digestion was assessed by

agarose gel analysis. To initiate clotting, 10 µl of the following mixtures: RNA or DNA, RNA pre-digested with RNase or DNA pre-digested with DNase, or RNase or DNase alone was added to wells containing 40 µl human plasma and incubated at 37^{o}C. Thrombin generation was initiated by adding a solution containing 15 mM $CaCl_2$ and 1 mM Z-Gly-Gly-Arg-AMC (Bachem, Bubendorf, Switzerland), a fluorescent thrombin-directed substrate; and substrate hydrolysis was monitored using a SpectraMax M5e plate reader (Molecular Devices). Thrombin generation profiles and data were analyzed using Technothrombin TGA software (Technoclone, Vienna, Austria).

6.6.7 $FeCl_3$-induced arterial thrombosis.

Wild type, $HRG^{+/-}$ and $HRG^{-/-}$ mice and $HRG^{-/-}$ mice supplemented with human HRG or saline were placed under gas anesthesia using 2-5% isofluorane (Baxter, Deerfield, IL). The right common carotid artery was isolated and vascular injury was induced by application of a 1x1 mm filter paper that was presoaked in 7.5% $FeCl_3$ to the external surface of the vessel for 1 min. Where indicated, the left jugular vein was cannulated with P10 Intramedic polyethylene tubing (BD Biosciences) and 5.8 mg/kg human HRG or an equivalent volume of saline was injected 40 min prior to $FeCl_3$ application. Plasma HRG levels were quantified by immunoassay. Briefly, plasma collected from wild type, $HRG^{-/-}$ mice or $HRG^{-/-}$ mice infused with purified HRG was added to wells of a Ni-coated plate (Thermoscientific) and HRG was detected using an affinity purified IgG directed against human HRG that was conjugated to horse radish peroxidase. The plasma concentration of HRG in control wild type mice was ~1-2 µM and in pilot studies, intravenous administration of 5.8 mg/kg of human HRG to $HRG^{-/-}$

mice resulted in similar HRG concentrations.

To assess the role of RNA or DNA in thrombus formation, the left jugular vein was cannulated and RNase (100 µl of a 2 mg/ml solution), DNase (200 µl of a 1 mg/ml solution), or an equivalent volume of saline was injected 15 min prior to injury induced by application of a 1x2 mm filter paper that was presoaked in 7.5% $FeCl_3$ for 1.5 min (Kannemeier *et al.*, 2007, Wang *et al.*, 2005, Wang *et al.*, 2006). Thrombosis was also assessed in wild type (10% $FeCl_3$, 1x2 mm filter paper, 1.5 min application) and $HRG^{-/-}$ mice (10% $FeCl_3$, 1x2 mm filter paper, 1 min application) treated with control, FXII, or FVII ASOs. In all experiments, thrombosis was assessed by monitoring changes in blood flow using a model T206 ultrasound flow probe (Transonic Systems Inc.) interfaced with a flow meter and a 0.5 mm flow probe (0.5V series) to assess blood flow prior to $FeCl_3$ application (baseline) and for 30 min thereafter. The TTO was determined as the time required for blood flow to decrease below 20% of the baseline value for at least 3 min (Owens, III *et al.*, 2011). The area under the plot of blood flow versus time was quantified using SigmaPlot (v.11).

6.6.8 Tail bleeding model.

The role of HRG in hemostasis was assessed using a tail bleeding model. Cumulative blood loss over the 30 min period after tail tip amputation was determined as described previously (Rand *et al.*, 2012, Vaezzadeh *et al.*, 2014). $HRG^{-/-}$, $HRG^{+/-}$ and wild type mice were anesthetized with an intraperitoneal injection of a solution containing 10% ketamine, 5% atropine and 5% xylazine. After transection at a position where the diameter was 1.5 mm, tails were immediately immersed in a tube containing 30 ml of

saline, pre-warmed to 37^{o}C, to collect the shed blood. Aliquots of saline were removed at intervals for up to 30 min; after subjecting the red blood cells to lysis using ZAP-OGLOBIN II lytic reagent (Beckman Coulter, Mississauga, ON), absorbance at 405 nm was determined and hemoglobin content was quantified by reference to a standard curve created by subjecting known amounts of mouse blood to lysis under the same conditions.

6.6.9 Histopathological analysis.

To assess the localization of HRG, RNA, DNA, fibrin, and platelets, thrombi collected from mice after $FeCl_3$-induced injury were embedded in Optimal Cutting Temperature (OCT) compound (Sakura Finetek, Torrence, CA) and cut into 4-10 μM sections using a Leica cryostat CM1900 (Wetzlar, Germany). For RNA and DNA detection, 100 μl of a 50 μM solution of SYTO RNASelect green fluorescent cell stain (Life Technologies, Eugene, OR) or SYTOX green fluorescent stain (Life Technologies), respectively, was injected into the left jugular vein prior to $FeCl_3$ application (Kannemeier *et al.*, 2007); for control mice, 100 μl of saline was injected instead of nucleic acid stain. In mice given RNase or DNase, stains were injected after RNase or DNase administration.

Tissue sections were blocked with 10% goat serum (Sigma Aldrich) prior to all histological analyses and with 120 μg/ml of an unconjugated AffiniPure Fab fragment anti-mouse IgG (H+L; Charles River) for studies with the anti-mouse fibrin IgG (T2G1, Accurate Westbury, NY). Slides were sequentially stained for fibrin, platelets and HRG. HRG was detected using 100 μg/ml sheep anti-human HRG IgG (Affinity Biologicals) conjugated to AlexaFluor 350 (Life Technologies) according to the manufacturer's

directions. Fibrin was detected with 50 μg/ml of anti-mouse fibrin IgG and visualized with a secondary anti-mouse AlexaFluor 488 or 647 IgG (Life Technologies). Platelets were detected with 10 μg/ml of rat anti-mouse CD41 IgG (BD Biosciences, Mississauga, ON) and visualized with secondary anti-rat AlexaFluor 488 or 647 IgG (Life Technologies). Slides were then rinsed with phosphate buffered saline (EMD, Gibbstown, NJ) and visualized using an Olympus BX41 microscope equipped with a DP72 camera (Center Valley, PA). Images were collected and analyzed using instrument software. After imaging, sections were subjected to hematoxylin and eosin staining prior to morphological analysis.

6.6.10 Binding of HRG, FXII and FXIIa to immobilized RNA using SPR.

The binding of proteins to biotinylated-RNA was determined using a Biacore T200 biosensor (GE Healthcare). SPR experiments were performed in HBS containing 0.05% Tw 20. Biotinylated-RNA was adsorbed to ~200-300 response units onto a flow cell of a streptavadin-coated chip (XanTec bioanalytics GmbH, Dusseldorf, Germany) at a flow rate of 5 μl/min. An unmodified streptavadin-containing flow cell served as the reference control. FXIIa (Enzyme Research Laboratories) was active site-blocked with FPR (Calbiochem) as described previously (Petrera *et al.*, 2009). Aliquots containing 0-0.125 μM HRG, 0-1 μM FXII (Enzyme Research Laboratories), or 0-4 μM FPR-FXIIa were injected at a flow rate of 40 μl/min followed by injection of buffer to monitor the off-rates. Flow cells were regenerated with 1 M NaCl, 250 mM imidazole and 5 mM EDTA between runs. The initial FXII and FPR-FXIIa off-rates from adsorbed RNA were

quantified using a two-state reaction binding equation and binding constants were determined by steady state analysis using instrument software.

6.6.11 Statistical analysis.

Data are presented as mean ± SD or SE as indicated. Significance of differences was determined using Student t-tests for paired data or analysis of variance (ANOVA) for group data. For all analyses, $p<0.05$ was considered statistically significant. GraphPad Prism4 software was used for all statistical analysis and for producing scatter diagrams, whereas the remaining data were graphed and analyzed using SigmaPlot.

6.7 Supplemental Information (SI) Tables and Figures

	Mouse Plasma		
	Wild type	$HRG^{+/-}$	$HRG^{-/-}$
Lag time (min)	3.8 ± 0.4	2.8 ± 0.4	3.3 ± 0.5
Peak thrombin (nM)	126.2 ± 14.8	150.5 ± 5.5*	116.7 ± 20.6
Time to peak (min)	5.3 ± 0.5	5.5 ± 0.5	5.3 ± 0.5
Velocity index (nM/min)	96.7 ± 38.2	101.1 ± 38.2	58.4 ± 9.4
ETP (nM·min)	2687.6 ± 96.5	2745.2 ± 32.3	2575.0 ± 122.0

SI Table 6.1 HRG does not modulate the extrinsic pathway in murine plasma. Clotting via the extrinsic pathway was initiated by adding Recombiplastin at a 1/1000 dilution to wild type, $HRG^{+/-}$ or $HRG^{-/-}$ murine plasma containing 50 μg/ml CTI and 30 μM PCPS vesicles followed by 15 mM $CaCl_2$. Thrombin generation was quantified by monitoring hydrolysis of Z-Gly-Gly-Arg-AMC. Data represent mean ± SD of 3 experiments, each performed in duplicate. *$p<0.05$, compared with results in wild type plasma.

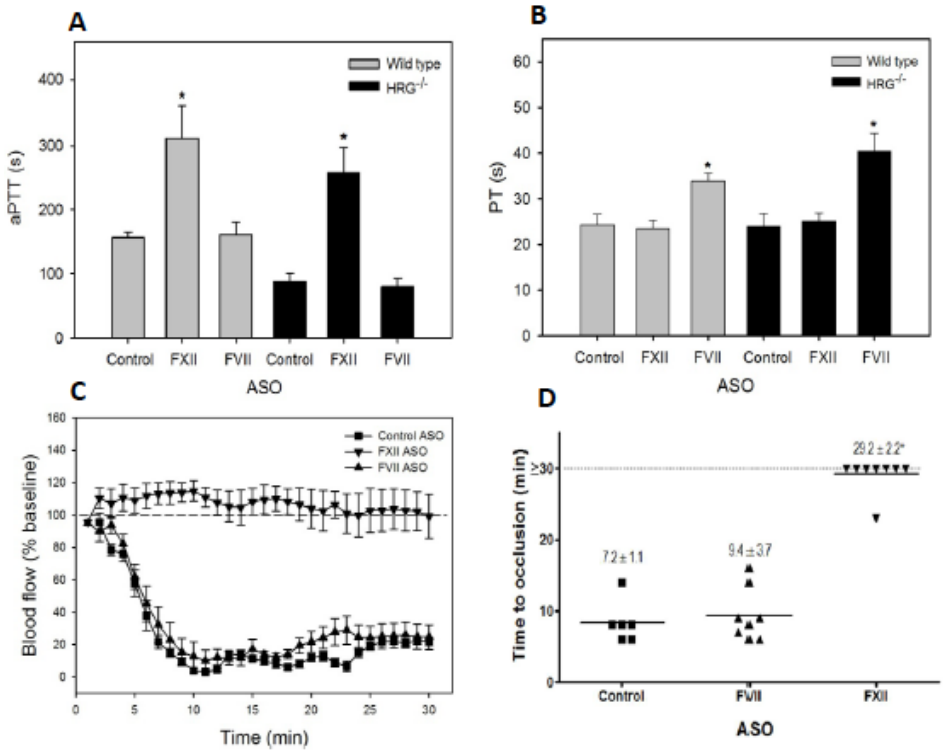

SI Figure 6.1 Effect of ASO treatment on the PT and aPTT.

(**A**-**B**) Plasma from wild type (*grey bars*) or $HRG^{-/-}$ (*black bars*) mice pre-treated with control, FXII- or FVII-directed ASOs was incubated with (**A**) a 1/5 dilution of aPTT reagent, or (**B**) 1/200 dilution of Recombiplastin. Clot times were determined after recalcification. (**C**-**D**) A 1x2 mm filter paper presoaked in 10% $FeCl_3$ was applied to the right carotid artery of ASO-treated $HRG^{-/-}$ mice for 1 min (n=6-8 per group). (**C**) Blood flow was continuously measured before and for 30 min after injury. Flow measurements at the times indicated are expressed as a percentage of baseline flow. Symbols represent the mean values, while the bars reflect SE. (**D**) TTO data are presented as a scatter diagram, where symbols represent individual values, and horizontal lines represent the mean values in each of the groups. *p<0.001, compared with saline controls.

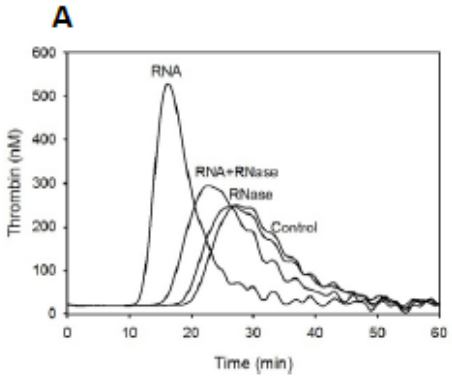

B

	Control	RNA	RNA+RNase	RNase
Lag time (min)	22.5 ± 2.1	12.5 ± 0.5†	15.8 ± 3.1†	20.2 ± 3.9
Peak thrombin (nM)	248.5 ± 13.3	548.8 ± 18.0‡	316.8 ± 65.7	259.8 ± 33.8
Time to peak (min)	29.5 ± 2.1	15.3 ± 0.5‡	22.0 ± 3.6‡	26.5 ± 4.4
Velocity index (nM/min)	35.4 ± 2.0	199.0 ± 40.7†	56.0 ± 26.3	41.8 ± 8.1
ETP (nM·min)	5185.8 ± 128.7	5801.2 ± 26.0†	5133.0 ± 129.0†	5164.7 ± 202.5

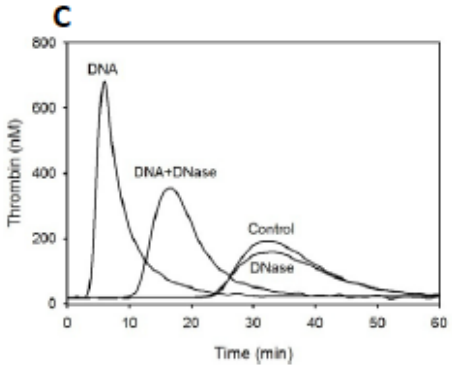

D

	Control	DNA	DNA+DNase	DNase
Lag time (min)	20.8 ± 3.8	4.8 ± 0.4†	11.7 ± 2.4*	20.3 ± 2.4
Peak thrombin (nM)	224.2 ± 36.9	661.3 ± 3.8†	452.4 ± 73.6*	242.1 ± 47.6
Time to peak (min)	27.2 ± 4.3	5.7 ± 0.5†	14.8 ± 3.1†	26.3 ± 3.6
Velocity index (nM/min)	36.4 ± 11.2	667.5 ± 18.1†	183.2 ± 74.8*	41.3 ± 14.8
ETP (nM·min)	46940 ± 140.5	4569.2 ± 403.7	5133.0 ± 228.5	4581.7 ± 186.5

SI Figure 6.2 RNase and DNase attenuate thrombin generation initiated by DNA and RNA, respectively.

(**A-D**) Effect of RNase and DNase on thrombin generation triggered by RNA and DNA, respectively. Human plasma containing 30 μM PCPS was incubated with 20 μg/ml RNA or DNA alone, RNase or DNase alone, RNA or DNA pre-treated with 20 μg/ml RNase or DNase, or with buffer prior to recalcification. The amount of thrombin generated was monitored by fluorescence. (**A, C**) Representative thrombin generation profiles are shown and (**B, D**) thrombin generation parameters are reported as means ± SD of 3 experiments, each performed in duplicate. *$p<0.05$ and ‡$p<0.005$, compared with control plasma without added nucleic acids and/or nucleases.

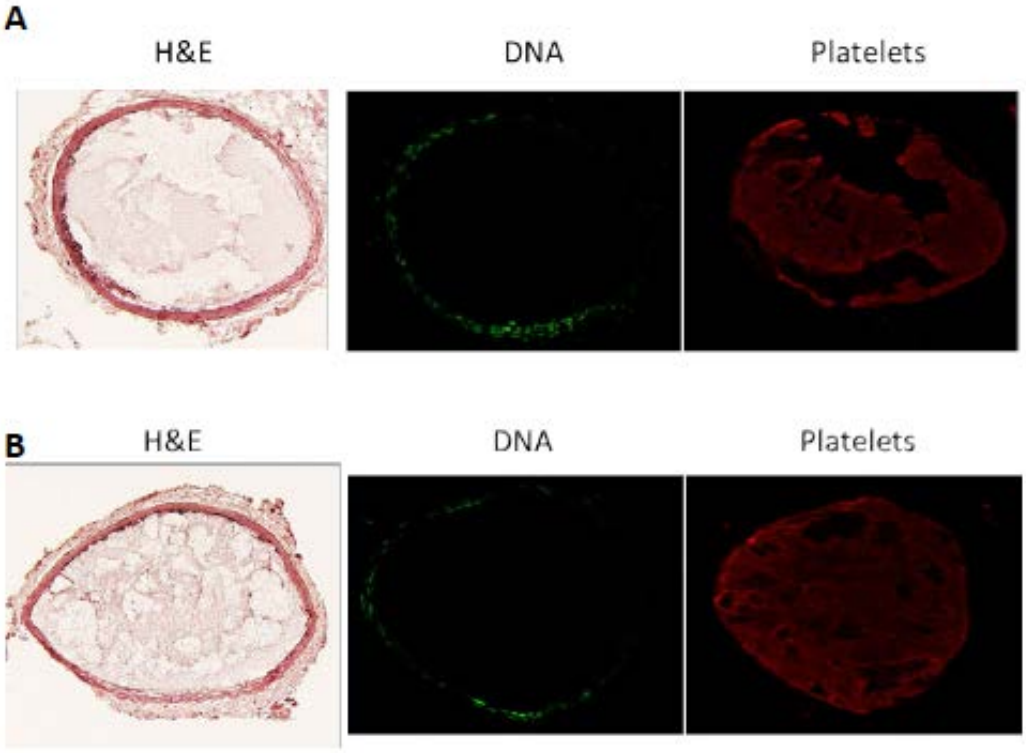

SI Figure 6.3 DNA is not detected in thrombi formed in mice after $FeCl_3$-injury.

(**A-B**) Staining for DNA and platelets in wild type mice pre-treated with (**A**) saline, or (**B**) 1 mg/ml DNase. Prior to injury, mice were given an intravenous injection of a DNA-specific fluorescent stain. Sections of thrombi harvested 30 min after $FeCl_3$-injury were subjected to immunohistochemical analysis using an antibody against platelets or were stained with H&E.

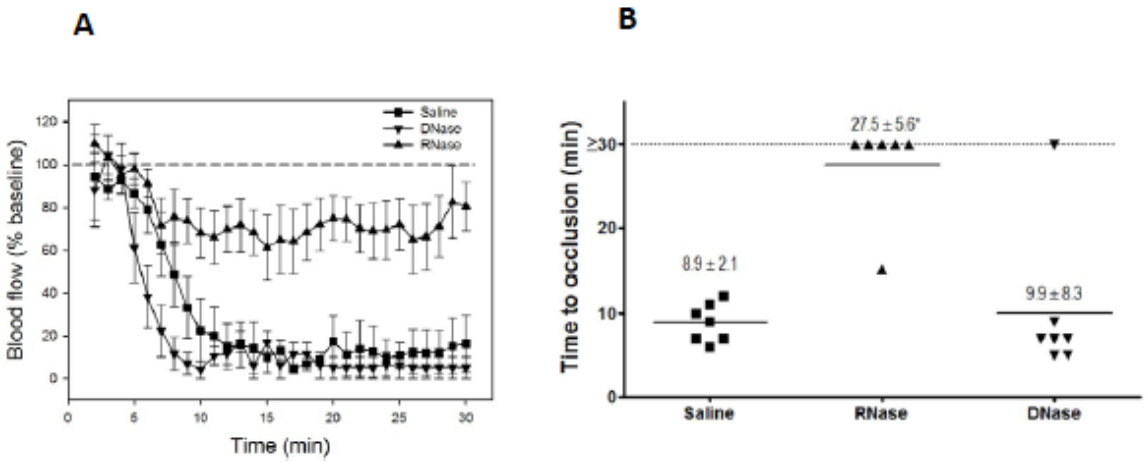

SI Figure 6.4 RNA induces thrombosis after $FeCl_3$-induced carotid artery injury in $HRG^{-/-}$ mice.

(**A-B**) Effect of RNase or DNase administration on thrombosis. After injection of 2 mg/ml RNase, 1 mg/ml DNase or saline into the left jugular vein, a 1x2 mm filter paper presoaked in 7.5% $FeCl_3$ was applied to the right carotid artery of $HRG^{-/-}$ mice for 1.5 min to initiate vascular injury (n=6-7 per group). (**A**) Blood flow was continuously measured. Symbols represent the means, while the bars reflect SE. (**B**) TTO data. The symbols represent individual values, and horizontal lines represent the mean values in each of the 3 groups. *$p<0.001$, compared with saline control.

Chapter 7: DISCUSSION & FUTURE DIRECTIONS

7.1 DISCUSSION

7.1.1 General Discussion

Recent studies have shed new light on the role of the intrinsic pathway in coagulation. Knock out of FXII, FXI, or HK in mice demonstrate that contact activation is important for the propagation of thrombosis, while having little or no role in hemostasis (Merkulov *et al.*, 2008, Renne *et al.*, 2005, Wang *et al.*, 2005, Wang *et al.*, 2006). Likewise, pharmacological interventions aimed at down-regulating the expression or activity of FXII or FXI demonstrate a similar phenotype to the knock out mice studies (Crosby *et al.*, 2013, Decrem *et al.*, 2009, Larsson *et al.*, 2014, Revenko *et al.*, 2011). Furthermore, the recent discovery that naturally occurring polyphosphates, such as polyP, DNA and RNA, are potent activators of FXII and that administration of phosphatase and nucleases protects mice from thrombosis (Kannemeier *et al.*, 2007, Muller *et al.*, 2009), provide additional support for the concept that the intrinsic pathway is important in pathological clot formation (Kannemeier *et al.*, 2007, Muller *et al.*, 2009). Therefore, the development of anticoagulants targeting the intrinsic pathway should mitigate thrombosis, without increasing the bleeding risk.

Because of the emerging importance of the intrinsic pathway in thrombosis, it is important to understand how this pathway is regulated. Our group showed that HRG binds FXIIa and attenuates its capacity to propagate contact activation of coagulation (MacQuarrie *et al.*, 2011). The effect of HRG on coagulation was specific to the intrinsic

pathway because HRG shortens the aPTT, but has no effect on the PT (MacQuarrie *et al.*, 2011). Recent studies demonstrate that there is an unidentified plasma protein that binds FXIIa (de Maat *et al.*, 2013), which is likely HRG because HRG-FXIIa complexes are detected in contact activated plasma (MacQuarrie *et al.*, 2011). Since HRG binds DNA (Gorgani *et al.*, 2002), we hypothesized that HRG also modulates nucleic acid-driven activation of the intrinsic pathway. In support of this concept, we show that HRG attenuates nucleic acid-mediated activation of the contact pathway at multiple levels. First, HRG binds nucleic acids (K_d of ~1 nM) and this localizes it to the site of contact activation, where it is poised to inhibit FXII activation and FXIIa activity (Chapters 5 and 6). Second, HRG impairs the capacity of nucleic acids to act as cofactors for thrombin activation of FXI, which is an important feedback step in coagulation (Chapter 5). Third, $HRG^{-/-}$ mice exhibit accelerated thrombosis compared with wild type controls in an arterial injury model that is driven by RNA and FXII (Chapter 6). Additionally, repletion with human HRG abrogates this effect, thereby confirming the role of HRG in contact activation. Lastly, hemostasis is normal in HRG-deficient mice. Therefore, these studies consistently demonstrate that HRG is a novel attenuator of thrombosis that acts by binding both FXIIa and contact activators (Chapter 6).

Downstream to the common pathway, HRG also modulates thrombin binding to the γ'-chain of fibrin(ogen) (Chapter 3). The γ'-chain is an unique thrombin binding site, since other thrombin-like serine proteases, such as batroxobin, do not interact with this region. These findings suggest that this is a newer evolutionary feature that distinguishes thrombin from other fibrinogen-cleaving enzymes (Chapter 4). By binding to the γ'-chain,

HRG competes with thrombin for binding to this region, thereby modulating the thrombin-γ'-chain interaction (Chapter 3). Taken together, these studies demonstrate that HRG is uniquely equipped to serve as a dynamic modulator of both the initiation and propagation phases of coagulation.

The overarching goal of this thesis was to explore the physiological roles of HRG in coagulation. The current chapter will: (a) highlight the biochemical and physiological importance of HRG in coagulation, (b) outline how HRG provides an unique link between coagulation and immunity, and (c) propose future experiments that will build on work presented in the thesis.

7.1.2 PHYSIOLOGICAL IMPORTANCE OF THE HRG-γ_A/γ'-FIBRINOGEN INTERACTION

The γ'-chain, which is the feature that distinguishes the two isoforms of fibrin(ogen), possesses an unique thrombin binding site (Meh *et al.*, 1996, Pospisil *et al.*, 2003). Like thrombin, snake venom proteases such as batroxobin can convert fibrinogen to fibrin; but unlike thrombin, batroxobin does not bind to the γ'-chain of fibrin(ogen) (Chapter 4). Thus, the capacity of thrombin to interact with γ'-chain is likely an evolutionary adaptation that augments the protease's specificity for its ligands (Chapter 4). Several studies have been undertaken to elucidate the physiological importance of the thrombin-γ'-chain interaction. Thrombin remains bound to fibrin following catalysis, and because this sequesters active thrombin, fibrin was originally termed anithrombin I (Mosesson, 2005). Because thrombin has a higher affinity for γ_A/γ'- than γ_A/γ_A-fibrin(ogen), it is hypothesized γ_A/γ'-fibrin has a greater capacity to sequester thrombin

(Meh *et al.*, 1996, Pospisil *et al.*, 2003). In support of this concept, we demonstrated that thrombin associated with γ_A/γ_A-fibrin has a greater propensity to promote clot expansion than thrombin bound to γ_A/γ'-fibrin clots (Chapter 4). Similarly, others have shown that infusion of γ_A/γ_A-fibrinogen, but not γ_A/γ'-fibrinogen, promotes arterial thrombosis in a murine model (Walton *et al.*, 2014). In addition, the levels of thrombin-AT complexes are lower in mice infused with γ_A/γ'-fibrinogen than in those given γ_A/γ_A-fibrinogen (Walton *et al.*, 2014), findings that support the contention that γ_A/γ'-fibrin sequesters thrombin to a greater extent than γ_A/γ_A-fibrinogen.

Other than FXIII and thrombin, there are very few proteins that are known to interact with the γ'-chain (Uitte de Willige *et al.*, 2009). We showed that HRG binds to the γ'-chain of γ_A/γ'-fibrin(ogen) in a zinc-dependent manner; and since this is also a thrombin binding site, HRG competes with thrombin for binding to γ_A/γ'-fibrin(ogen) (Chapter 3). HRG is a modular protein that possesses a high content of His residues concentrated in the HRR. Because the imidazole groups within the His side chains are exposed, they can interact with zinc ions to facilitate ligand binding (Jones *et al.*, 2005). Platelets store zinc and HRG in their α-granules and upon activation, release both components into the blood (Leung *et al.*, 1983, Marx *et al.*, 1993). The absolute requirement for zinc suggests that zinc acts as a molecular switch that directs HRG binding to the γ'-chain and by so doing, displaces thrombin (Chapter 3). Why is this mechanism necessary? When thrombin binds to γ_A/γ'-fibrin clots both of its exosites are occupied, which attenuates thrombin's capacity to propagate clotting by activating other coagulation factors or by binding to platelets (Fredenburgh *et al.*, 2008, Meh *et al.*, 1996,

Pospisil *et al.*, 2003). However, the capacity of platelets to release both zinc and HRG into the environment provides a dynamic switch that displaces thrombin from γ_A/γ'-fibrin clots, thereby enabling the protease to propagate clotting. Consequently, the capacity of HRG to displace thrombin from γ_A/γ'-fibrin clots provides an important positive feedback step that augments the procoagulant response. Alternatively, our group demonstrated that thrombin bound to γ_A/γ'-fibrin clots is more protected from inhibitors such as AT than thrombin bound to γ_A/γ_A-fibrin clots (Becker *et al.*, 1999, Fredenburgh *et al.*, 2008). Since clot-bound thrombin can promote clot expansion (Weitz *et al.*, 1990), this suggests that thrombin bound to γ_A/γ'-fibrin may be more thrombogenic than thrombin bound to γ_A/γ_A-fibrin clots (Fredenburgh *et al.*, 2008). From this perspective, by displacing thrombin from γ_A/γ'-fibrin, HRG renders it more susceptible to inhibition; and therefore, HRG may provide a switch to attenuate the activity of clot-associated thrombin. Since γ_A/γ'-fibrinogen comprises up to 15% of the total fibrinogen and its levels are associated with cardiovascular risk (Mosesson, 2005), the HRG-γ'-chain interaction provides an important regulatory mechanism to modulate the activity of clot-bound thrombin.

7.1.3 HRG IS A DYNAMIC MODULATOR OF FXIIa AND NUCLEIC ACID ACTIVITY

By binding to and attenuating the activity of FXIIa and nucleic acids, HRG is poised to serve as a dynamic modulator of the contact system. Although C1-Inh is postulated to be the major regulator of FXIIa, its rate of inhibition is slow and FXIIa is protected from inhibition when it is bound to polyanions, such as kaolin (Pixley *et al.*, 1987). Surface protection likely facilitates initiation and propagation of contact activation.

However, by binding polyanions such as DNA and RNA (Chapters 5 and 6) and polyP (Table 1.1), HRG is poised to interact with FXIIa and inhibit its activity in a milieu where FXIIa is protected from inhibition by C1-Inh. Therefore, HRG is more likely to inhibit FXIIa in the presence of nucleic acids than is C1-Inh.

The affinities of HRG for FXIIa and nucleic acids are comparable (K_d values of 21 and 1 nM, respectively). Thus, how is HRG regulated in the presence of both FXIIa and nucleic acids? Platelets store zinc and HRG in their α-granules and upon activation, both components are released into the blood (Leung *et al.*, 1983, Marx *et al.*, 1993). Since the HRG-FXIIa interaction is augmented 10^3-fold in the presence of zinc (K_d value of 7.5 pM) (MacQuarrie *et al.*, 2011), the surge of zinc provides a dynamic switch that directs HRG binding to FXIIa. However, under pathological conditions such as sepsis or cancer, where extracellular DNA and RNA levels are elevated, HRG may be sequestered by nucleic acids. In support of this concept, HRG levels are decreased in murine models of sepsis (Vu 2013, unpublished observations) and cancer (Rolny *et al.*, 2011).

7.1.4 PUTATIVE ROLES FOR THE FIBRIN-FXIIa-HRG INTERACTION

In addition to its role in contact activation of coagulation, FXII(a) has auxiliary roles in modulating fibrin clot formation and lysis (Konings *et al.*, 2011). Although HRG can bind FXIIa in the absence of zinc with a K_d value of 21 nM (MacQuarrie *et al.*, 2011), zinc is required for the HRG-fibrin interaction (Chapter 3). In the presence of zinc, HRG binds FXIIa with a K_d value of 7.5 pM (MacQuarrie *et al.*, 2011), which is an affinity that is three orders of magnitude greater than the affinity of HRG for fibrin (K_d of ~ 9 nM) (Chapter 3); thus, HRG is more likely to interact with FXIIa than with fibrin.

When FXII(a) interacts with fibrin, it increases the clot density and stiffness (Konings *et al.*, 2011), although the physiological importance of these changes is unclear. FXII(a) is linked to fibrinolysis because the protease directly converts plasminogen to plasmin, although it does so less efficiently than tissue-type or urokinase-type plasminogen activators (Colman and Schmaier, 1997). By binding to FXIIa and attenuating its activity, HRG may hinder the capacity of FXIIa to promote fibrinolysis, thereby rendering HRG-rich fibrin clots more resistant to lysis. In support of the concept that HRG exhibits anti-fibrinolytic properties, clots formed in plasma from HRG-deficient mice were shown to be more susceptible to lysis than clots formed in plasma from wild type controls (Tsuchida-Straeten *et al.*, 2005).

7.1.5 $FeCl_3$ MODEL OF THROMBOSIS

Several rodent models have been established for the study of thrombosis (*for review see* (Westrick *et al.*, 2007)), but of these, $FeCl_3$ is the most commonly used agent to initiate vascular injury and thrombosis (Owens, III *et al.*, 2011). The precise mechanisms leading to thrombosis in the $FeCl_3$ model are heavily debated. However, the general consensus is that application of $FeCl_3$ to the surface of the vessels leads to denudation of the endothelium, which results in exposure of subendothelial components, such as collagen and TF (Owens, III *et al.*, 2011). However, recent studies using scanning electron micrographs of vessels after $FeCl_3$ application demonstrate that the endothelium is intact (Barr *et al.*, 2013). An often overlooked aspect of the $FeCl_3$ model is the influence of the severity of injury, which is dependent on the $FeCl_3$ concentration (typically 2.5-20%), the filter paper size and the duration of its application on the surface

of the vessel (Owens, III *et al.*, 2011). Thus, whether the endothelium is denuded or not may depend on the extent of vascular injury.

Several studies using antibodies against TF have shown that the extrinsic pathway contributes to thrombosis in the $FeCl_3$ model (Eckly *et al.*, 2011, Massberg *et al.*, 2010). However, in our studies, selective depletion of FVII using an ASO had no effect on $FeCl_3$-induced thrombosis in wild type or HRG-deficient mice. Although we cannot completely exclude a role for the extrinsic pathway, in this model because ASO treatment does not fully eliminate FVII, the fact that FXII knock down abolished thrombosis in the FeCl model makes it unlikely that the extrinsic pathway plays a major part in thrombosis in this model (Chapter 6).

There is substantial evidence that the intrinsic pathway is an important driver of thrombosis in the $FeCl_3$ model. Others have shown that $FXII^{-/-}$ and $FXI^{-/-}$ mice are protected from $FeCl_3$-induced thrombosis (Renne *et al.*, 2005, Wang *et al.*, 2005, Wang *et al.*, 2006). Similarly, we showed that a FXII-directed, but not a FVII-directed ASO, exerted a thromboprotective effect (Chapter 6). In addition, using RNase and DNase, we confirmed that RNA activates the FXII in the $FeCl_3$ model (Chapter 6). Therefore, our observations support the contention that arterial thrombosis in the $FeCl_3$ model is driven by RNA in a FXII-dependent manner (Chapter 6).

7.1.6 RELATIVE CONTRIBUTION OF RNA AND DNA TO THROMBOSIS

Both RNA and DNA activate the intrinsic pathway of coagulation with comparable potencies *in vitro* (Chapter 5). Although RNA and DNA levels are elevated in patients with thrombotic microangiopathies (Fuchs *et al.*, 2012, Preissner, 2007), little is

known about the contribution of RNA and DNA to thrombosis. In rodent models, the relative contribution of RNA and/or DNA to thrombosis appears to vary depending on the method or technique used to initiate vascular injury. Regardless of whether thrombosis is initiated in the arterial or venous systems, RNA is consistently detected in thrombi and administration of RNase protects rodents from occlusion after $FeCl_3$ application, findings that support the concept that thrombosis in the $FeCl_3$ model is triggered by RNA, and not DNA (Fischer *et al.*, 2007, Kannemeier *et al.*, 2007). The origin of RNA in the $FeCl_3$-model is currently unknown. A recent report implicates red blood cells in the pathogenesis of $FeCl_3$-induced thrombosis (Barr *et al.*, 2013) and *in vitro* work suggests that when activated, red blood cells promote thrombin generation (Whelihan *et al.*, 2012). Consequently, RNA may be derived from red blood cells, or other cells that are injured or activated after $FeCl_3$-induced injury. However, others have shown that an antibody directed against the histone H2A-H2B-DNA complex attenuates thrombosis after $FeCl_3$ injury, thereby suggesting that DNA in NETs may also contribute to thrombosis in this model (Massberg *et al.*, 2010). However, we and others have shown that DNase has no impact on thrombosis in the $FeCl_3$ model, suggesting that DNA is not the activator of FXII in this model ((Kannemeier *et al.*, 2007); Chapter 6). Because histones can trigger thrombin generation in a platelet-dependent manner (Semeraro *et al.*, 2011), it is possible that they may contribute to thrombosis by enhancing RNA-mediated contact activation.

DNA and NETs contribute to thrombosis in inferior vena cava (IVC) ligation models (Brill *et al.*, 2012, von Bruhl *et al.*, 2012). In this model, application of a ligature reduces blood flow through the IVC by 80-90% and the resultant stasis induces

thrombosis (Geddings *et al.*, 2014, von Bruhl *et al.*, 2012). Although the precise mechanisms are not known, the prevailing thought is that the IVC ligation model does not result in vascular damage, but thrombosis is the result of perturbations in blood flow and subsequent activation of the endothelium, leukocytes and platelets (Geddings *et al.*, 2014, von Bruhl *et al.*, 2012). DNA in association with NETs is detected in deep vein thrombi, and administration of DNase reduces NET formation and suppresses DVT (Brill *et al.*, 2012, von Bruhl *et al.*, 2012). During NETosis, the nuclear membranes of neutrophils disintegrate and the contents of the nucleoplasm (e.g., DNA and histones) mix with those of the cytoplasm (e.g. RNA and ribosomes) prior to NET extrusion (Yipp and Kubes, 2013). However, RNA is rarely investigated in the context of NETs and thus, it is still unclear whether RNA contributes to venous thrombosis. Furthermore, while there is substantial evidence that neutrophils release extracellular DNA in various thrombosis models (Brill *et al.*, 2012, De Meyer *et al.*, 2012, Fuchs *et al.*, 2010, Massberg *et al.*, 2010, von Bruhl *et al.*, 2012), it is unclear whether other cells also release their nucleic acid contents. Partial ligation of the IVC often induces local ischemia (Geddings *et al.*, 2014), conditions known to produce cell necrosis and/or apoptosis. Nucleic acids are also released from cells undergoing necrosis or apoptosis (Edinger and Thompson, 2004), but the contribution of these pathways to the pathogenesis of venous thrombosis remains to be elucidated. Consequently, it is unclear whether RNA and DNA contribute equally to the pathogenesis of arterial and venous thrombosis; but emerging evidence suggests that the relative contribution of DNA and/or RNA to thrombosis may differ depending on the method used to induce injury and the vascular bed that is injured.

7.1.7 HRG IS A PATTERN RECOGNITION PROTEIN

Pattern recognition proteins (PRPs) are a class of molecules that recognize "danger signals" derived from pathogens or released from cells upon injury or death. PRPs recognize danger-associated molecular patterns (DAMPs). DAMPs are a broad class of molecules that include (a) pathogen associated molecular patterns (PAMPs) that are released from microorganisms during infection and (b) host-cell derived "danger signals" termed alarmins that are released upon tissue damage or injury (Delvaeye and Conway, 2009). PAMPs include the gram-negative bacteria cell wall component lipopolysaccharide (LPS), whereas alarmins include nucleic acids because they are normally found within cells. PRPs recognize DAMPs and present these patterns to macrophages for clearance. When cells are dying or dead, they release nucleic acids into the blood, which can trigger autoimmune responses (Rumore and Steinman, 1990). Thus, it is important to activate mechanisms that facilitate clearance of alarmins, such as nucleic acids. Consistent with the role of HRG as a PRP, HRG binds DNA on dying cells and this marks the cells for phagocytosis and clearance by macrophages (Gorgani *et al.*, 2002). In support of its role as an accessory protein, HRG can simultaneously binding to DNA exposed on dead cells and to Fc receptors on macrophages to bridge the two components together (Gorgani *et al.*, 2002).

In addition to recognizing nucleic acids (Chapters 5 and 6), HRG also binds to cell wall components on bacteria and yeast and induces lysis of these pathogens (Rydengard *et al.*, 2006, Rydengard *et al.*, 2007, Rydengard *et al.*, 2008, Shannon *et al.*, 2010). Microbial proteins on cell surfaces can also activate the intrinsic and extrinsic pathways

of coagulation to trigger fibrin formation. The fibrin clot effectively captures and localizes the invading pathogens at the site of infection (Esmon *et al.*, 2011). In the presence of zinc, HRG binds both isoforms of fibrinogen with comparable affinities (composite K_d value of ~ 9 nM) (Chapter 3). The HRG-fibrin interaction takes on new significance because HRG exhibits antimicrobial activity and modulates innate immunity and inflammation in a fibrin-dependent fashion (Shannon *et al.*, 2010). HRG is anchored to the fibrin network and mediates bacterial entrapment and killing (Shannon *et al.*, 2010). HRG binds bacteria (and fungi) and induces pore formation in their outer membranes in a manner that is dependent on zinc and pH, causing these pathogens to lyse (Rydengard *et al.*, 2006, Rydengard *et al.*, 2007, Rydengard *et al.*, 2008); consequently, the fibrin clot provides an antimicrobial milieu. Therefore, $HRG^{-/-}$ mice are more prone to bacterial dissemination and death compared with wild type controls (Shannon *et al.*, 2010). Thus, the HRG-fibrin interaction provides an important link between immunity and inflammation.

The view that HRG is a PRP provides a framework for assessing the physiological role of HRG. The observation that HRG exhibits antimicrobial activity and facilitates dead cell clearance via the canonical PRP mechanism supports the contention that HRG is an important modulator of the immune system. However, our observation that HRG attenuates contact activation of coagulation by binding FXIIa (MacQuarrie *et al.*, 2011) and nucleic acids (Chapters 5 and 6) indicates that HRG also plays an important role in coagulation. The capacity of HRG to serve as a link between immunity and coagulation is a property that it shares with the other contact components such as nucleic acids, HK and

PK/kallikrein. Cleavage of HK by elastase releases antimicrobial peptides (Poon *et al.*, 2011) and bacterial membrane surfaces can also activate FXII and PK (Frick *et al.*, 2007). Thus, the capacity of HRG to interact with nucleic acids that are released from lysed pathogen, FXII and fibrin during infection mirrors the interaction of HRG with the contact pathway components during thrombosis. Therefore, HRG is an important link between immunity and coagulation and it is likely that HRG contributes to arterial and venous thrombosis since both of pathologies are driven by dysregulation of immune cells and coagulation.

7.1.8 REGULATION OF HRG ACTIVITY

HRG is a multidomain protein that interacts with a wide variety of ligands, including fibrin(ogen) (Chapter 3), FXIIa (MacQuarrie *et al.*, 2011) and nucleic acids (Chapters 5 and 6). What mechanisms regulate HRG binding to its ligands? Distinguishing features of HRG that enable it to interact with multiple ligands and modulate processes important in coagulation and immunity include its: (a) modular structure, (b) capacity to sense environmental changes in pH and ion fluctuations and (c) susceptibility to cleavage by regulatory proteases. First, HRG is a modular protein and each of its domains exhibits ligand specificity (*reviewed in* (Jones *et al.*, 2005)). For instance, the NH_2-terminal region interacts with polyanions, such as heparin and heparan sulfate, whereas the HRR modulates fibrin(ogen) binding (Chapter 3). Second, the HRR is characterized by a high content of His residues. Imidazole groups exposed to solvent can interact with hydrogen ions or cations such as zinc (Fig. 1.5B), which induces a conformational change in the HRR that is transmitted throughout the molecule (Borza *et*

al., 1996, Borza and Morgan, 1998). Consequently, binding of hydrogen ions or zinc directs HRG binding to ligands such as fibrin(ogen). Therefore, ion binding may provide an important regulatory switch at sites of injury and/or infection where activated platelets release zinc and local ischemia lowers the pH. Third, HRG activity is regulated by cleavage by proteases such as plasmin, kallikrein and neutrophil elastase (Poon *et al.*, 2009, Poon *et al.*, 2011). This regulatory mechanism is best characterized in solid tumour models. Through modulation of the inflammatory and immune pathways, HRG suppresses tumour growth (Rolny *et al.*, 2011). As tumorigenesis progresses, however, plasma levels of HRG decrease, but HRG fragments are found in the tumour stroma (Rolny *et al.*, 2011). Plasmin activity is upregulated in solid tumours and because of its capacity to degrade extracellular matrix, plasmin contributes to tumour migration and metastasis (Dano *et al.*, 2005). Consequently, plasmin may attenuate HRG activity, thereby facilitating cancer progression. Likewise, neutrophil elastase cleaves HK to release antimicrobial peptides that are rich in His residues, providing a mechanism by which the HRR is released from HRG during infection (Poon *et al.*, 2011). Consequently, proteases can dampen the effects of HRG under different pathophysiological conditions. The capacity of HRG to sense dynamic changes in the environment and direct its binding accordingly provides a mechanism by which HRG regulates different biological processes.

7.1.9 HRG IS A MEMBER OF A GROUP OF MULTIFUNCTIONAL PROTEINS

During infection and subsequent healing, the innate immune system functions in a coordinated fashion with the coagulation, fibrinolytic and inflammatory pathways. The intertwining of these pathways supports the contention that during evolution, the coagulation system was an integral part of innate immunity (Delvaeye and Conway, 2009, Esmon *et al.*, 2011). From this perspective, it is evident that proteins such as HRG evolved so as to facilitate their interaction with all of these systems. Importantly, there are a group of multifunctional, plasma proteins that like HRG, bind multiple ligands and mediate crosstalk among several pathways. This group includes HK, C-reactive protein, and the complement component C1q, to name but a few (*reviewed* in (Poon *et al.*, 2011)). Although most of these proteins are structurally unrelated, they bind common ligands and have similar functions. Their ligands include cations (e.g., calcium and zinc) and polyanions (e.g. heparin, DNA and phospholipids), and these proteins regulate host defense, coagulation/fibrinolysis and dead cell clearance (*reviewed* in (Poon *et al.*, 2011)).

7.2 FUTURE DIRECTIONS

Although we have demonstrated that HRG serves as a potent inhibitor of contact activation and likely links coagulation and inflammation, there are several avenues of research that would broaden our understanding of its physiological functions, clinical relevance and therapeutic potential. This section proposes 3 such projects aimed at increasing our understanding of: (i) the HRG-FXIIa interaction, so as to identify novel antithrombotic drugs; (ii) the role of HRG in a DNA-driven model of venous thrombosis

to complement our studies with the $FeCl_3$ model; and (iii) HRG as novel link between coagulation and inflammation in a murine model of sepsis.

7.2.1 PROJECT #1: CHARACTERIZATION OF THE HRG-FXIIA INTERACTION

7.2.1.1 Rationale:

Anticoagulants are used for the prevention and treatment of arterial and venous thrombosis. Current anticoagulation therapy is based mainly on heparin or heparin derivatives, vitamin K antagonists and direct inhibitors of FXa or thrombin (Yeh *et al.*, 2012). However, a major drawback of these anticoagulants is the significant risk of bleeding (Gailani and Renne, 2007, Muller *et al.*, 2011). Thrombin-like serine proteases from snake venom such as batroxobin have been investigated for the prevention and treatment of thrombosis (Latallo, 1983, Wang *et al.*, 2010, Xu *et al.*, 2007). Batroxobin is a defibrinogenating agent that reduces blood viscosity, but studies with batroxobin and other snake venom enzymes for treatment of acute ischemic stroke have yielded disappointing results largely because of increased bleeding (Liu *et al.*, 2011). Therefore, there is an ongoing search for safer anticoagulants. Although FXII plays an important role in thrombosis, it is not important for hemostasis; a concept that has been consistently demonstrated in rodent, rabbit and non-human primate models (Larsson *et al.*, 2014, Matafonov *et al.*, 2014, Revenko *et al.*, 2011). The capacity of FXIIa to activate the intrinsic pathway makes it a prime target for therapeutic intervention because its inhibition would attenuate thrombosis without increasing the risk of bleeding (Gailani and Renne, 2007, Muller *et al.*, 2011). There are two approaches that could be used to target

FXII. First, ASOs could be used to decrease plasma FXII levels. Alternatively, FXIIa could be inhibited with aptamers, antibodies/nanonobodies, or small molecule inhibitors (de Maat *et al.*, 2013, Larsson *et al.*, 2014, Woodruff *et al.*, 2013). As an alternative approach, we propose to generate FXIIa-directed derivatives of HRG that specifically modulate the procoagulant activity of FXIIa. In addition to its role as an initiator of coagulation, FXIIa is also important in inflammation and vessel dilation (*reviewed in* (Schmaier and McCrae, 2007)); thus, it is important to develop specific FXIIa inhibitors that attenuate thrombosis without impacting on other physiological functions of the protease. α-FXIIa has a prominent role in thrombosis largely owing to its capacity to bind polyanion activators, such as nucleic acids. In contrast, β-FXIIa, which is composed of the catalytic domain and lacks any surface binding properties, is implicated in the regulation of inflammatory processes (Colman and Schmaier, 1997).

We recently identified HRG as a novel inhibitor of α-FXIIa, but not β-FXIIa, thereby suggesting that HRG binds to an allosteric region on the heavy chain (MacQuarrie *et al.*, 2011). We will further characterize the HRG-α-FXIIa interaction to identify the region(s) of HRG that mediate FXIIa binding. With this information, fragments of HRG may be identified that recapitulate the inhibitory effects of HRG on FXIIa activity. These fragments could then be reverse engineered to develop small molecule inhibitors.

7.2.1.2 Proposed Experiments:

7.2.1.3 ***Aim 1: To identify the domain(s) of HRG that bind to α-FXIIa.*** HRG fragments will be generated by limited plasmin digestion to produce N1N2-, COOH-, HRR-PRR

regions, which will be separated by chromatography (Poon *et al.*, 2009). In addition, other proteases or chemicals, such as trypsin and cyanogen bromide, will be used to generate alternative fractionation patterns. SPR will be used to compare the binding of the HRG fragments to α-FXIIa, β-FXIIa and FXII with that of intact HRG. Although the goal is to identify fragments that bind α-FXIIa with affinity similar to that of HRG, binding to β-FXIIa and FXII also will be investigated as negative controls. As part of the validation process, we can assess the capacity of HRG and its derivatives to compete with molecules that are known to bind to the heavy chain of FXIIa. These include the RNA aptamer R4cXII-1, and the nanobody A10, which bind to the heavy chain of FXIIa and inhibit FXIIa activity (de Maat *et al.*, 2013, Woodruff *et al.*, 2013); thus, it would be interesting if HRG and these two other heavy chain-directed inhibitors attenuate FXIIa activity by interacting with the same region. In summary, we will first identify HRG fragments that bind FXIIa and then prepare synthetic peptides analogs or use the HRG cDNA to generate recombinant HRG fragments in mammalian cell lines.

7.2.1.4 ***Aim 2: Characterization of FXIIa-directed HRG derivatives in murine models of thrombosis.*** Once inhibitory HRG fragments are identified, their antithrombotic effects will be investigated in $HRG^{-/-}$ mice to determine whether like intact HRG, the fragments rescue the prothrombotic phenotype of $HRG^{-/-}$ mice in the $FeCl_3$ model. This study will enable us to compare the potencies of the HRG fragments to that of intact HRG. As a control, we will also assess the effect of these fragments on bleeding in a tail amputation model.

7.2.2 PROJECT #2: CHARACTERIZATION OF THE ROLE OF HRG IN VENOUS THROMBOSIS

7.2.2.1 Rationale:

HRG attenuates both RNA- and DNA-mediated activation of coagulation (Chapter 5). In the $FeCl_3$ arterial injury model, we demonstrated that RNA drives thrombosis in a FXII-dependent fashion (Chapter 6). RNA and DNA are equally potent activators of the intrinsic pathway (Chapter 5) and thus, it is of interest to determine if HRG can also modulate the procoagulant activity of DNA in a model of thrombosis. In the IVC ligation model, DNase administration protects mice from thrombosis (Brill *et al.*, 2012, von Bruhl *et al.*, 2012). Therefore, by performing this model in $HRG^{-/-}$ and wild type mice, we can determine whether HRG deficiency endows mice with a prothrombotic phenotype in a DNA-driven model like it does in a RNA-driven model and whether HRG infusion restores the normal phenotype.

7.2.2.2 Proposed Experiments:

7.2.2.3 ***Aim 1: Characterization of the role of HRG in venous thrombosis***. Using the partial ligation model, blood flow in the IVC of HRG-deficient and wild type mice will be reduced by 80-90% for up to 48 hr to induce thrombosis (Brill *et al.*, 2012, Geddings *et al.*, 2014). Thrombi will be harvested and the weights of thrombi from $HRG^{-/-}$ and $HRG^{+/-}$ mice will be compared with those of thrombi harvested from wild type mice. We expect that thrombi in $HRG^{-/-}$ mice will be larger than those in wild type controls and that thrombi in $HRG^{+/-}$ mice will be of intermediate weight.

7.2.2.4 ***Aim 2: Relative contribution of DNA and RNA to venous thrombosis.*** It is currently unclear if RNA contributes to the pathogenesis of venous thrombosis. To evaluate the relative contribution of the DNA and RNA to thrombosis in the IVC ligation model, we will first quantify the levels of DNA and RNA in the plasma after surgery. In addition, DNase or RNAse will be injected into wild type mice to determine whether, like DNase, RNase also protects mice from thrombosis. Finally, the thrombi of these mice will be harvested, weighed and subjected to immunofluorescence using DNA- or RNA-selective dyes as described in Chapter 6 to determine their nucleic acid content.

7.2.3 PROJECT #3: CHARACTERIZATION OF THE ROLE OF HRG IN SEPSIS

7.2.3.1 Rationale:

Sepsis is characterized by systemic activation of the inflammatory and coagulation pathways as the result of bacterial infection in normally sterile parts of the body (Toltl *et al.*, 2008). The host response to infection leads to a coagulopathy that is mediated by both the intrinsic and extrinsic pathways (see (Levi *et al.*, 2003) *for review*). Evidence for a role of the intrinsic pathway in sepsis pathogenesis includes: (a) bacterial membranes contain negatively charged structural elements such as LPS and lipoteichoic acid and bacteria release cellular components such as polyP that can activate FXII and PK (Frick *et al.*, 2007, Tucker *et al.*, 2012); (b) a FXI directed antibody (14E11) attenuates the release of pro-inflammatory cytokines and reduced the formation thrombin-AT complexes in the cecal ligation and puncture (CLP) model of murine sepsis, but has no impact on tail bleeding (Tucker *et al.*, 2012); and (c) as part of the host-response in CLP models, neutrophils release NETs, which contain DNA and trigger contact activation (Kannemeier

et al., 2007, Meng *et al.*, 2012, Swystun *et al.*, 2011). Therefore, during sepsis, activation of the intrinsic pathway contributes to both microvascular thrombosis and inflammation.

The molecular brakes normally in place to prevent excessive clotting and inflammation are impaired during sepsis. Although C1-Inh inhibits FXIIa and FXIa, C1-Inh is degraded by elastase released from neutrophils during sepsis, which attenuates its activity (Caliezi *et al.*, 2000). Similarly, plasma HRG levels are significantly lower in septic patients than in non-septic controls (Stafford 2013, unpublished observations). Organ dysfunction is a common complication of severe sepsis and results from microvascular thrombosis and subsequent ischemia and infarction. Dead and damaged cells likely contribute to the elevated levels of DNA and RNA observed in septic patients (Dwivedi *et al.*, 2012, Preissner, 2007). In addition to promoting contact activation of coagulation, RNA is a pro-inflammatory agent that stimulates the release of inflammatory cytokines (Fischer *et al.*, 2012). Because HRG is a potent inhibitor of contact activation and recognizes nucleic acids as DAMPs to facilitates their clearance (Gorgani *et al.*, 2002), we hypothesize that the decrease in HRG levels during sepsis likely contributes to the systemic inflammation and coagulation that characterize sepsis.

7.2.3.2 Proposed Experiments:

7.2.3.3 *Aim 1: Characterization of the role of HRG in a murine model of CLP-induced sepsis*. In the CLP model, the cecum is ligated and then punctured to induce a slow leak of bacterial into the peritoneum (Doi *et al.*, 2009). To validate the role of HRG in this model of sepsis, wild type mice will be subjected to CLP and blood will be collected to quantify levels of HRG, nucleic acids, inflammatory markers (e.g., IL-6 and IL-10) and

thrombin-AT complexes. Additionally, organs will be harvested for further analysis of inflammation and coagulation using immunofluorescence (e.g., antibodies directed against neutrophils, histones, platelets and fibrin). We hypothesize that like the situation in septic patients, levels of HRG will decrease significantly in this model. Based on our preliminary results with an LPS model, the HRG levels were reduced by ~50% (Vu, unpublished 2013). Thus, there is a good possibility that HRG levels will drop during CLP-induced sepsis. We hypothesize that the effects of sepsis will be more severe in $HRG^{-/-}$ mice than in wild type controls. For repletion studies, HRG will be injected into $HRG^{-/-}$ mice at regular intervals before and after CLP to sustain high HRG levels during sepsis. We can then assess if HRG repletion attenuates inflammation and intravascular coagulation in HRG-deficient mice.

7.3 CONCLUSIONS

HRG is a relatively abundant plasma protein that binds to several ligands that include heparin, FXIIa, fibrinogen and nucleic acids (Table 1.1). Although HRG has been implicated in diverse biological processes such as immunity, vascular remodeling, cogulation, and fibrinolysis, its physiological function is unclear. We demonstrated that HRG is a dynamic modulator of coagulation. A secondary role of HRG in coagulation is modulation of thrombin binding to γ_A/γ'-fibrin clots. This phenomenon takes on new significance since circulating levels of γ_A/γ'-fibrinogen have been correlated with cardiovascular disease. The capacity of HRG to compete with thrombin for binding to the γ'-chain also has important implications since thrombi harvested from humans are rich in active thrombin that can promote clot expansion and growth. Other than thrombin and

perhaps FXIII, very few proteins have been shown to interact with the γ′-region; therefore, HRG binding to this region likely provides a unique mechanism that regulates the activity of clot-bound thrombin.

However, in the presence of zinc, HRG's affinity for FXIIa is three orders of magnitude greater than fibrin(ogen), demonstrating that FXIIa is the preferred ligand. HRG is a potent inhibitor of FXIIa and attenuates nucleic acid mediated activation of the contact pathway of coagulation. Using a murine model of thrombosis, we demonstrated that an HRG-deficiency results in a prothrombotic phenotype and that repletion with human HRG rescues the mice from thrombosis. Consistent with the role of HRG as a modulator of the intrinsic pathway, we also showed that an HRG-deficiency has minimal impact on bleeding in a murine tail amputation study.

A significant drawback of the current anticoagulants is they can increase a patient's risk of severe bleeding. Several pioneering studies with rodents, rabbits and non-human primates have consistently demonstrated that down-regulation of FXII or FXI or inhibition of FXIIa or FXIa protects these animals from thrombosis, while having only minimal effects on bleeding. Thus, there has been considerable interest in developing antithrombotics that inhibit one or more of the key players in the intrinsic pathway, as a means to develop safer drugs. HRG specifically binds FXIIa and inhibits propagation of contact activation of coagulation and likely modulates the activity of clot-bound thrombin. Therefore, further characterization of the role of HRG in coagulation may lead to the development of safer anticoagulants.

8.0 REFERENCES

Adams, T. E. and Huntington, J. A. (2006) Thrombin-cofactor interactions: structural insights into regulatory mechanisms. *Arterioscler. Thromb. Vasc. Biol.* **26**, 1738-1745.

Allan, P., Uitte, d. W., Abou-Saleh, R. H., Connell, S. D. and Ariens, R. A. (2012) Evidence that fibrinogen gamma' directly interferes with protofibril growth: implications for fibrin structure and clot stiffness. *J. Thromb. Haemost.* **10**, 1072-1080.

Aronson, D. L. (1976) Comparison of the actions of thrombin and the thrombin-like venom enzymes ancrod and batroxobin. *Thromb. Haemost.* **36**, 9-13.

Barr, J. D., Chauhan, A. K., Schaeffer, G. V., Hansen, J. K. and Motto, D. G. (2013) Red blood cells mediate the onset of thrombosis in the ferric chloride murine model. *Blood* **121**, 3733-3741.

Becker, D. L., Fredenburgh, J. C., Stafford, A. R. and Weitz, J. I. (1999) Exosites 1 and 2 are essential for protection of fibrin-bound thrombin from heparin-catalyzed inhibition by antithrombin and heparin cofactor II. *J. Biol. Chem.* **274**, 6226-6233.

Bernardo, M. M., Day, D. E., Halvorson, H. R., Olson, S. T. and Shore, J. D. (1993a) Surface-independent acceleration of factor XII activation by zinc ions. II. Direct binding and fluorescence studies. *J. Biol. Chem.* **268**, 12477-12483.

Bernardo, M. M., Day, D. E., Olson, S. T. and Shore, J. D. (1993b) Surface-independent acceleration of factor XII activation by zinc ions. I. Kinetic characterization of the metal ion rate enhancement. *J. Biol. Chem.* **268**, 12468-12476.

Binnie, C. G. and Lord, S. T. (1993) The fibrinogen sequences that interact with thrombin. *Blood* **81**, 3186-3192.

Bird, J. E., Smith, P. L., Wang, X., Schumacher, W. A., Barbera, F., Revelli, J. P. and Seiffert, D. (2012) Effects of plasma kallikrein deficiency on haemostasis and thrombosis in mice: murine ortholog of the Fletcher trait. *Thromb. Haemost.* **107**, 1141-1150.

Blomback, B., Hessel, B., Hogg, D. and Therkildsen, L. (1978) A two-step fibrinogen--fibrin transition in blood coagulation. *Nature* **275**, 501-505.

Bode, W., Mayr, I., Baumann, U., Huber, R., Stone, S. R. and Hofsteenge, J. (1989) The refined 1.9 A crystal structure of human alpha-thrombin: interaction with D-Phe-Pro-Arg chloromethylketone and significance of the Tyr-Pro-Pro-Trp insertion segment. *EMBO J.* **8**, 3467-3475.

Borissoff, J. I., Joosen, I. A., Versteylen, M. O., Brill, A., Fuchs, T. A., Savchenko, A. S., Gallant, M., Martinod, K., Ten Cate, H., Hofstra, L. *et al.* (2013) Elevated levels of

circulating DNA and chromatin are independently associated with severe coronary atherosclerosis and a prothrombotic state. *Arterioscler. Thromb. Vasc. Biol.* **33**, 2032-2040.

Borza, D. B. and Morgan, W. T. (1998) Histidine-proline-rich glycoprotein as a plasma pH sensor. Modulation of its interaction with glycosaminoglycans by ph and metals. *J Biol. Chem.* **273**, 5493-5499.

Borza, D. B., Tatum, F. M. and Morgan, W. T. (1996) Domain structure and conformation of histidine-proline-rich glycoprotein. *Biochemistry* **35**, 1925-1934.

Bosshart, H. and Heinzelmann, M. (2003) Endotoxin-neutralizing effects of histidine-rich peptides. *FEBS Lett.* **553**, 135-140.

Braud, S., Bon, C. and Wisner, A. (2000) Snake venom proteins acting on hemostasis. *Biochimie* **82**, 851-859.

Brill, A., Fuchs, T. A., Savchenko, A. S., Thomas, G. M., Martinod, K., De Meyer, S. F., Bhandari, A. A. and Wagner, D. D. (2012) Neutrophil extracellular traps promote deep vein thrombosis in mice. *J Thromb. Haemost.* **10**, 136-144.

Bugge, T. H., Xiao, Q., Kombrinck, K. W., Flick, M. J., Holmback, K., Danton, M. J., Colbert, M. C., Witte, D. P., Fujikawa, K., Davie, E. W. *et al.* (1996) Fatal embryonic bleeding events in mice lacking tissue factor, the cell-associated initiator of blood coagulation. *Proc. Natl. Acad Sci. U. S. A* **93**, 6258-6263.

Caliezi, C., Wuillemin, W. A., Zeerleder, S., Redondo, M., Eisele, B. and Hack, C. E. (2000) C1-Esterase inhibitor: an anti-inflammatory agent and its potential use in the treatment of diseases other than hereditary angioedema. *Pharmacol. Rev.* **52**, 91-112.

Castro, H. C., Zingali, R. B., Albuquerque, M. G., Pujol-Luz, M. and Rodrigues, C. R. (2004) Snake venom thrombin-like enzymes: from reptilase to now. *Cell Mol. Life Sci.* **61**, 843-856.

Cesarman-Maus, G. and Hajjar, K. A. (2005) Molecular mechanisms of fibrinolysis. *Br. J. Haematol.* **129**, 307-321.

Choi, S. H., Smith, S. A. and Morrissey, J. H. (2011) Polyphosphate is a cofactor for the activation of factor XI by thrombin. *Blood* **118**, 6963-6970.

Chung, D. W. and Davie, E. W. (1984) gamma and gamma' chains of human fibrinogen are produced by alternative mRNA processing. *Biochemistry* **23**, 4232-4236.

Citarella, F., te, V. H., Helmer-Citterich, M. and Hack, C. E. (2000) Identification of a putative binding site for negatively charged surfaces in the fibronectin type II domain of

human factor XII--an immunochemical and homology modeling approach. *Thromb. Haemost.* **84**, 1057-1065.

Colman, R. W. and Schmaier, A. H. (1997) Contact system: a vascular biology modulator with anticoagulant, profibrinolytic, antiadhesive, and proinflammatory attributes. *Blood* **90**, 3819-3843.

Cool, D. E., Edgell, C. J., Louie, G. V., Zoller, M. J., Brayer, G. D. and MacGillivray, R. T. (1985) Characterization of human blood coagulation factor XII cDNA. Prediction of the primary structure of factor XII and the tertiary structure of beta-factor XIIa. *J. Biol. Chem.* **260**, 13666-13676.

Cooper, A. V., Standeven, K. F. and Ariens, R. A. (2003) Fibrinogen gamma-chain splice variant gamma' alters fibrin formation and structure. *Blood* **102**, 535-540.

Crosby, J. R., Marzec, U., Revenko, A. S., Zhao, C., Gao, D., Matafonov, A., Gailani, D., MacLeod, A. R., Tucker, E. I., Gruber, A. *et al.* (2013) Antithrombotic effect of antisense factor XI oligonucleotide treatment in primates. *Arterioscler. Thromb. Vasc. Biol.* **33**, 1670-1678.

Cushman, M., O'Meara, E. S., Folsom, A. R. and Heckbert, S. R. (2009) Coagulation factors IX through XIII and the risk of future venous thrombosis: the Longitudinal Investigation of Thromboembolism Etiology. *Blood* **114**, 2878-2883.

Da Graca Salomao, M., Wuster, W., Thorpe, R. S. and Touzet, J.-M. (1997) DNA evolution of South American pitvipers of the genus Bothrops (REptilia:Serpentes:Viperidae). *Symp. Zool. Soc. Lond.* **70**, 89-98.

Dano, K., Behrendt, N., Hoyer-Hansen, G., Johnsen, M., Lund, L. R., Ploug, M. and Romer, J. (2005) Plasminogen activation and cancer. *Thromb. Haemost.* **93**, 676-681.

de Agostini, A., Lijnen, H. R., Pixley, R. A., Colman, R. W. and Schapira, M. (1984) Inactivation of factor XII active fragment in normal plasma. Predominant role of C-1-inhibitor. *J. Clin. Invest* **73**, 1542-1549.

De Cristofaro, R., De Candia, E., Landolfi, R., Rutella, S. and Hall, S. W. (2001) Structural and functional mapping of the thrombin domain involved in the binding to the platelet glycoprotein Ib. *Biochemistry* **40**, 13268-13273.

de Maat, S., van Dooremalen, S., de Groot, P. G. and Maas, C. (2013) A nanobody-based method for tracking factor XII activation in plasma. *Thromb. Haemost.* **110**, 458-468.

De Meyer, S. F., Suidan, G. L., Fuchs, T. A., Monestier, M. and Wagner, D. D. (2012) Extracellular chromatin is an important mediator of ischemic stroke in mice. *Arterioscler. Thromb. Vasc. Biol.* **32**, 1884-1891.

Decrem, Y., Rath, G., Blasioli, V., Cauchie, P., Robert, S., Beaufays, J., Frere, J. M., Feron, O., Dogne, J. M., Dessy, C. *et al.* (2009) Ir-CPI, a coagulation contact phase inhibitor from the tick Ixodes ricinus, inhibits thrombus formation without impairing hemostasis. *J Exp. Med.* **206**, 2381-2395.

Delvaeye, M. and Conway, E. M. (2009) Coagulation and innate immune responses: can we view them separately? *Blood* **114**, 2367-2374.

Di Cera, E. and Cantwell, A. M. (2001) Determinants of thrombin specificity. *Ann. N. Y. Acad. Sci.* **936**, 133-146.

Dias, N. and Stein, C. A. (2002) Antisense oligonucleotides: basic concepts and mechanisms. *Mol. Cancer Ther.* **1**, 347-355.

Diaz, J. A., Obi, A. T., Myers, D. D., Jr., Wrobleski, S. K., Henke, P. K., Mackman, N. and Wakefield, T. W. (2012) Critical review of mouse models of venous thrombosis. *Arterioscler. Thromb. Vasc. Biol.* **32**, 556-562.

Doi, K., Leelahavanichkul, A., Yuen, P. S. and Star, R. A. (2009) Animal models of sepsis and sepsis-induced kidney injury. *J Clin. Invest* **119**, 2868-2878.

Drasin, T. and Sahud, M. (1996) Blood-type and age affect human plasma levels of histidine-rich glycoprotein in a large population. *Thromb. Res.* **84**, 179-188.

Dwivedi, D. J., Toltl, L. J., Swystun, L. L., Pogue, J., Liaw, K. L., Weitz, J. I., Cook, D. J., Fox-Robichaud, A. E. and Liaw, P. C. (2012) Prognostic utility and characterization of cell-free DNA in patients with severe sepsis. *Crit Care* **16**, R151.

Eckly, A., Hechler, B., Freund, M., Zerr, M., Cazenave, J. P., Lanza, F., Mangin, P. H. and Gachet, C. (2011) Mechanisms underlying FeCl3-induced arterial thrombosis. *J Thromb. Haemost.* **9**, 779-789.

Edinger, A. L. and Thompson, C. B. (2004) Death by design: apoptosis, necrosis and autophagy. *Curr. Opin. Cell Biol.* **16**, 663-669.

Eigenbrot, C. and Kirchhofer, D. (2002) New insight into how tissue factor allosterically regulates factor VIIa. *Trends Cardiovasc. Med.* **12**, 19-26.

El Hefnawy, T., Raja, S., Kelly, L., Bigbee, W. L., Kirkwood, J. M., Luketich, J. D. and Godfrey, T. E. (2004) Characterization of amplifiable, circulating RNA in plasma and its potential as a tool for cancer diagnostics. *Clin. Chem.* **50**, 564-573.

Esmon, C. T. (2003) The protein C pathway. *Chest* **124**, 26S-32S.

Esmon, C. T., Xu, J. and Lupu, F. (2011) Innate immunity and coagulation. *J Thromb. Haemost.* **9 Suppl 1**, 182-188.

Falls, L. A. and Farrell, D. H. (1997) Resistance of gammaA/gamma' fibrin clots to fibrinolysis. *J Biol. Chem.* **272**, 14251-14256.

Faxalv, L., Boknas, N., Strom, J. O., Tengvall, P., Theodorsson, E., Ramstrom, S. and Lindahl, T. L. (2013) Putting polyphosphates to the test: evidence against platelet-induced activation of factor XII. *Blood* **122**, 3818-3824.

Fischer, S., Gerriets, T., Wessels, C., Walberer, M., Kostin, S., Stolz, E., Zheleva, K., Hocke, A., Hippenstiel, S. and Preissner, K. T. (2007) Extracellular RNA mediates endothelial-cell permeability via vascular endothelial growth factor. *Blood* **110**, 2457-2465.

Fischer, S., Grantzow, T., Pagel, J. I., Tschernatsch, M., Sperandio, M., Preissner, K. T. and Deindl, E. (2012) Extracellular RNA promotes leukocyte recruitment in the vascular system by mobilising proinflammatory cytokines. *Thromb. Haemost.* **108**, 730-741.

Fischer, S., Nishio, M., Dadkhahi, S., Gansler, J., Saffarzadeh, M., Shibamiyama, A., Kral, N., Baal, N., Koyama, T., Deindl, E. *et al.* (2011) Expression and localisation of vascular ribonucleases in endothelial cells. *Thromb. Haemost.* **105**, 345-355.

Foote, J. W. and Delves, H. T. (1984) Albumin bound and alpha 2-macroglobulin bound zinc concentrations in the sera of healthy adults. *J Clin. Pathol.* **37**, 1050-1054.

Fornace, A. J., Jr., Cummings, D. E., Comeau, C. M., Kant, J. A. and Crabtree, G. R. (1984) Structure of the human gamma-fibrinogen gene. Alternate mRNA splicing near the 3' end of the gene produces gamma A and gamma B forms of gamma-fibrinogen. *J. Biol. Chem.* **259**, 12826-12830.

Fredenburgh, J. C., Stafford, A. R., Leslie, B. A. and Weitz, J. I. (2008) Bivalent binding to gammaA/gamma'-fibrin engages both exosites of thrombin and protects it from inhibition by the antithrombin-heparin complex. *J. Biol. Chem.* **283**, 2470-2477.

Fredenburgh, J. C., Stafford, A. R., Pospisil, C. H. and Weitz, J. I. (2004) Modes and consequences of thrombin's interaction with fibrin. *Biophys. Chem.* **112**, 277-284.

Fredenburgh, J. C., Stafford, A. R. and Weitz, J. I. (2001) Conformational changes in thrombin when complexed by serpins. *J Biol. Chem.* **276**, 44828-44834.

Frick, I. M., Bjorck, L. and Herwald, H. (2007) The dual role of the contact system in bacterial infectious disease. *Thromb. Haemost.* **98**, 497-502.

Fuchs, T. A., Brill, A., Duerschmied, D., Schatzberg, D., Monestier, M., Myers, D. D., Jr., Wrobleski, S. K., Wakefield, T. W., Hartwig, J. H. and Wagner, D. D. (2010) Extracellular DNA traps promote thrombosis. *Proc. Natl. Acad Sci. U. S. A* **107**, 15880-15885.

Fuchs, T. A., Kremer Hovinga, J. A., Schatzberg, D., Wagner, D. D. and Lammle, B. (2012) Circulating DNA and myeloperoxidase indicate disease activity in patients with thrombotic microangiopathies. *Blood* **120**, 1157-1164.

Gailani, D. and Renne, T. (2007) Intrinsic pathway of coagulation and arterial thrombosis. *Arterioscler. Thromb. Vasc. Biol.* **27**, 2507-2513.

Gaipl, U. S., Beyer, T. D., Heyder, P., Kuenkele, S., Bottcher, A., Voll, R. E., Kalden, J. R. and Herrmann, M. (2004) Cooperation between C1q and DNase I in the clearance of necrotic cell-derived chromatin. *Arthritis Rheum.* **50**, 640-649.

Gansler, J., Jaax, M., Leiting, S., Appel, B., Greinacher, A., Fischer, S. and Preissner, K. T. (2012) Structural requirements for the procoagulant activity of nucleic acids. *PLoS. One.* **7**, e50399.

Geddings, J., Aleman, M. M., Wolberg, A., von Bruhl, M. L., Massberg, S. and Mackman, N. (2014) Strengths and weaknesses of a new mouse model of thrombosis induced by inferior vena cava stenosis: communication from the SSC of the ISTH. *J Thromb. Haemost.* **12**, 571-573.

Gersh, K.C. and Lord, S.T. (2006) An investiatioin of factor XIII binding to recombinant gamma'/gamma' and gammaA/gamma' fibrinogen. *Blood (ASH Annual Meeting Abstracts)* **108**,

Ghosh, S., Shukla, D., Suman, K., Lakshmi, B. J., Manorama, R., Kumar, S. and Bhandari, R. (2013) Inositol hexakisphosphate kinase 1 maintains hemostasis in mice by regulating platelet polyphosphate levels. *Blood* **122**, 1478-1486.

Gilbert, G. E., Novakovic, V. A., Kaufman, R. J., Miao, H. and Pipe, S. W. (2012) Conservative mutations in the C2 domains of factor VIII and factor V alter phospholipid binding and cofactor activity. *Blood* **120**, 1923-1932.

Girolami, A., Scarparo, P. and Vettore, S. (2009) The association of a mild FXII deficiency with myocardial infarction and venous thrombosis is completely unjustified. *J. Thromb. Thrombolysis.* **27**, 454-455.

Gorgani, N. N., Altin, J. G. and Parish, C. R. (1999) Histidine-rich glycoprotein prevents the formation of insoluble immune complexes by rheumatoid factor. *Immunology* **98**, 456-463.

Gorgani, N. N., Smith, B. A., Kono, D. H. and Theofilopoulos, A. N. (2002) Histidine-rich glycoprotein binds to DNA and Fc gamma RI and potentiates the ingestion of apoptotic cells by macrophages. *J Immunol.* **169**, 4745-4751.

Gormally, E., Caboux, E., Vineis, P. and Hainaut, P. (2007) Circulating free DNA in plasma or serum as biomarker of carcinogenesis: practical aspects and biological significance. *Mutat. Res.* **635**, 105-117.

Griffith, M. J. (1982) The heparin-enhanced antithrombin III/thrombin reaction is saturable with respect to both thrombin and antithrombin III. *J. Biol. Chem.* **257**, 13899-302.

Guo, F., Liu, J., Wang, C., Liu, N. and Lu, P. (2009) Fibrinogen, fibrin, and FDP induce C-reactive protein generation in rat vascular smooth muscle cells: pro-inflammatory effect on atherosclerosis. *Biochem. Biophys. Res. Commun.* **390**, 942-946.

Henschen-Edman, A. H., Theodor, I., Edwards, B. F. and Pirkle, H. (1999) Crotalase, a fibrinogen-clotting snake venom enzyme: primary structure and evidence for a fibrinogen recognition exosite different from thrombin. *Thromb. Haemost.* **81**, 81-86.

Houlihan, L. M., Davies, G., Tenesa, A., Harris, S. E., Luciano, M., Gow, A. J., McGhee, K. A., Liewald, D. C., Porteous, D. J., Starr, J. M. *et al.* (2010) Common variants of large effect in F12, KNG1, and HRG are associated with activated partial thromboplastin time. *Am. J. Hum. Genet.* **86**, 626-631.

Huntington, J. A. (2005) Molecular recognition mechanisms of thrombin. *J. Thromb. Haemost.* **3**, 1861-1872.

Isbister, G. K. (2010) Snakebite doesn't cause disseminated intravascular coagulation: coagulopathy and thrombotic microangiopathy in snake envenoming. *Semin. Thromb. Hemost.* **36**, 444-451.

Jackman, M. P., Parry, M. A., Hofsteenge, J. and Stone, S. R. (1992) Intrinsic fluorescence changes and rapid kinetics of the reaction of thrombin with hirudin. *J Biol. Chem.* **267**, 15375-15383.

Jancso, A., Kolozsi, A., Gyurcsik, B., Nagy, N. V. and Gajda, T. (2009) Probing the Cu(2+) and Zn(2+) binding affinity of histidine-rich glycoprotein. *J Inorg. Biochem.* **103**, 1634-1643.

Jensen, T., Kierulf, P., Sandset, P. M., Klingenberg, O., Joo, G. B., Godal, H. C. and Skjonsberg, O. H. (2007) Fibrinogen and fibrin induce synthesis of proinflammatory cytokines from isolated peripheral blood mononuclear cells. *Thromb. Haemost.* **97**, 822-829.

Jones, A. L., Hulett, M. D., Altin, J. G., Hogg, P. and Parish, C. R. (2004a) Plasminogen is tethered with high affinity to the cell surface by the plasma protein, histidine-rich glycoprotein. *J Biol. Chem.* **279**, 38267-38276.

Jones, A. L., Hulett, M. D. and Parish, C. R. (2004b) Histidine-rich glycoprotein binds to cell-surface heparan sulfate via its N-terminal domain following Zn2+ chelation. *J Biol. Chem.* **279**, 30114-30122.

Jones, A. L., Hulett, M. D. and Parish, C. R. (2005) Histidine-rich glycoprotein: A novel adaptor protein in plasma that modulates the immune, vascular and coagulation systems. *Immunol. Cell Biol.* **83**, 106-118.

Kaczmarek, E. and McDonagh, J. (1988) Thrombin binding to the A alpha-, B beta-, and gamma-chains of fibrinogen and to their remnants contained in fragment E. *J Biol. Chem.* **263**, 13896-13900.

Kannemeier, C., Shibamiya, A., Nakazawa, F., Trusheim, H., Ruppert, C., Markart, P., Song, Y., Tzima, E., Kennerknecht, E., Niepmann, M. *et al.* (2007) Extracellular RNA constitutes a natural procoagulant cofactor in blood coagulation. *Proc. Natl. Acad Sci. U. S. A* **104**, 6388-6393.

Kariko, K., Buckstein, M., Ni, H. and Weissman, D. (2005) Suppression of RNA recognition by Toll-like receptors: the impact of nucleoside modification and the evolutionary origin of RNA. *Immunity.* **23**, 165-175.

Kleinschnitz, C., Stoll, G., Bendszus, M., Schuh, K., Pauer, H. U., Burfeind, P., Renne, C., Gailani, D., Nieswandt, B. and Renne, T. (2006) Targeting coagulation factor XII provides protection from pathological thrombosis in cerebral ischemia without interfering with hemostasis. *J Exp. Med.* **203**, 513-518.

Konings, J., Govers-Riemslag, J. W., Philippou, H., Mutch, N. J., Borissoff, J. I., Allan, P., Mohan, S., Tans, G., Ten Cate, H. and Ariens, R. A. (2011) Factor XIIa regulates the structure of the fibrin clot independently of thrombin generation through direct interaction with fibrin. *Blood* **118**, 3942-3951.

Koopman, J., Haverkate, F., Lord, S. T., Grimbergen, J. and Mannucci, P. M. (1992) Molecular basis of fibrinogen Naples associated with defective thrombin binding and thrombophilia. Homozygous substitution of B beta 68 Ala----Thr. *J. Clin. Invest* **90**, 238-244.

Korneeva, V. A., Trubetskov, M. M., Korshunova, A. V., Lushchekina, S. V., Kolyadko, V. N., Sergienko, O. V., Lunin, V. G., Panteleev, M. A. and Ataullakhanov, F. I. (2014) Interactions Outside the Proteinase-Binding Loop Contribute Significantly to the Inhibition of Activated Coagulation Factor XII by its Canonical Inhibitor from Corn. *J. Biol. Chem.*

Kretz, C. A., Cuddy, K. K., Stafford, A. R., Fredenburgh, J. C., Roberts, R. and Weitz, J. I. (2010) HD1, a thrombin- and prothrombin-binding DNA aptamer, inhibits thrombin

generation by attenuating prothrombin activation and thrombin feedback reactions. *Thromb. Haemost.* **103**, 83-93.

Kretz, C. A., Stafford, A. R., Fredenburgh, J. C. and Weitz, J. I. (2006) HD1, a thrombin-directed aptamer, binds exosite 1 on prothrombin with high affinity and inhibits its activation by prothrombinase. *J Biol. Chem.* **281**, 37477-37485.

Kumar, R., Beguin, S. and Hemker, H. C. (1995) The effect of fibrin clots and clot-bound thrombin on the development of platelet procoagulant activity. *Thromb. Haemost.* **74**, 962-968.

Lakomaa, E. L., Sato, S., Goldberg, A. M. and Frazier, J. M. (1982) The effect of sodium diethyldithiocarbamate treatment on copper and zinc concentrations in rat brain. *Toxicol. Appl. Pharmacol.* **65**, 286-290.

LaManna, J. C. (1996) Hypoxia/ischemia and the pH paradox. *Adv. Exp. Med. Biol.* **388**, 283-292.

Lancellotti, S., Rutella, S., De, F., V, Pozzi, N., Rocca, B. and De Cristofaro, R. (2008) Fibrinogen-elongated gamma chain inhibits thrombin-induced platelet response, hindering the interaction with different receptors. *J. Biol. Chem.* **283**, 30193-30204.

Larsson, M., Rayzman, V., Nolte, M. W., Nickel, K. F., Bjorkqvist, J., Jamsa, A., Hardy, M. P., Fries, M., Schmidbauer, S., Hedenqvist, P. *et al.* (2014) A factor XIIa inhibitory antibody provides thromboprotection in extracorporeal circulation without increasing bleeding risk. *Sci. Transl. Med.* **6**, 222ra17.

Latallo, Z. S. (1983) Retrospective study on complications and adverse effects of treatment with thrombin-like enzymes--a multicentre trial. *Thromb. Haemost.* **50**, 604-609.

Leung, L. L. (1986) Interaction of histidine-rich glycoprotein with fibrinogen and fibrin. *J. Clin. Invest* **77**, 1305-1311.

Leung, L. L., Harpel, P. C., Nachman, R. L. and Rabellino, E. M. (1983) Histidine-rich glycoprotein is present in human platelets and is released following thrombin stimulation. *Blood* **62**, 1016-1021.

Levi, M., Keller, T. T., van Gorp, E. and Ten Cate, H. (2003) Infection and inflammation and the coagulation system. *Cardiovasc. Res.* **60**, 26-39.

Li, C. Q., Vindigni, A., Sadler, J. E. and Wardell, M. R. (2001) Platelet glycoprotein Ib alpha binds to thrombin anion-binding exosite II inducing allosteric changes in the activity of thrombin. *J. Biol. Chem.* **276**, 6161-6168.

Lijnen, H. R., Hoylaerts, M. and Collen, D. (1980) Isolation and characterization of a human plasma protein with affinity for the lysine binding sites in plasminogen. Role in the regulation of fibrinolysis and identification as histidine-rich glycoprotein. *J Biol. Chem.* **255**, 10214-10222.

Lijnen, H. R., Jacobs, G. and Collen, D. (1981) Histidine-rich glycoprotein in a normal and a clinical population. *Thromb. Res.* **22**, 519-523.

Liu, L. W., Vu, T. K., Esmon, C. T. and Coughlin, S. R. (1991) The region of the thrombin receptor resembling hirudin binds to thrombin and alters enzyme specificity. *J Biol. Chem.* **266**, 16977-16980.

Liu, M., Counsell, C., Zhao, X. L. and Wardlaw, J. (2004) Fibrinogen-depleting agents for acute ischemic stroke. *Stroke* **36**, 173-174.

Liu, S., Marder, V. J., Levy, D. E., Wang, S. J., Yang, F., Paganini-Hill, A. and Fisher, M. J. (2011) Ancrod and fibrin formation: perspectives on mechanisms of action. *Stroke* **42**, 3277-3280.

Lo, Y. M., Zhang, J., Leung, T. N., Lau, T. K., Chang, A. M. and Hjelm, N. M. (1999) Rapid clearance of fetal DNA from maternal plasma. *Am. J. Hum. Genet.* **64**, 218-224.

Lorand, L. (2001) Factor XIII: structure, activation, and interactions with fibrinogen and fibrin. *Ann N. Y. Acad Sci.* **936**, 291-311.

Lord, S. T., Rooney, M. M., Hopfner, K. P. and Di Cera, E. (1995) Binding of fibrinogen A alpha 1-50-beta-galactosidase fusion protein to thrombin stabilizes the slow form. *J. Biol. Chem.* **270**, 24790-24793.

Lovely, R. S., Falls, L. A., Al Mondhiry, H. A., Chambers, C. E., Sexton, G. J., Ni, H. and Farrell, D. H. (2002) Association of gammaA/gamma' fibrinogen levels and coronary artery disease. *Thromb. Haemost.* **88**, 26-31.

Lovely, R. S., Moaddel, M. and Farrell, D. H. (2003) Fibrinogen gamma' chain binds thrombin exosite II. *J. Thromb. Haemost.* **1**, 124-131.

Ma, D., Mizurini, D. M., Assumpcao, T. C., Li, Y., Qi, Y., Kotsyfakis, M., Ribeiro, J. M., Monteiro, R. Q. and Francischetti, I. M. (2013) Desmolaris, a novel factor XIa anticoagulant from the salivary gland of the vampire bat (Desmodus rotundus) inhibits inflammation and thrombosis in vivo. *Blood* **122**, 4094-4106.

Macfarlane, R. G. (1964) An enzyme cascade in the blood clotting mechanism, and its function as a biochemical amplifier. *Nature* **202**, 498-499.

Mackman, N. (2008) Triggers, targets and treatments for thrombosis. *Nature* **451**, 914-918.

Mackman, N. (2009) The role of tissue factor and factor VIIa in hemostasis. *Anesth. Analg.* **108**, 1447-1452.

Mackman, N., Tilley, R. E. and Key, N. S. (2007) Role of the extrinsic pathway of blood coagulation in hemostasis and thrombosis. *Arterioscler. Thromb. Vasc. Biol.* **27**, 1687-1693.

MacQuarrie, J. L., Stafford, A. R., Yau, J. W., Leslie, B. A., Vu, T. T., Fredenburgh, J. C. and Weitz, J. I. (2011) Histidine-rich glycoprotein binds factor XIIa with high affinity and inhibits contact-initiated coagulation. *Blood* **117**, 4134-4141.

Mann, K. G., Jenny, R. J. and Krishnaswamy, S. (1988) Cofactor proteins in the assembly and expression of blood clotting enzyme complexes. *Annu. Rev. Biochem.* **57**, 915-956.

Marder, V. J., Shulman, N. R. and Carroll, W. R. (1969) High molecular weight derivatives of human fibrinogen produced by plasmin. I. Physicochemical and immunological characterization. *J Biol. Chem.* **244**, 2111-2119.

Maret, W. (2004) Exploring the zinc proteome. *J. Anal. At. Spectrom* **19**, 15-19.

Mariani, G., Konkle, B. A. and Ingerslev, J. (2006) Congenital factor VII deficiency: therapy with recombinant activated factor VII -- a critical appraisal. *Haemophilia.* **12**, 19-27.

Maroun, R. C. and Serrano, S. M. (2004) Identification of the substrate-binding exosites of two snake venom serine proteinases: molecular basis for the partition of two essential functions of thrombin. *J Mol. Recognit.* **17**, 51-61.

Martinod, K., Demers, M., Fuchs, T. A., Wong, S. L., Brill, A., Gallant, M., Hu, J., Wang, Y. and Wagner, D. D. (2013) Neutrophil histone modification by peptidylarginine deiminase 4 is critical for deep vein thrombosis in mice. *Proc. Natl. Acad. Sci. U. S. A* **110**, 8674-8679.

Marx, G., Korner, G., Mou, X. and Gorodetsky, R. (1993) Packaging zinc, fibrinogen, and factor XIII in platelet alpha-granules. *J. Cell Physiol* **156**, 437-442.

Massberg, S., Grahl, L., von Bruehl, M. L., Manukyan, D., Pfeiler, S., Goosmann, C., Brinkmann, V., Lorenz, M., Bidzhekov, K., Khandagale, A. B. *et al.* (2010) Reciprocal coupling of coagulation and innate immunity via neutrophil serine proteases. *Nat. Med.* **16**, 887-896.

Matafonov, A., Leung, P. Y., Gailani, A. E., Grach, S. L., Puy, C., Cheng, Q., Sun, M. F., McCarty, O. J., Tucker, E. I., Kataoka, H. *et al.* (2014) Factor XII inhibition reduces thrombus formation in a primate thrombosis model. *Blood* **123**, 1739-1746.

Meh, D. A., Siebenlist, K. R. and Mosesson, M. W. (1996) Identification and characterization of the thrombin binding sites on fibrin. *J. Biol. Chem.* **271**, 23121-23125.

Meng, W., Paunel-Gorgulu, A., Flohe, S., Hoffmann, A., Witte, I., Mackenzie, C., Baldus, S. E., Windolf, J. and Logters, T. T. (2012) Depletion of neutrophil extracellular traps in vivo results in hypersusceptibility to polymicrobial sepsis in mice. *Crit Care* **16**, R137.

Merkulov, S., Zhang, W. M., Komar, A. A., Schmaier, A. H., Barnes, E., Zhou, Y., Lu, X., Iwaki, T., Castellino, F. J., Luo, G. *et al.* (2008) Deletion of murine kininogen gene 1 (mKng1) causes loss of plasma kininogen and delays thrombosis. *Blood* **111**, 1274-1281.

Miyata, T., Kawabata, S., Iwanaga, S., Takahashi, I., Alving, B. and Saito, H. (1989) Coagulation factor XII (Hageman factor) Washington D.C.: inactive factor XIIa results from Cys-571----Ser substitution. *Proc. Natl. Acad. Sci. U. S. A* **86**, 8319-8322.

Moen, J. L., Gorkun, O. V., Weisel, J. W. and Lord, S. T. (2003) Recombinant BbetaArg14His fibrinogen implies participation of N-terminus of Bbeta chain in desA fibrin polymerization. *Blood* **102**, 2466-2471.

Monroe, D. M. and Hoffman, M. (2006) What does it take to make the perfect clot? *Arterioscler. Thromb. Vasc. Biol.* **26**, 41-48.

Monroe, D. M., Hoffman, M. and Roberts, H. R. (2002) Platelets and thrombin generation. *Arterioscler. Thromb. Vasc. Biol.* **22**, 1381-1389.

Morgan, W. T. (1986) Serum histidine-rich glycoprotein levels are decreased in acquired immune deficiency syndrome and by steroid therapy. *Biochem. Med. Metab Biol.* **36**, 210-213.

Morrissey, J. H. (2011) Taking the brakes off? *Blood* **117**, 3939-3940.

Morrissey, J. H., Choi, S. H. and Smith, S. A. (2012) Polyphosphate: an ancient molecule that links platelets, coagulation, and inflammation. *Blood* **119**, 5972-5979.

Mosesson, M. W. (2005) Fibrinogen and fibrin structure and functions. *J. Thromb. Haemost.* **3**, 1894-1904.

Mosesson, M. W. (2007) Update on antithrombin I (fibrin). *Thromb. Haemost.* **98**, 105-108.

Mosesson, M. W., Cooley, B. C., Hernandez, I., Diorio, J. P. and Weiler, H. (2009) Thrombosis risk modification in transgenic mice containing the human fibrinogen thrombin-binding gamma' chain sequence. *J. Thromb. Haemost.* **7**, 102-110.

Muller, F., Gailani, D. and Renne, T. (2011) Factor XI and XII as antithrombotic targets. *Curr. Opin. Hematol.* **18**, 349-355.

Muller, F., Mutch, N. J., Schenk, W. A., Smith, S. A., Esterl, L., Spronk, H. M., Schmidbauer, S., Gahl, W. A., Morrissey, J. H. and Renne, T. (2009) Platelet polyphosphates are proinflammatory and procoagulant mediators in vivo. *Cell* **139**, 1143-1156.

Mullin, J. L., Gorkun, O. V., Binnie, C. G. and Lord, S. T. (2000) Recombinant fibrinogen studies reveal that thrombin specificity dictates order of fibrinopeptide release. *J Biol. Chem.* **275**, 25239-25246.

Mutch, N. J., Robbie, L. A. and Booth, N. A. (2001) Human thrombi contain an abundance of active thrombin. *Thromb. Haemost.* **86**, 1028-1034.

Nadano, D., Yasuda, T. and Kishi, K. (1993) Measurement of deoxyribonuclease I activity in human tissues and body fluids by a single radial enzyme-diffusion method. *Clin. Chem.* **39**, 448-452.

Nagata, S., Nagase, H., Kawane, K., Mukae, N. and Fukuyama, H. (2003) Degradation of chromosomal DNA during apoptosis. *Cell Death. Differ.* **10**, 108-116.

Nikula, T. K., Bocchia, M., Curcio, M. J., Sgouros, G., Ma, Y., Finn, R. D. and Scheinberg, D. A. (1995) Impact of the high tyrosine fraction in complementarity determining regions: measured and predicted effects of radioiodination on IgG immunoreactivity. *Mol. Immunol.* **32**, 865-872.

Olexa, S. A. and Budzynski, A. Z. (1979) Binding phenomena of isolated unique plasmic degradation products of human cross-linked fibrin. *J. Biol. Chem.* **254**, 4925-4932.

Olman, M. A., Williams, W. F., Strickland, J. H., Jr., Hagood, J. S., Simmons, W. L. and Rivera, K. E. (1998) Facile purification of fibrinogen fragments using a computer-based model with general applicability to the generation of salt gradients. *Protein Expr. Purif.* **14**, 71-78.

Owens, A. P., III, Lu, Y., Whinna, H. C., Gachet, C., Fay, W. P. and Mackman, N. (2011) Towards a standardization of the murine ferric chloride-induced carotid arterial thrombosis model. *J Thromb. Haemost.* **9**, 1862-1863.

Parry, M. A., Jacob, U., Huber, R., Wisner, A., Bon, C. and Bode, W. (1998) The crystal structure of the novel snake venom plasminogen activator TSV-PA: a prototype structure for snake venom serine proteinases. *Structure.* **6**, 1195-1206.

Pawlinski, R., Fernandes, A., Kehrle, B., Pedersen, B., Parry, G., Erlich, J., Pyo, R., Gutstein, D., Zhang, J., Castellino, F. *et al.* (2002) Tissue factor deficiency causes

cardiac fibrosis and left ventricular dysfunction. *Proc. Natl. Acad. Sci. U. S. A* **99**, 15333-15338.

Pechik, I., Madrazo, J., Mosesson, M. W., Hernandez, I., Gilliland, G. L. and Medved, L. (2004) Crystal structure of the complex between thrombin and the central "E" region of fibrin. *Proc. Natl. Acad. Sci. U. S. A* **101**, 2718-2723.

Perzborn, E., Roehrig, S., Straub, A., Kubitza, D. and Misselwitz, F. (2011) The discovery and development of rivaroxaban, an oral, direct factor Xa inhibitor. *Nat. Rev. Drug Discov.* **10**, 61-75.

Petrera, N. S., Stafford, A. R., Leslie, B. A., Kretz, C. A., Fredenburgh, J. C. and Weitz, J. I. (2009) Long range communication between exosites 1 and 2 modulates thrombin function. *J Biol. Chem.* **284**, 25620-25629.

Pieters, M., Kotze, R. C., Jerling, J. C., Kruger, A. and Ariens, R. A. (2013) Evidence that fibrinogen gamma' regulates plasma clot structure and lysis and relationship to cardiovascular risk factors in black Africans. *Blood* **121**, 3254-3260.

Pixley, R. A., Cassello, A., De La Cadena, R. A., Kaufman, N. and Colman, R. W. (1991) Effect of heparin on the activation of factor XII and the contact system in plasma. *Thromb. Haemost.* **66**, 540-547.

Pixley, R. A., Schapira, M. and Colman, R. W. (1985) The regulation of human factor XIIa by plasma proteinase inhibitors. *J Biol. Chem.* **260**, 1723-1729.

Pixley, R. A., Schmaier, A. and Colman, R. W. (1987) Effect of negatively charged activating compounds on inactivation of factor XIIa by Cl inhibitor. *Arch. Biochem. Biophys.* **256**, 490-498.

Poon, I. K., Olsson, A. K., Hulett, M. D. and Parish, C. R. (2009) Regulation of histidine-rich glycoprotein (HRG) function via plasmin-mediated proteolytic cleavage. *Biochem. J.* **424**, 27-37.

Poon, I. K., Patel, K. K., Davis, D. S., Parish, C. R. and Hulett, M. D. (2011) Histidine-rich glycoprotein: the Swiss Army knife of mammalian plasma. *Blood* **117**, 2093-2101.

Pospisil, C. H., Stafford, A. R., Fredenburgh, J. C. and Weitz, J. I. (2003) Evidence that both exosites on thrombin participate in its high affinity interaction with fibrin. *J. Biol. Chem.* **278**, 21584-21591.

Preissner, K. T. (2007) Extracellular RNA. A new player in blood coagulation and vascular permeability. *Hamostaseologie.* **27**, 373-377.

Rand, M. L., Wang, H., Pluthero, F. G., Stafford, A. R., Ni, R., Vaezzadeh, N., Allison, A. C., Kahr, W. H., Weitz, J. I. and Gross, P. L. (2012) Diannexin, an annexin A5

homodimer, binds phosphatidylserine with high affinity and is a potent inhibitor of platelet-mediated events during thrombus formation. *J Thromb. Haemost.* **10**, 1109-1119.

Rasche, H. (2001) Haemostasis and thrombosis:an overview. *European Heart Journal Supplements* **Supplement Q**, Q3-Q7.

Rau, J. C., Beaulieu, L. M., Huntington, J. A. and Church, F. C. (2007) Serpins in thrombosis, hemostasis and fibrinolysis. *J. Thromb. Haemost.* **5 Suppl 1**, 102-115.

Renne, T., Pozgajova, M., Gruner, S., Schuh, K., Pauer, H. U., Burfeind, P., Gailani, D. and Nieswandt, B. (2005) Defective thrombus formation in mice lacking coagulation factor XII. *J Exp. Med.* **202**, 271-281.

Renne, T., Schmaier, A. H., Nickel, K. F., Blomback, M. and Maas, C. (2012) In vivo roles of factor XII. *Blood* **120**, 4296-4303.

Revenko, A. S., Gao, D., Crosby, J. R., Bhattacharjee, G., Zhao, C., May, C., Gailani, D., Monia, B. P. and MacLeod, A. R. (2011) Selective depletion of plasma prekallikrein or coagulation factor XII inhibits thrombosis in mice without increased risk of bleeding. *Blood* **118**, 5302-5311.

Riedel, T., Suttnar, J., Brynda, E., Houska, M., Medved, L. and Dyr, J. E. (2011) Fibrinopeptides A and B release in the process of surface fibrin formation. *Blood* **117**, 1700-1706.

Rojkjaer, R. and Schousboe, I. (1997) The surface-dependent autoactivation mechanism of factor XII. *Eur. J. Biochem.* **243**, 160-166.

Rolny, C., Mazzone, M., Tugues, S., Laoui, D., Johansson, I., Coulon, C., Squadrito, M. L., Segura, I., Li, X., Knevels, E. *et al.* (2011) HRG inhibits tumor growth and metastasis by inducing macrophage polarization and vessel normalization through downregulation of PlGF. *Cancer Cell* **19**, 31-44.

Rose, T., LeMosy, E. K., Cantwell, A. M., Banerjee-Roy, D., Skeath, J. B. and Di Cera, E. (2003) Three-dimensional models of proteases involved in patterning of the Drosophila Embryo. Crucial role of predicted cation binding sites. *J. Biol. Chem.* **278**, 11320-11330.

Rosen, E. D., Chan, J. C., Idusogie, E., Clotman, F., Vlasuk, G., Luther, T., Jalbert, L. R., Albrecht, S., Zhong, L., Lissens, A. *et al.* (1997) Mice lacking factor VII develop normally but suffer fatal perinatal bleeding. *Nature* **390**, 290-294.

Rumore, P. M. and Steinman, C. R. (1990) Endogenous circulating DNA in systemic lupus erythematosus. Occurrence as multimeric complexes bound to histone. *J. Clin. Invest* **86**, 69-74.

Rydengard, V., Andersson, N. E. and Schmidtchen, A. (2006) Zinc potentiates the antibacterial effects of histidine-rich peptides against Enterococcus faecalis. *FEBS J* **273**, 2399-2406.

Rydengard, V., Olsson, A. K., Morgelin, M. and Schmidtchen, A. (2007) Histidine-rich glycoprotein exerts antibacterial activity. *FEBS J* **274**, 377-389.

Rydengard, V., Shannon, O., Lundqvist, K., Kacprzyk, L., Chalupka, A., Olsson, A. K., Morgelin, M., Jahnen-Dechent, W., Malmsten, M. and Schmidtchen, A. (2008) Histidine-rich glycoprotein protects from systemic Candida infection. *PLoS. Pathog.* **4**, e1000116.

Sabbatini, A. R., Mattii, L., Battolla, B., Polizzi, E., Martini, D., Ranieri-Raggi, M., Moir, A. J. and Raggi, A. (2011) Evidence that muscle cells do not express the histidine-rich glycoprotein associated with AMP deaminase but can internalise the plasma protein. *Eur. J. Histochem.* **55**, e6.

Saha, P., Humphries, J., Modarai, B., Mattock, K., Waltham, M., Evans, C. E., Ahmad, A., Patel, A. S., Premaratne, S., Lyons, O. T. *et al.* (2011) Leukocytes and the natural history of deep vein thrombosis: current concepts and future directions. *Arterioscler. Thromb. Vasc. Biol.* **31**, 506-512.

Samuel, M., Pixley, R. A., Villanueva, M. A., Colman, R. W. and Villanueva, G. B. (1992) Human factor XII (Hageman factor) autoactivation by dextran sulfate. Circular dichroism, fluorescence, and ultraviolet difference spectroscopic studies. *J. Biol. Chem.* **267**, 19691-19697.

Schaefer, A. V., Leslie, B. A., Rischke, J. A., Stafford, A. R., Fredenburgh, J. C. and Weitz, J. I. (2006) Incorporation of fragment X into fibrin clots renders them more susceptible to lysis by plasmin. *Biochemistry* **45**, 4257-4265.

Schmaier, A. H. and McCrae, K. R. (2007) The plasma kallikrein-kinin system: its evolution from contact activation. *J Thromb. Haemost.* **5**, 2323-2329.

Schmaier, A. H., Silverberg, M., Kaplan, A. P. and Colman, R. W. (1987) Contact activation and its abnormalities, in *Hemostasis and Thrombosis Basic Principles and Clinical Practice*, 2 edition, eds. Colman, R. W., Hirsh, J., Marder, V. J., and Salzman, E. pp. 18-38.

Scott, C. F. and Colman, R. W. (1992) Fibrinogen blocks the autoactivation and thrombin-mediated activation of factor XI on dextran sulfate. *Proc. Natl. Acad Sci. U. S. A* **89**, 11189-11193.

Semeraro, F., Ammollo, C. T., Morrissey, J. H., Dale, G. L., Friese, P., Esmon, N. L. and Esmon, C. T. (2011) Extracellular histones promote thrombin generation through

platelet-dependent mechanisms: involvement of platelet TLR2 and TLR4. *Blood* **118**, 1952-1961.

Serrano, S. M. and Maroun, R. C. (2005) Snake venom serine proteinases: sequence homology vs. substrate specificity, a paradox to be solved. *Toxicon* **45**, 1115-1132.

Shannon, O., Rydengard, V., Schmidtchen, A., Morgelin, M., Alm, P., Sorensen, O. E. and Bjorck, L. (2010) Histidine-rich glycoprotein promotes bacterial entrapment in clots and decreases mortality in a mouse model of sepsis. *Blood* **116**, 2365-2372.

Siebenlist, K. R., Meh, D. A. and Mosesson, M. W. (1996) Plasma factor XIII binds specifically to fibrinogen molecules containing gamma chains. *Biochemistry* **35**, 10448-10453.

Siebenlist, K. R., Mosesson, M. W., Hernandez, I., Bush, L. A., Di Cera, E., Shainoff, J. R., Di Orio, J. P. and Stojanovic, L. (2005) Studies on the basis for the properties of fibrin produced from fibrinogen-containing gamma' chains. *Blood* **106**, 2730-2736.

Smith, A., Nuiry, I. and Morgan, W. T. (1985) Proteolysis of histidine-rich glycoprotein in plasma and in patients undergoing thrombolytic therapy. *Thromb. Res.* **40**, 653-661.

Smith, S. A., Choi, S. H., Collins, J. N., Travers, R. J., Cooley, B. C. and Morrissey, J. H. (2012) Inhibition of polyphosphate as a novel strategy for preventing thrombosis and inflammation. *Blood* **120**, 5103-5110.

Smith, S. A., Choi, S. H., Davis-Harrison, R., Huyck, J., Boettcher, J., Rienstra, C. M. and Morrissey, J. H. (2010) Polyphosphate exerts differential effects on blood clotting, depending on polymer size. *Blood* **116**, 4353-4359.

Smith, S. A., Mutch, N. J., Baskar, D., Rohloff, P., Docampo, R. and Morrissey, J. H. (2006) Polyphosphate modulates blood coagulation and fibrinolysis. *Proc. Natl. Acad. Sci. U. S. A* **103**, 903-908.

Standeven, K. F., Carter, A. M., Grant, P. J., Weisel, J. W., Chernysh, I., Masova, L., Lord, S. T. and Ariens, R. A. (2007) Functional analysis of fibrin {gamma}-chain cross-linking by activated factor XIII: determination of a cross-linking pattern that maximizes clot stiffness. *Blood* **110**, 902-907.

Stewart, A. J., Blindauer, C. A. and Sadler, P. J. (2009) Plasma fatty acid levels may regulate the Zn(2+)-dependent activities of histidine-rich glycoprotein. *Biochimie* **91**, 1518-1522.

Stocker, K. F. (1998) , in *Hemostasis and Animal Venoms* edition, eds. Pirkle, H. and Markland, F. (Marcel Dekker, Inc., Los Angeles), pp. 525-540.

Stone, S. R. and Hofsteenge, J. (1986) Kinetics of the inhibition of thrombin by hirudin. *Biochemistry* **25**, 4622-4628.

Sulikowski, T., Bauer, B. A. and Patston, P. A. (2002) alpha(1)-Proteinase inhibitor mutants with specificity for plasma kallikrein and C1s but not C1. *Protein Sci.* **11**, 2230-2236.

Swartz, M. J., Mitchell, H. L., Cox, D. J. and Reeck, G. R. (1977) Isolation and characterization of trypsin inhibitor from opaque-2 corn seeds. *J. Biol. Chem.* **252**, 8105-8107.

Swystun, L. L., Mukherjee, S. and Liaw, P. C. (2011) Breast cancer chemotherapy induces the release of cell-free DNA, a novel procoagulant stimulus. *J Thromb. Haemost.* **9**, 2313-2321.

Tamkovich, S. N., Cherepanova, A. V., Kolesnikova, E. V., Rykova, E. Y., Pyshnyi, D. V., Vlassov, V. V. and Laktionov, P. P. (2006) Circulating DNA and DNase activity in human blood. *Ann. N. Y. Acad. Sci.* **1075**, 191-196.

Taylor, F. B., Jr., Chang, A., Ruf, W., Morrissey, J. H., Hinshaw, L., Catlett, R., Blick, K. and Edgington, T. S. (1991) Lethal E. coli septic shock is prevented by blocking tissue factor with monoclonal antibody. *Circ. Shock* **33**, 127-134.

Tesselaar, M. E., Romijn, F. P., Van, D. L., I, Prins, F. A., Bertina, R. M. and Osanto, S. (2007) Microparticle-associated tissue factor activity: a link between cancer and thrombosis? *J. Thromb. Haemost.* **5**, 520-527.

Toltl, L. J., Swystun, L. L., Pepler, L. and Liaw, P. C. (2008) Protective effects of activated protein C in sepsis. *Thromb. Haemost.* **100**, 582-592.

Tsuchida-Straeten, N., Ensslen, S., Schafer, C., Woltje, M., Denecke, B., Moser, M., Graber, S., Wakabayashi, S., Koide, T. and Jahnen-Dechent, W. (2005) Enhanced blood coagulation and fibrinolysis in mice lacking histidine-rich glycoprotein (HRG). *J Thromb. Haemost.* **3**, 865-872.

Tucker, E. I., Verbout, N. G., Leung, P. Y., Hurst, S., McCarty, O. J., Gailani, D. and Gruber, A. (2012) Inhibition of factor XI activation attenuates inflammation and coagulopathy while improving the survival of mouse polymicrobial sepsis. *Blood* **119**, 4762-4768.

Turcotte, A. and Bergeron, M. G. (1992) Pharmacodynamic interaction between RP 59500 and gram-positive bacteria infecting fibrin clots. *Antimicrob. Agents Chemother.* **36**, 2211-2215.

Uitte de Willige, S., de Visser, M. C., Houwing-Duistermaat, J. J., Rosendaal, F. R., Vos, H. L. and Bertina, R. M. (2005) Genetic variation in the fibrinogen gamma gene increases the risk for deep venous thrombosis by reducing plasma fibrinogen gamma' levels. *Blood* **106**, 4176-4183.

Uitte de Willige, S., Standeven, K. F., Philippou, H. and Ariens, R. A. (2009) The pleiotropic role of the fibrinogen gamma' chain in hemostasis. *Blood* **114**, 3994-4001.

Vaezzadeh, N., Ni, R., Kim, P. Y., Weitz, J. I. and Gross, P. L. (2014) Comparison of the effect of coagulation and platelet function impairments on various mouse bleeding models. *Thromb. Haemost.* **112**.

van den Herik, E. G., Cheung, E. Y., de Lau, L. M., den Hertog, H. M., Leebeek, F. W., Dippel, D. W., Koudstaal, P. J. and de Maat, M. P. (2011) gamma'/total fibrinogen ratio is associated with short-term outcome in ischaemic stroke. *Thromb. Haemost.* **105**, 430-434.

van der Meijden, P. E., Munnix, I. C., Auger, J. M., Govers-Riemslag, J. W., Cosemans, J. M., Kuijpers, M. J., Spronk, H. M., Watson, S. P., Renne, T. and Heemskerk, J. W. (2009) Dual role of collagen in factor XII-dependent thrombus formation. *Blood* **114**, 881-890.

van der Vaart, M. and Pretorius, P. J. (2008) Circulating DNA. Its origin and fluctuation. *Ann N. Y. Acad Sci.* **1137**, 18-26.

van Montfoort, M. L. and Meijers, J. C. (2013) Anticoagulation beyond direct thrombin and factor Xa inhibitors: indications for targeting the intrinsic pathway? *Thromb. Haemost.* **110**, 223-232.

van't Veer, C. and Mann, K. G. (1997) Regulation of tissue factor initiated thrombin generation by the stoichiometric inhibitors tissue factor pathway inhibitor, antithrombin-III, and heparin cofactor-II. *J. Biol. Chem.* **272**, 4367-4377.

von Bruhl, M. L., Stark, K., Steinhart, A., Chandraratne, S., Konrad, I., Lorenz, M., Khandoga, A., Tirniceriu, A., Coletti, R., Kollnberger, M. *et al.* (2012) Monocytes, neutrophils, and platelets cooperate to initiate and propagate venous thrombosis in mice in vivo. *J Exp. Med.* **209**, 819-835.

Vu, T.T., Zhou, J., Leslie, B.A., Stafford, A.R., Fredenburgh, J.C., and Weitz, J.I. (2013) Histidine rich glycoprotein binds to DNA, RNA and FXIIa with high affinity and attenuates contact-mediated coagulation in a mouse model of arterial thrombosis. *J Thromb.Haemost.(International Society on Thrombosis and Hemostasis)* **11**, 20. Abstract

Vu, T. T., Stafford, A. R., Leslie, B. A., Kim, P. Y., Fredenburgh, J. C. and Weitz, J. I. (2011) Histidine-rich glycoprotein binds fibrin(ogen) with high affinity and competes with thrombin for binding to the gamma'-chain. *J Biol. Chem.* **286**, 30314-30323.

Wagenaar-Bos, I. G. and Hack, C. E. (2006) Structure and function of C1-inhibitor. *Immunol. Allergy Clin. North Am.* **26**, 615-632.

Walton, B. L., Getz, T. M., Bergmeier, W., Lin, F.-C., Uitte, d. W. and Wolberg, A. S. (2014) The fibrinogen gammaA/gamma'-isoform does not promote acute arterial thrombosis in mice. *J. Thromb. Haemost.* **12**, 680-689.

Wang, J., Zhu, Y. Q., Liu, F., Li, M. H., Zhao, J. G., Tan, H. Q., Wang, J. B., Cheng, Y. S. and Zhang, P. L. (2010) Batroxobin for prevention of restenosis in diabetic patients after infrapopliteal arterial angioplasty: a small randomized pilot trial. *Ann. Vasc. Surg.* **24**, 876-884.

Wang, X., Cheng, Q., Xu, L., Feuerstein, G. Z., Hsu, M. Y., Smith, P. L., Seiffert, D. A., Schumacher, W. A., Ogletree, M. L. and Gailani, D. (2005) Effects of factor IX or factor XI deficiency on ferric chloride-induced carotid artery occlusion in mice. *J Thromb. Haemost.* **3**, 695-702.

Wang, X., Smith, P. L., Hsu, M. Y., Gailani, D., Schumacher, W. A., Ogletree, M. L. and Seiffert, D. A. (2006) Effects of factor XI deficiency on ferric chloride-induced vena cava thrombosis in mice. *J Thromb. Haemost.* **4**, 1982-1988.

Weisel, J. W., Veklich, Y. and Gorkun, O. (1993) The sequence of cleavage of fibrinopeptides from fibrinogen is important for protofibril formation and enhancement of lateral aggregation in fibrin clots. *J Mol. Biol.* **232**, 285-297.

Weitz, J. I. and Bates, E. R. (2003) Direct thrombin inhibitors in cardiac disease. *Cardiovasc. Toxicol.* **3**, 13-25.

Weitz, J. I., Hudoba, M., Massel, D., Maraganore, J. and Hirsh, J. (1990) Clot-bound thrombin is protected from inhibition by heparin-antithrombin III but is susceptible to inactivation by antithrombin III-independent inhibitors. *J. Clin. Invest* **86**, 385-391.

Wencel-Drake, J. D., Boudignon-Proudhon, C., Dieter, M. G., Criss, A. B. and Parise, L. V. (1996) Internalization of bound fibrinogen modulates platelet aggregation. *Blood* **87**, 602-612.

Westrick, R. J., Winn, M. E. and Eitzman, D. T. (2007) Murine models of vascular thrombosis (Eitzman series). *Arterioscler. Thromb. Vasc. Biol.* **27**, 2079-2093.

Whelihan, M. F., Zachary, V., Orfeo, T. and Mann, K. G. (2012) Prothrombin activation in blood coagulation: the erythrocyte contribution to thrombin generation. *Blood* **120**, 3837-3845.

White, J. (2005) Snake venoms and coagulopathy. *Toxicon* **45**, 951-967.

Wolberg, A. S. (2012) Determinants of fibrin formation, structure, and function. *Curr. Opin. Hematol.* **19**, 349-356.

Wolfenstein-Todel, C. and Mosesson, M. W. (1980) Human plasma fibrinogen heterogeneity: evidence for an extended carboxyl-terminal sequence in a normal gamma chain variant (gamma'). *Proc. Natl. Acad. Sci. U. S. A* **77**, 5069-5073.

Woodruff, R. S., Xu, Y., Layzer, J., Wu, W., Ogletree, M. L. and Sullenger, B. A. (2013) Inhibiting the intrinsic pathway of coagulation with a factor XII-targeting RNA aptamer. *J Thromb. Haemost.* **11**, 1364-1373.

Xu, G., Liu, X., Zhu, W., Yin, Q., Zhang, R. and Fan, X. (2007) Feasibility of treating hyperfibrinogenemia with intermittently administered batroxobin in patients with ischemic stroke/transient ischemic attack for secondary prevention. *Blood Coagul. Fibrinolysis* **18**, 193-197.

Yau, J. W., Liao, P., Fredenburgh, J. C., Stafford, A. R., Revenko, A. S., Monia, B. P. and Weitz, J. I. (2014) Selective depletion of factor XI or factor XII with antisense oligonucleotides attenuates catheter thrombosis in rabbits. *Blood* **123**, 2102-2107.

Yeh, C. H., Fredenburgh, J. C. and Weitz, J. I. (2012) Oral direct factor Xa inhibitors. *Circ. Res.* **111**, 1069-1078.

Yipp, B. G. and Kubes, P. (2013) NETosis: how vital is it? *Blood* **122**, 2784-2794.

You, W. K., Choi, W. S., Koh, Y. S., Shin, H. C., Jang, Y. and Chung, K. H. (2004) Functional characterization of recombinant batroxobin, a snake venom thrombin-like enzyme, expressed from Pichia pastoris. *FEBS Lett.* **571**, 67-73.

Younis, H. S., Crosby, J., Huh, J. I., Lee, H. S., Rime, S., Monia, B. and Henry, S. P. (2012) Antisense inhibition of coagulation factor XI prolongs APTT without increased bleeding risk in cynomolgus monkeys. *Blood* **119**, 2401-2408.

Zhang, H., Lowenberg, E. C., Crosby, J. R., MacLeod, A. R., Zhao, C., Gao, D., Black, C., Revenko, A. S., Meijers, J. C., Stroes, E. S. *et al.* (2010) Inhibition of the intrinsic coagulation pathway factor XI by antisense oligonucleotides: a novel antithrombotic strategy with lowered bleeding risk. *Blood* **116**, 4684-4692.

Zhang, Y., Wisner, A., Maroun, R. C., Choumet, V., Xiong, Y. and Bon, C. (1997) Trimeresurus stejnegeri snake venom plasminogen activator. Site-directed mutagenesis and molecular modeling. *J Biol. Chem.* **272**, 20531-20537.

Zhou, J., May, L., Liao, P., Gross, P. L. and Weitz, J. I. (2009) Inferior vena cava ligation rapidly induces tissue factor expression and venous thrombosis in rats. *Arterioscler. Thromb. Vasc. Biol.* **29**, 863-869.

Zimmerman, B. and Valentino, L. A. (2013) Hemophilia: in review. *Pediatr. Rev.* **34**, 289-294.